UNIVERSITAT DE
BARCELONA

Role of p38 MAPK in breast cancer

Begoña Cánovas Bilbao

ADVERTIMENT. La consulta d'aquesta tesi queda condicionada a l'acceptació de les següents condicions d'ús: La difusió d'aquesta tesi per mitjà del servei TDX (**www.tdx.cat**) i a través del Dipòsit Digital de la UB (**diposit.ub.edu**) ha estat autoritzada pels titulars dels drets de propietat intel·lectual únicament per a usos privats emmarcats en activitats d'investigació i docència. No s'autoritza la seva reproducció amb finalitats de lucre ni la seva difusió i posada a disposició des d'un lloc aliè al servei TDX ni al Dipòsit Digital de la UB. No s'autoritza la presentació del seu contingut en una finestra o marc aliè a TDX o al Dipòsit Digital de la UB (framing). Aquesta reserva de drets afecta tant al resum de presentació de la tesi com als seus continguts. En la utilització o cita de parts de la tesi és obligat indicar el nom de la persona autora.

ADVERTENCIA. La consulta de esta tesis queda condicionada a la aceptación de las siguientes condiciones de uso: La difusión de esta tesis por medio del servicio TDR (**www.tdx.cat**) y a través del Repositorio Digital de la UB (**diposit.ub.edu**) ha sido autorizada por los titulares de los derechos de propiedad intelectual únicamente para usos privados enmarcados en actividades de investigación y docencia. No se autoriza su reproducción con finalidades de lucro ni su difusión y puesta a disposición desde un sitio ajeno al servicio TDR o al Repositorio Digital de la UB. No se autoriza la presentación de su contenido en una ventana o marco ajeno a TDR o al Repositorio Digital de la UB (framing). Esta reserva de derechos afecta tanto al resumen de presentación de la tesis como a sus contenidos. En la utilización o cita de partes de la tesis es obligado indicar el nombre de la persona autora.

WARNING. On having consulted this thesis you're accepting the following use conditions: Spreading this thesis by the TDX (**www.tdx.cat**) service and by the UB Digital Repository (**diposit.ub.edu**) has been authorized by the titular of the intellectual property rights only for private uses placed in investigation and teaching activities. Reproduction with lucrative aims is not authorized nor its spreading and availability from a site foreign to the TDX service or to the UB Digital Repository. Introducing its content in a window or frame foreign to the TDX service or to the UB Digital Repository is not authorized (framing). Those rights affect to the presentation summary of the thesis as well as to its contents. In the using or citation of parts of the thesis it's obliged to indicate the name of the author.

UNIVERSITAT DE BARCELONA

IRB BARCELONA
INSTITUTE FOR RESEARCH IN BIOMEDICINE

UNIVERSITAT DE BARCELONA

FACULTAD DE FARMACIA

PROGRAMA DE DOCTORADO EN BIOMEDICINA

ROLE OF p38 MAPK IN BREAST CANCER

Memoria presentada por Begoña Cánovas Bilbao para optar al título de doctor por la Universitat de Barcelona

Esta tesis ha sido realizada en el Instituto de Investigación Biomédica de Barcelona (IRB Barcelona)

Dr. Ángel Rodríguez Nebreda
(Director de la tesis)

Begoña Cánovas Bilbao
(Doctoranda)

Dra. Isabel Fabregat Romero
(Tutora de la tesis)

Begoña Cánovas Bilbao
Barcelona, 2017

En la vida no hay cosas que temer,

sólo cosas que comprender

Marie Curie

CONTENTS

ABBREVIATIONS 13

ABSTRACT/RESUMEN 17

INTRODUCTION 23

1. CANCER 25
    1.1. ONCOGENE and NON-ONCOGENE ADDICTION 26
    1.2. BREAST CANCER 28
        1.2.1. BREAST CANCER MODELS: PyMT TRANSGENIC MOUSE 29
        1.2.2. BREAST CANCER MODELS: HUMAN DERIVED XENOGRAFTS 31
2. CHROMOSOME INSTABILITY 31
    2.1. CIN and ANEUPLOIDY in NON TRANSFORMED CELLS 32
    2.2. CIN AND ANEUPLOIDY in CANCER 32
3. CELL CYCLE PROGRESSION AND CELL CYCLE CHECKPOINTS 35
    3.1. G1/S CHECKPOINT 36
    3.2. INTRA S CHECKPOINT 37
    3.3. G2 CHECKPOINT 37
    3.4. SPINDLE ASSEMBLY CHECKPOINT 37
4. DNA REPLICATION 38
    4.1. REPLICATION STRESS 39
5. DNA DAMAGE RESPONSE 41
    5.1. DNA REPAIR 43
        5.1.1. NON HOMOLOGOUS END JOINING 44
        5.1.2. HOMOLOGOUS RECOMBINATION 44
6. p38 MAPK 46
    6.1. MAPK SUPERFAMILY 46
    6.2. DISCOVERY 47
    6.3. p38 MAPK FAMILY 47
    6.4. ACTIVATION 48
    6.5. DOWNSTREAM TARGETS 49
    6.6. p38α IN CANCER 51
        6.6.1. p38α role in cell cycle regulation and cell cycle checkpoints 52
        6.6.2. p38α role in DNA replication and replication stress 53
        6.6.3. p38α role in DNA Damage 53

AIM OF THE WORK 55

Specific objectives 57

MATERIALS AND METHODS 59

1. MATERIALS 61

1.1. Buffers and solutions 61
1.2. Commercial Reagents and Kits 62
1.3. Antibodies 65
1.4. Primers 67
1.5. Plasmids 68
2. METHODS **68**
2.1. MOUSE WORK ***68***
2.1.1 Generation of PyMT mice with inducible Cre 68
2.1.2 Patient-derived xenografts 68
2.1.3 Animal treatments 69
2.1.4. Histological analysis 69
2.1.5. FISH 69
2.2. MAMMALIAN CELL CULTURE ***70***
2.2.1. Generation of epithelial cell lines from PyMT tumors 70
2.2.2. Maintenance and subculture 70
2.2.3. Cell collection 70
2.2.4. Freezing and thawing 70
2.2.5. Mycoplasma detection 71
2.2.6. Cell pellet preparation for IHC 71
2.2.7. Cell treatments 71
2.2.8. Retroviral Infection 73
2.3. MOLECULAR BIOLOGY ***73***
2.3.1. Protein extraction 73
2.3.2. Determination of protein concentration 73
2.3.3. Western Blot 74
2.3.4. Subcellular fractionation 74
2.3.5. Immunoprecipitation 74
2.3.6. RNA isolation 74
2.3.7. cDNA synthesis 75
2.3.8. Quantitative real time PCR 75
2.3.9. Epithelial cell isolation for p38α deletion analysis 75
2.3.10. Kinase Assay 76
2.3.11. Mass Spectrometry 76
2.4. CELLULAR BIOLOGY ***76***
2.4.1. Cell Cycle Analysis 76
2.4.2. MTT proliferation assay 76
2.4.3. BrdU Uptake 77
2.4.4. Annexin V staining 77
2.4.5. Epithelial status verification 77
2.4.6. Phospho H3 S10 staining 78
2.4.7. Clonogenic Assays 78

2.4.8. Metaphase spread preparation 78
2.4.9. Immunofluorescence 78
2.4.10. Telomere staining 79
2.4.11. Time-lapse imaging......79
2.4.12. DNA replication fiber assay......79
2.4.13. COMET assays......80
2.4.13.1. *Neutral COMET* 80
2.4.13.2. *Alkaline COMET* 81
2.4.14. Intracellular ROS quantification 81
2.4.15. 8-OHdG determination 81
2.4.16. Homologous recombination assay......81
2.5. STATISTICAL ANALYSIS ***82***

RESULTS 83

1. Characterization of PyMT mice with inducible p38α deletion **86**
2. p38α expression in tumor epithelial cells is essential for PyMT-induced breast cancer progression *in vivo* **87**
3. Establishment and characterization of cell lines derived from PyMT tumors **89**
4. Functional characterization of p38α deletion in immortalized PyMT epithelial cells......**91**
4.1. p53 status characterization **94**
4.2. Receptor status characterization **95**
4.3. p38α is not directly involved in PyMT signaling **96**
5. p38α is required for chromosome segregation in PyMT epithelial cells and its deletion increases chromosome instability **99**
6. Mitotic defects do not explain the increased chromosome instability found in the absence of p38α **103**
7. p38α deletion results in elevated DNA damage and replication stress in PyMT cells **109**
8. p38α deletion hampers ATR signaling and DNA repair in response to replication associated DNA damage **116**
9. Inhibition of p38α potentiates the anti-tumoral effect of CIN-inducing chemotherapeutic drugs **122**

DISCUSION 127

1. p38α as an example of non-oncogene in breast cancer cells **129**
2. Novel role of p38α in replication-associated DNA damage response **131**
3. p38α deletion increases chromosome instability and sensitizes breast cancer cells to CIN-inducing agents **133**
4. Collateral damage of p38α targeting **135**

CONCLUSIONS ……………………………………………………………………………………………………139

APPENDIX ……………………………………………………………………………………………………143

REFERENCES ……………………………………………………………………………………………………148

ACKNOWLEDGMENTS ……………………………………………………………………………………………………167

ABBREVIATIONS

4-OHT	4-hydroxitamoxifen
53BP1	p53 binding protein 1
8-OHdG	8-hydroxy-2' -deoxyguanosine
A.U.	Arbitrary Units
ACA	Anti-centromere antibody
APC	Adenomatous polyposis coli
APS	Ammonium persulfate
ATM	ataxia telangiectasia mutated
ATP	Adenosine triphosphate
ATR	ATM and Rad3-related
BRCA1	Breast cancer 1
BrdU	5-bromo-2'-deoxyuridine
BSA	Bovine serum albumin
CDK	Cyclin-dependent kinase
Chk1	Checkpoint kinase 1
CldU	5-Chloro-2’-deoxyuridine thymidine
CIN	Chromosomal instability
CK	Cytokeratin
CPT	Campothecin
CreERT2	Cre Recombinase-estrogen receptor T2 mutant
CSK	Cytoskeletal
CtIP	CtBP-interacting protein
DAB	3,3-di-amino-benzidine
DAPI	4',6-diamidino-2-phenylindole
DCF	2’,7’-dichlorofluorescin
DCFDA	2’,7’-dichlorofluorescin diacetate
DDR	DNA damage response
dH$_2$O	Distilled water
DMEM	Dulbecco's Modified Eagle Medium
DMSO	Dimethyl sulfoxide
DNA	Deoxyribonucleic acid
DNAse	deoxyribonuclease
DPX	Distyrene, plasticizer, xylene
DSB	DNA double strand break
dsDNA	Double stranded DNA
DTT	Dithiothreitol
E2	17β-estradiol
EDTA	Ethylenediamine tetraacetic acid
EGTA	Ethylene glycol tetraacetic acid
EPCAM	Epithelial cell adhesion molecule
ERα	Estrogen receptor-alpha
FACS	Fluorescence-activated cell sorting
FBS	Fetal bovine serum
FISH	Fluorescence In Situ Hybridization
FITC	Fluorescein isothiocyanate
FS	Forward scatter
GAPDH	Glyceraldehyde 3-phosphate dehydrogenase
GFP	Green fluorescent protein

Gy	Greys
H&E	Hematoxylin & Eosin
H2AX	Histone H2AX
H3	Histone 3
HBS	HEPES buffered saline
HEPES	4-(2-hydroxyethyl)-1-piperazineethanesulfonic acid
Her2	Human epidermal growth factor receptor 2
HPRT	Hypoxanthine-guanine phosphoribosyltransferase
HR	Homologous recombination
HSP27	Heat shock protein 27
IdU	5-iodo-2'-deoxyuridine
LC	Liquid chromatography
Lum	Luminal
LY	LY2228820
MAPK	Mitogen-activated protein kinase
MCM	Minichromosome maintenance protein
MDM2	Murine doble minute 2
MEF	Mouse embryo fibroblast
MK2	Mitogen-activated protein kinase-activated protein kinase 2
MKK	Mitogen-activated protein kinase kinase
MNK	MAP Kinase Signal-Integrating Kinase 1
MSK	Mitogen and stress-activated protein kinase 1
MPS1	Monopolar spindle 1
MRN	Mre11-Rad50-Nbs1
mRNA	Messenger RNA
MS	Mass spectrometry
MTT	3-(4,5-Dimethylthiazol-2-yl)-2,5-diphenyltetrazolium bromide
NHEJ	Non-homologous end joining
Noco	Nocodazole
NOD/Scid	Non-obese diabetic/severe combined immunodeficiency
NT	Non treated
O/N	Overnight
PAGE	Polyacrylamide Gel Electrophoresis
PARP	PolyADP ribose polymerase
PBS	Phosphate buffer solution
PDX	Patient-derived xenograft
PE	Phycoerythrin
PgR	Progesterone Receptor
PH	PH797804
PI	Propidium Iodide
PI3K	Phosphatidylinositol 3-kinase
PMSF	Phenylmethanesulfonyl fluoride
PVDF	Polyvinylidene fluoride
PyMT	Polyoma Middle T
qRT-PCR	Quantitative real time Polymerase chain reaction
RIPA	Radioimmunoprecipitation assay
RNA	Ribonucleic acid
Rnase	Ribonuclease

ROS	Reactive oxygen species
RPA	Replication protein A
rpm	revolutions per minute
RT	Room temperature
SAC	Spindle assembly checkpoint
SB	SB203580
SDS	Sodium dodecyl sulfate
SEM	Standart error mean
Ser	Serine
SMA	Smooth muscle actin
SSB	Single strand break
SSC	saline-sodium citrate
ssDNA	single-stranded DNA
TEMED	N,N,N´,N´-tetramethylethylenediamine
Thr	Threonine
TN	Triple Negative
TUNEL	Terminal deoxynucleotidyl transferase dUTP nick-end labeling
Tyr	Tyrosine
UV	Ultraviolet
WT	Wild type
Z-VAD-FMK	carbobenzoxy-valyl-alanyl-aspartyl-[O-methyl]- fluoromethylketone

ABSTRACT/RESUMEN

Cancer refers to a group of diseases characterized by the presence of cells that divide uncontrollably and have the ability to spread to other tissues.

During the past years, the protein kinase p38α has emerged as an important regulator of tumorigenesis that often functions as a tumor suppressor in normal epithelial cells. However, recent studies provided evidence for a function of p38α promoting tumor cell proliferation and survival in some cancer types. Moreover, p38α inhibition has been shown to cooperate with chemotherapeutic drugs such as cisplatin and sorafenib. Given that the role of p38α in cancer seems to be cell and context dependent, in this work we have addressed the function of p38α in the particular context of breast cancer progression.

Using the Polyoma middle T mammary tumorigenesis model, we have found that p38α expression in epithelial cancer cells is essential for tumor cell survival. In order to analyze the underlying molecular mechanisms, we established cell lines from the PyMT-induced mammary tumors. We observed that p38α downregulation resulted in replication stress, elevated DNA damage, and increased chromosome missegregation, which correlated with decreased viability of the PyMT-expressing cancer cells.

The defects in replication fork progression and the increased DNA damage led us to investigate the status of the DNA damage response in p38α-deficient cancer cells. We observed impaired single strand-DNA generation, ATR activation and RAD51 recruitment after DNA damage, indicating that homologous recombination DNA repair was defective in p38α deficient cells. Moreover, we identified CtIP, a key factor that promotes DNA-end resection in mammalian cells, as a p38α substrate. De-regulation of CtIP due to decreased p38α-mediated phosphorylation is likely to affect the DNA damage response and explain many of the observed phenotypes. Altogether, our results indicated that p38α was required for effective DNA damage response and repair, which in turn impinged on proper DNA replication and maintenance of chromosome stability in breast cancer epithelial cells.

The above results suggested that targeting p38α could increase tumor cell sensitivity to chromosome instability-inducing agents such as taxanes. We confirmed this hypothesis using both PyMT-induced tumors and patient-derived xenografts, in which p38α inhibitors enhanced, accelerated or prolonged the anti-tumoral response observed with the taxanes alone.

In summary, we describe a novel role of p38α in coordinating the DNA damage response and limiting chromosome instability in cancer cells, and propose the combination of p38α inhibitors and taxanes as a potential therapeutic option in breast cancer treatment.

Cáncer es un término que engloba a un amplio grupo de enfermedades caracterizadas por un crecimiento descontrolado de células que pueden propagarse a otros tejidos.

Durante los últimos años, la proteína quinasa p38α se ha identificado como un importante regulador de la actividad tumoral y está considerada como un supresor tumoral. Sin embargo, estudios recientes sugieren que p38α puede promover el crecimiento y la supervivencia en algunos tipos de células tumorales, así como que su inhibición coopera con agentes quimioterapéuticos como el cisplatino o el sorafenib. Así pues, la función de p38α parece depender tanto del tipo de célula como del contexto. Por ello, este trabajo abordó el papel de p38α en el contexto concreto de la progresión del cáncer de mama.

Usando el modelo de cáncer de mama "Polyoma middle T" (PyMT), hemos observado que la expresión de p38α en las células epiteliales que conforman el tumor es esencial para la supervivencia y crecimiento del mismo. Para analizar los mecanismos moleculares implicados establecimos un sistema *ex vivo* consistente en líneas celulares derivadas de tumores de mama inducidos por PyMT. Observamos que en ausencia de p38α estas células mostraban estrés replicativo, un mayor daño en el ADN y un incremento en los errores de segregación que correlacionaban con una menor viabilidad celular.

Los defectos durante la replicación y el aumento en el daño en el ADN nos llevaron a investigar el estado de la ruta de respuesta al daño en el ADN. Así pues, encontramos que las células tumorales deficientes en p38α mostraban defectos en la generación de ADN monocatenario, en la activación de ATR y en el reclutamiento de RAD51 a los focos de daño, lo que sugería que la reparación de ADN por recombinación homóloga estaba afectada. Además identificamos CtIP, un factor esencial para la resección del ADN, como sustrato directo de p38α. La desregulación de CtIP debido a la ausencia de fosforilación por p38α influiría negativamente en la respuesta al daño en el ADN y explicaría en gran medida los fenotipos descritos anteriormente. En conjunto, nuestros datos sugieren que p38α es necesaria para una eficiente reparación del ADN y por tanto para la óptima replicación del ADN y el mantenimiento de la estabilidad cromosómica en las células epiteliales de cáncer de mama.

Los resultados anteriores sugerían que la intervención farmacológica de p38α podría incrementar la sensibilidad a agentes inductores de inestabilidad cromosómica como los taxanos. Confirmamos esta teoría tanto en tumores inducidos por PyMT como en xenografías derivadas de pacientes; en ambos casos la inhibición de p38α potenció, aceleró o prolongó el efecto anti-tumoral de los taxanos.

En resumen, nuestros resultados demuestran una nueva función de p38α en la coordinación de la repuesta al daño en el ADN y el mantenimiento de la estabilidad cromosómica, y apoyan la combinación de los inhibidores de p38α con taxanos como una opción a tener en cuenta en el tratamiento del cáncer de mama.

INTRODUCTION

1. CANCER

Cancer is the second leading cause of cell death throughout the world and, despite the huge amounts of efforts and money, control of the advanced disease has not been achieved (World Health Organization).

Cancer is not one disease, but a large group of almost 100 diseases. According to the American National Institutes of Health (NIH), cancer refers to any of the diseases characterized by the development of abnormal cells that divide uncontrollably and have the ability to infiltrate and destroy normal body tissues.

Although there are more than 100 different types of cancer and although every single cancer has its own mutational profile, Hanahan and Weinberg suggested in 2000 that all cancer genotypes are manifestations of six essential alterations in cell physiology. Cancer cells would acquire these functional capabilities through different mechanisms and at different times of the transformation process, but eventually, they will allow the cancer cells to survive, proliferate and disseminate. These six so-called "hallmarks" are: self-sufficiency in growth signals, evasion of programmed cell death, limitless replicative potential, sustained angiogenesis, tissue invasion and metastasis (Hanahan and Weinberg, 2000). This seminal paper was reviewed eleven years later, when four additional hallmarks were added: deregulation of cellular metabolism, avoidance of immune system, genomic instability and inflammation (Hanahan and Weinberg, 2011). These characteristics are thus a way of summarizing the complexity of cancer biology in a set of phenotypes that almost all malignant cells must acquire in order to form a tumor (Fig.1).

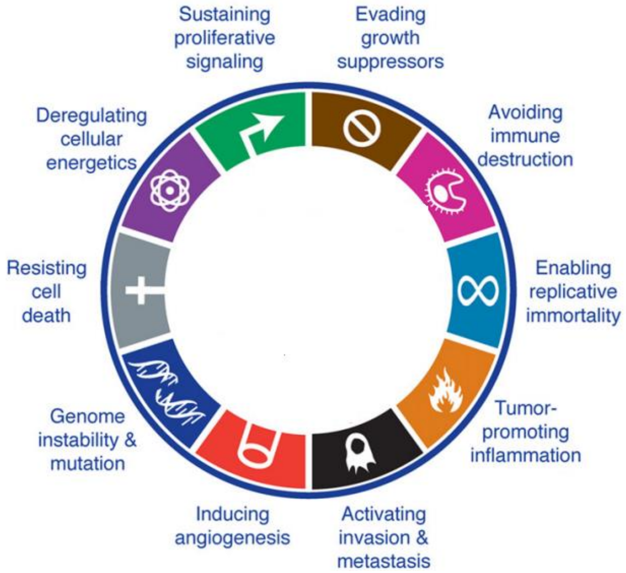
Sustaining proliferative signaling
Evading growth suppressors
Avoiding immune destruction
Enabling replicative immortality
Tumor-promoting inflammation
Activating invasion & metastasis
Inducing angiogenesis
Genome instability & mutation
Resisting cell death
Deregulating cellular energetics

Figure 1. Hallmarks of cancer (Hanahan and Weinberg, 2011). Self-sufficiency in growth signals, evasion of apoptosis, limitless replicative potential, angiogenesis, tissue invasion and metastasis were initially proposed as the six cancer hallmarks. Eleven year later, two additional hallmarks were included, deregulation of cellular energetics and avoidance of immune response, together with two enabling characteristics: genomic instability and tumor-promoted inflammation.

How normal cells evolve in order to obtain all the mentioned characteristics is a topic that has been widely studied. Cancer is nowadays accepted to be an evolutionary process driven by stepwise somatic mutations with sequential and subclonal selection; a parallel to Darwinian natural selection that was established in 1996 (Nowell, 1976). The mutational process is very diverse and the number of mutations in a cancer can vary from 10-20 to hundreds or thousands. The great majority are passengers and modest, but an undefined number of them are functionally relevant drivers of the disease.

Cancer becomes cancer, in part, by reactivating and modifying many existing cellular programs often used during development. These programs control processes such as cell proliferation, migration, polarity, apoptosis, and differentiation (Luo et al., 2009). In summary, following the Darwinian principles, cancer evolves through random mutations and epigenetic changes that alter these pathways followed by the clonal selection of cells that can survive and proliferate under adverse circumstances.

1.1. ONCOGENE and NON-ONCOGENE ADDICTION

Despite the extensive genetic and epigenetic alterations found in a tumor, including point mutations, translocations, rearrangements, deletions or transcriptional silencing that help and contribute to tumorigenicity, a given tumor is likely to be driven by certain few changes (Luo et al., 2009). Mutations in oncogenes are likely to be one of the most important examples of “cancer drivers”. Many cancers require increased activity of oncogenes for tumor initiation and maintenance, and this dependency was coined as “oncogene addiction” by Bernard Weinstein in 2002 (Weinstein, 2002). This concept arose, among others, from the work of Jain *et al*. (Jain et al., 2002), where brief inactivation of Myc resulted in the sustained regression and differentiation of the tumors, suggesting that Myc inactivation may be effective in certain tumors. Similar addictions were shown for H-RAS in melanoma (Chin et al., 1999) or BCR-ABL in leukemia (Huettner et al., 2000); in both cases the inactivation of these genes induced apoptosis and increased the survival of the mice. This “oncogene addiction” theory has been proved to be applicable to some human cancers, and in some cases it has been therapeutically exploited as in the case of Her2/Neu. This tyrosine kinase receptor is known to be functionally involved in the pathogenesis of human breast cancer (Slamon et al., 1987). Her2/Neu antisense oligonucleotides prevented proliferation of breast cancer cells with amplified Her2/Neu, but had no effect on other breast cancer types (Colomer et al., 1994). These “Her2 oncogene hypothesis” led to the development of anti-Her2 antibodies like Trastuzumab, which have resulted in a significantly improved clinical efficacy, transforming the clinical approach to cancer therapy (Moasser, 2007). Other examples of addiction in the clinics are *EGFR*-mutant non-small cell lung cancers, *BRAF*-mutant melanomas or *ALK*-mutated lung tumors; a high percentage of these tumors respond to drugs that selectively inhibit these mutationally activated kinases (Settleman, 2012).

Oncogenes, however, may display increased dependence on other genes, neither mutated nor overexpressed, that are known to be non-oncogenic *per se*, but turn out to be essential for supporting the tumorigenic phenotype. In other words, the survival of malignant cells also relies on a set of proteins that are not inherently tumorigenic. This strong dependency of tumors on normal functions is known as “non oncogene addiction” (Solimini et al., 2007). Importantly, these genes are rate-limiting for tumor cells but are not required to the same extent for the viability of normal cells. The biological reason underlying this “non-oncogene addiction” is that developing tumors are subjected to adverse microenvironmental conditions and to elevated intracellular stress, such as DNA damage and replication stress, metabolic or oxidative stress, or protein missfolding, making them more dependent on stress support pathways for their survival (Fig. 2). Non-oncogene addiction genes can be classified as intrinsic or extrinsic. Intrinsic genes, including those involved in DNA damage and replicative stress protection, mitotic stress, metabolic stress, hypoxia, etc. are those which support the tumor in a cell-autonomous manner. Extrinsic genes function in stromal and vascular cells and are often related to angiogenesis.

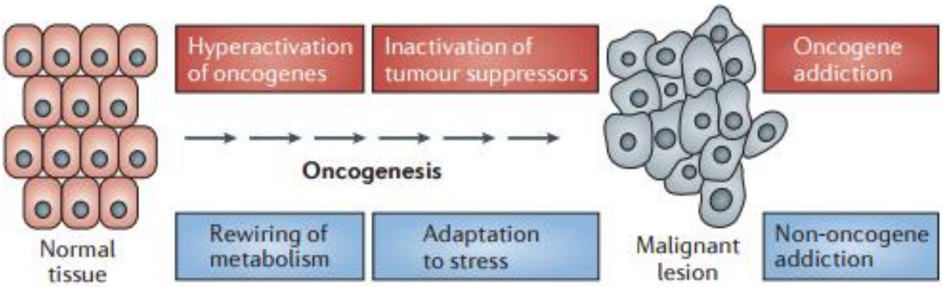

Figure 2. Schematic of oncogene and non-oncogene addiction during the transformation process (Galluzzi et al., 2013). Oncogene addiction is a phenomenon where the tumor development and survival depend on the continuous activation of certain pathways. Non-oncogene addiction genes, however, are usually not required for oncogenesis itself, but help the cancer cell to buffer the increased stress levels.

Many authors agree that non-oncogene addiction may constitute an attractive approach for the development of novel therapeutic strategies. Investigation of the genetic interactions taking place in cancer, both *in vivo* and *in vitro* might help in the identification of new therapeutic strategies, being the base for synthetic lethality (Freije et al., 2011). The synthetic lethality concept arose in yeast and describes the functional interaction between two genes, in which defects in any of them are viable, while in combination they lead to fitness impairment or cell death. This concept can be applied to cancer therapy as malignant cells with alterations in specific genes or pathways or with a particular dependency on a stress signaling pathway would be especially sensitive to certain therapies. This could be achieved by either stress sensitizing, diminishing the activity of the stress support pathways, or by stress overload, which involves the exacerbation of an existing oncogenic stress in order to overload the cell (Solimini et al., 2007). PARP inhibitors are one of the best examples of non-oncogene addiction and synthetic lethality. Although PARP is not mutated in cancer, its inhibition has shown to be effective in tumors with defective DNA damage response pathways (Esposito et al., 2015) or in tumors harboring mutations in certain DNA damage repair genes as in the case of BRCA1/2 (Farmer et al., 2005, Bryant et al., 2005).

1.2. BREAST CANCER

Breast cancer refers to a malignant tumor that has developed from cells in the breast. About 95% of malignant breast tumors are carcinomas that are initiated in the epithelium of the mammary gland. The formation of a carcinoma usually proceeds from a benign, well-differentiated localized tumor called carcinoma *in situ*, to an invasive cancer that penetrates the basal membrane infiltrating the adjacent tissue, and ultimately to a metastatic tumor that disseminates to other parts of the body through the lymphatic system and blood vessels.

Breast cancer can be traced up to Ancient Egypt, where Edwin Smith papyrus described the first recorded case around 1600 BC. In 460 BC Hippocrates described breast cancer as a humoral disease and it was considered as a whole body illness. This humoral hypothesis was not challenged till the 17th century, and it was not until mid-18th when breast cancer started to be considered a local illness and when surgery came up. This breakthrough gave rise to breast cancer etiology study and in 19th century the first non-invasive treatments such as hormone therapy or radiation appeared.

Nowadays, although breast cancer is the most frequently diagnosed cancer, the most common invasive cancer in females and the second leading cause of cancer in woman worldwide (Siegel et al., 2016), its life expectancy has been greatly increased thanks to the improvement both in surgery and adjuvant methods. Further improvements require not only better prevention and diagnosis, but also better understanding of tumor biology for developing more targeted therapies and avoiding recurrence and resistance.

There is a high degree of diversity within breast tumors, as well as among patients, and all of these factors together determine the risk of disease progression and therapeutic resistance (Polyak, 2011). This heterogeneity evidences the importance of understanding the breast cancer biology and developing better clinically useful classifications in terms of prognosis, prediction and therapy design.

There are several ways to classify breast cancers according to several parameters. Classically, breast tumor have been classified according to their pathology, mainly into *in situ* or invasive carcinomas; according to their grade in grade I, II or III depending on their differentiation status and growth pattern; according to the stage from 0 to 4, depending on the size, the spreading and the metastasis of the tumor; or according to the status of the estrogen receptor, progesterone receptor and Her2 receptors. Recently, new approaches have tried to put together the former classifications and the new knowledge obtained from gene expressions profiles of different breast cancers, giving rise to the "molecular subtypes" (Fig.3). Several subtypes have been proposed, but maybe the most spread classification would be the one where breast cancers are divided into four groups: Luminal A, Luminal B, Her2 and Basal subtypes, which not only differ in their molecular features but also in their prognosis and responsiveness to treatments (Prat et al., 2015, Sorlie et al., 2001).

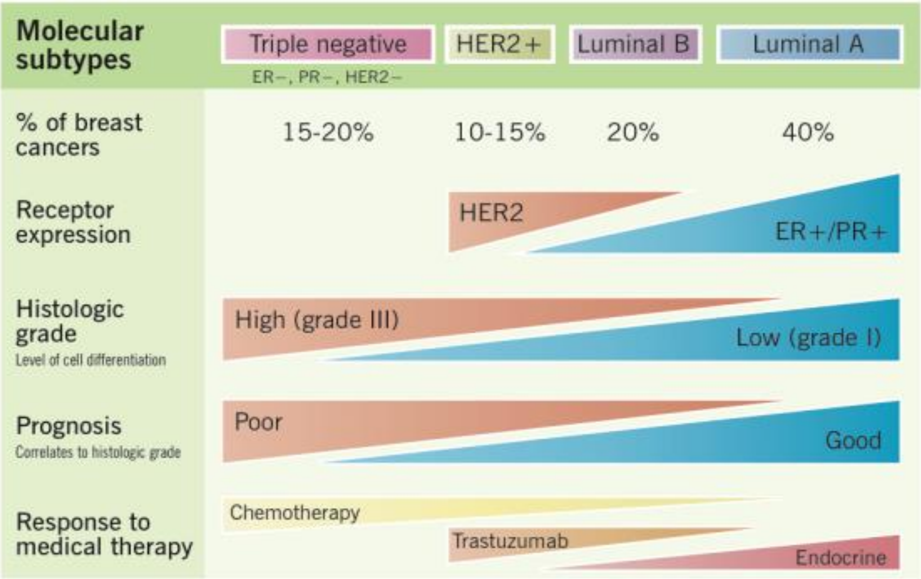
Molecular subtypes
Triple negative
ER−, PR−, HER2−
HER2+
Luminal B
Luminal A
% of breast cancers
15-20%
10-15%
20%
40%
Receptor expression
HER2
ER+/PR+
Histologic grade
Level of cell differentiation
High (grade III)
Low (grade I)
Prognosis
Correlates to histologic grade
Poor
Good
Response to medical therapy
Chemotherapy
Trastuzumab
Endocrine

Figure 3. Main features of the different molecular subtypes. Obtained from McMaster Pathophysiology Reviews. Summary of the histological features, prognosis and therapy response in the main molecular subtypes. ER: Estrogen receptor; PR: Progesterone receptor.

1.2.1. BREAST CANCER MODELS: PyMT TRANSGENIC MOUSE

Polyoma middle T (PyMT) transgenic mice have been widely used to study breast tumorigenesis and metastasis not only due to their short latency and high penetrance, but also because of the PyMT tumors similarities to human breast cancers, both in terms of disease morphology and expression markers.

This transgenic mouse model is driven by the ectopic expression of the middle T antigen of the polyomavirus in the mammary gland under control of the MMTV promoter. It results in the transformation of the mammary epithelial cells, the development of multifocal mammary adenocarcinomas and later metastatic lesions in the lymph nodes and the lungs (Guy et al., 1992).

PyMT anchors to the plasma membrane through its hydrophobic C-terminus. It interacts with and activates the non-receptor tyrosine kinase c-Src, which in turn phosphorylates PyMT on several Tyr residues. These phosphorylated residues serve as docking sites for SH2 or PTB domains, leading to the recruitment of intracellular signaling molecules such as PI3K, SHC and PLC-γ (Dilworth et al., 1994, Whitman et al., 1985, Su et al., 1995, Lee et al., 2011b). Although PyMT has no intrinsic enzymatic activity itself, it mimics the activation process of constitutively activated receptor tyrosine kinases, which are activated by ligand binding and autophosphorylated, leading to the subsequent activation of similar downstream signaling pathways.

Tumor progression in these mice shows four distinct stages: hyperplasia, adenoma, early carcinoma and late carcinoma (Fig. 4), which are comparable to the human breast cancer development from *in situ* proliferative lesions to invasive carcinomas (Lin et al., 2003).

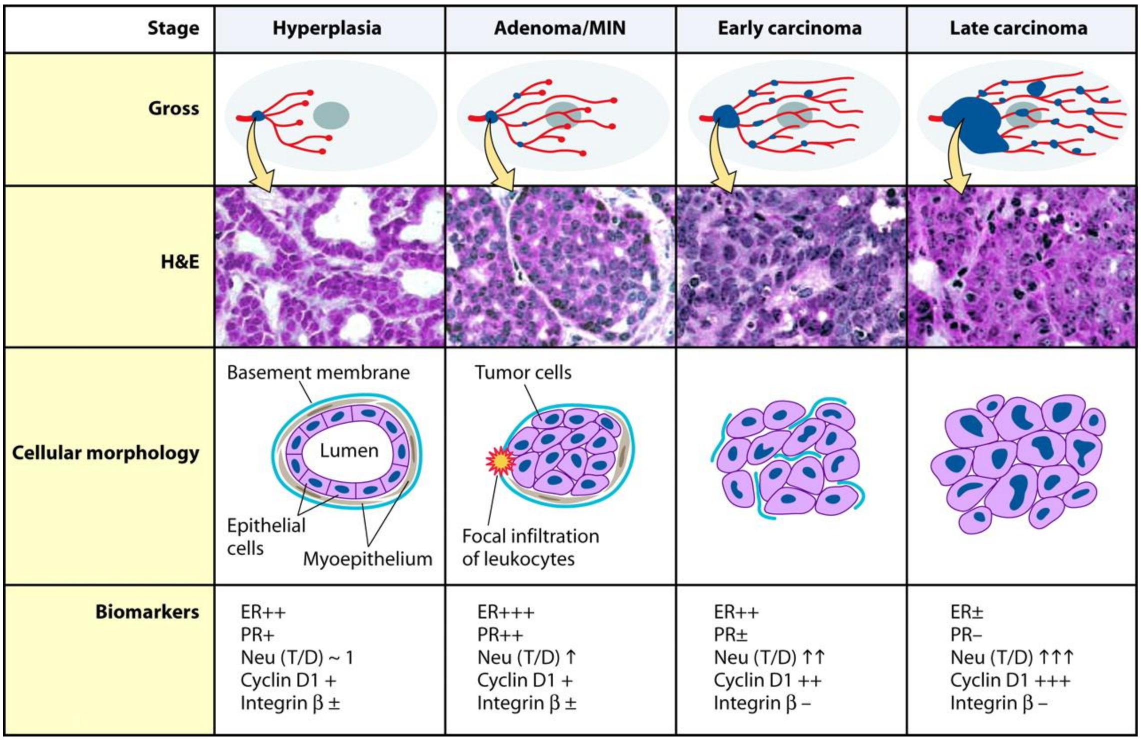

Stage	Hyperplasia	Adenoma/MIN	Early carcinoma	Late carcinoma
Gross				
H&E				
Cellular morphology				
Biomarkers	ER++ PR+ Neu (T/D) ~ 1 Cyclin D1 + Integrin β ±	ER+++ PR++ Neu (T/D) ↑ Cyclin D1 + Integrin β ±	ER++ PR± Neu (T/D) ↑↑ Cyclin D1 ++ Integrin β –	ER± PR– Neu (T/D) ↑↑↑ Cyclin D1 +++ Integrin β –

Figure 4. Summary of PyMT-induced tumorigenesis (Fluck and Schaffhausen, 2009). Gross panel shows the overall development of lesions (indicated by blue dots) in the mammary gland. H&E panel displays the histology of the lesions. Cellular morphology boxes represent changes in the morphology of cancer cells and integrity of basement membrane in every stage. Lower panel summarizes the expression tendency of the main biomarkers during tumor progression.

Moreover, PyMT mice progressively loss the estrogen and progesterone hormone receptors and increase Her2 and cyclin D1 (Fig. 4) (Lin et al., 2003, Maglione et al., 2001), characteristics associated to poor-outcome human breast cancer.

Altogether, PyMT has proven a useful model for studying breast cancer biology, being especially interesting because its resemblance to poor prognosis human tumors.

1.2.2. BREAST CANCER MODELS: HUMAN DERIVED XENOGRAFTS

Genetically engineered mouse models allow the study of tumor initiation and progression in an immunocompetent context. However, in most of them, including PyMT model, tumorigenesis is induced by the expression of a powerful oncogene, and do not fully recapitulate the diversity of human tumor mutations in the primary or metastatic sites (Whittle et al., 2015). This problem has been recently overcome by the generation and generalization of the human patient derived xenografts (PDXs). PDXs consist of engraftments of actual human tumor tissues into immunodeficient mice, which can be propagated by serial transplantation without any *in vitro* step, avoiding the selective pressure imposed by cell culture conditions. This “tumorgrafts” resemble the original characteristics of the tumors from the patients in terms of clinical and histological markers, hormone responsiveness, genomic features and metastasis preferences (DeRose et al., 2011), and more importantly, they conserve the intra-tumor heterogeneity, which is involved in therapy response and resistance development (Cassidy et al., 2015)

2. CHROMOSOME INSTABILITY

Genomic instability is defined as a process prone to genomic changes or increased tendency of genomic alterations in cells. These alterations include mutations on genes, amplifications, deletions or rearrangements of chromosomes segments or whole chromosome gain or loss among others. Genomic instability is associated with the failure of cells to properly duplicate the genome and accurately segregate the genetic material among daughter cells (Shen, 2011). There are several forms of genomic instability in cancers, but most of them exhibit a form called chromosomal instability (CIN), defined by a high rate of chromosome structural and numerical abnormalities (Negrini et al., 2010).

The main recognized outcome or consequence of CIN is aneuploidy, defined as the abnormal number of chromosomes in a cell, a state where certain chromosomes no longer come in pairs. Aneuploidy, especially in cancer, is a byproduct of CIN and karyotypic complexity frequently correlates with CIN (Nicholson and Cimini, 2013). However, although aneuploidy and CIN often coexist, these concepts are not equivalent. CIN can originate aneuploidy due to a single misssegregation event, resulting in a chromosomal imbalance that can be stably propagated (Zasadil et al., 2013). Although less obvious, aneuploidy can, though not necessarily does, induce CIN by unbalancing the expression of genes required for mitosis (Duesberg et al., 1998). An interesting proof of principle was carried out in yeast (Sheltzer et al., 2011), where 69% of *S. cerevisiae* strains carrying an extra chromosome showed higher missegregation than the haploid strains. More recently, this fact was further corroborated using mammalian cells (Passerini et al., 2016); the addition of one or two extra chromosomes in colorectal HCT116 or retinal RPE cell lines promoted misssegregation and chromosome instability by deregulating in this case replication-required genes, elevating DNA damage and replication stress.

2.1. CIN and ANEUPLOIDY in NON TRANSFORMED CELLS

Last century, Theodor Boveri observed that aneuploid sea urchin embryos died while polyploid ones survived. Nowadays polyploidy is known to be physiologically found in nature, especially in plants and non-vertebrates. In human cells, however, it is restricted to liver and placental tissues. In contrast, aneuploidy interferes with growth and development and is associated with disease, sterility and tumor formation. Indeed, just three trisomies are not embryonically lethal in humans (chromosomes 13, 18 and 21) and just trisomy 21 is viable more than a year. Meanwhile, no trisomy has found to be viable in mice (Torres et al., 2008).

Most of the work done in aneuploidy and CIN in cell physiology has been performed in yeast. Aneuploid *Saccharomyces cerevisiae* showed defects in growth, altered metabolism and proteotoxic stress, independently of the exact additional chromosomes (Torres et al., 2007). Interestingly, duplication of the entire genome is not as deleterious as the duplication of a subset of chromosomes, indicating that genomic imbalances underlie the detrimental effect of aneuploidy. Similar results were obtained in MEFs, were aneuploidy also impairs the kinetic of spontaneous immortalization in culture (Williams et al., 2008). Most of the mammalian cells showing CIN also proliferate poorly as shown for example in BUB1 or MAD2 deregulated MEFs (Baker et al., 2004, Sotillo et al., 2007), evidencing the detrimental consequences of CIN and aneuploidy in the cellular and organismal fitness of every organism studied.

2.2. CIN AND ANEUPLOIDY in CANCER

Defects on chromosome structure and number, together with abnormal mitoses were first observed in cancer samples more than 100 years ago by David Hanseman. Based on these studies and his own observations, Theodor Boveri proposed in 1914 (Boveri, 1914) that abnormal chromosome constitution might enhance cancer. It was not until 1997 when a direct link between chromosome missegregation and cancer was found in cancer cell lines (Lengauer et al., 1997). Nowadays, CIN is an established cancer hallmark (Hanahan and Weinberg, 2011) and it is a general feature of most cancer types: 86% of epithelial tumors are aneuploidy according to the "*Database of Chromosome Aberrations and Gene Fusions*" and 50% of them exhibit CIN (Zasadil et al., 2013). Accordingly, CIN has been correlated with poor prognosis (Carter et al., 2006, Habermann et al., 2009, Chibon et al., 2010) and with drug resistance (Duesberg et al., 2000, Swanton et al., 2009, Swanton et al., 2007, Lee et al., 2011a).

The mechanism by which CIN determines cancer outcome can be considered from the Darwinian point of view (Cahill et al., 1999) (Fig.5). Natural selection depends on cell to cell variations and CIN, together with epigenetic plasticity, originates a plethora of phenotypic heterogeneity of cancer cell populations. Progression to a malignant state would involve genetic diversification and non-linear clonal evolution (Tsao et al., 1999), as evidenced by the fact that metastases often contain aberrations not found in the primary tumor or detected at a low frequency in the primary site (Roschke and Rozenblum, 2013). CIN-derived subclones would provide almost endless options in a selection process providing opportunities for the cells to adapt to environmental and stromal pressures, explaining why CIN is found at early stages in tumor development.

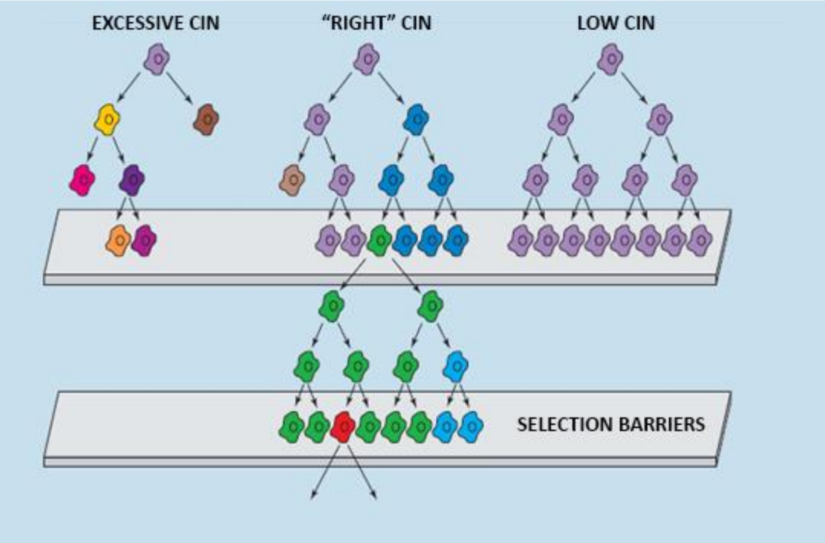

Figure 5. Model for clonal selection during tumorigenesis. Adapted from (Cahill et al., 1999)**.** Normal cells carry low rates of instability, the diversity of the population is low and therefore tumor progression is blocked. If CIN is too high, the accumulated damage is excessive and cells dye, blocking thus the transformation process. In tumor cells, however, the increased genetic instability gives a broad genotype heterogeneity which ensures that at least one cell contains the required alteration to overcome the first barrier. This cell can expand and keep on changing, originating different clones. Consequently, these mutations that allowed every transformation step will be present in the final tumor.

In this line, MAD2-induced CIN has been shown to facilitate recurrence after oncogene withdrawal in both KRAS and Her2 models (Sotillo et al., 2010, Rowald et al., 2016) and it would explain why some tumors relapse after apparently effective therapies. Indeed, from a Darwininan perspective, anticancer therapies can be considered selective pressures and increased heterogeneity may increase the probability of a resistant population to emerge (McGranahan et al., 2012), giving rise to resistances.

How CIN originates such heterogeneity? CIN modifies the chromosomal configuration, resulting in a wide range of karyotypes showing a plethora of genetic alterations such as the formation of fusion gene products, unbalance of the gene dosage favoring gene amplification of tumor promoter genes like MYC or loss of heterozygosity of tumor suppressors as p53, besides general changes in gene expression. This massive alterations in the gene and the protein expression profiles affect the physiological equilibrium of essential cell functions such as metabolism, cell cycle checkpoints, cell division or cell-to cell communication (Masuda and Takahashi, 2002). This would lead to a relaxation of the strict control of cell growth and give cells enough flexibility to adapt and respond to their microenvironment and undergo malignant transformation.

Despite their high prevalence in human cancers, aneuploidy and CIN do not always elevate tumor incidence in mice. Although CIN and aneuploidy increases or accelerates the spontaneous or carcinogen-induced appearance of tumors (Sotillo et al., 2007, Ricke et al., 2011, Schvartzman et al., 2011), in other models they do not affect the tumor fate (Malureanu et al., 2010, Cowley et al., 2005) or even show a tumor suppressor function (Godek et al., 2016, Maia et al., 2015, Silk et al., 2013). Interestingly, in some cases CIN enhances or inhibits tumor growth depending on the context (Weaver et al., 2007). Moreover, high CIN signatures have been associated with improved prognosis relative to intermediate ones in ER(-) breast cancer (Birkbak et al., 2011, Roylance et al., 2011, Jamal-Hanjani et al., 2015) and the same tendency has been observed in ovarian, gastric and lung cancers (Roylance et al., 2011). Therefore, the relationship between CIN and tumor outcome is not as straightforward as initially predicted and it seems to depend on the CIN levels, the development stage of the tumor and the cellular context. Altogether, there may be a certain degree of CIN or specific karyotypes that would promote tumorigenesis and aggressiveness, while excessive levels would be detrimental for cell survival, leading to lower tumor incidence or tumor regression. This fact suggests enhancing CIN as a plausible therapy strategy (Martin et al., 2010). On the one hand, inactivating the genome instability survival pathways may potentiate the efficacy of anticancer drugs and enhance the therapeutic window, independently of the individual mutations (Swanton et al., 2011). On the other hand, the higher instability of cancer cells makes them more susceptible to stress-inducing agents. Therefore, the identification of CIN-related genes has been shown to be a promising approach to fight cancer (Tang et al., 2011).

During the cell cycle, chromosome stability relies in the proper functioning of four essential mechanisms: high fidelity DNA replication in S-phase, precise chromosome segregation in mitosis, error free repair of sporadic DNA damage and a coordinated cell cycle progression. Errors in any of these functions, which will be addressed in the following sections, have been described to originate CIN (Giam and Rancati, 2015).

3. CELL CYCLE PROGRESSION AND CELL CYCLE CHECKPOINTS

The cell cycle is a collection of highly ordered events whose goal is to ensure that DNA is faithfully replicated once and that identical chromosomal copies are distributed equally to two daughter cells (Sherr, 2000). It is composed of four phases: G1, the gap before DNA replication, S, the DNA synthetic phase, G2, the gap after DNA replication, and M, the mitotic phase that culminates in cell division. Cells in G1 can also enter in a resting state known as G0. In mammals most of the adult cells but the gut epithelium and the hematopoietic system are in this quiescent phase. During G1, S and G2 phases the nucleus seems morphologically uniform and that is why these phases are collectively known as interphase. At the molecular level, however, during interphase the cell both grows and replicates its DNA in an orderly manner, accounting thus for the 90-95% of the total cell cycle time. Mitosis is the time where a cell divides into two genetically identical daughter cells and is probably the most complex and delicate phase of the cell cycle, since errors during segregation can generate aneuploidy and CIN hampering cell viability. According to morphological features, mitosis can be divided into five different phases: prophase, prometaphase, metaphase, anaphase and telophase, after which the cell divides in a process called cytokinesis. Prophase is characterized by the condensation of the chromatin into chromosomes and the migration of the centrosomes to the opposite sides of the cell. Prometaphase is marked by the nuclear envelope breakdown and the invasion of the nuclear space by the microtubules. In metaphase, chromosomes form the “metaphase plate” where the two sister chromatids are tightly associated at the centromeric region and still bind the microtubules. In anaphase, chromosome cohesion is lost and sister chromatids are split apart towards opposite spindle poles. In telophase, chromosomes reach the poles of the spindle, chromatin starts to decondense and the nuclear envelop reforms around the two masses of chromatin. Finally, cell division occurs in cytokinesis. During this stage that starts in anaphase and progress through telophase, a contractile ring assembles at the cell cortex and shrinks forming the so-called cleavage furrow, which eventually separate the whole cytoplasm into two daughter cells.

A correct cell cycle involves the ordered and unidirectional transition from one phase to another. The timing and ordering of cell cycle progression is dependent on positive and negative regulatory circuits that allow passage only after completion of critical events. At the molecular level, this cell cycle progression is regulated by a family of cyclin dependent kinases (CDKs) together with their activators (cyclins) and inhibitors (Ink4, Cip and Kip families). Deregulation of any of these proteins have been detected in cancer (Malumbres and Barbacid, 2009).

During unperturbed proliferation, mammalian cells can only withdraw from the cell cycle on experiencing growth-factor deprivation or growth inhibitory signals in early-to-mid G1 phase (Massague, 2004). In cancer, however, cells are continuously cycling and they are particularly susceptible to DNA damage (Kaufmann and Paules, 1996). Upon different genotoxic stresses, cells can transiently delay or even temporarily arrest cell cycle in several points of the cell cycle known as checkpoints. This control machinery ensures the proper division of the cell and limits genomic instability by preventing DNA damage, being thus especially important in DNA damage-prone cells as cancer cells.

3.1. G1/S CHECKPOINT

During G1 phase the cell tests the availability of mitogens and nutrients and the cellular environment. If favorable, the decision is made in the restriction point in middle to late G1. In case of DNA damage the ATM/ATR and Chk1/Chk2 kinases are activated, which in turn target two independent but complementary effectors of the G1 checkpoint, the Cdc25A phosphatase and the p53 transcription factor. On the one hand, the phosphorylation of Cdc25A leads to its ubiquitination and degradation, preventing thus the Cdc25A-mediated activatory dephosphorization of CDK2 and the consequent loading onto chromatin of Cdc45, a protein required for replication initiation. On the other hand, p53 activation leads to the accumulation of its downstream target p21 (WAF1/Cip1) and the inhibition of the G1/S promoter CDK2. Importantly, the Cdc25A cascade is a faster response than the p53 pathway since it does not require transcription and newly synthesized proteins. However, p21 accumulation requires up to several hours. Therefore, this mechanism complements and eventually replaces the transient acute inhibition of CDK2 trough the Cdc25A degradation pathway, leading to a sustained and even sometimes permanent cell cycle blockage (Lukas et al., 2004).

3.2. INTRA S CHECKPOINT

The intra-S-phase checkpoint involves a transient and reversible inhibition of the DNA replication activated by genotoxic stresses. It is described to work through two parallel branches, a Cdc25A dependent pathway described above, that prevents the initiation of new origin firing, and a NBS1 and BRCA1 dependent route. Furthermore, this signaling is involved in protecting the integrity of stalled replication forks, preventing the conversion of primary lesions into DNA breaks (Kastan and Bartek, 2004).

3.3. G2 CHECKPOINT

The G2 or G2/M checkpoint prevents damaged cells from entering mitosis. Similarly to G1, G2 checkpoint can delay or arrest cell cycle via post-translational modifications of Cdc25C or alteration of the p53 transcriptional programs. The main target in this phase is the cyclin B/CDK1 complex, whose activation is inhibited by the subcellular sequestration, degradation or inhibition of the Cdc25 phosphatases (especially Cdc25c) trough ATM/ATR, CHK1/CHK2 or p38 MAPK. Moreover, other proteins such as PLKs, 53BP1 or BRCA1 also contribute to the G2 checkpoint responses. The maintenance of this G2 checkpoint relies on the transcriptional programs of BRCA1 and p53, leading to the upregulation of proteins such as p21, Gadd45 and 14-3-3 (Kastan and Bartek, 2004).

3.4. SPINDLE ASSEMBLY CHECKPOINT

The spindle assembly checkpoint (SAC), also known as the mitotic checkpoint, is a crucial mechanism for ensuring fidelity in chromosome segregation during mitosis and defects in this machinery have been shown to induce CIN (Cahill et al., 1998) and increase cancer incidence (Kops et al., 2005). SAC delays the anaphase onset until all chromosomes are properly bi-oriented on the mitotic spindle, avoiding the premature separation of the sister chromatids and the subsequent missegregation and chromosome copy number alterations (Fig.6).

The SAC is activated in every cell cycle immediately upon entry into mitosis. The inhibitory signal coming from unattached kinetochores results in the recruitment of Mad2, BubR1, Bub3 and MPS1. Additional proteins such as the complex formed by Aurora B, Survivin, and INCENP are known to collaborate by sensing tension between sister chromatids. Upon chromosome alignment, Mad2 is released from the complex, resulting in the activation of APC/C-CDC20, which in turn targets securin and cyclin B1 for degradation. Consequently, separase is activated, leading to the separation of the sister chromatids, and CDK1 is inactivated, an essential requirement for mitotic exit (Perez de Castro et al., 2007).

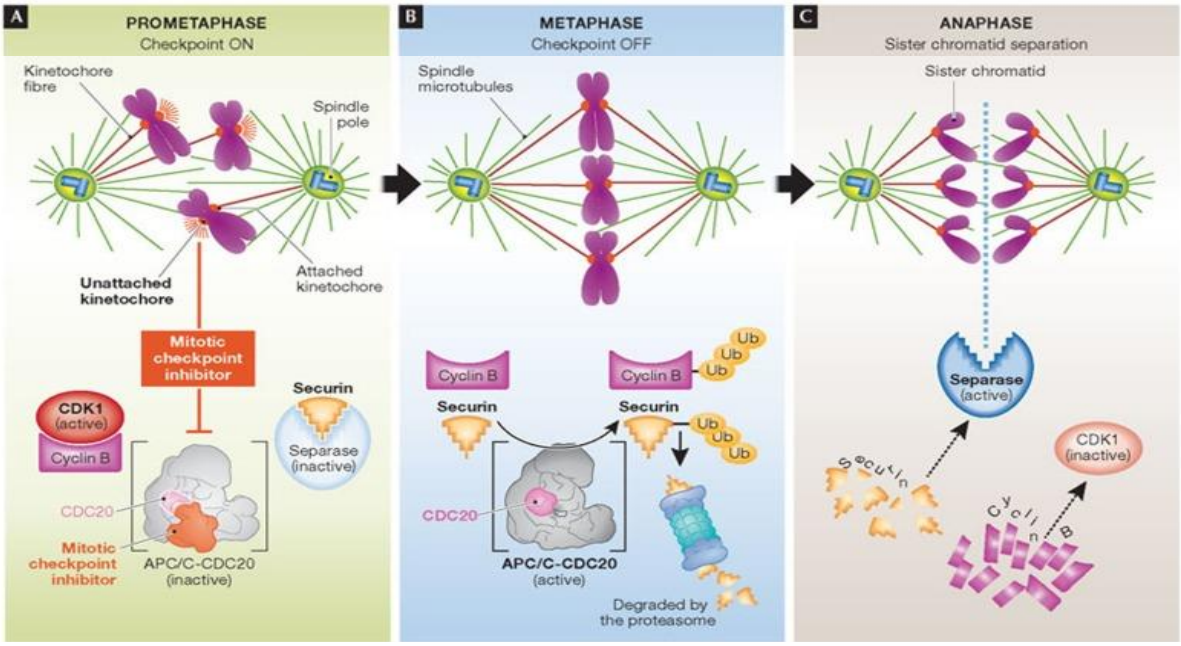
A
PROMETAPHASE
Checkpoint ON
Kinetochore fibre
Spindle pole
Unattached kinetochore
Attached kinetochore
Mitotic checkpoint inhibitor
CDK1 (active)
Cyclin B
Securin
Separase (inactive)
CDC20
Mitotic checkpoint inhibitor
APC/C-CDC20 (inactive)
B
METAPHASE
Checkpoint OFF
Spindle microtubules
Cyclin B
Cyclin B
Ub
Securin
Securin
CDC20
APC/C-CDC20 (active)
Degraded by the proteasome
C
ANAPHASE
Sister chromatid separation
Sister chromatid
Separase (active)
CDK1 (inactive)
Securin
Cyclin B

Figure 6. Schematic of the SAC. Adapted from (Holland and Cleveland, 2012)**.** A) Unattached kinetochores release a diffusible signal that inhibits ubiquitination of securin and cyclin B1 by the APC/CDC20 complex. B) When all kinetochores are properly attached, APC/CDC20 ubiquitinates securin and cyclin B1, which are degraded by the proteasome, silencing SAC. C) Securin destruction activates separase and cyclin B1 degradation inactivates CDK1, inducing sister chromatid separation and exit from mitosis.

4. DNA REPLICATION

DNA replication is essential for cell proliferation and most mutations that affect this process are deleterious. However, some mutations or differential expression in core DNA replication proteins have been identified in human cancers (Pillaire et al., 2010, Suzuki and Takahashi, 2013). Proper control and execution of DNA replication is critical for faithful transmission of the genome and defects in this process can cause genomic instability, compromise cell proliferation and promote cancer susceptibility.

This process is organized into three distinct phases: initiation, elongation and termination. DNA replication is initiated at defined loci known as replication origins and comprises two step processes: origin licensing and firing. Origin licensing starts in late mitosis or early G1 and is characterized by the assembly of the pre-replication complex (pre-RC) at the origins. This pre-RC comprises the origin recognition complex (Orc 1-6), Cdc6, Cdt1 and the core replicative helicase component Mcm2-7. Origin firing occurs in S phase and involves the activation of the Mcm2-7, which is now capable of unwinding the DNA and allow DNA synthesis (Mazouzi et al., 2014). Interestingly, eukaryotic chromosomes have a wide distribution of licensed origins, but not all of them are activated and used during normal replication, providing a backup in case of replication slow-down or failure (Blow et al., 2011). Once the DNA duplex is unwound, the single strand DNA generated is stabilized by RPA and DNA polymerases are recruited to proceed with the replication elongation. Much less is known about the termination step and several mechanisms as the existence of termination regions (Fachinetti et al., 2010), the convergence of two forks (Santamaria et al., 2000) or encountering of telomeric sequences have been described to participate in this final process.

Given its high complexity, DNA replication is considered one of the biggest challenges for genomic integrity since every step intrinsically makes DNA vulnerable to damage. Any damage generated by errors during DNA replication is referred as replication stress (Mazouzi et al., 2014).

4.1. REPLICATION STRESS

Replication stress is defined as slowing or stalling in replication fork progression, which can lead to replication fork collapse and DNA breaks. Defects during DNA replication are thought to be especially deleterious; since the double-strand nature of the DNA is temporarily lost, a mild single strand break (SSB) can be, upon convergence with progressing replication forks, converted into a double strand break (DSB), a much more serious lesion (Ruzankina et al., 2008). It has been shown that even mild replication stress levels increase the frequency of chromosomal lesions that are transmitted to daughter cells (Lukas et al., 2011) and replication stress was recently proposed as the link between structural and numerical chromosome aberrations (Burrell et al., 2013) and the major driving force of CIN in cancer (Gorgoulis et al., 2005, Halazonetis et al., 2008).

The detrimental potential of replication stress relies on its deleterious consequences in the subsequent phases of the cell cycle, especially in mitosis, ultimately impairing chromosome segregation and genome stability. One reason is that the DNA damage response may not be activated following a moderate replication stress (Koundrioukoff et al., 2013, Wilhelm et al., 2014), allowing damaged cells to enter mitosis and leading to chromosome breaks at under-replicated regions. Consequently, unreplicated or not-fully replicated regions originate anaphase bridges and ultra-fine bridges. These chromatids might break, potentially leading to breakage-fusion-bridge events that are found in cancer cells (Gisselsson et al., 2000). These structures create a physical link between the two sister chromatids which is subjected to a mechanical tension during cytokinesis. If broken, these bridges lead to an uneven segregation of the broken chromosome arms and therefore to potential translocations. If not resolved, the two sister chromatids can be pulled toward the same mitotic spindle pole leading to aneuploidy (Gelot et al., 2015), again evidencing the potential of replication stress to create both structural and numerical CIN. The result of these replicative and mitotic stresses is inherited and the main sign in the daughter cells is the presence of micronuclei and 53BP1 bodies. The protein 53BP1 is thought to surround non-repaired mitotic DSBs to allow their repair in G1 (Lukas et al., 2011). Micronuclei are the consequence of lagging chromosomes, acentric chromosomes or broken fragments that have been embedded into their own nuclear envelope (Fenech et al., 2011); micronuclei replication is defective and provokes DNA damage in G2, giving rise to chromosome aberrations (Crasta et al., 2012) and further rearrangements.

One of the most accepted source of replication stress are unrepaired DNA lesions (Fig. 7), which impact on DNA replication both due to the generation of physical barriers to replication fork progression and the activation of cell cycle checkpoints. Such lesions can be originated by exogenous agents (e.g. ionizing radiation, ultraviolet light or chemical compounds used in cancer therapy as alkylating agents such as cisplatin or topoisomerase inhibitors like camptothecin) or endogenous sources such as defects in the DNA replication itself or the oxidized bases generated from the reactive oxygen species (ROS), derived from the normal cellular metabolism (Ciccia and Elledge, 2010).

Collisions between replication and transcription complexes have also been identified as a source of replication stress (Fig. 7), illustrated by the identification of certain DSB-prone regions in highly transcribed regions (Barlow et al., 2013). Additionally, other loci known as “fragile sites” have been identified as DSB-prone, although the reason why is still under debate.

Another major cause of replication stress relies on the inappropriate regulation of origin firing (Fig. 7). Insufficient firing can lead to loss of genetic information while excessive firing can deplete nucleotide pool, an essential component of the replication machinery that has been recently proposed as an essential player regulating replication stress and genomic instability (Poli et al., 2012, Bester et al., 2011). Interestingly, overexpression or activation of oncogenes such as Myc, HRas or cyclin E promotes increased origin firing, leading to depletion of nucleotide pools and collisions with transcription complexes (Zeman and Cimprich, 2014).

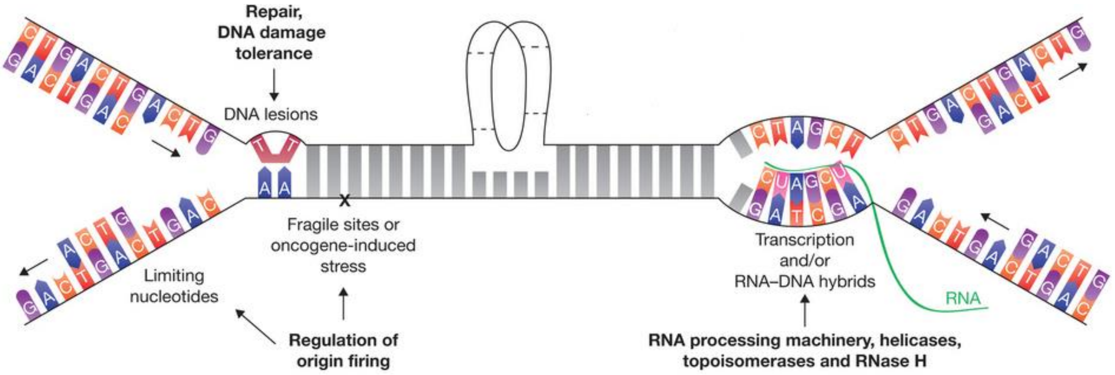
Repair, DNA damage tolerance
DNA lesions
Fragile sites or oncogene-induced stress
Limiting nucleotides
Regulation of origin firing
Transcription and/or RNA–DNA hybrids
RNA
RNA processing machinery, helicases, topoisomerases and RNase H

Figure 7. Causes of replication stress. Adapted from (Zeman and Cimprich, 2014). Several conditions or obstacles can lead to DNA replication slow-down or stalled replication forks. DNA lesions, nucleotides scarceness, fragile sites, or collisions with transcription machinery are among the most recognized ones. Some of the key resolution pathways for each source of stress are indicated in bold.

5. DNA DAMAGE RESPONSE

Correct duplication of the genome requires the coordination between DNA replication and DNA damage response machineries. As cancer cells often show higher levels of replication stress and consequently higher levels of DNA damage, they usually rely more on the DNA damage signaling compared to normal cells in order to maintain genomic integrity and survive. Therefore, DNA damage sensing and repair mechanisms become especially important in a tumorigenic context. DNA damage in the cell is combated by the DNA damage response (DDR), which consists of a collection of mechanisms in charge of detecting DNA lesions, signaling their presence and promoting their repair (Jackson and Bartek, 2009). In response to damage, DDR coordinates two general but essential processes: activation of cell cycle checkpoints, which have been addressed above, and DNA repair. Therefore, DDR normally suppresses CIN and its status influence cancer progression and treatment responses.

DDR comprises a network of interacting pathways that cooperate to elaborate a response and is organized in sensors, transducers and effector proteins (Fig. 8). Sensor proteins recognize the diverse DNA lesions. DSBs are mainly detected by the MRN complex, which consists of Mre11, Rad50 and Nbs1 proteins, or by Ku, formed by Ku70 and Ku80 (Ciccia and Elledge, 2010). Both MRN and Ku are localized to DSBs within seconds after DNA damage occurs (Hartlerode et al., 2015) and contribute to the recruitment and activation of ATM and DNA-PKcs respectively. Meanwhile, RPA binds single-stranded DNA (ssDNA), generated by the unwinding of the DNA after fork stalling during replication stress or by DNA resection during DSB homologous recombination repair. RPA coating of ssDNA prevents formation of secondary structures and localizes ATR to the damaged forks (Zou and Elledge, 2003). Interestingly, RPA not only recruits ATR, but it is also an ATR target and its phosphorylation seems to play a role in DNA repair and checkpoint activation (Marechal and Zou, 2015).

ATR and ATM are the main transducers in this network (Fig. 8). ATR (Ataxia telangiectasia mutated- and Rad3-related) is the main kinase sensing replication stress and is activated in S phase by its physical recruitment to the ssDNA binding protein RPA. Of note, not all sources of replication related damage produce long ssDNA, and replication stress is not necessarily linked to ATR activation (Koundrioukoff et al., 2013, Wilhelm et al., 2014); accordingly, mild insults may induce few forks to stall and a global cellular response may not be required. However, when activated and once assembled at a DNA lesion or stalled fork, ATR coordinates replication, cell cycle progression and DNA repair through the phosphorylation of numerous substrates. The best characterized mediator of ATR is Chk1, which in turn can phosphorylate effector proteins that stabilize stalled forks, repair collapsed forks and prevent late origin firing (Allen et al., 2011).

However, the most studied function of Chk1 is its role in cell cycle progression. Once activated, Chk1 is taken away from chromatin and signals DNA damage along the nucleus, leading to growth arrest by the modulation of CDK regulators (Smits et al., 2006), especially the Cdc25 family. Moreover, Chk1 also activates p53, which contributes to the maintenance of the cell cycle arrest. While Chk1 is spread, other ATR substrates act on the chromatin, more specifically in the replication forks such as RPA1, RPA2, MCMs, or DNA polymerases that are suggested to contribute to fork stabilization (Cimprich and Cortez, 2008). Finally, ATR substrates are also involved in DNA repair. ATR function in repair is likely restricted to breaks arising at the replication fork (Lopez-Contreras and Fernandez-Capetillo, 2010) and involved in the repair of DNA breaks by homologous recombination (Wang et al., 2004, Brown et al., 2014, Bakr et al., 2015).

Ataxia Telangectasia Mutated (ATM) kinase is activated upon DSBs. ATM is recruited to DSBs by interacting with Nbs1 in the called MRN complex (Lee and Paull, 2004) and once activated, it phosphorylates a plethora of downstream effectors that modulate processes such as DNA repair, cell cycle checkpoints, cell death or senescence, being thus essential to the cell fate following DNA damage (Shiloh and Ziv, 2013). ATM is considered less important in response to replication stress; however ATM signaling has been proposed to inhibit origin firing by promoting stabilization and repair of damaged replication forks (Bakr et al., 2015).

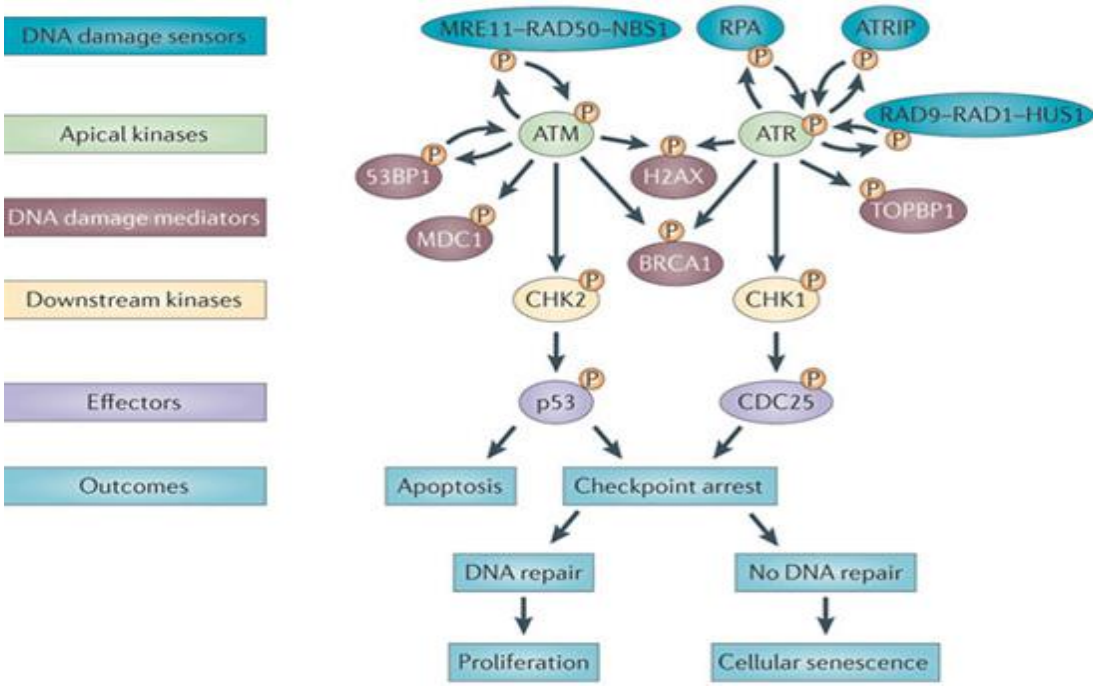
DNA damage sensors
Apical kinases
DNA damage mediators
Downstream kinases
Effectors
Outcomes
MRE11–RAD50–NBS1
RPA
ATRIP
RAD9–RAD1–HUS1
P
ATM
ATR
53BP1
H2AX
TOPBP1
MDC1
BRCA1
CHK2
CHK1
p53
CDC25
Apoptosis
Checkpoint arrest
DNA repair
No DNA repair
Proliferation
Cellular senescence

Figure 8. DNA Damage Response network (Sulli et al., 2012). Depending on the damaging source, sensor proteins can activate ATM, which responds mainly to DSBs, and ATR, which is activated by ssDNA. Recruitment of these kinases to the damaged foci occurs through the interaction with NBS1 and ATRIP. Once activated, they phosphorylate downstream kinases such as Chk1/2, which in turn regulate the activity of downstream effectors that coordinate cell cycle progression and DNA repair.

5.1. DNA REPAIR

DSBs are considered the most toxic of all DNA lesions, as it is believed that a unique unresolved DSB can induce apoptosis (Sonoda et al., 2006). If unrepaired, they lead to broken chromosomes; if repaired improperly, they can lead to chromosome translocation, often resulting in CIN. Endogenous DSBs can directly arise from ROS generated during cellular metabolism or can be a consequence of milder lesions or replication stalled forks that could not be properly overcome. Moreover, many exogenous chemicals induce DNA lesions that interfere with replication fork progression, eventually resulting in DSBs such as the alkylating agent cisplatin, DNA synthesis inhibitors (hydroxyurea or aphidicolin) or topoisomerase inhibitors (such as camptothecin or etoposide). On the contrary, ionizing radiation or bleomycin cause replication-independent DSBs (Helleday et al., 2008) (Fig. 9).

DNA repair is cell-cycle regulated and direct DSBs are mainly repaired by non-homologous end joining (NHEJ) while replication-associated DSBs are preferentially repaired by homologous recombination (HR) and related replication pathways.

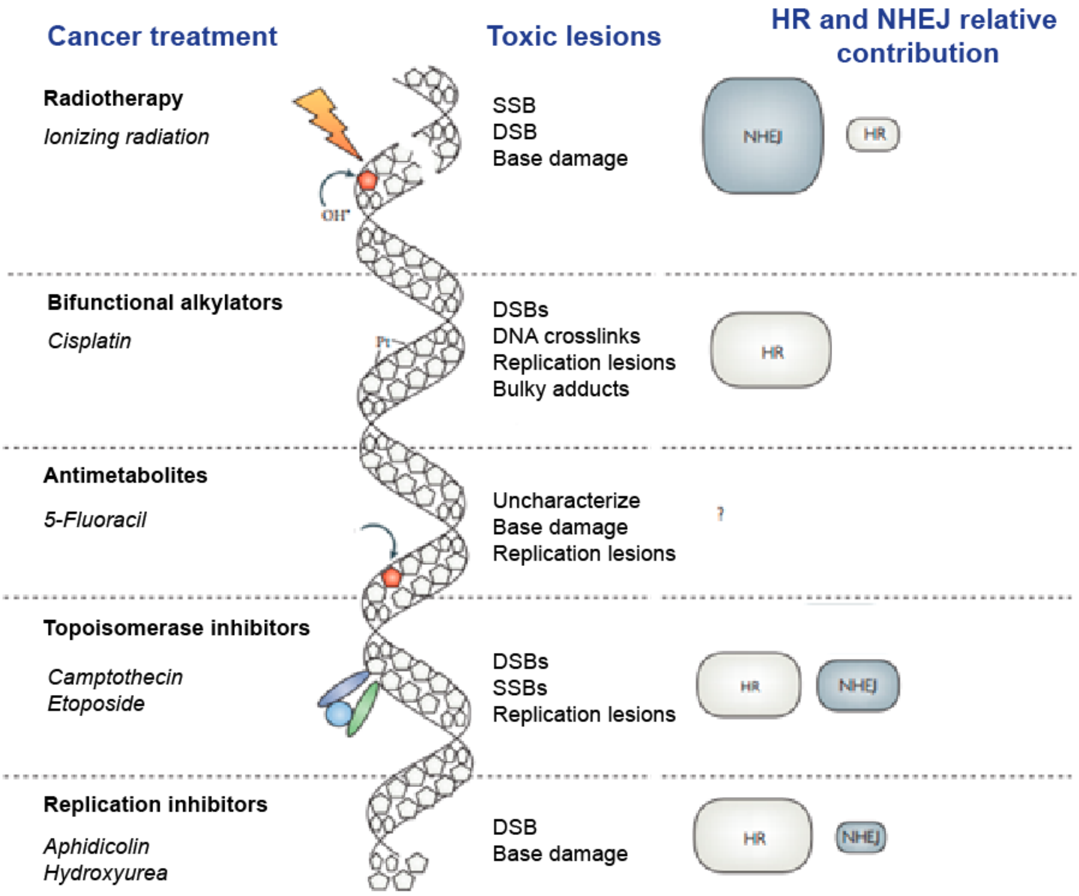
Cancer treatment
Toxic lesions
HR and NHEJ relative contribution
Radiotherapy
Ionizing radiation
OH•
SSB
DSB
Base damage
NHEJ
HR
Bifunctional alkylators
Cisplatin
Pt
DSBs
DNA crosslinks
Replication lesions
Bulky adducts
HR
Antimetabolites
5-Fluoracil
Uncharacterize
Base damage
Replication lesions
?
Topoisomerase inhibitors
Camptothecin
Etoposide
DSBs
SSBs
Replication lesions
HR
NHEJ
Replication inhibitors
Aphidicolin
Hydroxyurea
DSB
Base damage
HR
NHEJ

Figure 9. DNA lesions derived from different cancer treatments and relative importance of HR and NHEJ in their repair. Adapted from (Helleday et al., 2008). Different exogenous insults form different DNA lesions in different phases of the cell cycle. Many routes are involved in their repair but in this graph just the relative implication of the HR and NHEJ is represented.

5.1.1. NON HOMOLOGOUS END JOINING

NHEJ pathway is more efficient than HR and can take place in every phase in the cell cycle, although it is mainly employed in G1 and early S phases, when sister chromatids are not available (Shrivastav et al., 2008). In NHEJ the ends of the break are ligated independently of their sequence, being thus error-prone. It is a relatively simple repair pathway where both ends of the break are initially bound by the Ku70/80 heterodimer, which in turn recruits the catalytic subunit of the complex, DNA-PKcs. Then, ends can be processed by nucleases or polymerases in order to create compatible ends. Finally, a ligation complex formed by DNA ligase IV, XRCC4 and XLF ligates the ends (Ciccia and Elledge, 2010). It often results in small insertions, deletions, substitutions or even translocations, especially when multiple DSBs are present, since there is no way to determine which breaks were contiguous (Huertas, 2010). Although apparently harmful, with this rapid repair mechanism, otherwise lethal DSBs are exchanged for “just” structural aberrations.

5.1.2. HOMOLOGOUS RECOMBINATION

Replication-associated DNA lesions are preferentially repaired by HR. HR repairs breaks by using the undamaged sister chromatid as a template; therefore, it usually results in a clean and accurate repair and that is why HR is known as an “error-free” pathway. Given that this repair option needs a sister chromatid, HR only occurs in late S and G2 phases. When DNA is packed and sister chromatids are significantly separated chromosome condensation makes homology search difficult and that is why HR is restricted in the cell cycle (Sonoda et al., 2006).

MRN complex recognizes DSBs, recruiting and activating ATM, which in turn triggers multiple signaling pathways and recruits repair proteins to the damaged sites (Falck et al., 2005). The basic step in HR is the resection of DSBs to generate extensive 3´ ssDNA overhangs on each side of the break, which are bound by RPA. Importantly, DNA resection decreases the occurrence of NHEJ since Ku complex has poor affinity for ssDNA (Dynan and Yoo, 1998), tipping the balance toward HR. RPA-coated ssDNA recruits the ATR-ATRIP complex, facilitating its recognition of substrates for phosphorylation and the initiation of checkpoint signaling and repair (Zou and Elledge, 2003). Thus, the conversion from dsDNA to ssDNA involves a switch from ATM to ATR signaling (Shiotani and Zou, 2009). RPA is then displaced from the ssDNA by RAD51 in a BRCA1/2 dependent process. RAD51-ssDNA filaments facilitate the homology searching and invasion of the ssDNA into homologous dsDNA. DNA synthesis takes place at the invading end using the homologous region of DNA as a template, eventually resulting in an error-free repair of the DSB (Fig. 10).

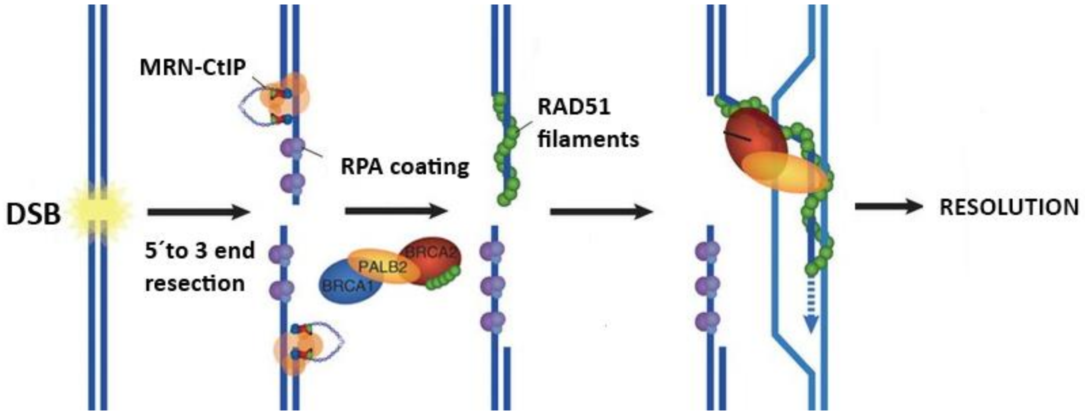

Figure 10. Simplified Homologous recombination process. Adapted from (Buisson et al., 2010)**.** The most important steps of HR are represented: DSB recognition, DNA end-resection, RPA coating, RAD51 filaments formation and strand invasion.

An essential factor in the DSB repair pathway choice is CtIP (CtBP-Interacting Protein). CtIP is a relatively conserved protein in mammals whose C-terminus is highly conserved from yeast to humans (Huertas and Jackson, 2009, You and Bailis, 2010). CtIP interacts with the MRN complex and facilitates ssDNA formation, ATR signaling and homologous recombination (Sartori et al., 2007). CtIP is believed to promote DNA end-resection in conjunction with Mre11, since its nuclease activity is under debate (Makharashvili et al., 2014). Interestingly, removal of both Mre11 and CtIP reduces HR to the same extent than CtIP or Mre11 downregulation individually (Sartori et al., 2007), further confirming that these proteins act in the same pathway. CtIP is subjected to a tight regulation, both at the transcriptional and post-transcriptional levels, in order to maintain chromosome stability. Although mRNA levels are pretty constant throughout the cell cycle, the CtIP protein expression is induced in S and G2 phases together with other HR-related proteins such as BRCA1 (Yu and Baer, 2000). Moreover, phosphorylation of CtIP has been shown to control its activity (Huertas and Jackson, 2009, Anand et al., 2016, Makharashvili et al., 2014, Wang et al., 2013), its protein stability (Steger et al., 2013, Lafranchi et al., 2014, Ferretti et al., 2016) or its interaction with other proteins such as ATM (Wang et al., 2013). Mutations in specific phosphorylation sites have been described to impact CtIP functionality and therefore impair the whole DSB repair pathway.

The relevance of HR for genome integrity is demonstrated by the fact that mice lacking key genes such as CtIP, BRCAs, or RAD51 are embryonically lethal and heterozygous mice are cancer prone. Interestingly, these HR-deficient cancers are hypersensitive to DNA damaging agents, including some chemotherapeutics drugs (reviewed in (Krajewska et al., 2015)).

6. p38 MAPK

6.1. MAPK SUPERFAMILY

Mitogen-activated protein kinases (MAPKs) are a family of proline-directed Ser/Thr kinases whose function and regulation have been conserved during evolution from yeast to humans (Widmann et al., 1999). MAPKs are key components in the signal transduction process, sensing changes in the extracellular environment and elaborating an appropriate cellular response. They are players in regulating several cellular processes such as cell proliferation, cell movement, cell differentiation or programmed cell death among others (Roux and Blenis, 2004).

In higher eukaryotes there are three well characterized MAPK arms: the extracellular signal-regulated kinases (ERK), composed by ERK1 and ERK2; the c-JUN NH2-terminal kinases, formed by JNK1, JNK2 and JNK3; and the p38 subfamily, containing four isoforms p38α, p38β, p38γ and p38δ. Other MAPK subfamilies have been identified as ERK5, ERK3, ERK4, ERK7 and ERK8, but their functions are not yet fully understood.

ERK 1/2 are known to be preferentially responsive to growth factors and mitogens, while JNKs and p38 MAPKs are strongly activated by environmental stresses and inflammatory cytokines (Morrison, 2012). In yeast, individual MAPK families often signal independently from each other, existing thus a pathway specificity even when individual components participate in more than one signaling pathway. In higher organisms, however, MAPK activation highly depends on the cell type and the biological context, and several MAPK branches can be activated at a time in order to elaborate the proper cellular response (Schaeffer and Weber, 1999).

MAPKs are typically organized in a three-kinase module consisting of a MAPK, a MAPK activator (MEK, MKK or MAP2K) and a MEK activator (MEKK or MAP3K). Each cascade is initiated by certain extracellular stimuli and the signal is transmitted through the sequential phosphorylation and consequent activation of these components. This three-step organization confers specificity to this phosphorelay system.

There are at least 20 MAP3Ks, which are often activated by interactions with a small GTPase and/or phosphorylation by protein kinases downstream from cell surface receptors (Cargnello and Roux, 2011). This large number of MAP3K allows for diversity of inputs to feed into particular MAPK pathways (Widmann et al., 1999). MAP3Ks selectively phosphorylate and activate different combinations of the seven MAP2Ks, resulting in a precise activation profile depending on the stimuli (Cuevas et al., 2007). In turn, these seven MAP2Ks generally recognize docking sites present in the at least 12 MAPKs (Bardwell and Thorner, 1996) and activate the MAPKs through a conserved dual Thr/Tyr phosphorylation in their activation loop (TxY motif). The tridimensional recognition of the docking site, and not simply a linear sequence surrounding the TxY motif confers another level of specificity, favoring the fidelity of the transmission between signal and response. Once activated, MAPKs can phosphorylate on Ser and Thr diverse substrates comprising transcription factors, protein kinases and many other kinds of proteins (Kyriakis and Avruch, 2012), eventually inducing the appropriate biological response.

6.2. DISCOVERY

The first human p38 MAPK was originally identified in a pharmacological screen to identify compounds modulating the production of the inflammatory cytokine tumor necrosis factor alpha (TNFα) in lipopolysaccharide-stimulated human monocytes (Lee et al., 1994). This new kinase had a high sequence homology to the *Saccaromyces cerevisieae* HOG1 kinase, involved in host protection from hyperosmotic stress. Further experiments suggested that p38 MAPKs participate not only in inflammatory responses but also in stress induced signaling, in cell proliferation and cell death (Cuadrado and Nebreda, 2010). The number of articles about p38 MAPK, and more specifically about p38α, has increased exponentially over the years and so has the knowledge about this protein (Fig. 11).

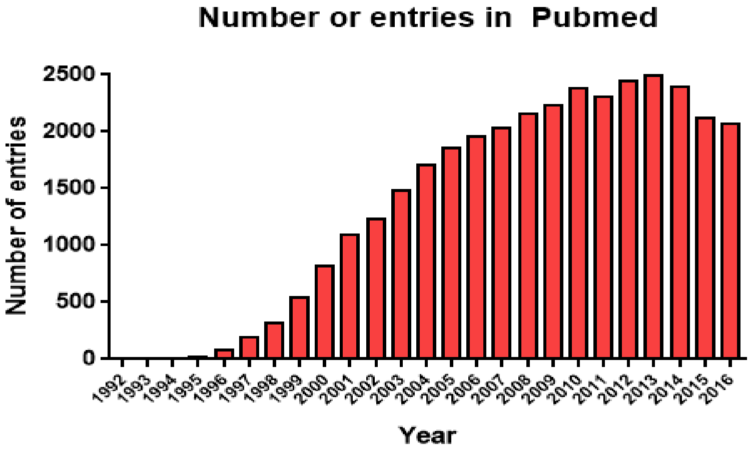

Figure 11. Number of PUBMED entries containing MAPK14 per year. Data obtained from NCBI showing the increasing interest on MAPK14 since its discovery.

6.3. p38 MAPK FAMILY

Four isoforms of p38 MAPKs encoded by four different genes have been identified in mammals; p38α, encoded by MAPK14, p38β, encoded by MAPK11, p38γ, encoded by MAPK12 and p38δ, encoded by MAPK13. They share more than 60% identity in their overall amino acid sequence and more than 90% within their kinase domains (Coulthard et al., 2009). Despite their high homology, these isoforms have notable differences in tissue expression, upstream activators and downstream effectors, as well as in their sensitivity to chemical inhibitors. These differences are so functionally important that p38α knockout mice are embryonically lethal

(Adams et al., 2000, Mudgett et al., 2000), while p38β, p38γ or p38δ deficiency does not affect embryonic viability (Beardmore et al., 2005, Sabio et al., 2005).

p38α and p38β are closely related proteins that are expressed in most tissues but to a different extent. While p38α is highly abundant in most of cell types, p38β is expressed at lower levels and its contribution to p38 MAPK signaling is not well defined (Kumar et al., 2003, Wagner and Nebreda, 2009). Meanwhile, p38γ and p38δ show a more restricted expression pattern. p38γ has been shown to be more prominent in skeletal muscle and p38δ in endocrine glands.

Different members of this family show overlapping substrate specificities. The genetic deletion of p38 MAPK family members has confirmed the existence of functional redundancy (Cuadrado and Nebreda, 2010). One example was carried out in MEFs, where SAP97/hDlg, is usually phosphorylated by p38γ, but in its absence other p38 MAPKs can perform this function (Sabio et al., 2005). Other cases have been found *in vivo*, such as p38α knockout embryos, where p38β is able, to a certain extent, to compensate for functions such as the lung developmental defect (del Barco Barrantes et al., 2011). However, in this same work, authors show the requirement of both p38α and p38β isoforms for a proper heart development, indicating the existence of specific roles of these isoforms. Taken together, the literature suggests that redundancy exists and compensation among isoforms takes place. Nevertheless, there are specific functions that are likely to be determined by the selectivity of the upstream activators and the identities and functions of the preferred downstream substrates.

6.4. ACTIVATION

Mammalian p38 MAPKs are activated in response to most environmental and cellular stresses, inflammation and other signals such as cytokines like TNF-α or IL-1 and growth factors (Zarubin and Han, 2005). Similar activation profiles have been described for the four p38 MAPK members (Jiang et al., 1996, Jiang et al., 1997, Cuenda et al., 1997), however, some differences have been observed in terms of kinetics and level of activation of these isoforms.

p38 MAPKs are mostly catalytically inactive in basal conditions, but become rapidly activated by MKK-dependent dual phosphorylation in the activation loop sequence Thr-Gly-Tyr. This phosphorylation induces a conformational change in the protein, enabling ATP and substrate to bind (Cuenda and Rousseau, 2007). Three MKKs have been described to activate the different p38 MAPKs: MKK6, MKK3 and MKK4. The relative contribution of the different MKKs in every case depends on both the stimulus and the cell type. MKK6 and MKK3 share 80% sequence homology (Stein et al., 1996) and are highly specific for p38 MAPKs (Enslen et al., 1998). MKK6 can phosphorylate the four p38 MAPK family members, while MKK3 activates the p38α, p38γ and p38δ isoforms, but not the p38β (Cuadrado and Nebreda, 2010). Additionally, p38α can also be phosphorylated by MKK4 (Derijard et al., 1995), a typical activator of the JNK pathway.

These MAP2Ks are in turn activated by around 10 of MAP3Ks (Cuadrado and Nebreda, 2010):ASK1, DLK1, TAK1, TAO1, TAO2, MLK3, TLP3, ZAK1, MEKK3 and MEKK4. Presumably, each MAP3K confers responsiveness to distinct stimuli but they are not specific for p38 MAPK. Some of them have been described to also activate the JNK pathway; actually, JNK and p38 MAPK cascades can be activated on overexpression of at least a dozen MAP3Ks, whose physiological roles and specificities remain elusive (Chang and Karin, 2001). ASK1, for example, plays a key role in the activation of p38 MAPKs by oxidative stress in mammals (Dolado et al., 2007), but it has also been described to activate both JNKs and p38 MAPKs upon H_2O_2 or TNFα in embryonic fibroblasts (Tobiume et al., 2001). Upstream of the cascade, the regulation of MAP3Ks is more complex, involving phosphorylation by STE20 family kinases and binding to small GTP-binding proteins of the Rho family such as Rac or Cdc42, as well as ubiquitination-based mechanisms (Cuadrado and Nebreda, 2010). The diversity of MAP3Ks and their flexibility provide the cell with versatility to respond to the external stimuli by differentially activating the different MAPK pathways.

Of note, inactivation of the pathway is as important as its activation. In the same way that MKK3 or MKK6 can phosphorylate p38 MAPKs in a matter of minutes, inactivation also occurs rapidly. Duration of the signaling is controlled by phosphatases, including generic phosphatases like phosphatase 1 and phosphatase 2A, or dedicated dual-specificity MAPK phosphatases such as MKP-1 and MKP-7 (Owens and Keyse, 2007, Masuda et al., 2001). These enzymes can be activated by phosphorylated p38 MAPK, creating a regulatory negative feedback loop that tightly controls the activation status of the pathway (Olson and Hallahan, 2004).

6.5. DOWNSTREAM TARGETS

Many p38 MAPK substrates have been identified by using pyrinidyl imidazole inhibitors such as SB203580, which targets p38α and p38β. The use of BIRB796 -a dyaril urea compound that at high concentrations inhibits not only p38α and p38β, but also p38γ and p38δ-and especially the use of specific knockout mice has provided new tools for identifying new and specific substrates (Cuenda and Rousseau, 2007). However, it is possible that the p38α and p38β substrates are overrepresented in the general p38 MAPKs substrate lists.

p38 MAPKs have been found both in the nucleus and the cytoplasm of quiescent cells, but upon stimulation, its cellular re-localization is not well understood. Some evidence suggests that upon activation, p38 MAPKs translocate from the cytoplasm to the nucleus (Raingeaud et al., 1995), but other reports show that activated p38 MAPKs preferentially accumulate in the cytosol (Ben-Levy et al., 1998).

p38 MAPK functions, independently of their physical localization, are mainly associated with the phosphorylation of Ser-Pro or Thr-Pro motifs in their substrates. However, some exceptions have been described. On the one hand, the phosphorylation of non-proline directed sites by p38 MAPKs like in Tau protein, where the phosphorylation of several non-canonical serines and a threonines have been detected (Reynolds et al., 2000). On the other hand, kinase-independent functions have been described for p38 MAPKs, where they would bind to their targets in the absence of phosphorylation. The first kinase-independent function of a MAPK was reported for Fus3 and Kss1 in *S. cerevisiae* in 1997 (Cook et al., 1997, Madhani et al., 1997). In this studies, apart from their kinase-dependent functions in mating and filamentation, these proteins show kinase-independent inhibitory functions, due in part to the interaction with distinct target transcription factors. This work was followed by others, both in yeast and in mammals, proposing kinase-independent functions in the regulation of mitotic progression by p38α (Fan et al., 2005), the nerve-growth factor induced apoptosis through the induction of gadd45 in medulloblastomas (Chou et al., 2001), or the K-Ras-induced transformation of rat intestinal epithelial cells, where K-Ras increases p38γ expression without increasing its phosphorylation (Tang et al., 2005). Although the underlying mechanisms are non-well determined, non-catalytic functions may include the scaffolding of protein complexes, the competition for protein interactions, the allosteric effects on other enzymes, or the change in the subcellular localization or DNA binding (Rauch et al., 2011).

In general, it has been estimated that MAPKs may have from 200 to 300 substrates each. The main substrates of p38 MAPKs are protein kinases and transcription factors; however, many other functions can be performed by p38 MAPK substrates such as chromatin remodeling, protein degradation and localization, endocytosis, apoptosis, cytoskeleton dynamics, or cell migration (Cuadrado and Nebreda, 2010).

The main protein kinases directly phosphorylated by p38 MAPKs are MK2/3, MNK1/2 and MSK1/2. These protein kinase substrates of p38 MAPKs appear to play a role in the intracellular amplification of signals. For example, MK2 –the first identified substrate for p38α-, together with its related family member MK3, are shown to activate various substrates including HSP27 (heat shock protein 27), LSP1 (lymphocyte-specific protein 1), CREB (cAMP response element-binding protein) or ATF1 (activating transcription factor 1). Moreover, MK2 has been found to phosphorylate TTP (tristetraprolin) (Mahtani et al., 2001), a protein that is known to destabilize mRNA, participating in the control of gene expression at the post-transcriptional level. MNK1 and MNK2 are believed to regulate translational initiation by phosphorylating eiF-

4E (eukaryotic initiation factor 4e) (Waskiewicz et al., 1997). Finally, p38 MAPKs can also activate MSK1 (Deak et al., 1998), which in turn participates in transcription activation by mediating CREB, NFkB or STATs activation and chromatin remodeling via histone phosphorylation.

Another group of substrates that are activated by p38 MAPKs comprises transcription factors. Many transcription factors accounting for a wide range of functions such as inflammation, angiogenesis or apoptosis have been observed to be phosphorylated and activated by p38 MAPKs. Examples include ATF-1/2/6 (activating transcription factor 1, 2 and 6), Sap1 (SRF accessory protein), CHOP (GADD153), p53, MEF2C (myocyte enhance factor 2C), MEF2A, or NFAT (nuclear factor of activated T cells) (Zarubin and Han, 2005). p38 MAPKs can also repress gene transcription by phosphorylating transcriptional repressors like HBP1 (HMG-Box Transcription Factor 1) (Xiu et al., 2003), which in turn blocks the expression of various genes regulating cell cycle progression.

Considering just p38α, almost 100 proteins were known to be phosphorylated by this p38 MAPK isoform up to 2013 (Trempolec et al., 2013) (Fig.12)

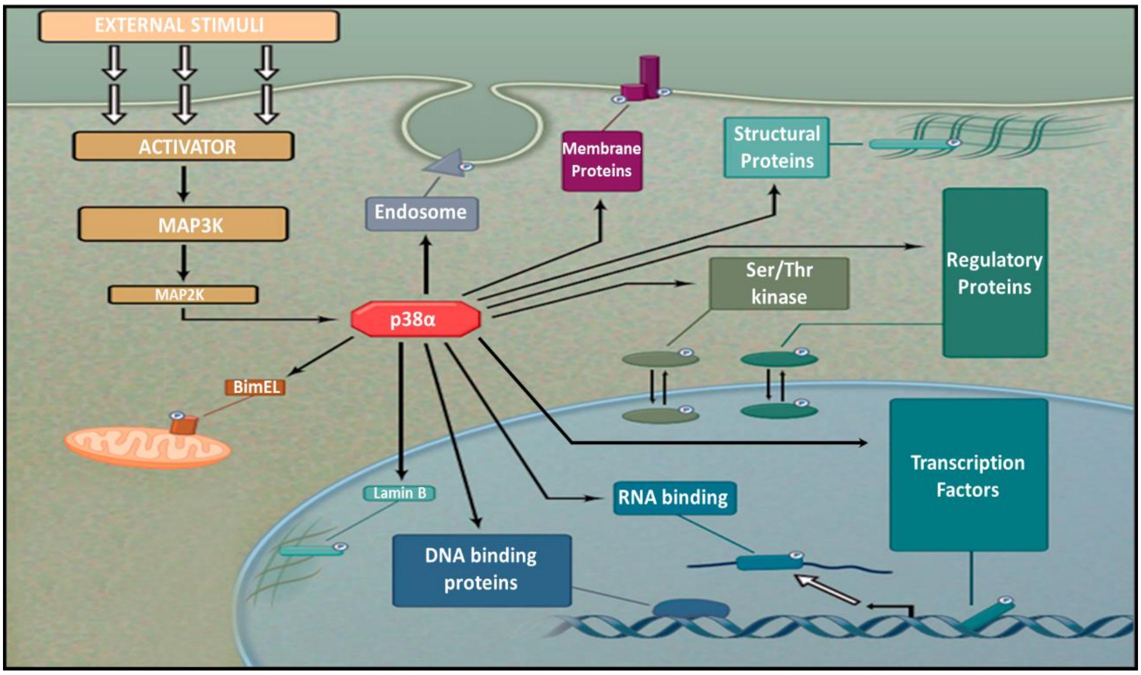
EXTERNAL STIMULI
ACTIVATOR
MAP3K
MAP2K
Endosome
Membrane Proteins
Structural Proteins
Ser/Thr kinase
Regulatory Proteins
p38α
BimEL
Transcription Factors
Lamin B
RNA binding
DNA binding proteins

Figure 12. p38α MAPK substrates. Adapted from (Trempolec et al., 2013). Schematic showing the functional diversity of p38α substrates.

6.6. p38α IN CANCER

p38 MAPKs participate in several processes important for normal tissue functioning and that are frequently deregulated in many diseases including cancer. Given the wide range of targets and the plethora of functions that they perform, p38MAPK in general, and p38α in particular, can impact on cancer cell homeostasis at different levels, including the regulation of several processes mentioned in previous sections.

6.6.1. p38α ROLE IN CELL CYCLE REGULATION AND CELL CYCLE CHECKPOINTS

p38α has been described to play an important role in the regulation of the G1 and G2 checkpoints.

p38α can contribute to the induction of the G1 checkpoint in response to several stimuli such as senescence, osmotic stimuli, ROS (Thornton and Rincon, 2009) or loss of centrosome integrity (Mikule et al., 2007). Of note, p38α has been shown to collaborate in the G1 arrest by regulating p21 levels following DNA damage through different mechanisms. Several studies describe p38α as a p53 activator which ultimately leads to p21 accumulation and subsequent induction or maintenance of the G1 arrest (Mikule et al., 2007, Shaltiel et al., 2014). However, p38α can directly regulate p21 levels by phosphorylation (Kim et al., 2002) or by posttranscriptional stabilization of its mRNA (Lafarga et al., 2009).

Meanwhile, the role of p38α in the G2/M transition is more studied. Using UV radiation, p38 MAPKs were shown to be required for cell cycle arrest (Bulavin et al., 2001, Warmerdam et al., 2013) and MK2 was identified as the key mediator by phosphorylating Cdc25B and Cdc25C (Manke et al., 2005). p38α inhibition also impairs topoisomerase inhibitor and histone deacetylase-induced checkpoints (Mikhailov et al., 2004). However, p38α role following γ-radiation is not so well-characterized and different outcomes have been proposed. This may raise the question of whether p38α function in G2/M is as universal as initially proposed and whether diverse DNA damage stresses and different degrees of damage would differentially activate p38α, originating distinct responses.

The amount of literature regarding p38α and the mitotic checkpoint is more reduced. p38α was shown to be activated following nocodazole-arrest in somatic cells and the introduction of an activated p38α form induced arrest in M phase in *Xenopus* egg extracts (Takenaka et al., 1998). p38α depletion in oocytes disturbed SAC, resulting in abnormal spindles and missaligned chromosomes (Ou et al., 2010). In mammals, p38MAPK has been shown to be activated upon nocodazole (Sayed et al., 2001) or cadmiun (Yen and Yang, 2010) and to indirectly participate in mitotic arrest. Some authors suggest that p38α would not act during SAC, but in a late-interphase checkpoint referred as "antephase", where p38α would mediate the transient decondensation of chromosomes and return to G2 upon certain insults (Lee et al., 2010, Matsusaka and Pines, 2004). However, the existence of this antephase checkpoint, as well as the potential function of p38α during the SAC is still unknown.

6.6.2. p38α ROLE IN DNA REPLICATION AND REPLICATION STRESS

p38α functions in cell cycle checkpoints in response to a plethora of DNA damage agents such as UV, ROS or chemotherapeutic agents such as cisplatin or doxorubicin have been extensively addressed along the literature. However, the function of p38α during replication or its involvement in the cellular fate following replication stress remains poorly characterized. Studies using arsenic trioxide (ATO), a chemical compound that increases ROS and impairs DNA repair among other effects, showed that p38α, together with other kinases, was required for Ccd6 protein stabilization and cell proliferation following ATO treatment, suggesting that p38α was required for proper DNA replication in stress conditions (Liu et al., 2010). p38α has also been shown to indirectly control DNA synthesis through the regulation of Myc. The negative regulation of Myc by p38α would avoid the Myc-dependent origin firing, restricting replication stress following etoposide treatment (Cannell et al., 2010). More focused studies using hydroxyurea and gemcitabine, two DNA replication inhibitors, however, showed contradictory outcomes. In some reports p38α and p38β were described to collaborate to inhibit mitotic entry and avoid genomic instability after hydroxiurea-induced DNA replication arrest (Llopis et al., 2012), while others showed how MK2, a direct substrate of p38α, promotes fork stalling and accumulation of DNA damage upon replication stress (Kopper et al., 2013). Therefore, the scarce bibliography and the discrepancy among the available results make the role of p38α in DNA replication and replication stress unclear.

6.6.3. p38α ROLE IN DNA DAMAGE

p38α deals with several kind of environmental insults. However, its role in response to DNA damage is not fully described. As mentioned in previous sections, p38α determines cell fate following UV radiation while its importance in γ-irradiation is still under debate. Interestingly, p38α and especially its substrate MK2 have been described to be activated in response to commonly used DNA-damaging agents such as cisplatin, doxorubicin and camptothecin. MK2 cell-cycle checkpoint functions have been proposed to be important in cells with a defective p53 signaling (Reinhardt et al., 2007) and to promote the maintenance of the checkpoint established by Chk1 (Reinhardt et al., 2010). Furthermore, p38α has been described to be activated by a particular kind of physiological DSBs produced upon V(D)J recombination in thymocytes. In this context, p38α would induce a p53-dependent G2/M arrest checkpoint, allowing DNA repair (Pedraza-Alva et al., 2006) and promote survival through the attenuation of GSK3β activity by its phosphorylation on Ser 389 (Thornton et al., 2016). Altogether, p38α seems to be involved in the cellular response to several damaging stimuli through the regulation of cell cycle checkpoints.

Due to these and other evidence, p38α has been classically associated with a tumor-suppressor role. However, recent reports have illustrated pro-tumorigenic functions of p38α by promoting tumor cell proliferation and survival (Gupta et al., 2014) or by facilitating cancer cell survival in response to chemotherapy treatments (Pereira et al., 2013, Rudalska et al., 2014). Given this duality and since p38α activity has been linked to several homeostatic mechanisms, we investigated the contribution of p38α to cancer cell survival and tumor progression in the particular context of breast cancer

AIM OF THE WORK

In normal epithelial cells, p38α has a well-established role as a tumor suppressor. However, novel functions promoting tumor cell survival and proliferation have been recently described. Moreover, p38α targeting has been shown to synergize with several therapeutic agents in diverse tumor types. Despite all the literature concerning p38 MAPKs and cancer, the roles of p38α during tumor progression and the response to chemotherapy are still elusive.

We decided to focus on the role of p38α in breast cancer progression and more specifically, in the homeostasis of breast cancer cells. Given that most of the bibliography concerning p38α and breast cancer is based on the use of p38 MAPK inhibitors, we decided to develop a genetic system to analyze the specific functions of p38α in breast cancer cells.

Specific objectives

- Development of a genetic system to study the role of p38α in breast cancer progression.
- Characterization of p38α functions in the homeostasis of breast cancer cells.
- Evaluation of the interest of using p38α inhibitors in breast cancer therapy as single agents or in combination with chemotherapeutic drugs.

MATERIALS AND METHODS

1. MATERIALS

1.1. Buffers and solutions

PBS 10X

1.37M NaCl
27mM KCl
100mM Na2HPO4
17.5mM KH2PO4
pH 7.4

Running Buffer 10X

0.25M Tris base
2M glycine
1% SDS
pH 8.3

Transfer Buffer 10X	**Transfer Buffer 1X**
0.2M Tris base	10% Transfer Buffer 10X
1.5M glycine	20% 2-propanol
1% SDS	70% H_2O

Protein Loading buffer 5X

250mM Tris pH 6.8
50% glycerol
250mM DTT
10% SDS
0.1% bromophenol blue

Ponceau Red

0.1% Ponceau Red powder
5% acetic acid
Disolved in dH_2O

HBS buffer (2X)

50mM HEPES
280 mM NaCl
1.5mM Na_2HPO_4
pH 7.12

RIPA buffer

50mM Tris-HCl
150mM NaCl
1% NP-40
5mM EDTA
1mM DTT
1mM PMSF
10µg/ml pepstatin
10µg/ml aprotinins
10µg/ml leupeptin
20mM NaF
1µM mycrocystin

Coomassie staining solution

0.5% Coomassie Blue R250
10% acetic acid
45% methanol

Coomassie Destaining solution

25% methanol
7% acetic acid

Kinase assay buffer

50 mM Tris-HCl (pH 7.5)
10 mM $MgCl_2$
2 mM DTT
200 µM ATP

NID Buffer

10 mM Tris pH 8.3
50 mM KCl
2 mM MgCl2
0.1 mg/ml gelatin
0.45% NP40
0.45% Tween20
1 mg/ml Proteinase K

SSC buffer 20X	**SSC buffer**
3M NaCl	10ml SSC 20X solution
0.3M Sodium citrate	90ml H_2O

1.2. Commercial Reagents and Kits

Reagent	Company	Reference
MOUSE WORK RELATED		
4-OHT	Sigma	H6278
Corn oil	Sigma	C8267
Docetaxel	Accord	691719.0
Methylcellulose	Sigma	M7140
Paclitaxel	Accord	676253.0
PH797804	Selleckchem	S2726
CELL CULTURE WORK RELATED		
17-β estradiol	Sigma	E8875
4-OHT (for cell culture)	Sigma	H7904
BrdU	Roche	10280879001
CldU	Sigma	C6891
Colcemide	Sigma	10295892001
Collagenase A	Roche	10103586001
DCFDA	Sigma	D6883
DMEM	Sigma	5796
DMSO (for cell culture)	Sigma	D5796
DNAse	Sigma	D4513
Docetaxel	Accord	691719.0
FBS	ThermoFisher	E6541L
Fluorobritte DMEM	ThermoFisher	A1896701

Glutamine	LabClinics	M11-004
H_2O_2	Sigma	H1009
Hanks Balance salt solution	GIBCO	14025092
Hyaluronidase	Sigma	H3506
IdU	Sigma	I7125
LY2228820	Selleckchem	S1494
MK2206	Selleckchem	S1078
Monastrol	Sigma	M8515
Nocodazole	Sigma	M1404
Nutlin	Sigma	N6287
Paclitaxel	Sigma	T7191
PBS 10X	Sigma	D1408
Penicillin/Streptomycin	LabClinics	P11-010
PH797801	Selleckchem	S2726
Polybrene	Sigma	H9268
Puromycin	Sigma	P9620
Reversine	Selleckchem	S7588
SB203580	Axon MEDCHEM	AX1363
Trypsin	Sigma	T3924
UO126	Calbiochem	662005
Z-VAD-FMK	SM Biochemicals LLC	SMFMK001

HISTOLOGY WORK RELATED

10% buffered formalin	Sigma	HT501128
BrightVision poly-HRP anti-IgG	ImmunoLogic	DPVO110HRP
DAB	Dako	K3468
DPX	Leica Biosystems	08600E
Eosin	Panreac	251301-1611
Hematoxylin	Panreac	254766-1611
Peroxidase blocking buffer	Dako	S2023
Sodium citrate	Sigma	71497
Superfrost glass slides	VWR	J1800AMNZ

CELLULAR AND MOLECULAR BIOLOGY WORK RELATED

Acetic acid	Panreac	131008.1611
Acrylamide 40% 29:1	BioRad	161-0146
Agarose	Conda	8019.22
Aprotinin	Sigma	A6279
APS	Sigma	A3678
Benzamide	Sigma	B6506
Boric acid	Sigma	B6768
Bromophenol blue	Sigma	B8026
BSA	Sigma	A7906
Chloridric acid	Sigma	258148
Chromosome 17 FISH probe	Empire genomics	CHR17-10-GO
Crystal Violet	Sigma	HT90132
DAPI	Life Technologies	P36935
dNTPs mix	Fermentas	R0192

DTT	GE Healthcare	17-1318-02
EDTA	Sigma	E46758
EGTA	Sigma	E4378
Ethanol	Panreac	141086.1214
Glicerol	Sigma	49782
HEPES	GIBCO	15630-049
Hoescht	ThermoFisher	62249
Leupeptin	Sigma	L2884
Low melting agarose	Sigma	A9414
Magna protein G magentic beads	Millipore	16-662
Magnesium chloride	Merck	1.05833.1000
Methanol	Panreac	131091.1214
Mycrocystin	Enzo LifeScience	ALX350012
Nitrocellulose Membrane 0.2µM	GE Healthcare	10600001
Nitrocellulose Membrane 0.45µM	GE Healthcare	10600002
NP40	AppliChem	A16960250
Paraformaldehyde	Aname	15710
Pepstatin	Sigma	P4265
PMSF	Sigma	P7626
Ponceau Red	Sigma	P3504
ProLong Gold Antifade Mountant with DAPI	Life Technologies	P36935
Propidium Iodide	Sigma	P4864
Proteinase K	Roche	03115852001
Random Primers	Invitrogen	48190-011
Rnase A	Roche	10109142001
Sarkozyl	Fluka	61743
SDS	Sigma	71725
Sodium fluoride	Sigma	S7920
Sodium Hydroxide	Sigma	S8045
Sodium orthovanadate	Sigma	S6508
Sucrose	Sigma	50389
Superfrost slides	VWR	J1800AMNZ
Superscript II Reverse Transcriptase	Invitrogen	18064-014
SYBER green	BioRad	1708886
TEMED	Sigma	T9281
Triton X-100	Sigma	T9284
TRIZMA-base	Sigma	T6066
TRIZMA-HCl	Sigma	T3253
Tween 20	Sigma	P7949
Wheat Germ Agglutinin Alexa Fluor 594	Invitrogen	W11262
β-mercaptoethanol	Sigma	M7154

COMMERCIAL KITS

Annexin V FITC Apoptosis Detection Kit	BD Biosciences	556547
Cell Growth Assay	Merck Millipore	CT02
FITC Mouse Anti- BrdU Set	BD Biosciences	556028
In Situ Cell Death Detection Kit (TUNEL)	Roche	11684795910
MycoAlert	Lonza	LT07-318

PureLink on column Dnase set	Invitrogen	121-85-010
RC DC protein assay kit II	BioRad	5000122
RNA PureLink Minikit	Ambion	12183018A
Telomere PNA FISH Kit/Cy3	Dako	K5326

1.3. Antibodies

Antibody	**Company**	**Reference**
	Western Blot	
Actin	Abcam	49846
AKT 1/2	Santa Cruz	sc-1619
AKT Phospho S473	Cell Signalling	9271
Caspase 3	Cell Signalling	9665
CDC20	Santa Cruz	5296
CDK1	Santa Cruz	54
Chk1 Phospho S345	Cell Signalling	2348
CtIP	Santa Cruz	271339
CtIP Phospho S276	*Gift from Alessandro Sartori*	*(Steger et al., 2013)*
CtIP Phospho S327	ThermoFisher	PA5-37337
CtIP Phospho T315	*Gift from Alessandro Sartori*	*(Steger et al., 2013)*
Cyclin E	Santa Cruz	247
CyclinB1	Santa Cruz	245
E2F1	Santa Cruz	193
ERα	Dako	M7047
GAPDH	Sigma	G8795
H2AX Phospho S139	Millipore	05-636
H3 Phospho S10	Millipore	06-570
HSP27	Santa Cruz	1049
HSP27 Phospho S82	Cell Signalling	2401
JNK	Santa Cruz	571
JNK Phospho T183/Y185	BD bioscience	612145
Lamin B1	Santa Cruz	20682
MAD2	MBL	K0167-3
MCM2	*Gift from Juan Mendez*	*(Alvarez et al., 2015)*
MCM3	*Gift from Juan Mendez*	*(Alvarez et al., 2015)*
MCM4	*Gift from Juan Mendez*	
MCM6	*Gift from Juan Mendez*	*(Alvarez et al., 2015)*
MK2	Cell Signalling	3042
MKK6	Home-made	(Ambrosino et al., 2003)
Myc	Abcam	32072
p21	Santa Cruz	397
p38 MAPK Phospho T180/Y182	Cell Signalling	9211
p38α	Santa Cruz	535
p38α	Cell Signalling	9218
p53	Cell Signalling	2524
PyMT	Abcam	15085
Ras	BD bioscience	610001

RPA32	Cell Signalling	2208
RPA32 Phospho S33	Bethyl	A300-246
RPA32 Phospho S4/S8	Bethyl	A300-245
Securin	Santa Cruz	56207
alpha-Tubulin	Sigma	T9026
Goat IgG (Alexa Fluor 680)	Invitrogen	A21084
Rabbit IgG (Alexa Fluor 680)	Invitrogen	A21076
Mouse IgG (Alexa Fluor 680)	Invitrogen	A21057
Mouse IgG (Alexa Fluor 800)	Rockland	611-131-122

Immunofluorescence

53BP1	Novus Biological	NB100-304
ACA	Antibodies incorporated	15-235
Alpha-Tubulin	Sigma	T9026
Aurora A Phospho T288	Abcam	83968
Aurora B	Abcam	2254
BrdU (ssDNA)	BD bioscience	347580
BrdU anti-CldU	AbD Serotec	OBT 0030
BrdU anti-IdU	BD bioscience	347580
CtIP Phospho T315	*Gift from Alessandro Sartori*	*(Steger et al., 2013)*
E-cadherin	BD bioscience	610181
H2AX Phospho S139	Millipore	05-636
MCM2	*Gift from Juan Mendez*	*(Alvarez et al., 2015)*
MCM3	*Gift from Juan Mendez*	*(Alvarez et al., 2015)*
MCM4	*Gift from Juan Mendez*	
MCM6	*Gift from Juan Mendez*	*(Alvarez et al., 2015)*
Rad51	Millipore	PC-130
RPA32	Cell Signalling	2208
Gamma-Tubulin	Sigma	T6557

Flow Cytometry

8-OHdG	Jaica	N45.1
APC-CD45	BD Bioscience	559864
BRDU	BD Bioscience	556028
EPCAM-FITC	Santa Cruz	53532
H2AX Phospho S139	Millipore	05-636
H3 Phospho S10	Millipore	06-570
PE-Pdgfrα	eBioscience	12-1401-81

Immunohistochemistry

8-OHdG	Jaica	N45.1
CK8	Fitzgeral	70R-30587
CK14	ThermoFischer	RB-9020
E-cadherin	BD bioscience	610181
ERα	Dako	M7047
H2AX Phospho S139	Millipore	05-636
H3 Phospho S10	Millipore	06-570
HER2	Dako	A0485

Ki67	Novacastra	NCL
PgR	Dako	A0098
SMA	BioGenex	MU128-UC

1.4. Primers

Gene	**Forward**	**Reverse**
BRCA1	AAGAGACAGTAACTAAGCCAGGT	GGGGCGGTCTGTAACAATTCC
BUB1	GTTCCTAGGAGTCAGGGTTCAG	ATGATCACCCTTTGTTCCCTAAT
BUBR1	GCTCTGAAAGCTCCAGGTCA	GACGCGGTATCGGCATTTTC
CAV1	ATACGTAGACTCCGAGGGACA	GCGCGTCATACACTTGCTTC
CDC6	CGGTCTGGAACCAAACCAGT	GGCATGATGGCCACACAAACTT
CDC20	GCCGAACTCCTGGCAAATCT	TTGGGGGATAAAGCGGTCAC
CDK1	GGTCCGTCGTAACCTGTTGA	CCACACCGTAAGTACCTTCTCC
CYCA2	GTC CTT CAT GGA AAG CAG	ACG TTC ACT GGC TTG TCT
CyclinB1	TGAAAAGGGAAGCAAAAACGCT	ATCGGGCTTGGAGAGGGATT
DCN	GCTCACGCAGTGAAACCTTAG	CTAACTATGCAGCCCAGGCA
E2F1	GGA TCT GGA GAC TGA CCA	CTC CAG GAC ATT GGT GA
ERα	CTGTGCTTGATTATTCTG	CTGTGGATAGAGTAAGTC
FOXA1	ATGAGAGCAACGACTGGAACA	TCATGGAGTTCATAGAGCCCA
FOXM1	CTGTGAGGGTCAAAGCTTGC	TCTGATGTTTCACTCGGGGC
GAPDH	CTTCACCACCATGGAGGAGGC	GGCATGGACTGTGGTCATGAG
GAPDH (human)	GTCGGAGTCAACGGATTTGG	TGAGCCCCAGCCTTCTCC
GATA3	AGCCACATCTCTCCCTTCAG	AGGGCTCTGCCTCTCTAACC
GREB1	TGCACAACGTTACCACCAGGAG	CCTCTGACGGTGGAATGCAA
GREB1 (human)	GTGGTAGCCGAGTGGACAAT	AAACCCGTCTGTGGTACAGC
HMBS (human)	GGAGTATTCGGGGAAACCTC	AAGCAGAGTCTCGGGATCG
HPRT	GAGAGCGTTGGGCTTACCTC	ATCGCTAATCACGACGCTGG
K14	TGAGAGCCTCAAGGAGGAGC	TCTCCACATTGACGTCTCCAC
K18	GCCAGGCCCAGGAATATGAA	AGGGCATCGTTGAGACTGAAA
K8	AGATCACCACCTACCGCAAG	TGAAGCCAGGGCTAGTGAGT
MAD2	TCAGAAACTGGTGGTGGTCA	ACGAACACCTTCCTCTTTTGC T
MAPK13	CAAGGGCAAGGACTACCTGG	TCTGGGGCAGGGACTGAATA
MAPK14 exon12	GCCCTCCCTCACTTCAGGAG	TGTGCTCGGCACTGGAGACC
MAPK14 exon2	GCATCGTGTGGCAGTTAAGA	GTCCTTTTGGCGTGAATGAT
MCM2	ACCAACGTATCCGCATCCAG	TCAGCTCTATCTCGTCCCCT
MCM3	CGAGGAGGACCAAGGCATTT	TTGTTCAGGAGGCGGTTAGC
MCM4	AGAGTGAACGTCACAGGCAT	GCAGACGTTTTGCATCCGTT
MCM5	CAGAGGCGATTCAAGGAGTTC	CGATCCAGTATTCACCCAGGT
MCM6	ACACACTACGATCACGTTCTGA	ACCAGGTAGGGGTCTTCCTC
MCM7	GCGTTCGTTTTCTGCTTCCC	CGATGAGCCAGATGAACCAACT
MDM2	CAAGAGACTCTGGTTAGACC	GGATCCTTCAGATCACTCCC
MKK6	GACCAGTTCCACGCCGCCTC	CGTCGCCCTCCCGGAAGAGT
ORC1	GCCCTATGTGGCTAAACTGA	GGAGGAACTTCAGCTCCATTTTG
p107	TCT TGT ATG CGG AAT CCT	ATC TCC ATT CCA TGA AGC
p21	TATCCAGACATTCAGAGCCACA	CACGGGACCGAAGAGACAAC
p21 (human)	CTGAGACTCTCAGGGTCGAA	CGGCGTTTGGAGTGGTAGAA

Securin	GTGGCGCAGTCTTCGAGTA	TCCTTAGATGCCAAACGGCG
SKPR1	AGCCTCATTCAGGGGAGGAT	CAGGGCGATGTGGTCTTCAT
SLC28a	AATCTGCCTAACGCTGTGCT	ATGGCTTCAAGGTAGGGCAC

1.5. Plasmids

Plasmid	Addgene Reference
pBABE-H2BGFP	Plasmid #26790
pCL-ECO	Plasmid #12371
pDR-GFP	Plasmid #46085
pCBASceI	Plasmid #26477

2. METHODS

2.1. MOUSE WORK

Colony management and animal handling were performed by Dra. Ana Igea Fernández.

2.1.1. Generation of PyMT mice with inducible Cre

Mice were housed according to national and European Union regulations, and protocols were approved by the animal care and use committee of the Barcelona Science Park (PCB-CEEA).

PyMT p38α$^{\text{lox/lox CreERT2 or lox/- CreERT2}}$ female mice were generated by crossing p38α$^{\text{lox/lox or lox/-}}$ mice (Ventura et al., 2007) with MMTV-PyMT, provided by William Muller (McGill University, Canada) and UbiquitinC-Cre-ERT2 mice (Ruzankina et al., 2007), being all mostly in FVB background.

Breast tumors were monitored twice a week with a caliper using the formula V= (π x length) x wide^2 and experiments were started when tumors reached 150-200mm^3, usually around 2.5 months old.

2.1.2. Patient-derived xenografts

PDX models were obtained from Dra. Violeta Serra (VHIO) and Dra. Eva Gonzalez (IDIBELL). Tumors were harvested when they reached a size of 1500mm^3 and tumor tissue was cut into 2- to 3-mm^3 pieces in Fetal Bovine Serum (FBS). Under anesthesia with isoflurane, one tumor piece was orthotopically implanted in the mammary fat pad by a small incision into 5-6 weeks old female NOD/Scid mice (Harlan Laboratories). For the experiments, xenografts were allowed to grow until they reached a size of 150-200mm^3 and then mice were subjected to the corresponding treatments. Tumor size was measured every other day by a digital caliper using the following formula: Tumor volume = (length × width^2)/2.

2.1.3. Animal treatments

For p38α deletion, 4-hydroxytamoxifen (4-OHT) was dissolved in 10% ethanol/90% corn oil and mice were intraperitoneally injected with 1mg each day for five consecutive days.

For chemotherapeutic treatments, PyMT mice were injected with 20mg/kg paclitaxel or docetaxel for three consecutive weeks. The p38α inhibitor PH797804 was dissolved in 0.05% methylcellulose in PBS and administered daily at 15 mg/kg by oral gavage during 21 days. In the case of PDXs, mice were injected once a week with 20mg/kg of docetaxel for four consecutive weeks or 20mg/kg paclitaxel for three consecutive weeks. PH797804 was administered daily at 15mg/kg by oral gavage during 21 days.

2.1.4. Histological analysis

Tumors dissected from mice were fixed in 10% buffered formalin overnight at RT and embedded in paraffin. 3µm sections were de-wax in xylene for 10min and the re-hydrated in consecutive ethanol solutions (100%, 95%, 75%, 50%) and H_2O. Re-hydrated sections were either stained with H&E or subjected to additional immunohistochemical analysis. In this case, sections were subjected to antigen retrieval (10mM sodium citrate pH 6 for or Tris-EDTA pH 9 20min in a steamer), washed in PBS, and endogenous peroxidase activity was inactivated using peroxidase blocking buffer for 15min at RT. Sections were blocked in blocking solution (0.05% BSA/PBS) for 20min at RT and incubated with primary antibodies. BrightVision Poly-HRP-Secondary antibodies and DAB were used for signal development. Slides were counter-stained with hematoxylin, de-hydrated in consecutive ethanol solutions (50%, 75%, 95% and 100%) and mounted using DPX.

Ki67 and γH2AX stainings were analyzed using Fiji macros written by the Advanced Digital Microscopy Core Facility (IRB Barcelona). In both cases microscopy images were split in H&E and DAB channels. For Ki67 quantification the ratio between DAB(+) area vs total H&E area was determined. In case of γH2AX, only the DAB(+) area was considered and taken as parameter (γH2AX(+) area).

2.1.5. FISH

Centromeric probe FISH was performed on PDX tumor sections. 5µm sections were de-paraffined by three xilol washes of 5min each, re-hydrated in consecutive 99% ethanol (three times, 5min), 96% ethanol(three times, 5min) and H_2O, and subjected to antigen retrieval by autoclaving slides 20min in 10mM sodium citrate buffer at pH6. Tissue was digested with proteinase K for 5min at RT, washed in SSC buffer for 5min at RT, fixed in formalin during 10min and dehydrated in successive washes (1min/each) in 70%, 95% and 100% ethanol. When dried, chromosome 17 centromeric probe was added and samples were denatured for

5min at 83°C and hybridized at 37°C O/N. Then, samples were washed with 73°C-pre-warmed 0.3% NP40 SSC buffer, washed again in the same buffer at RT and air-dried. Finally, slides were mounted using mounting media containing DAPI. Samples were visualized using a Leica TCS SPE confocal microscope.

2.2. MAMMALIAN CELL CULTURE

2.1.1. Generation of epithelial cell lines from PyMT tumors

Tumors were chopped using razors and digested at 37°C rocking for 1h in DMEM medium containing Collagenase A (1mg/ml) and Hyaluronidase (1.5units/ml). After digestion, cell suspension was filtered through a 70µm cell strainer and centrifuged 5min at 1500rpm. The cell pellet was resuspended in 10ml DMEM and centrifuged at 1500rpm for 30s. The supernatant was discarded and the cell pellet was resuspended and spun again four more times. The final cell pellet enriched in epithelial cells was plated. Cells were passaged until spontaneously immortalized, usually after 16 passages.

2.1.2. Maintenance and subculture

Cells were maintained in DMEM media supplemented with 10% heat inactivated fetal bovine serum (FBS), 1% penicillin/streptomycin and 1% glutamine at 37°C and 5% CO_2.

For subculturing, cells were washed twice in PBS and incubated in 750µl trypsin at 37°C until detached. Then, complete media was added and cells were diluted as desired (1:8-1:12) depending on the confluence and re-plated in a new culture dish.

2.1.3. Cell collection

For harvesting, sub-confluent cell cultures were washed twice with PBS and trypsinized. Cells were resuspended in 5ml of complete fresh media and the suspension was transferred to a 15ml conical tube and centrifuged at RT at 1200rpm for 5min. Afterwards, media was aspirated and the pellet was washed in 1ml of PBS. Cell suspension was centrifuged again in the same conditions and supernatant was discarded.

For western blot or RNA analysis purposes, cell pellets were immediately frozen in dry ice and kept at -80°C. For fixation for flow cytometry analysis, cell pellets were resuspended in 0.5ml of PBS and then 4.5ml of ice-cold 70% ethanol were added drop-wise while slowly vortexing. Suspension was kept at -20°C for at least 24h before proceeding.

2.1.4. Freezing and thawing

For freezing, cells were collected as described above and resuspended in freezing media consisting of 90% FBS and 10% DMSO. Cells from a 70-85% confluent p10cm culture dish were resuspended in 1-2ml of freezing media and transferred to 1-2 1.5ml cryo-tubes. Cryo-tubes were stored in a Mr. Frosty container (ThermoFisher) at -80°C for up to one week and then transferred to liquid nitrogen for long term storage.

For thawing, frozen cells were quickly placed in a 37°C water bath until completely thawed. Then cells were transferred to a conical tube and resuspended in 5ml of pre-warmed media. Cell suspension was centrifuged at RT at 1200rpm for 5min. Media was aspirated and pellet was resuspended in 10ml media and plated in a 10cm dish.

2.1.5. Mycoplasma detection

Cells were routinely tested for mycoplasma using Mycoplasma Detection Kit. 100µl from the cell media were taken and centrifuged for 5min at 200g. The supernatant was transferred to a test tube. 100µl of MycoAlert reagent were added and luminescence was measured after 5 min incubation. Then, 100µl of MycoAlert substrate were added and luminescence was measured after 10min incubation. The ratio of reading B/reading A was used to determine the mycoplasma status according to manufacturer´s parameters.

2.1.6. Cell pellet preparation for IHC

Cells were harvested, washed in PBS and pelleted in a 1.5ml Eppendorf tube. 1ml of 10% buffered formalin was carefully added and pellet was incubated at 4°C O/N. The next day the pellet was extracted by pipetting, transferred to a cassette and embedded in paraffin. Paraffin blocks were processed as described in the Histological analysis section.

2.1.7. Cell treatments

4-hydroxytamoxifen (4-OHT)

4-OHT is the active metabolite of tamoxifen. When 4-OHT is used in a CreERT2/lox system, it binds to a modified fragment of the estrogen receptor, which is bound to the Cre recombinase. Therefore, addition of 4-OHT relocates Cre into the nucleus, where it recombines the loxP sites, resulting in p38α downregulation.

Cells were treated with 100nM 4-OHT for 48h. A 10mM stock was prepared in ethanol and stored at -20°C.

17-β-estradiol (E2)

E2 is a steroid hormone that binds to estrogen receptor and activates gene transcription.

Cells were treated with 10nM E2 for 24h in 0.1% FBS media. A 10mM stock was prepared in ethanol and stored at -20°C.

p38 MAPK inhibitors

SB203580 inhibits p38α and p38β activity by binding to the ATP binding pocket.

Cells were treated with 5µM SB203580. A 10mM stocks were prepared in DMSO and kept at -20°C.

PH797804 is an ATP-competitive inhibitor that preferentially acts on p38α.

Cells were treated with 2µM PH797804. A 2mM stock was prepared in DMSO and kept at -20°C.

LY2228820 is an ATP-competitive inhibitor of p38MAPK, highly selective for p38α and p38β isoforms.

Cells were treated with 100nM LY2228820. A 1mM stock was prepared in DMSO and kept at -20°C.

None of the inhibitor aliquots were thawed more than three times.

BrdU

BrdU is a synthetic analog of thymidine that is incorporated in newly synthesized DNA, allowing the measurement of cell proliferation.

Cells were incubated in 10µM BrdU for 2 hours.

When BrdU was used to measure ssDNA, 10µM BrdU was incubated for 48h.

A 10mM stock was prepared in H_2O and stored at -20°C.

Nutlin

Nutlin is an inhibitor of the MDM2/p53 interaction which leads to p53 activation.

Cells were incubated with 10µM nutlin for 24h unless indicated. A 10mM stock was prepared in DMSO and stored at -20°C

Spindle Poisons

Most of these drugs bind tubulin interfering with microtubules dynamic and arresting cells in mitosis in a spindle assembly checkpoint (SAC) dependent manner.

Nocodazole was used at 3µM. A 500ng/ml stock was prepared in DMSO and stored at -20°C.

Colcemide was used at 100ng/ml. A 1mg/ml stock was prepared in ethanol and stored at -20°C.

Paclitaxel was used at 25 or 100nM depending on the experiment. A 1mM stock was prepared in DMSO and stored at -20°C.

Docetaxel was used at 5nM. A commercial 25mM stock was stored at 4°C.

Monastrol is an Eg5 kinesin inhibitor that does not affect microtubule polymerization. It was used at 100nM. A 100µM stock was prepared in DMSO and stored at -20°C.

Reversine

Reversine is an inhibitor of the kinase MPS1 that inhibits SAC in a dose dependent manner.

Cells were incubated with 250nM reversine unless indicated. A 1mM stock was prepared in DMSO and stored at -20°C.

Campothecin (CPT)

CPT is a Topoisomerase I inhibitor that causes replication-associated DNA damage by creating SSBs that are converted into DSBs during replication.

Cells were incubated with 1µM CPT for 1h or 100nM overnight. A 1mM stock was prepared in DMSO and stored at -20°C.

2.1.8. Retroviral Infection

Retroviral infection was used to create stable cell lines. Initially, a transient transfection of the HEK293T with the desired plasmid was performed; 5µg of the desired DNA and 5µg of the pCL-Eco packaging plasmid were mixed with 50µl of 2.5M $CaCl_2$ and H_2O up to 500µl. After 5min incubation at RT, 500µl of 2XHBS were added drop-wise and incubated at RT for 20min. This mixture was added drop-wise to the HEK293T cells and about 8-16h later, cells were carefully washed with PBS and fresh media was added. After 24h, the HEK293T supernatant was harvested and filtered through a 0.45µm PVDF filter. 5ml of this media, 5ml of fresh media and 8µg/ml polybrene were added to a p10cm dish containing the exponentially-growing cells to be infected. This step was repeated twice. 24h after finishing the second infection round, the corresponding antibiotics were added and selection was carried out for 5-10 days.

2.3. MOLECULAR BIOLOGY

2.3.1. Protein extraction

Frozen cell pellets were directly resuspended in RIPA lysis buffer, mixed by vortexing and kept on ice for 15min. Lysates were subjected to water-bath sonication when needed, incubated on ice for 15min and centrifuged at 13200rpm for 15min at 4°C.

Mouse tissues were immersed in RIPA lysis buffer and homogenized using Precellys homogenization and lysis instrument (Bertin Technologies). Lysates were incubated 15min on ice and centrifuged 15min at 13200rpm at 4°C.

Supernatants were recovered and kept at -80°C.

2.3.2. Determination of protein concentration

Protein concentration was estimated using the RC DC protein assay kit II. 2µl of protein sample were mixed with 25µl of working reagent A (coming from a mixture of 10µl of Protein Assay Reagent S and 500µl of Reagent A); 200µl of Protein Assay reagent C were added afterwards. The solution was incubated 6min at RT and absorbance at 750nm was measured. Concentrations were calculated using a BSA standard curve.

2.3.3. Western Blot

Total protein (20-40µg) were separated by SDS-PAGE using 8%, 10%, 12% or 14% Laemmli gel, depending on the protein molecular weight. After electrophoresis, proteins were transferred from the polyacrylamide gel to a nitrocellulose membrane using a wet transfer system (Bio-Rad). Ponceau Red was used to check transfer quality and efficiency. After washing out Ponceau Red with PBS, the membrane was blocked during 1h with 5% non-fat milk in PBS at RT. Primary antibody was diluted in 5% BSA in PBS-0.05% Tween and incubated O/N at 4°C. Then, membranes were washed three times in PBS and incubated with the secondary antibodies diluted in 1% BSA in PBS-0.05% Tween for 1h at RT. Finally, membranes were extensively washed with PBS and proteins were detected using Odyssey Infrared Imaging System. Antibodies are indicated in the Materials section.

2.3.4. Subcellular fractionation

At least 1 million cells were harvested and resuspended in 200µl of Buffer A (10mM Hepes pH7.9, 10mM KCl, 1.5mM $MgCl_2$, 0.34M sucrose and 10% glycerol)/1mM DTT/0.1% Triton X100 and protease inhibitors, and incubated for 5min on ice. After centrifugation for 5min at 3500rpm at 4°C, the supernatant contains cytosolic proteins and the pellet contains the intact nuclei. This nuclear pellet was washed with buffer A/1mM DTT and resuspended in cold 3mM EDTA/0.2mM EGTA with protease inhibitors and incubated 30min on ice. This solution was centrifuged 5min at 4000rpm at 4°C; the supernatant contained the soluble nuclear proteins and the pellet, which was resuspended in 1X Laemmli Loading buffer and sonicated twice for 15s at 20% amplitude, corresponds to the chromatin fraction.

2.3.5. Immunoprecipitation

Magnetic Protein-G beads were washed in cold PBS and incubated in 300µl ice cold PBS containing 3µl of CtIP antibody (Bethyl, A300-488A) for 4h rotating at 4°C. Meanwhile, cell lysates were pre-cleared by incubation with 20µl of washed beads during 45min rotating at 4°C. Beads with CtIP were recovered and beads from the lysates were discarded using a magnetic stand (Millipore). Pre-cleared lysates were incubated with CtIP-bound beads O/N rotating at 4°C. The next day beads were recovered, washed twice in ice cold RIPA buffer, resuspended in 1X loading buffer, boiled at 95°C for 5min and analyzed by western blot.

2.3.6. RNA isolation

Total RNA was isolated from frozen cell pellets using RNA Purelink MiniKit and residual DNA was digested using PureLink on column DNase set following manufacturer´s instructions.

RNA purity and concentration was determined by measuring the absorbance at 260 and 280nM using NanoDrop 2000 spectophotometer (Thermo Scientific).

2.3.7. cDNA synthesis

500ng-1µg of total RNA was reverse transcribed using Random Primers and SuperScript II Reverse Transcriptase following manufacturer's protocol.

2.3.8. Quantitative real time PCR

5-25µg of cDNA were mixed with 2.5µM of each primer, SYBR green and autoclaved H_2O in a 20µl reaction volume. Samples were run in a Bio-Rad C1000 thermal cycler machine. HPRT and GAPDH were used as reference genes in mouse cells. HMBS and GAPDH were used as reference genes in human cells. Primers used are listed in the Materials section. PCR conditions are indicated below:

50°C 2min
95°C 10min

$$\left.\begin{array}{ll} 95^\circ\mathrm{C} & 15\mathrm{s} \\ 56^\circ\mathrm{C} & 15\mathrm{s} \\ 72^\circ\mathrm{C} & 60\mathrm{s} \end{array}\right\} \text{40 cycles}$$

95°C 15s
60°C 2min
95°C 15s

The fold changes in gene expression were calculated using the ΔCt method.

2.3.9. Epithelial cell isolation for p38α deletion analysis

Tumors were digested as previously described and the cell suspension was filtered through a 70µm cell strainer and centrifuged 5min at 1500rpm. Cell pellets were resuspended in Hanks Balance media containing 1mM HEPES and 1% FBS and digested first with 1ml trypsin for 3-5min and then with 0.4mg DNAse for 2-3min. Cells were washed again with Hanks Balance media and cell density was quantified. 100000 cells were stained using APC-CD45 for leukocytes, PE-Pdgfr-α for fibroblasts and EPCAM-FITC for epithelial cells detection. Cells were stained in darkness for 30min on ice, washed in PBS and resuspended in PBS containing DAPI. EPCAM(+) cells were sorted in NID buffer to isolate genomic DNA. Sorted cells were digested O/N at 56°C and after inactivation of the proteinase K at 95°C for 10min, 2µl of the cell lysate were used for the qRT-PCR reaction. Deletion levels were analyzed using specific primers for the exon 2 (floxed) and exon 12 (control) of the p38α gene (MAPK14).

2.3.10. Kinase Assay

Purified CtIP (500ng) and activated p38α (100ng) were incubated in a total volume of 20µl kinase buffer supplemented with protease inhibitors for 30min at 30°C. Reaction was stopped by adding 1X sample loading buffer and boiling for 5min. Proteins were resolved by SDS-PAGE, transferred onto a nitrocellulose membrane and detected with the corresponding phospho-antibodies.

2.3.11. Mass Spectrometry

Kinase assays with p38α were performed in triplicates using full-length human CtIP (500 ng, Abcam, ab152651) and incubating with 500µM ATP for 2h. Samples were run in a SDS-PAGE and Coomassie stained. Bands were cut and in-gel digested using trypsin (Shevchenko et al., 2006). Sample processing was performed by the IRB Mass Spectrometry Facility. Briefly, digested solutions were speed vacuum-dried and reconstituted in 1% formic acid for LC-MS/MS analysis. Peptide mixture was separated in a C18 analytical column and column outlet was directly connected to an Advion TriVersa NanoMate fitted on an Orbitrap Fusion Lumos Tribrid, operated in a data-dependent acquisition (DDA) mode. Database search was performed with Proteome Discoverer software v2.1 using Sequest HT search engine. SwissProt Human database and MaxQuant common contaminants fasta file were used. Searches were run against targeted and decoy databases to determine the false discovery rate (FDR). Peptides with a q-value lower than 0.1 and a FDR< 1% were considered as positive identifications with a high confidence level. The PhosphoRS node in Proteome Discoverer was used to provide a confident measure of the localization of phosphorylation in the peptide sequences. Further p-site assignment validation was made by manual spectra inspection. Ratios of the peptides with or without phosphorylation were calculated and p-sites relative abundance was determined. Average p-site abundance was calculated and those sites with a value > 0.25 were considered as main hits.

2.4. CELLULAR BIOLOGY

2.4.1. Cell Cycle Analysis

Cells were harvested, fixed in 70% cold ethanol and kept at -20°C for at least 24h. Cells were then washed twice in PBS and incubated in PBS containing 20µg/ml propidium iodide, 0.1mg/ml RNaseA, and 0.1% Tween 20 for 30min at 37°C in the dark. 10000 cells were acquired on an EPICS XL flow cytometer and cell cycle distribution was analyzed with the FlowJo software.

2.4.2. MTT proliferation assay

500-2000 cells/well were seeded in 96well plates in a final volume of 100µl. Cell viability was determined at the desired days post-seeding using the MTT Cell Growth Assay; 10µl of reagent A were added to every well and 4h later 100µl of reagent B were added. The next day, absorbance at 570nm was read using absorbance at 750nm as reference. Absorbance was proportional to the viable number of cells and values were normalized to day 1.

2.4.3. BrdU Uptake

This protocol allows quantification of cells undergoing DNA synthesis, indicating cell proliferation.

Growing cells were incubated with 10µM BrdU for 2h, harvested and fixed in cold 70% ethanol for at least 24h. Fixed cells were centrifuged at 2000rpm for 5min at RT. Ethanol was aspirated and cells were washed with PBS. Afterwards, cell pellet was resuspended in an ice-cold denaturizing solution (0.1M HCl, 0.5% Tween 20 in H_2O) and incubated for 10min in ice. After centrifugation, cells were resuspended in H_2O and incubated at 95°C for 5min. Cells were centrifuged again, washed once in blocking buffer (1% BSA, 0.5% Tween 20 in PBS) and resuspended in 100µl of blocking buffer containing 10µl of anti-BRDU-FITC. After 1h incubation at RT in the dark, cells were washed once in blocking solution and resuspended in a PI staining solution (10µg/ml PI, 200µg/ml RNAase A, 0.05% Tween 20 in PBS). 20000 cells were acquired on an EPICS XL flow cytometer and FlowJo software was used for analysis.

2.4.4. Annexin V staining

Annexin V is a protein that binds to the negatively charged phospholipid phosphatidylserine (PS). PS is translocated from the inner to the outer leaflet of the plasma membrane during apoptosis; therefore, determination of exposed PS by annexin V is a measurement of cell death.

Cells were freshly harvested together with their media. Annexin V FITC Apoptosis Detection Kit was used and cells were stained following manufacturer's instructions. Briefly, cells were centrifuged at 1500rpm for 5 min, washed in cold PBS and resuspended in 100µl of 1X annexin V binding buffer with 5µl of annexin V-FITC. Samples were incubated 20min at RT in the dark and finally, 400µl of propidium iodide staining buffer were added. 10000 cells were acquired on a Gallios Flow Cytometer and FlowJo was used for analysis.

2.4.5. Epithelial status verification

EPCAM is a transmembrane protein commonly used as an epithelial marker. After immortalization, cell lines derived from PyMT tumors were tested for EPCAM in order to test their epithelial status.

Cells were harvested, washed in PBS and resuspended in 100µl of fresh DMEM containing 2µl of EPCAM-FITC antibody. After 30min incubation on ice in the darkness, cells were washed and resuspended in 500µl of fresh DMEM. 10000 cells were acquired on a Gallios Flow Cytometer and FlowJo software was used for analysis.

2.4.6. Phospho H3 S10 FACS staining

H3 phosphorylation on Ser10 correlates with chromatin condensation and is widely used as a mitotic marker.

Cells were harvested and fixed in cold 70% ethanol. After fixation, cells were centrifuged at 2400rpm, washed once in PBS and once in blocking buffer (2%BSA/0.25%TritonX-100 in PBS). Then cells were resuspended in 50µl of blocking buffer containing 1µl of pH3S10 antibody and incubated for 2h at RT with occasionally vortex. Cells were washed in PBS and resuspended in 100 µl of 2%BSA/PBS containing 1µl of the α-rabbit Alexa-Fluor 488 antibody (Invitrogen). After 45min incubation at RT in the darkness, cells were washed in PBS and incubated in DNA staining solution (200µg/ml RNAase A, 20µg/ml PI in PBS) at RT for 30min. 10000 cells were acquired in a Gallios Flow Cytometer and analyzed using FlowJo.

2.4.7. Clonogenic Assays

Cells were trypsinized and 1200 cells were plated in 60 mm dishes. Media was renewed every three days and cells were allowed to grow until visible colonies were formed (7-10 days depending on the treatment). Then cells were washed in PBS, fixed in 4% paraformaldehyde for 20min and stained with crystal Violet for 30min. Repeated H_2O washes were performed until clean colonies were visible. The colony area was measured using Fiji.

2.4.8. Metaphase spreads preparation

Cells were treated with 100ng/ml colcemide for 2h for arresting cells in metaphase and then trypsinized. Pelleted cells were hypotonically swollen in 75mM KCl for 20min at 37°C and fixed in fixative solution (ice cold 75% methanol/25% acetic acid). After three washes in fixative solution, cells were spread on superfrost glass slides, steam treated for 5s, heat dried and stained with mounting media containing DAPI. Spreads were imaged using a Nikon E1000 epifluorescence microscope. Chromosome number and chromosome aberrations were analyzed using Fiji software.

2.4.9. Immunofluorescence

Cells grown on coverslips were washed in PBS and fixed firstly in 4% paraformaldehyde in PBS for 20min at RT. After PBS washing, cells were incubated in 100% ice-cold methanol for 10min at -20°C. Then, cells were permeabilized in 0.1%Triton X-100 in PBS for 10min at RT and blocked in 1%BSA in PBS for 1h at RT. Primary antibodies were diluted in blocking buffer and incubated O/N at 4°C. Cover slips were washed with PBS and subsequently incubated with 1:400

Alexa-conjugated secondary antibodies (Invitrogen) for 45min at RT in the darkness. Finally, cells were washed and mounted using mounting media containing DAPI. Cells were visualized using a Nikon E1000 epifluorescence microscope, a Leica TCS SPE confocal microscope or a SCANR confocal microscope.

In the case of RPA, a pre-extraction step using CSK I buffer (10mM PIPES, 100mM NaCl, 300mM sucrose, 3mM $MgCl_2$, 1mM EGTA, 0.5% Triton X-100) was performed prior to fixation in order to remove the soluble RPA fraction.

For ssDNA detection using non denaturating BdrU staining, cells were incubated for 48h with 10µM BrdU and fixed in methanol at -20°C for 1h. Blocking and staining was performed as previously.

Nuclear signal intensity (γ-H2AX and MCMs) and dot detection (53BP1, RPA and BrdU) were performed using Fiji Macros written by the Advanced Digital Microscopy Unit (IRB Barcelona). Briefly, these macros detect the nuclei in the DAPI channel. Then, signal intensity or number of dots are quantified inside every pre-detected nuclei. The outcome of the macros are the mean intensity or the number of dots in every single nuclei.

2.4.10. Telomere staining

Telomeres were detected in chromosome spreads using Telomere PNA FISH Kit following manufacturer´s manual. Briefly, metaphase spreads preparations were pretreated with a commercial buffer, dehydrated in increasing concentrations of ethanol and air-dried. The telomeric probe was added and samples were subjected to denaturation at 80°C for 5min and hybridization at RT for 4h. Then, the probe was rinsed using a commercial buffer, washed at 65°C, de-hydrated again in the same alcohol series and air-dried. Finally, slides were mounted with media containing DAPI. Spreads were visualized using a Leica TCS SPE confocal microscope.

2.4.11. Time-lapse imaging

For time-lapse imaging, cells were seeded in 6well plates and images were taken in a SCANR confocal microscope. Images were taken every 5-15min depending on the experiment. In case of H2B-GFP cells, Fluorobritte DMEM was used in order to optimize fluorescence acquisition. Videos were analyzed using Fiji Software.

2.4.12. DNA replication fiber assay

Labeling actively progressing replication forks with BrdU analogs allows the analysis of the DNA replication process at the single molecule level.

Cells were pulsed with 10µM IdU for 20min, washed in warm media and pulsed again with 100µM CldU for the same time. Cells were resuspended in ice cold PBS, and 2µl of the cell solution were transferred to a microscope slide and incubated with 7µl of spreading buffer (200mM Tris-HCl pH 7.5, 50mM EDTA and 0.5% SDS) for 5min. Slides were then tilted to allow DNA to spread. Fixation was perform with methanol:acetic acid (3:1) for 10min. DNA was denatured in 2.5M HCl for 1h at RT, rinsed in PBS and blocked in 1% BSA/1% Triton X-100 in PBS for 1h at RT before staining with primary antibodies: anti-BrdU (AbD Serotec, OBT 0030G) and mouse anti-BrdU (Becton Dickinson, 347580) antibodies to detect CldU and IdU, respectively. Alexa Fluor-conjugated antibodies were incubated for 1h at RT and after several PBS washes, slides were mounted in mounting media containing DAPI. Tracks were imaged on a Leica TCS SPE confocal microscope, images were analyzed using Fiji software and fork rate was calculated using ((length(µm)*2.59kb/µm)/pulse time). At least 200 tracks were analyzed in every experiment. For asymmetry rate determination, bidirectional fibers were imaged. CIdu-labeled tracks were measured and left versus right length was calculated. At least 30 bidirectional fibers were analyzed in every experiment. For inter-origin distance measurement, fibers with at least two origins were used and distance between two origins was determined.

2.4.13. COMET assays

COMET assay, also known as Single Cell Gel Electrophoresis assay (SCGE) is a method for measuring DNA breaks at the single cell level. It is based on the measurement of the migration of DNA supercoils; if DNA is damaged, supercoils are relaxed and broken ends are able to migrate, while if undamaged, the lack of free ends and the large size of the fragments prevent migration. Two variants exist: neutral COMET for DSB detection and alkaline COMET for SSBs detection.

For both neutral and alkaline COMET, three agarose solutions were prepared in PBS: 2% agarose, 1% low-melting agarose and 0.5% low-melting agarose and kept at 37°C. Slides were pre-coated with 2% agarose before starting the experiment. Then, cells were harvested in ice cold PBS at a 10^6 cells/ml density. 15µl of this cell suspension were mixed with 90µl of 0.5% low-melting agarose and transferred onto pre-coated slides. Cell-containing agarose was incubated for 30min at 4°C and a second layer of 90µl of 1% low-melting agarose was added and incubated for 30min at 4°C. Lysis and the subsequent procedure depend on the COMET variant.

2.4.13.1. Neutral COMET

Slides were immersed in neutral lysis solution (0.5mg/ml proteinase K, 2% sarkozyl in 500mM EDTA pH8) at 37°C for 16-20h. Slides were subjected to 3 washes of 10min with neutral electrophoresis buffer (90mM Tris buffer, 90mM boric acid and 2mM EDTA, pH 8.5) and run in an agarose gel tank for 25min at 20V. After washing in dH_2O, nuclei were stained with Hoechst for 20min and washed once in PBS and twice in dH_2O. Pictures were taken using a Nikon E1000 epifluorescence microscope and tail moment was calculated using the OPENCOMET plugin for Fiji.

2.4.13.2. Alkaline COMET

Slides were immersed in alkaline lysis solution (2.5M NaCl, 100mM EDTA, 10mM Trizma base and 1% sarkozyl, pH 10) at 4°C for 18-20 h. Slides were subjected to 3 washes of 10min with alkaline electrophoresis buffer (30mM NaOH and 2mM EDTA, pH 12.5) and run for 25min at 10V. After washing in dH_2O, nuclei were stained with Hoechst for 20min and washed once in PBS and twice in dH_2O. Pictures were taken using a Nikon E1000 epifluorescence microscope and tail moment was calculated using the OPENCOMET plugin for Fiji.

2.4.14. Intracellular ROS levels quantification

Reactive oxygen species were quantified using DCFDA (2′,7′-dichlorodihydrofluorescein diacetate), a fluorogenic dye that becomes highly fluorescent following oxidation by intracellular ROS**.**

Cells were incubated for 30min at 37°C with 10µM DCFDA. Then, cells were trypsinized and resuspended in PBS containing 1.4µg/ml aprotinin. DCF fluorescence of 10000 cells was measured using a Gallios Flow Cytometer. DCF fluorescence intensity was analyzed using FlowJo software.

2.4.15. 8-OHdG level determination

ROS and other free radical cause oxidative damage to several biomolecules including DNA. 8OHdG is one type of oxidative DNA damage that has been used a biomarker for oxidative stress.

Cells were harvested and fixed in 70% cold ethanol. After fixation, DNA was denatured in 2M HCl for 20 min in ice, washed in PBS, resuspended in H_2O and incubated at 95°C for 5min. After centrifugation, cells were stained with 8-OHdG antibody diluted in 2%BSA/0.25% Tween 20 in PBS for 1h at RT. Cells were washed in PBS and incubated for 1h at RT with an Alexa-Fluor secondary antibody (Invitrogen). After washing, fluorescence intensity was measured using a Gallios Flow Cytometer and data was analyzed using FlowJo software.

2.4.16. Homologous recombination assay

The DR-GFP construct was used to measure homologous recombination efficiency. DR-GFP consists of two mutated GFP genes; the upstream repeat contains the recognition site for the I-SceI endonuclease and the downstream repeat is a 5´and 3´truncated GFP fragment. Transient expression of I-SceI causes a DSB in the upstream gene, which is repaired through HR using the downstream copy, resulting in GFP(+) cells.

Cells from a 10cm culture dish were trypsinized, washed in PBS and resuspendend in 100µl of Resuspension Buffer R (Invitrogen). 5µg of DR-GFP plasmid were added to the cell suspension and electroporated with 1pulse of 30ms width and 1350V in a Neon Transfection System (Invitrogen). Cells were plated again on a 10cm plate and the next day puromycin was added in order to initiate the antibiotic selection. Once selected, DR-GFP cells were electroporated again with I-SceI and 24h later 4-OHT treatment was performed. Two days after Cre induction and p38α deletion, cells were harvested, resuspended in PBS and 20000 cells were acquired in a Gallios Flow Cytometer. The percentage of GFP(+) cells was analyzed using FlowJo software.

2.5. STATISTICAL ANALYSIS

Data, unless indicated otherwise, are presented as mean±SEM. Statistical significance was determined by Student´s test using Graph Pad Prism software. p-values < 0.05 (*), < 0.1 (**) and < 0.01 (***) were considered statistically different.

Statistical analysis in PDX model treatments was performed by Camille Stephan-Otto (IRB Biostatistics Unit) using R programming language. For all time points volumes were divided by the size of the corresponding lesion at time 0 of treatment. For each time point a linear model was fitted with experimental batch and mouse as nested random effects. Coefficients and p-values for the comparisons of interest were computed through the "glht" function from the multcomp (Hothorn et al., 2008) R package using the "Westfall" multiplicity adjustment method. p-values < 0.05 (*), < 0.1 (**) and < 0.01 (***) were considered statistically different.

RESULTS

1. ***Characterization of PyMT mice with inducible p38α deletion***

To investigate the influence of p38α in breast tumor progression *in vivo*, we combined the PyMT mouse model with floxed conditional alleles of p38α. Mice expressing the PyMT transgene were crossed with mice carrying p38α$^{lox/-}$ and Ubiquitin-CreERT2 (CreERT2) alleles. This way, p38α could be deleted at any time of the tumor development upon 4-hydroxitamofixen (4-OHT) administration.

We initially tested the efficiency of p38α deletion in different organs, since Cre recombinase expression was expected in all tissue types. We observed almost a 100% downregulation on most of the studied organs, including the mammary tissue. The ones with higher residual p38α expression, spleen and thymus, corresponded to the tissues with higher turnover of the panel (Fig. 13).

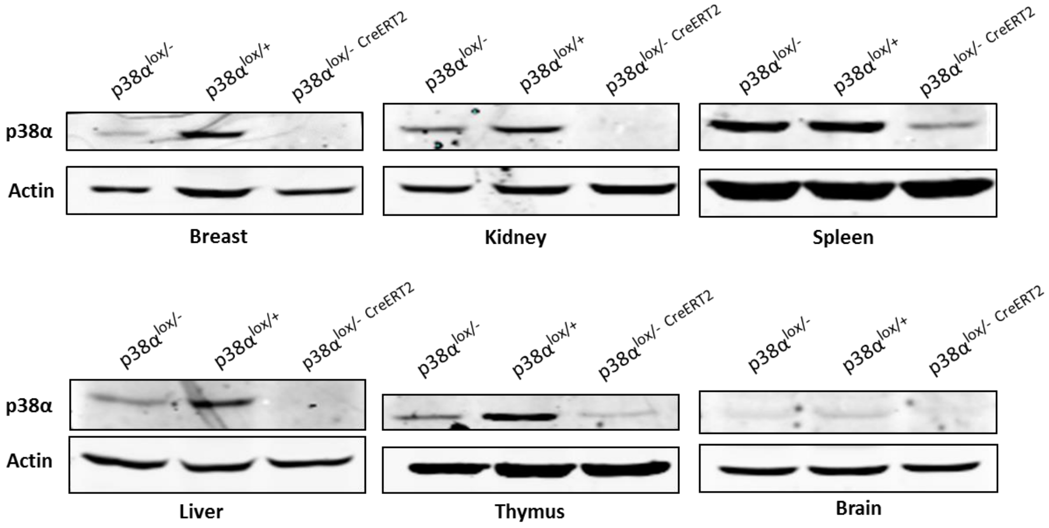

Figure 13. Cre efficiency in different tissues. Mice were subjected to 4-OHT treatment and sacrificed 10 days after the last 4-OHT injection. Western blot analysis of p38α was performed in lysates from different tissues. p38α$^{lox/+}$ and p38α$^{lox/-}$ animals were chosen as references for complete dose and half dose of the protein. Cre efficiency was assayed in a p38α$^{lox/- CreERT2}$ mouse.

Additionally, we studied the expression and activation pattern of p38α during PyMT-induced tumor progression. PyMT mice start showing hyperplasia at 4 weeks, adenomas are visible at 8 weeks and carcinomas appear between 8 and 12 weeks (Lin et al., 2003). We sacrificed mice at different stages of tumor development and analyzed p38α protein status. Tumor growth was evidenced by the increased expression of PyMT, the driving oncogene present in the epithelial cancer cells, and E-cadherin, an epithelial marker that correlates with increased cellular mass. Although we observe a transient increase of p38 MAPK phosphorylation at six weeks, p38α did not show significant changes, neither at the expression nor at the phosphorylation level, compared to age-matched tumor-free littermates (Fig. 14), suggesting that p38α is not involved in tumor initiation in this context.

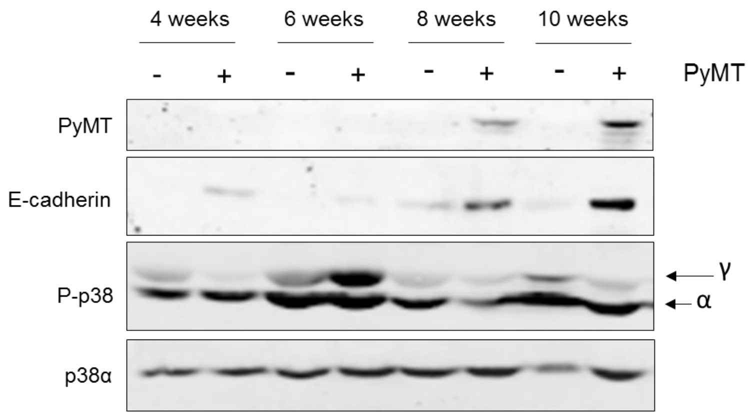

Figure 14. p38α expression and activation pattern during PyMT-induced tumorigenesis. Western blot of mammary tissue from PyMT mice and age-related littermates at the indicated times.

2. p38α expression in tumor epithelial cells is essential for PyMT-induced breast cancer progression in vivo

In order to study the role of p38α in breast cancer progression and not initiation, mammary tumors were allowed to grow and once developed, mice were treated with 4-OHT in order to induce Cre activation and delete p38α. We found that p38α deletion (p38αΔ) resulted in a regression of the tumor while PyMT WT littermates, either p38α$^{+/-\ \mathrm{CreERT2}}$ or p38α$^{\mathrm{lox/-}}$, showed continuous tumor growth (Fig. 15A). The downregulation of p38α was confirmed by quantitative real time PCR (qRT-PCR), where we also observed an upregulation of its direct activator MKK6 (Fig. 15B), likely due to a negative feedback loop (Ambrosino et al., 2003). At the protein level, together with p38α downregulation, we detected the downregulation of MK2, one of its direct substrates, and the upregulation of MKK6 (Fig. 15C) indicating that p38α signaling was impaired.

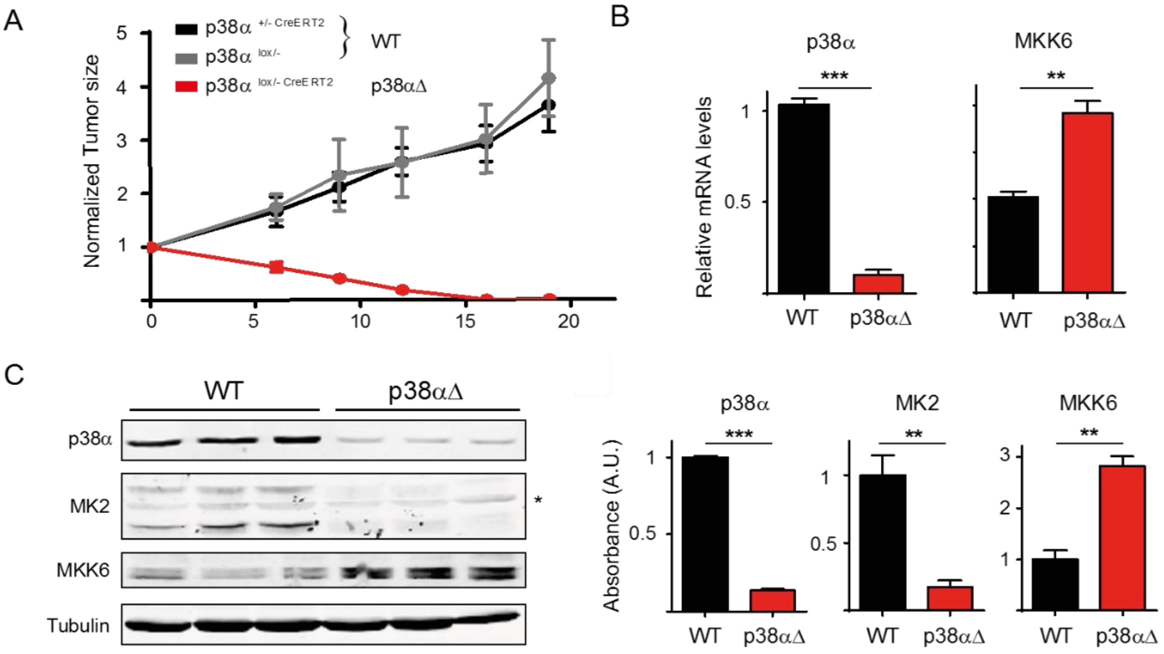

Figure 15. Analysis of p38α downregulation in PyMT mice. A) Tumor growth curves of mice expressing MMTV-PyMT treated with 4-OHT for 5 days. Measurements were normalized to the initial tumor size. At least six animals were analyzed in every group. B) Relative p38α and MKK6 mRNA levels in three independent WT and p38αΔ tumors at day 15. C) Western blot for the indicated proteins in WT and p38αΔ tumors at day 15. Quantification is represented in the bar graphs.

Histological analysis of the mammary fat pads revealed that although p38αΔ mice had no palpable tumors, their mammary tissue was not completely normal. These mice showed mainly hyperplastic tissue and small carcinoma areas, while WT littermates displayed histology more consistent with advanced tumor stages, as shown by the solid sheet of epithelial cells where no acinar structures were visible (Fig. 16A). In agreement with a reduced tumor mass, the mammary tissue of p38αΔ mice showed a 75% reduction in the epithelial cell compartment compared to WT mice (Fig. 16A). Moreover, Ki67 and TUNEL stainings showed a decreased proliferation (Fig. 16B) and an increased cell death (Fig. 16C) in p38αΔ mice, which was consistent with the tumor regression observed following p38α deletion. Additionally, we observed a four-fold increase in the levels of phosphorylated histone variant H2AX, referred to as γ-H2AX (Figure 16D), indicating that p38α downregulation resulted in higher levels of DNA damage.

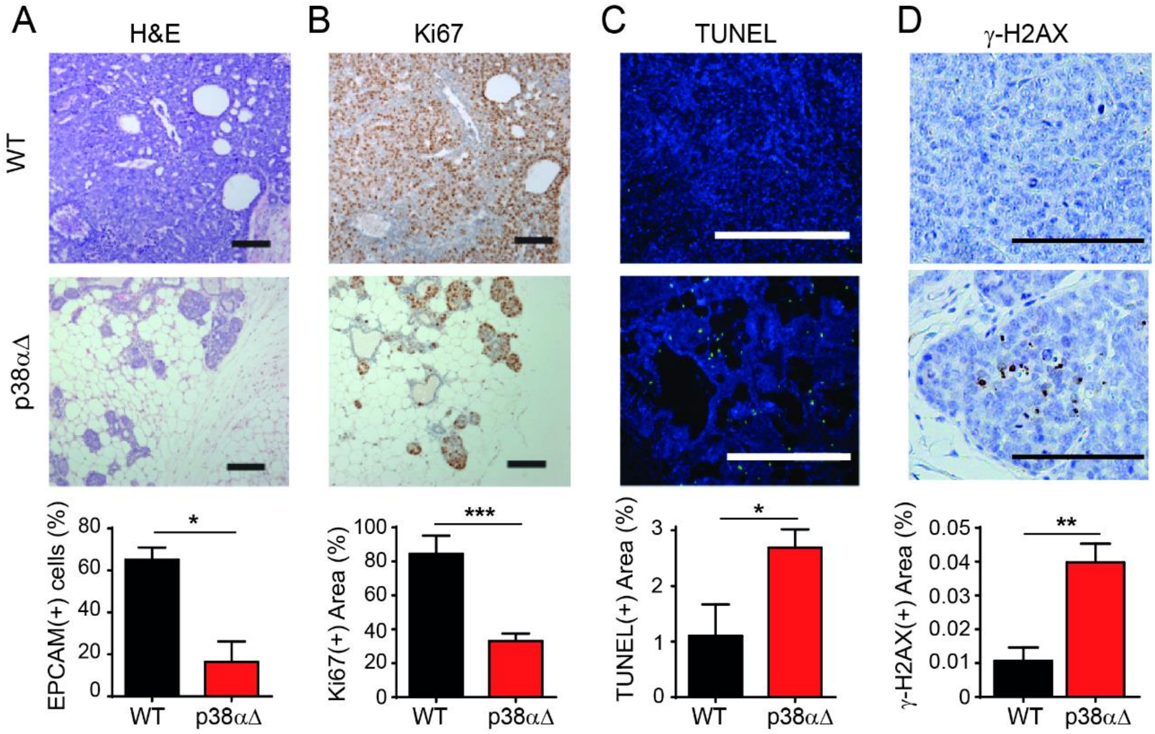

Figure 16. p38αΔ tumors show milder histological lesions, together with lower cell proliferation and increased cell death and DNA damage. Representative images of WT and p38αΔ tumors at day 15 are shown**.** At least three independent animals per group were analyzed**.** A) H&E images. Graph represents the percentage of epithelial cells of the tumor. B) Ki67 staining. Quantification of Ki67(+) area is shown in the graph. C) TUNEL staining. Quantification of TUNEL(+) area is shown in the graph. D) γ-H2AX staining. Quantification of γH2AX(+) area is shown in the graph. Bars = 100µm

When PyMT p38α$^{lox/-CreERT2}$ mice were followed for longer times after 4-OHT administration, we noticed that at later timepoints tumors started to re-grow (Fig. 17A). These relapsing tumors were almost identical to initial WT tumors in terms of proliferation (Fig. 17B), cell death (Fig. 17C) and epithelial content (Fig. 17D). We sorted epithelial cells from these tumors (Fig. 17E) at different timepoints, extracted DNA, and examined the extent of p38α deletion at the genomic level. At day 15, when tumors were not palpable, around 25% of the remaining epithelial cells contained the floxed exon 2 of p38α. However, by day 40, when re-grown tumors were as big as initial tumors, the floxed exon 2 was detected in most of the epithelial cells (Fig. 17F), suggesting that relapsed tumor masses arose mainly from escaper cells that never deleted p38α. These results indicated that p38α deletion did not occur in all the cancer epithelial cells and those retaining p38α expression had a competitive advantage that made them repopulate the tumors.

Altogether, these results supported the essential role of p38α in tumor homeostasis by promoting mammary tumor cell proliferation and survival.

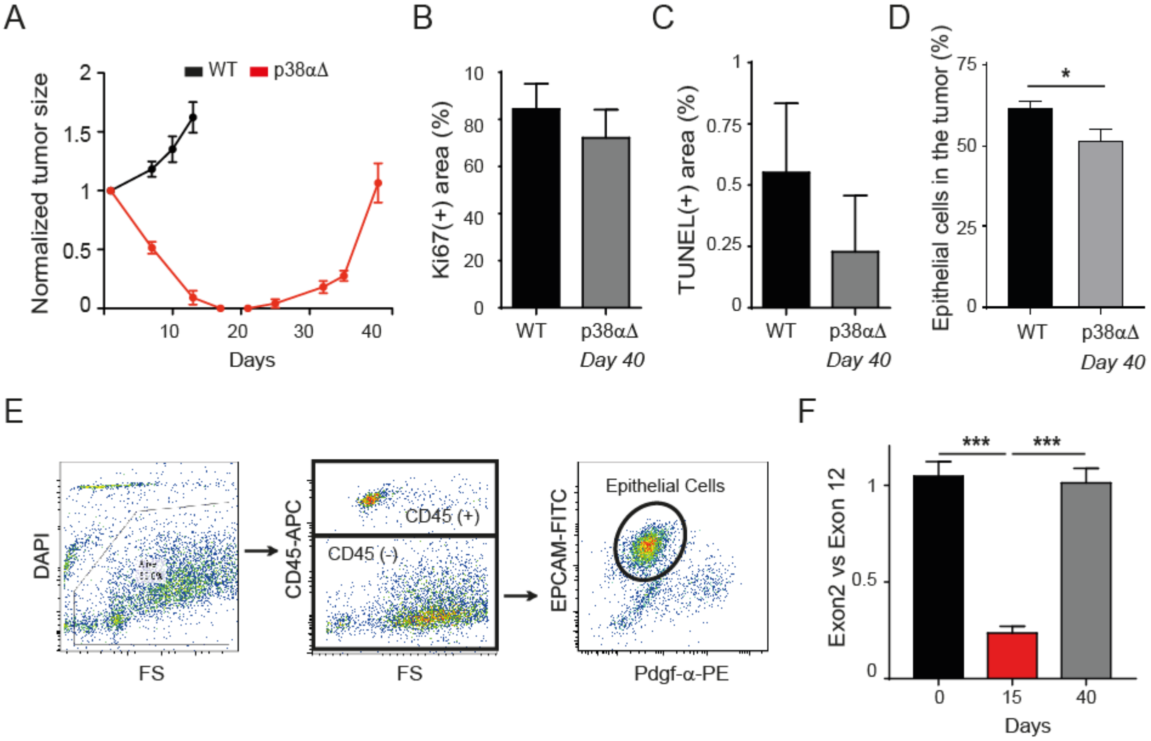

Figure 17. p38α expressing escaper cells repopulate tumors. A) Tumor growth curves in mice expressing MMTV-PyMT treated with 4-OHT for 5 days. Measurements were normalized to the initial tumor size. At least 8 animals were analyzed in each group. B) Percentage of Ki67(+) area in at least two WT and p38α$^{lox/-CreERT2}$ mice at day 40. C) Percentage of TUNEL(+) area in at least two WT and p38α$^{lox/- CreERT2}$ mice at day 40. D) Percentage of epithelial cells in the tumors from three independent WT and p38αΔ mice at day 40. E) Workflow for sorting of epithelial cells from PyMT-induced mammary tumors. F) Analysis of genomic deletion of the floxed exon2 of p38α in in p38α$^{lox/- CreERT2}$ tumors before 4-OHT administration and at day 15 and 40. At least three independent mice were analyzed in every timepoint.

3. Establishment and characterization of cell lines derived from PyMT tumors

To study the role of p38α in PyMT epithelial breast cancer cells and to investigate the molecular mechanisms underlying mammary tumor regression *in vivo*, we established epithelial cell cultures derived from PyMT-induced tumors (Fig. 18).

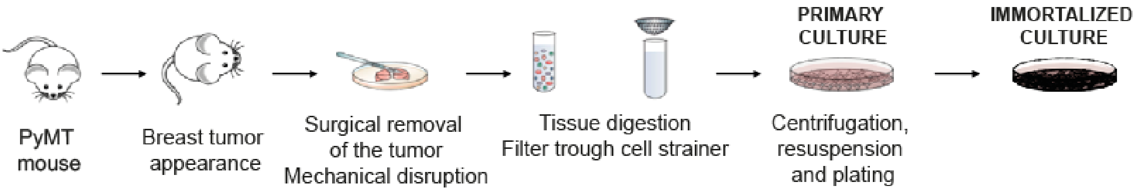
PyMT mouse
Breast tumor appearance
Surgical removal of the tumor Mechanical disruption
Tissue digestion Filter trough cell strainer
PRIMARY CULTURE
Centrifugation, resuspension and plating
IMMORTALIZED CULTURE

Figure 18. Schematic of the protocol used to derive cell lines from PyMT-induced mammary tumors. Advanced tumors from mice around 3 months old were used for deriving cell cultures. Immortalized cultures were achieved at around passage 16, after approximately two months in culture.

We initially obtained primary cultures from p38α$^{lox/-}$ and p38α$^{lox/-CreERT2}$ tumors and corroborated that 4-OHT incubation efficiently deleted p38α in these cells. We also examined the phosphorylation of HSP27, a target of the p38α pathway, and confirmed that it was decreased (Fig 19), indicating the downregulation of the signaling pathway.

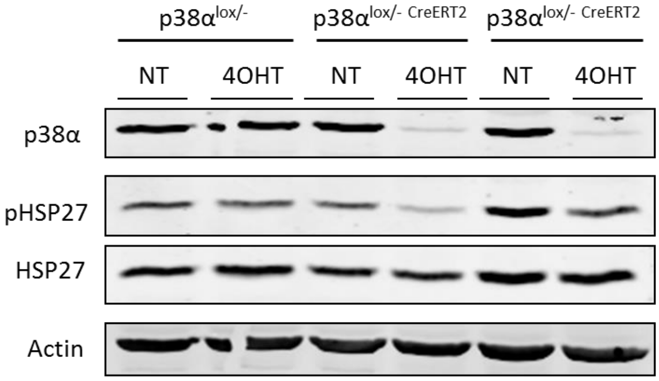
p38αlox/-
p38αlox/- CreERT2
p38αlox/- CreERT2
NT
4OHT
NT
4OHT
NT
4OHT
p38α
pHSP27
HSP27
Actin

Figure 19. 4-OHT incubation efficiently deletes p38α from primary tumor cells in culture. Western blot analysis for the indicated proteins were performed in three tumor-derived primary cell cultures: one control line (p38α$^{lox/-}$) and two independent p38α$^{lox/- CreERT2}$ lines. NT: non treated

We performed basic cell proliferation and cell death analysis on these primary tumor cells. We observed that 4-OHT did not have any effect on the proliferation rate or cell death of p38α$^{lox/-}$ cells. In p38α$^{lox/- CreERT2}$, however, 4-OHT incubation lead to Cre induction and p38α deletion, and these p38αΔ cells consistently showed decreased proliferation and increased cell death in two independent cell lines (Fig. 20A and 20B). This indicated that p38α was essential for the homeostasis of PyMT epithelial cancer cells and suggested that the tumor regression following p38α deletion observed *in vivo* was, at least in part, due to the impaired survival of the epithelial tumor cells.

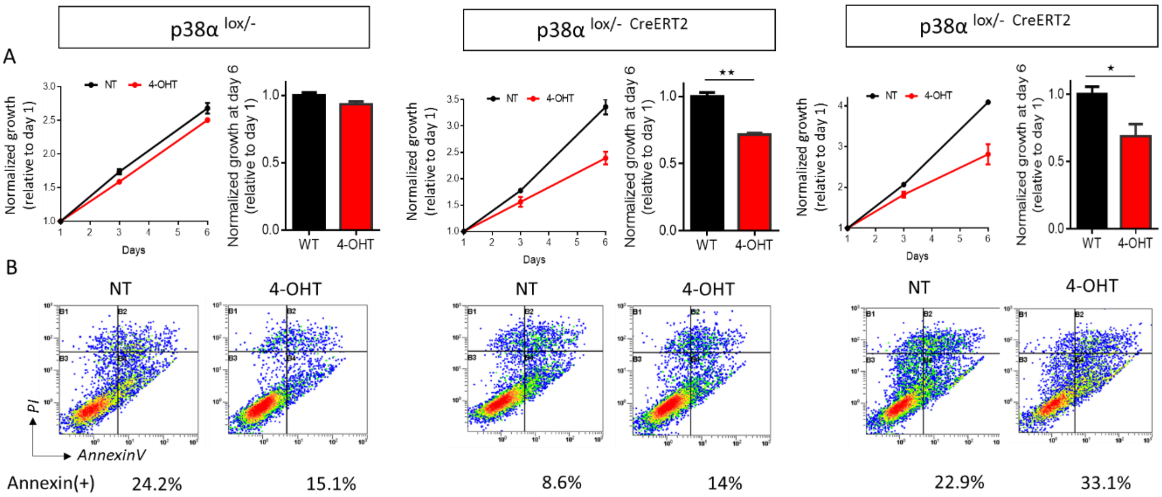

Figure 20. p38α deletion results in decreased proliferation and increased cell death in primary PyMT cancer cells. One control line (p38α$^{lox/-}$) and two independent p38α$^{lox/-\ CreERT2}$ lines were analyzed. A) Cell cultures were subjected to MTT analysis during six days. Values were normalized to the initial day. Bar graphs show the normalized tumor growth at the end of the experiment. B) Annexin V staining was performed 4 days after 4-OHT incubation. Dot plots of non-treated (NT) and 4-OHT treated cells are shown. Percentages of annexin V (+) cells are indicated below.

The primary cultures recapitulated the *in vivo* behavior of the PyMT-induced tumors in terms of proliferation and cell death; however, they showed a high basal death as shown in Fig. 20B and started to enter senescence between passages 5-7. Therefore, we decided to establish cell lines by passaging these primary cultures until spontaneously immortalized, which took about 16 passages.

The immortalized cancer cell lines grew well, showed a typical epithelial morphology (Fig. 21A) and were 100% positive for the epithelial marker EPCAM (Fig. 21B). In addition, we phenotypically characterized these cells (Fig. 21C) and confirmed that PyMT tumor-derived cell cultures retained the differentiation features of epithelial cancer cells *in vivo*. Of note, cells were mostly ERα(-), PgR(-), which is a typical feature of the advanced stages of PyMT tumors and of poor prognosis breast human cancers. Therefore, the immortalized cell lines recapitulated important features of the breast tumors and provided a relevant system to analyze the molecular basis for the enhanced tumor cell death and reduced tumor size observed upon p38α deletion *in vivo*.

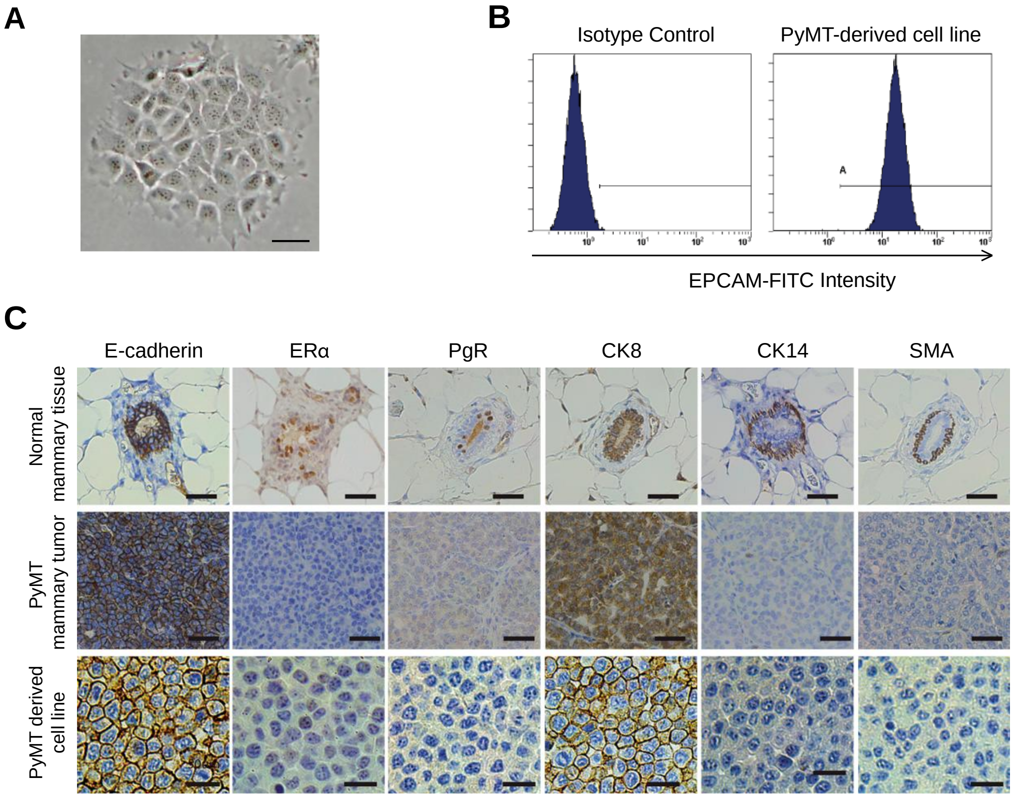
A
B
Isotype Control
PyMT-derived cell line
A
EPCAM-FITC Intensity
C
E-cadherin
ERα
PgR
CK8
CK14
SMA
Normal mammary tissue
PyMT mammary tumor
PyMT derived cell line

Figure 21. Characterization of immortalized PyMT epithelial cell lines. A) Bright field image of PyMT-expressing cell line. Bar=25µm. B) EPCAM-FITC fluorescence intensity plot and its corresponding isotype control. C) Immunohistological characterization of the cell lines derived from PyMT-induced tumors compared to PyMT-induced advanced tumors and normal mammary fat pads. Bars = 50 µm.

4. Functional characterization of p38α deletion in immortalized PyMT epithelial cells

We initially tested the Cre-recombinase efficiency and specificity in the immortalized PyMT epithelial cell lines. For this purpose, we examined the expression of the MAPK14 gene and its surrounding genes (Fig. 22A). We confirmed that 4-OHT-induced Cre activation efficiently deleted the exon 2 of MAPK14, but did not affect the expression of its nearby genes MAPK13, SKRP1 and SLC26a8 (Fig. 22B). Therefore, although we cannot rule out other unspecific recombination events far away from the target sequence, these results indicated that Cre recombinase effectively deleted exon 2 of MAPK14 without affecting adjacent sequences in the PyMT cancer cells.

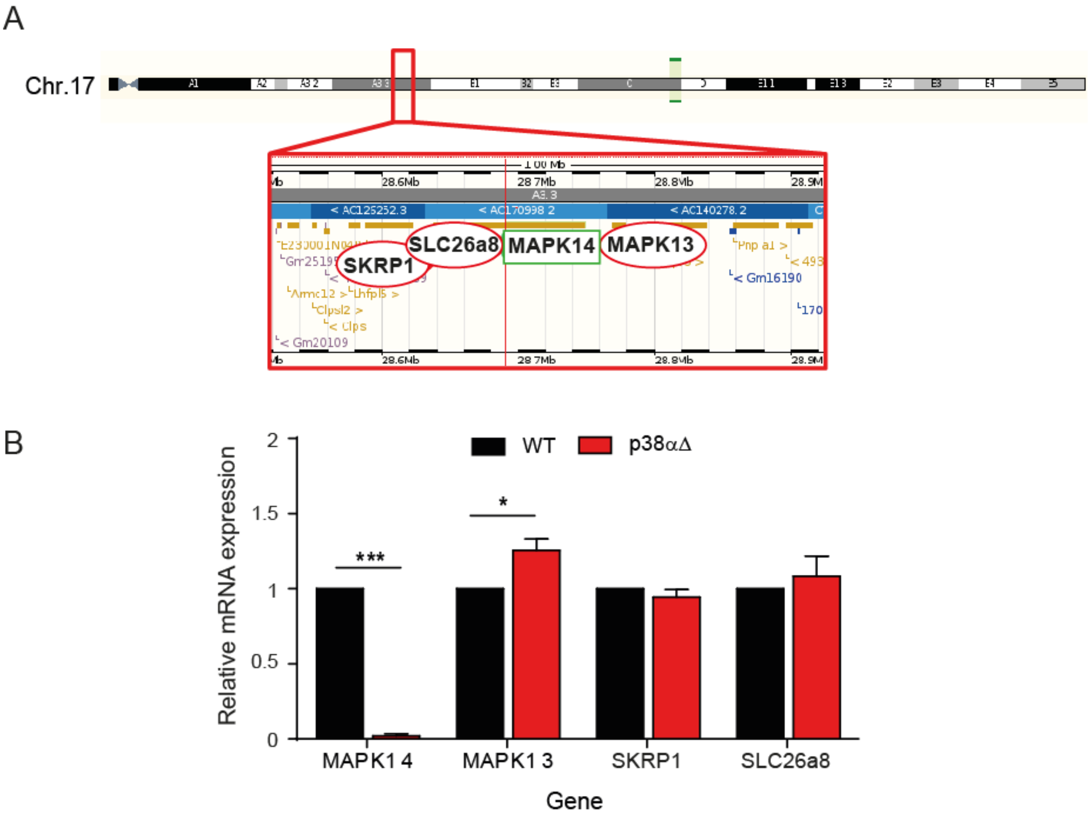

Figure 22. Cre recombinase efficiently deletes MAPK14 exon 2 without affecting the expression of adjacent genes. A) Map of chromosome 17 with a zoom on the MAPK14 locus. Modified from ensembl.org. B) Relative mRNA expression levels of MAPK14 exon 2 and the indicated surrounding genes. Data correspond to three independent experiments including two different PyMT-expressing cell lines.

Then, we functionally studied the effects of p38α deletion in the immortalized cancer cell lines. We verified that the tumor cells in culture efficiently deleted p38α protein upon treatment with 4-OHT (Fig. 23A). Consequently, we also found decreased phosphorylation of the downstream target HSP27 and increased levels of its activator MKK6 (Fig. 23A), indicating that p38α signaling pathway was impaired. We confirmed that p38α was also essential for the viability of these immortalized tumor cells, as p38α depletion greatly reduced the ability of the cells to form colonies (Fig. 23B). We did not find significant differences in the cell cycle of WT and p38αΔ cells, except for a slight decrease in S-phase (Fig. 23C). However, we observed decreased levels of DNA replication, which were evident at early time points (Fig. 23D), and increased cell death, mainly observed at later time points (Fig. 23E), which correlated with the lower viability of p38αΔ cells. Biochemical analysis supported these results, as we observed the downregulation of the proliferation-associated AKT pathway, and the upregulation of JNK signaling and cleaved-caspase 3, both indicative of increased cell death (Fig. 23F).

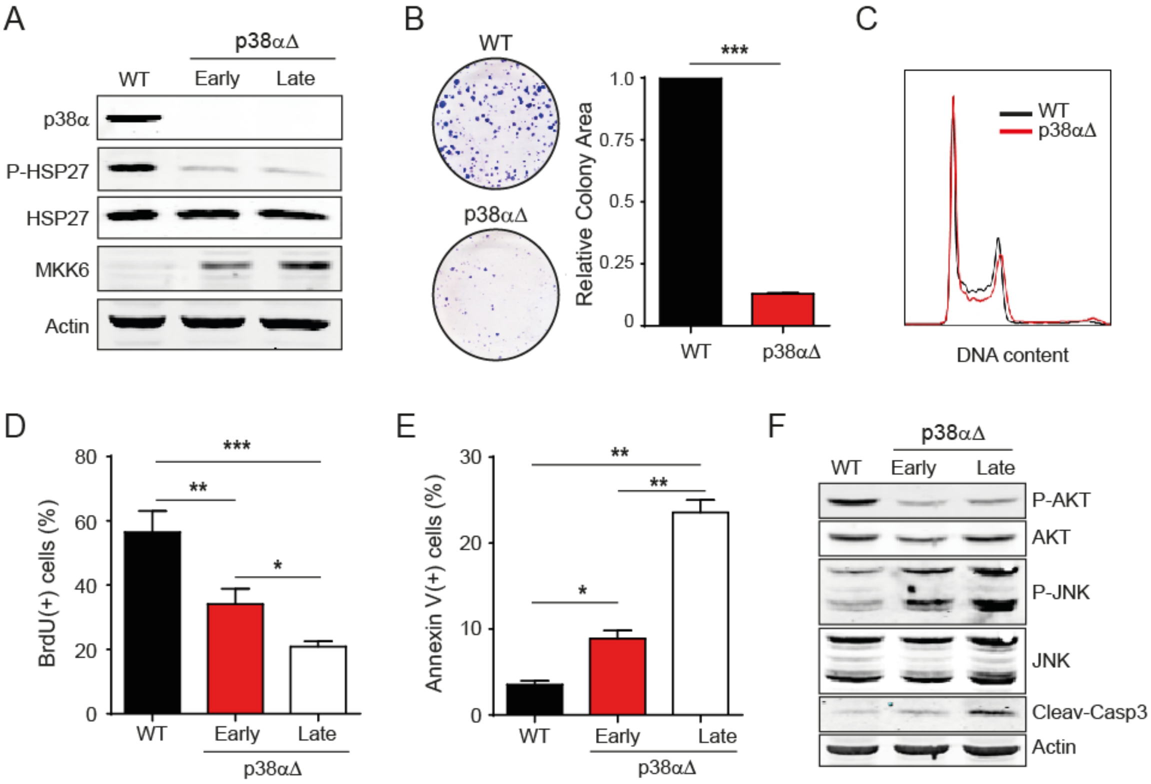

Figure 23. Cancer cells derived from PyMT-induced mammary tumors reproduce the *in vivo* tumor behavior. Early and Late refer to two and six days after the 4-OHT treatment, respectively. If not indicated, experiments were performed at the early timepoint. A) Cells were analyzed by western blot for the indicated antibodies. B) Colony formation assay using WT and p38αΔ cells. Bar graph shows the quantification of two independent experiments. C) Representative cell cycle profiles of WT and p38αΔ cells. D) BrdU uptake in WT and p38αΔ cells. Bar graph represents the quantification of three independent experiments. E) Annexin V staining of WT and p38αΔ cells. Bar graph represents the quantification of two independent experiments. F) WT and p38αΔ cells were analyzed by western blot using antibodies against the indicated proteins.

To further characterize the cell death mechanism, we treated p38αΔ cells with the caspase inhibitor Z-VAD-FMK (ZVAD) and performed an annexin V cell death assay. We chose nutlin as a positive control, a compound that inhibits the interaction between p53 and its negative regulator MDM2, stabilizing thus p53 and ultimately leading to caspase dependent apoptosis. ZVAD incubation neither reverted nor lowered cell death in p38αΔ cells (Fig. 24A), while a complete rescue was obtained in the case of nutlin (Fig. 24B). This suggested that cell death following p38α deletion was not uniquely caspase-dependent and that other cell death mechanisms, apart from apoptosis, were taking place. Of note, cell death was detected at late timepoints (six days after 4-OHT incubation and p38α deletion). Therefore, it was likely not a direct effect of p38α deletion, but rather a consequence of cellular defects accumulated during this time in the absence of p38α. This would explain on the one hand the later appearance of cell death compared to the early drop in proliferation and, on the other hand, it would also explain why inhibiting caspase 3 (and caspase 1 to a less extent) was not enough to stop the massive cell death.

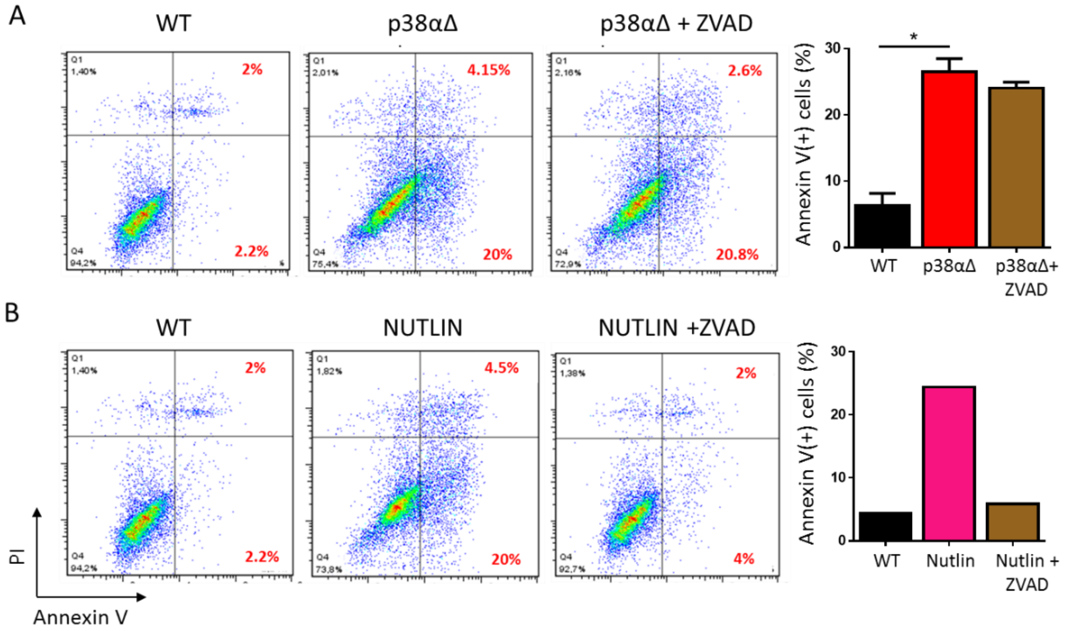

Figure 24. ZVAD caspase inhibitor does not revert cell death in p38αΔ cells. A) 50µM ZVAD was added every other day to p38αΔ cells till day 6 after 4-OHT incubation. Dot plots show annexin V and PI staining in the indicated conditions. Bar graph represents the percentage of annexin V(+) cells in two independent experiments. B) As positive control, WT cells were incubated in 10µM nutlin for 48h with or without 50µM ZVAD. Quantification of the percentage of annexin V(+) cells is shown in the bar graph. The percentage of annexin V (+)/PI(-) and annexin V (+)/PI(+) in every plot is indicated in red.

Altogether, our results indicated that p38α was required for breast cancer cell viability, both *in vivo* and *in vitro*, and that its deletion resulted in cancer cell death and mammary tumor regression in a PyMT tumorigenesis model.

4.1. p53 status characterization

The tumor suppressor p53 is essential for maintaining cellular genomic integrity and it has been described to be mutated in about half of all cancers (Muller and Vousden, 2013). In response to several signals, p53 can mediate a plethora of cellular outcomes such as cell cycle arrest, senescence, differentiation or apoptosis. Therefore, p53 status is important to understand the role of other proteins in a tumor cell.

In order to functionally test p53, we treated PyMT epithelial cells with the p53 activator nutlin and analyzed the expression of p21, one of its main downstream targets. $p53^{WT}$ cells HCT116 upregulated p21 following p53 activation, while $p53^{MUT}$ SW620 did not show any response. PyMT tumor cells, as shown in Fig. 25A and 25B, upregulated p21 both at the mRNA and the protein levels following nutlin incubation, indicating that they expressed a functional p53 gene.

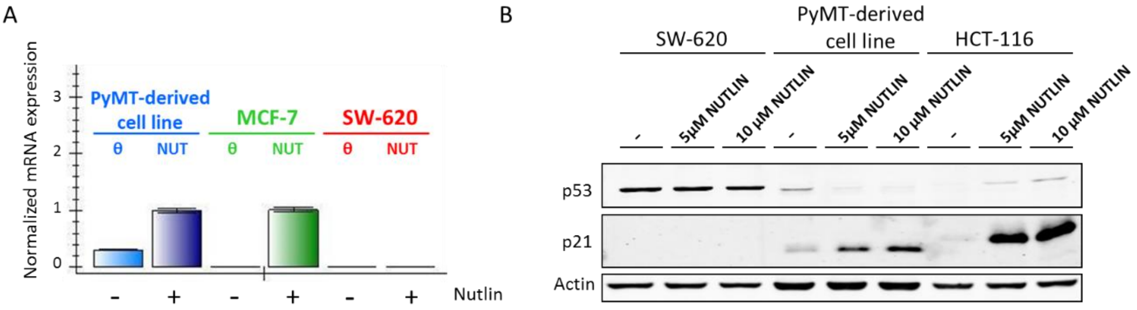

Figure 25. PyMT epithelial cells express a functional p53 gene. A) Cells were incubated with 10µM nutlin for 24h and p21 mRNA levels were analyzed by qRT-PCR. MCF-7 and SW620 human cells were used as $p53^{WT}$ and $p53^{MUT}$ cells respectively. B) Cells were incubated with 5 or 10µM nutlin for 24h and p53 and p21 protein levels were analyzed by western blot. HCT-116 and SW620 human cell lines were used as $p53^{WT}$ and $p53^{MUT}$ controls respectively.

Of note, in the absence of p38α, p21 and MDM2 mRNA levels were upregulated after p53 activation, indicative of the transcriptional activity of p53 (Fig. 26A). However, protein levels did not respond accordingly and p21 did not increase upon nutlin incubation in p38αΔ cells (Fig. 26B). This probably reflects that p38α can modulate p21 protein expression independently of transcription.

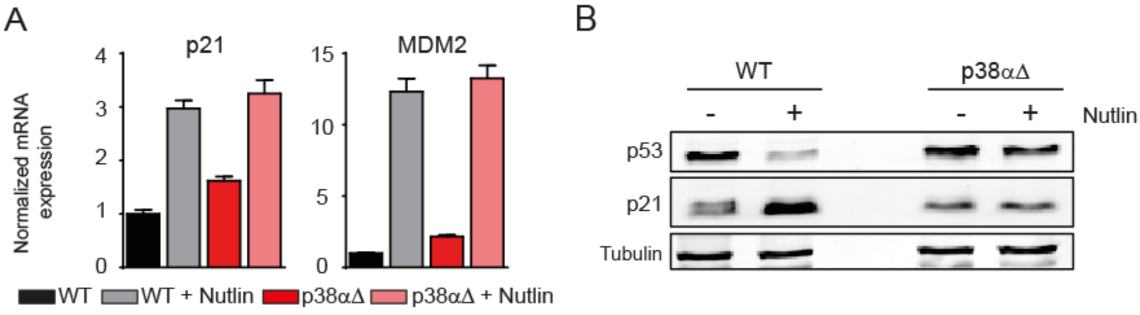

Figure 26. p38α cooperates in the p21 regulation at the post-transcriptional level. WT and p38αΔ cells were treated with 10µM nutlin for 24h. A) p21 and MDM2 mRNA levels were analyzed by qRT-PCR. Bar graphs show the data of one representative experiment. Similar results were obtained in a second independent experiment. B) p53 and p21 protein levels were analyzed by western blot. Results were reproducible in three independent experiments.

These results correlated with previous work where p38 MAPK signaling was shown to be required for the p21 mRNA stabilization and protein accumulation following γ-radiation (Lafarga et al., 2009).

4.2. Receptor status characterization

Another important feature of breast cancer is the status of certain membrane receptors: ERα, PgR, and Her2. These hormone and growth receptors, when bound by their ligands, activate several signaling pathways that contribute to cellular proliferation and to sustain tumor growth. Determination of the status of ERα, PgR, and Her2 is of great interest since their expression is used to classify breast cancers into different subgroups which predict the outcome and contribute to treatment decision.

We immunohistochemically analyzed the expression of these three receptors in PyMT cancer cell pellets and found that ERα expression was increased following p38α deletion, while no difference was found in the case of PgR and Her2 (Fig. 27A). We then examined the mRNA (Fig. 27B) and protein levels (Fig. 27C) of ERα, confirming that this receptor was upregulated in the absence of p38α.

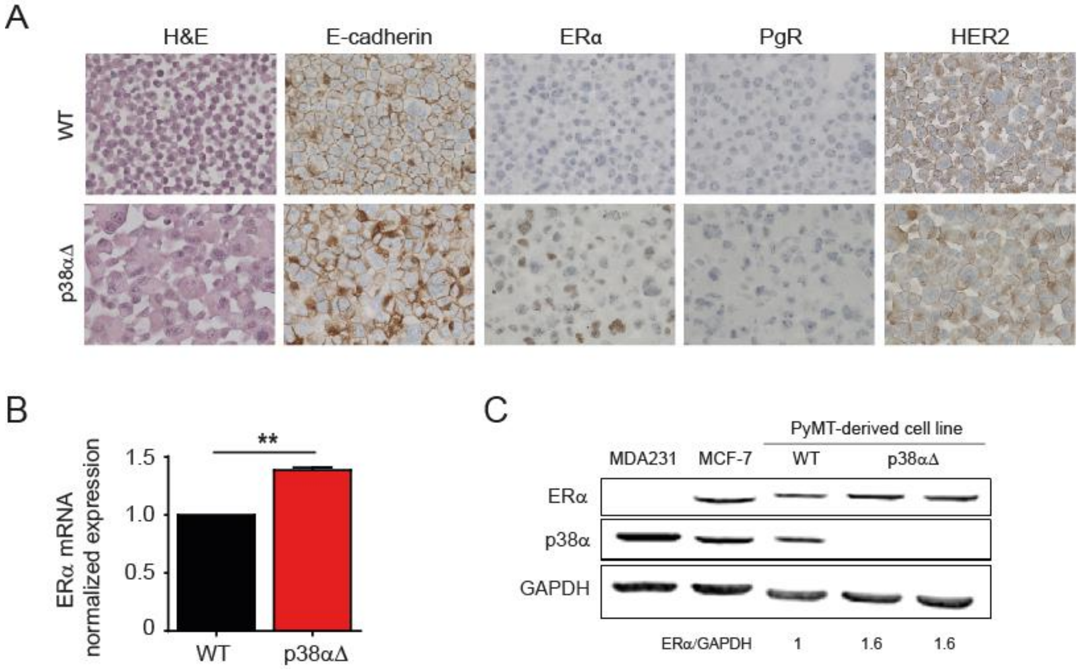

Figure 27. ERα expression is regulated by p38α in PyMT epithelial cells. A) WT and p38αΔ cell pellets were stained with the indicated antibodies. B) ERα mRNA levels were analyzed by qRT-PCR. Bar graph shows the results from two independent experiments. C) ERα protein levels were analyzed in total lysates of WT and p38αΔ cells by western blot. Two independent p38αΔ samples are shown. The relative ERα protein levels are indicated below.

The importance of ERα relies on its transcriptional activity, since it activates growth-related genes and promotes cell proliferation. Therefore, we studied whether the increased protein levels correlated with a more functional signaling. For this, we treated both WT and p38αΔ cells with the ERα ligand 17β-estradiol (E2) and analyzed the transcriptional response using GREB1 as readout and MCF-7 cells as positive control. As expected, GREB1 was upregulated in MCF7 following E2 stimulation. WT PyMT cancer cells showed no response to E2, while p38αΔ cells upregulated GREB1 mRNA expression (Fig. 28A), indicating that p38α interferes with the biological activity of ERα. Although the role of p38 MAPKs in estrogen signaling is not clear (Antoon et al., 2012, Lee and Bai, 2002), our data was in line with previous work describing a phosphorylation-dependent negative regulation of ERα by p38α (Bhatt et al., 2012). Moreover, it fitted with the activation of p38 MAPK signaling found in tamoxifen-resistant tumors (Gutierrez et al., 2005, Aesoy et al., 2008).

ERα, however, is not just a growth factor, but it is also a well-known marker of luminal differentiation in breast cells. The epithelium of the mammary gland is formed by two main lineages, luminal and basal cells, which have distinct characteristics and play different roles in a tumorigenesis context. Importantly, epithelial luminal differentiation has been shown to inhibit tumor progression and metastasis (Kouros-Mehr et al., 2008). Therefore, we investigated whether p38α could be involved in mammary epithelial cell differentiation by analyzing a set of genes known to correlate with estrogen receptor expression and to be involved in tumor cell differentiation. We found no differences in the mRNA expression of luminal-associated genes such as GATA3, FOXA1, CK8, or CK18, while reduced expression of some basal-associated genes such as CK14 or FOXM1 was detected in p38αΔ cells (Fig. 28B). However, no differences in the luminal phenotype were detected according to EPCAM and CD49f expression (Fig. 28C), two surface markers commonly used to classify mammary cell populations.

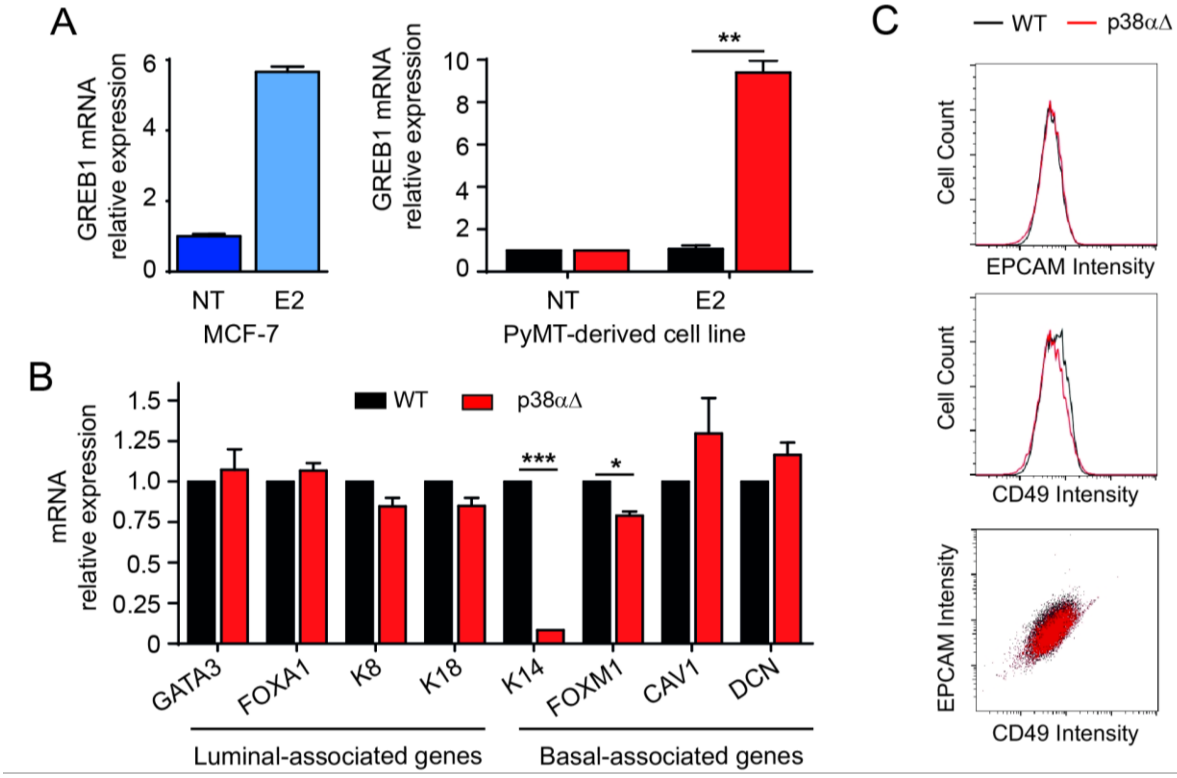

Figure 28. p38α regulates ERα functionality but the differentiation status is not affected in p38αΔ cells. A) GREB1 mRNA expression was determined in WT and p38αΔ cells after 24h incubation in 10nM E2 in 0.1%FBS media. Graph represents two independent experiments. MCF7 cells were used as positive control for ER function. B) Relative mRNA expression levels of luminal and basal associated genes were analyzed in WT and p38αΔ cells. Graph summarizes the results of two independent experiments. C) EPCAM (up), CD49f (middle) and combined (down) intensity plots of WT and p38αΔ cells obtained by flow cytometry.

This suggests that the observed changes in mRNA levels upon p38α deletion were not enough to influence the differentiation fate of the cancer cells.

Altogether, our results indicated that estrogen receptor signaling was upregulated in the absence of p38α. However, this increase was not accompanied by important transcriptional or phenotypical changes. Therefore, although interesting from a therapeutic point of view, the increase in ERα signaling following p38α deletion could not explain the cell death and tumor regression observed in the PyMT tumorigenesis model.

4.3. p38α is not directly involved in PyMT signaling

p38 MAPK signaling has never been described to be required for PyMT-induced tumorigenesis, but we wanted to make sure that the tumor enabling function of p38α in this model was not due to a requirement of p38α for PyMT signaling itself. PyMT, by mimicking the activity of receptor tyrosine kinases, recruits cytoplasmic signaling proteins, ultimately activating PI3K and RAS pathways, which are therefore essential for its transforming capacity (Schaffhausen and Roberts, 2009). In order to confirm that p38α was not directly involved in PyMT signaling, PyMT cancer cells were incubated with an AKT inhibitor (MK2206), an ERK inhibitor (UO126) and a p38 MAPK inhibitor (PH797804). As expected, incubation in MK2206 or UO126 resulted in immediate and massive cell death, while cells treated with PH797804 showed reduced proliferation, but did not die at this short timepoint (Fig. 29A, 29B).

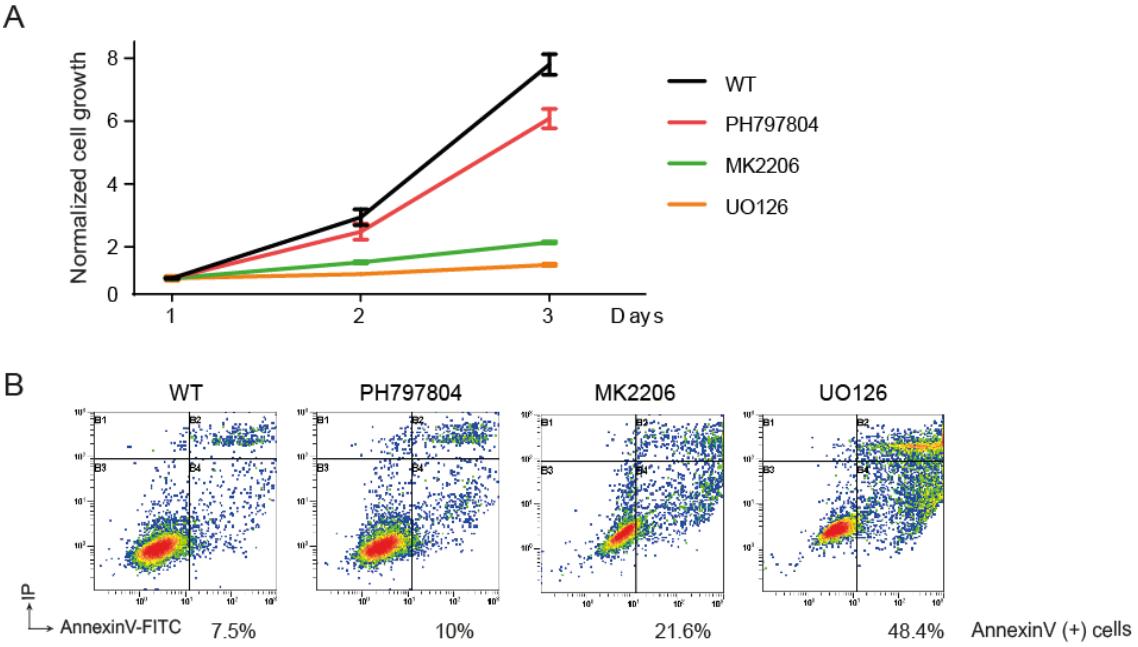

Figure 29. p38α is not required for PyMT signaling. Cells were treated for 72h with either vehicle, 2μM PH797804, 3μM MK2206 or 5μM UO126. A) Cell growth was analyzed by MTT. B) Cell death after 72h was determined by annexin V staining. The percentage of Annexin V(+) cells is shown below.

Indirectly, these results indicated that although p38α is essential for PyMT tumor progression, it is not likely a downstream effector of PyMT signaling.

5. p38α is required for chromosome segregation in PyMT epithelial cells and its deletion increases chromosome instability

Observing PyMT cancer cells before and after p38α deletion under the microscope, we realized that they presented slight different morphologies. We observed that p38αΔ cells were slightly bigger and the abundance of multinucleated cells was increased compared to WT cells (Fig. 30A). We quantified cell size using the Forward-scatter signal by flow cytometry (Fig. 30B) and multinucleated cells using DAPI and E-cadherin staining (Fig. 30C), and confirmed that both parameters increased after p38α deletion, suggesting potential defects in cell division.

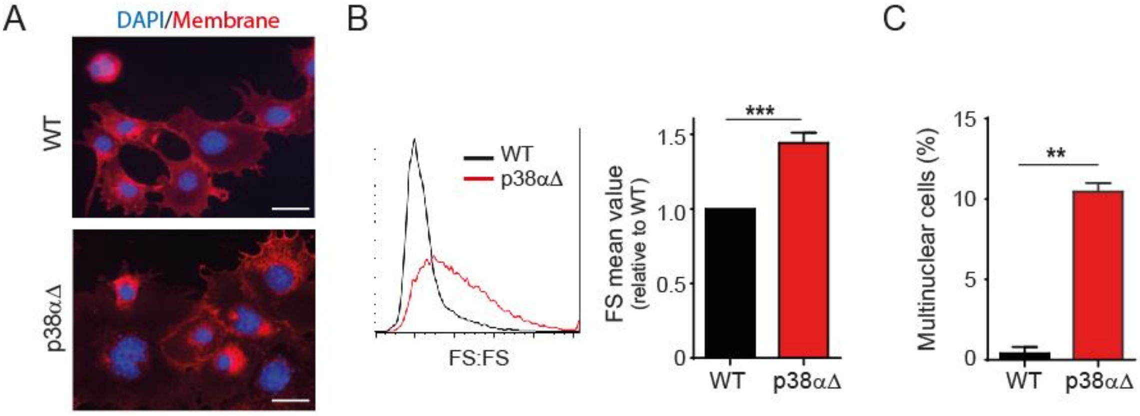

Figure 30. Cancer cells become bigger and multinucleated following p38α deletion. A) Representative images of WT and p38αΔ cells stained with DAPI and Wheat germ agglutinin as membrane marker. Bar=20µm. B) Representative Forward-scatter plot of WT and p38αΔ cells. Bar graph shows quantification of six independent experiments. C) Immunofluorescence based quantification of cells exhibiting two or more nuclei in two independent experiments. At least 100 cells were counted in each replicate.

The larger cells and the higher multinucleation rate observed upon p38α downregulation suggested potential defects during chromosome segregation. In order to test this hypothesis, we performed time-lapse video analysis and observed that WT cells completed mitosis in around 35min, while some p38αΔ cells showed a delay in anaphase resolution and cytokinesis completion (Fig. 31). To further validate the mitotic defects, we stably expressed H2B-GFP, which allowed high resolution imaging of DNA. We observed that both WT and p38αΔ cells condensed and de-condensed DNA normally and that cells progressed normally through prophase and metaphase in the absence of p38α. Cytokinesis, however, was physically obstructed by inter-cellular DNA structures known as DNA bridges (Fig. 32). Nevertheless, even in the presence of the DNA bridges, most of the p38αΔ cells were able to eventually divide, but exhibited micronuclei after mitosis (Fig 32).

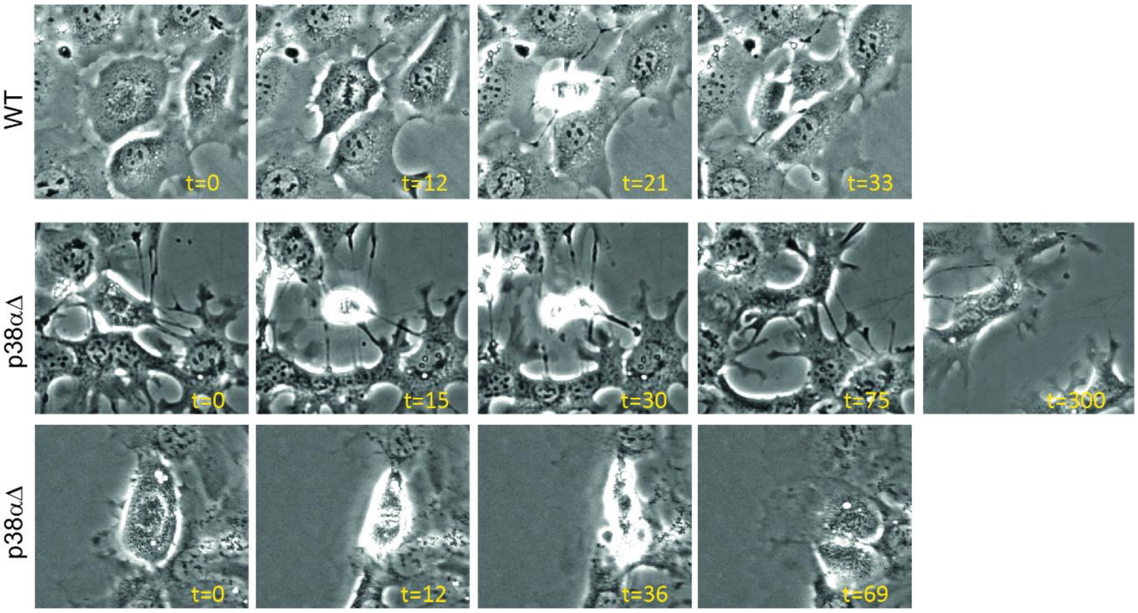
WT
t=0
t=12
t=21
t=33
p38αΔ
t=0
t=15
t=30
t=75
t=300
p38αΔ
t=0
t=12
t=36
t=69

Figure 31. p38αΔ cells show impaired anaphase resolution and cytokinesis defects. Representative images from WT and p38αΔ cells are shown. The time in minutes is indicated in yellow.

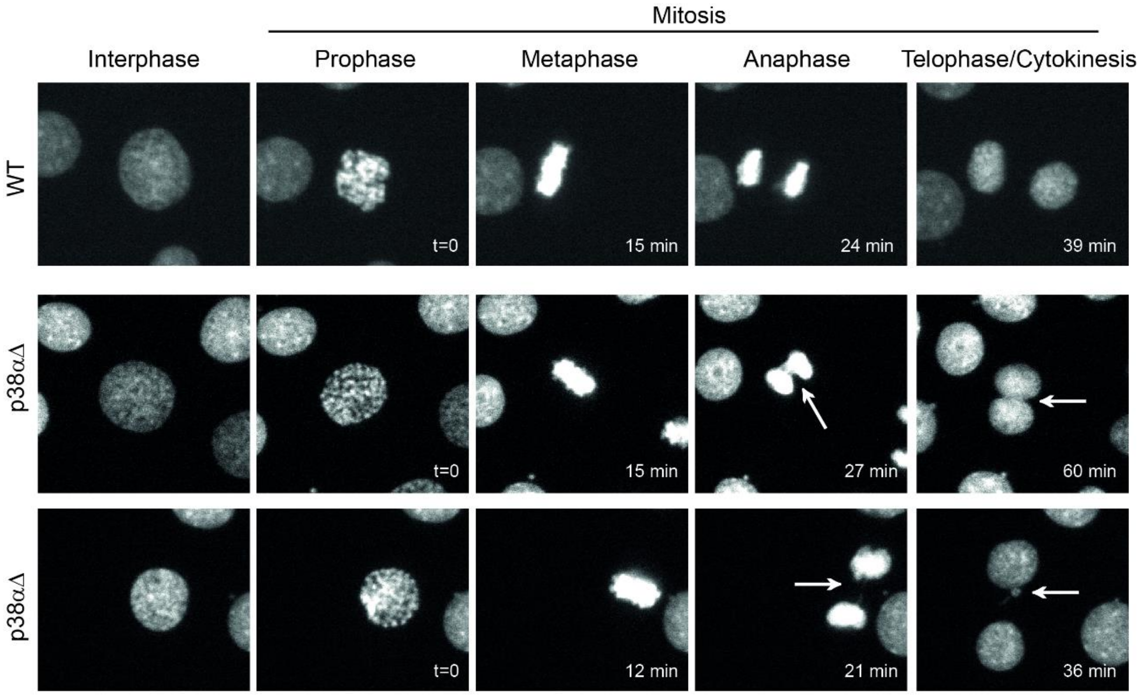
Mitosis
Interphase
Prophase
Metaphase
Anaphase
Telophase/Cytokinesis
WT
t=0
15 min
24 min
39 min
p38αΔ
t=0
15 min
27 min
60 min
p38αΔ
t=0
12 min
21 min
36 min

Figure 32. Defective mitoses after p38α deletion. Representative images from H2B-GFP WT and p38αΔ cells are shown. The time in minutes is indicated below. Arrows mark mitotic defects such as DNA bridges and micronuclei.

Immunofluorescence-based quantifications showed that both DNA bridges and micronuclei were strongly increased in p38αΔ cells (Fig. 33A and 33B). These defects are classical CIN markers; therefore, we examined additional characteristics of CIN. An increased number of cells with more than two centrosomes (Fig. 33C) as well as with multipolar prophases and metaphases were observed in the absence of p38α (Fig. 33D), indicating an increased CIN following p38α deletion. Moreover, we detected a higher rate of chromosome fragments and non-telomeric fusions (Fig. 33E) in p38αΔ metaphase spreads, which might reflect the defects in anaphase resolution and cytokinesis. In order to study this CIN phenotype *in vivo*, we stained PyMT mammary tumor sections with phospho-histone H3 and detected an increased percentage of aberrant mitoses after p38α downregulation (Fig. 33F), confirming the occurrence of CIN not only *ex-vivo* in cell cultures, but also *in vivo* in mouse tumors.

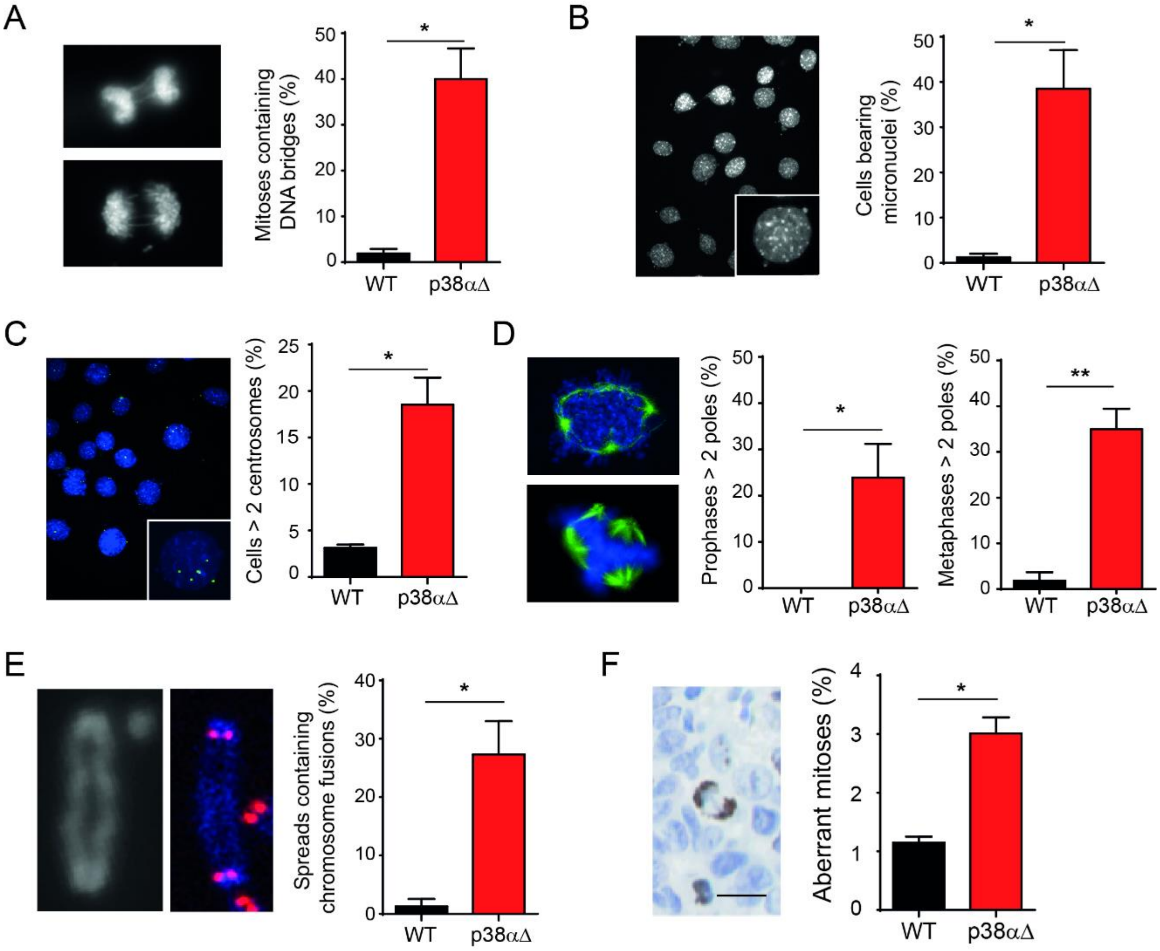

Figure 33. p38α deletion increases CIN in PyMT epithelial cells. A) Representative images of DNA bridges in p38αΔ cells. Bar graph shows the quantification of three independent experiments. At least 60 mitoses per condition were analyzed in each experiment. B) Representative image of p38αΔ cells with micronuclei. Bar graph shows the quantification of two independent experiments. At least 500 cells were analyzed in each experiment. C) Representative image of p38αΔ cells stained with γ-tubulin. Bar graph shows the percentage of cells showing > 2 centrosomes in two independent experiments. At least 500 cells were analyzed in each experiment. D) Representative images of p38αΔ cells stained with α-tubulin. Graphs show the quantification of multipolar prophases and metaphases of three independent experiments. At least 50 mitoses per condition were analyzed in each experiment. E) Representative picture from a chromosome fusion in p38αΔ cells (left) and telomere-FISH staining in red (right). Percentage of spreads containing fusions was quantified in three independent experiments. At least 50 spreads were analyzed in each experiment. F) Representative image of an aberrant mitosis in sections of p38α-deficient PyMT mammary tumors stained with phospho-H3 S10. Bar graph shows the quantification of two independent mice. At least 20 fields per tumor were quantified. Bars = 10 µm.

CIN cells accumulate karyotype alterations during cell cycles, creating numerical changes in the cell population or, in other words, aneuploidy. To confirm this idea metaphase spreads from WT and p38αΔ cells were performed and the number of chromosomes per metaphase was counted (Fig. 34A). On the one hand, we found that these cells were 3n, as the median number of chromosome in WT cells was 69 (Fig. 34B). This indicated that PyMT epithelial cells were polyploid. On the other hand, p38αΔ cells showed a heterogeneous distribution in terms of chromosome loading (Fig. 34B), indicating that they were not just polyploid but aneuploid. This marked increase in aneuploidy (Fig. 34C) may explain the slower proliferation and later cell death, since CIN and aneuploidy have been shown to have detrimental effects in most of the organisms (Lynch et al., 1993, Torres et al., 2007, Williams et al., 2008) and even a single chromosome gain can cause tumor suppression (Sheltzer et al., 2017).

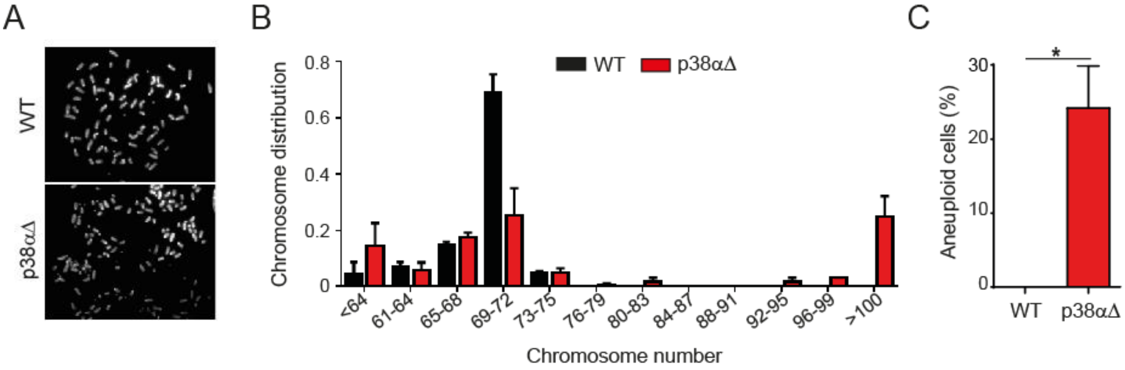

Figure 34. p38α deletion results in increased aneuploidy in PyMT epithelial cells. A) Representative metaphase spreads of WT and p38αΔ cells. B) The number of chromosomes in at least 50 spreads was counted. Histogram shows chromosome number distribution in WT and p38αΔ cells in three independent experiments. C) Spreads containing more or less chromosomes than the median ±30% were considered aneuploid. Bar graph shows the quantification of aneuploid cells in the three independent experiments. At least 50 spreads were analyzed in each experiment.

Taken together, p38α downregulation in the PyMT breast cancer cells resulted in a variety of mitotic aberrations, abnormal cytokinesis, increased aneuploidy and a CIN phenotype, which were consistent with the larger and multinucleated cells, and would explain the lower fitness, the increased cell death and the tumor regression.

As a control, we derived cell lines from PyMT-induced tumors in p38α$^{+/+\ CreERT2}$ mice, which activated Cre upon 4-OHT treatment but did not carry loxP sites and did not delete p38α (Fig. 35A). Treatment of these cells with 4-OHT barely affected proliferation and cell death (Fig. 35B, 35C), and these cells were also able to form colonies to a similar extent as the non-treated ones (Fig. 35D). Moreover, spreads from these cells, incubated or not with 4-OHT, showed no major differences in the number of chromosomes. These results indicated that the observed phenotypes can be specifically ascribed to p38α downregulation, rather than to 4-OHT treatment or Cre activation.

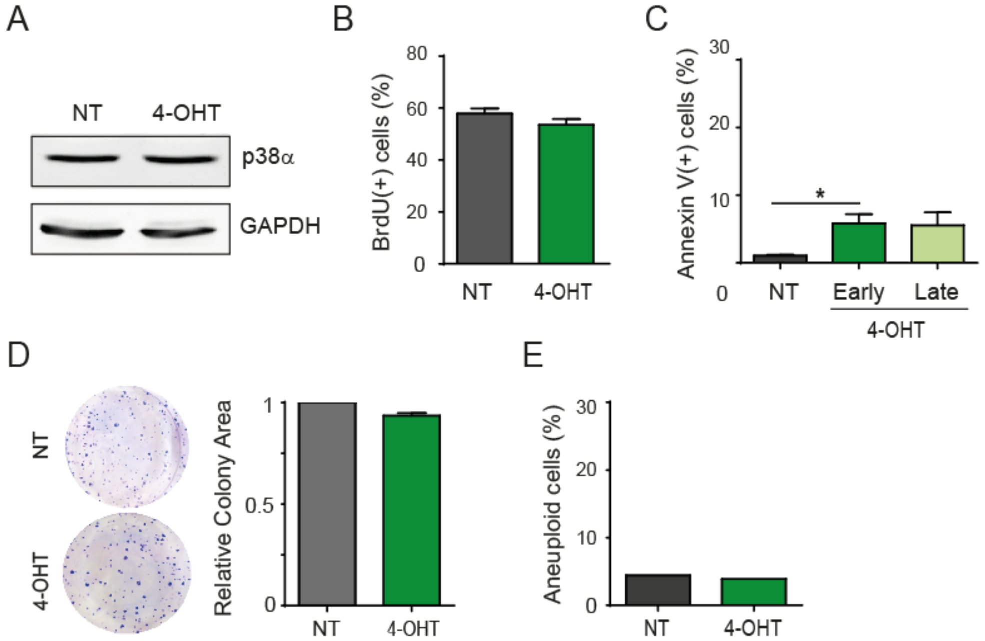

Figure 35. 4-OHT incubation and Cre induction are not responsible for the phenotypes observed in p38αΔ cells. Control p38$^{+/+\ CreERT2}$ cells were incubated or not with 4-OHT for 48h and released. A) p38α levels were analyzed by western blot. B) BrdU uptake in two independent experiments. C) Annexin V staining in three independent experiments. Early and Late corresponds to two and six days after 4-OHT treatment. D) Colony formation assay. Graph represents the quantification of two independent experiments. E) Metaphase spreads were performed, the number of chromosomes were counted and all the cells containing more or less than the median+30% chromosomes were considered aneuploid.

6. Mitotic defects do not explain the increased chromosome instability found in the absence of p38α

Several mechanisms can lead to CIN and aneuploidy, but perhaps the most obvious one is a failure during mitotic progression. Mitosis is a tightly regulated process that involves the temporal and spatial control of several kinases such as CDK1 and Auroras, and that is monitored by a special checkpoint known as SAC. Defects in several mitotic players have been associated with segregation errors and CIN (Welburn et al., 2010, Gonzalez-Loyola et al., 2015, Vazquez-Novelle et al., 2014).

We initially analyzed the chromosome condensation. This factor is important since loss of chromatid cohesion causes premature chromatid separation that results in missegregation and aneuploidy (Solomon et al., 2011, Iwaizumi et al., 2009). We indirectly studied chromosome condensation by measuring the chromosome area in metaphase spreads, and found no difference between WT and p38αΔ cells (Fig. 36).

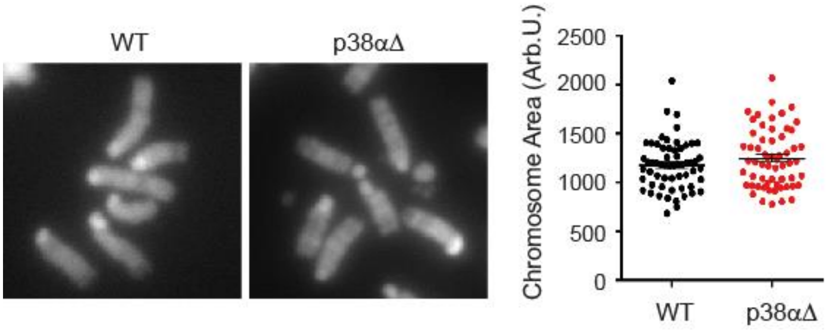

Figure 36. p38α deletion does not affect chromosome condensation. Representative images of chromosomes from WT and p38αΔ metaphase spreads. Graph shows the quantification of the chromosome area. At least 60 chromosomes in different spreads were analyzed.

We next analyzed the status of Aurora B, an essential sensor of tension at the centromere-kinetochore interphase whose targeting leads to attachment failures and miss-segregation, and Aurora A, required for mitotic entry and proper spindle formation. We stained WT and p38αΔ cells with antibodies for Aurora B (Fig. 37A) and Phospho Aurora A T288 (Fig. 37B), which corresponds to an autophosphorylation site and is indicative of its activity. We did not find any difference, neither in Aurora B nor in P-Aurora A, in terms of localization or signal intensity, suggesting that Aurora A/B functionality was maintained after p38α deletion.

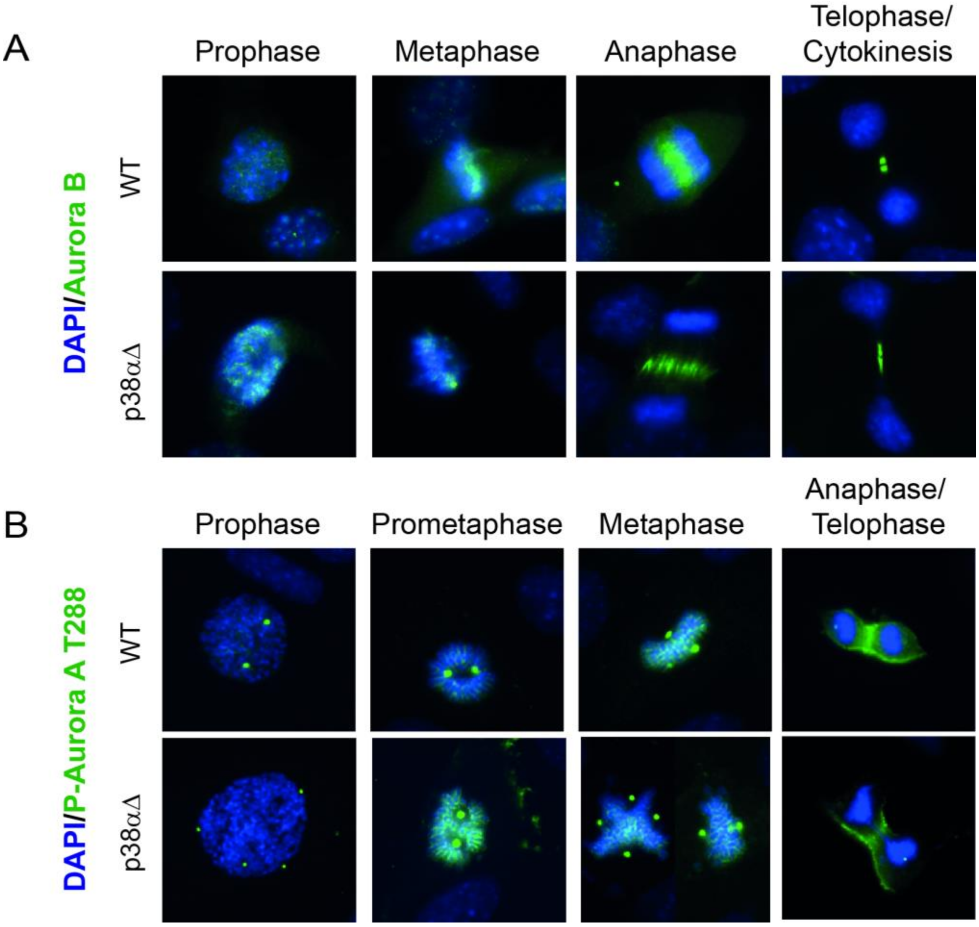
A
Prophase
Metaphase
Anaphase
Telophase/ Cytokinesis
DAPI/Aurora B
WT
p38αΔ
B
Prophase
Prometaphase
Metaphase
Anaphase/ Telophase
DAPI/P-Aurora A T288
WT
p38αΔ

Figure 37. p38α deletion does not affect Aurora B or Phospho-Aurora A localization. Representative images of Aurora B (A) and Aurora A P-T288 (B) in different mitotic phases.

Although de-regulation of Aurora A and Aurora B and defects in chromosome condensation can originate aneuploidy, the SAC could be considered the main guardian of the genome integrity during mitotic progression. To study the SAC status, we initially analyzed its main components at the transcriptional level. We found a reproducible decrease in the mRNA levels of BUB1, MAD2 and CDK1 (Fig. 38A) and confirmed the MAD2 and CDK1 reduction, together with a cyclin B1 downregulation, at the protein level (Fig. 38B). Of note, expression of these proteins is cell-cycle dependent. Although we have previously shown that cell cycle profile barely changed following p38α deletion (Fig. 23C), cell proliferation was impaired in p38α deficient cells (Fig. 23D), and likely account for the reduction of the mitosis-associated proteins.

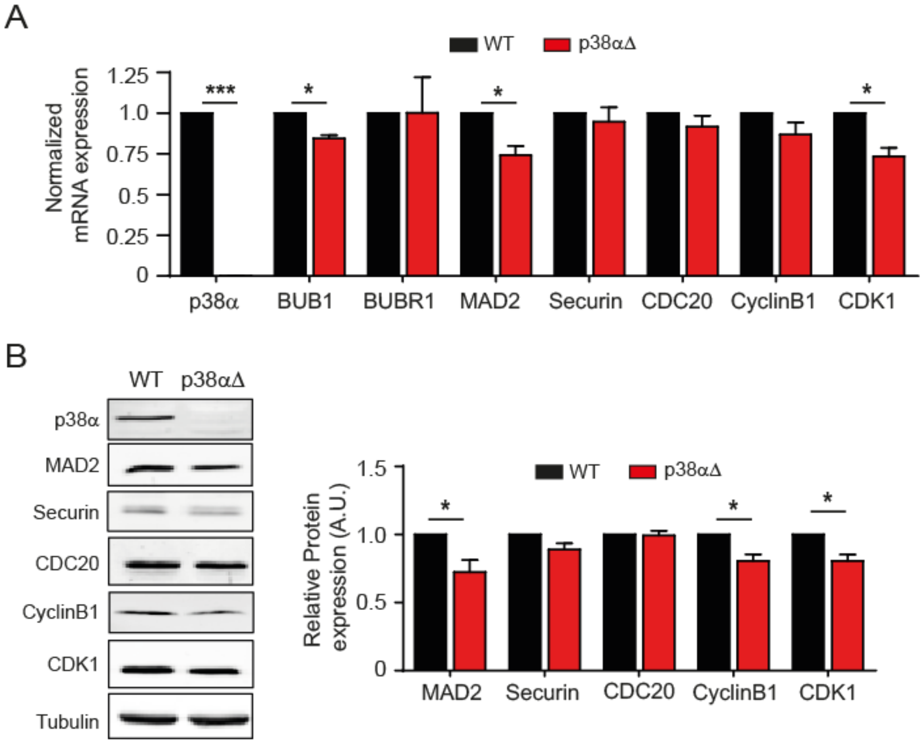

Figure 38. p38αΔ cells show decreased levels of some SAC-related proteins. WT and p38αΔ cells were analyzed. A) mRNA levels of the indicated genes were analyzed by qRT-PCR in three independent samples. B) Representative western blots of SAC-related proteins. Quantification of three independent experiments is shown in the graph.

We next functionally assayed SAC by incubating cells with mitotic poisons. We initially treated WT and p38αΔ cells with paclitaxel, also known as taxol, a microtubule-stabilizing drug that arrests cells in prometaphase, activating the SAC and temporarily blocking mitotic progression. We observed a lower accumulation in mitosis in p38α deficient cells, marked by the reduced pH3(+) cell percentage upon paclitaxel incubation (Fig. 39A). However, p38αΔ cells consistently showed a decreased basal mitotic rate (about 35% lower), which can in part explain the lower expression of MAD2, cyclin B1 and CDK1 proteins. Therefore, we normalized the pH3(+) cells to the initial mitotic rate and re-analyzed the results. Again, we detected a lower accumulation of mitotic cells, but the difference between WT and p38αΔ was reduced to a 30% (Fig. 39B). These results were corroborated by performing western blot in the same conditions. We confirmed the lower expression of pH3 and CDK1 and detected a lower accumulation of cyclin B1 (Fig. 39C). A lower mitotic accumulation in the presence of paclitaxel can be due to a bypass of the checkpoint or to other reasons like a lower mitotic entry. To further analyze the behavior of these cells upon SAC activation, we performed time-lapse video using the H2B-GFP expressing cells in the presence of paclitaxel. We measured the time cells were arrested in prometaphase and confirmed that p38αΔ cells exited the prometaphase arrest a 25% faster than WT cells (Fig. 39D).

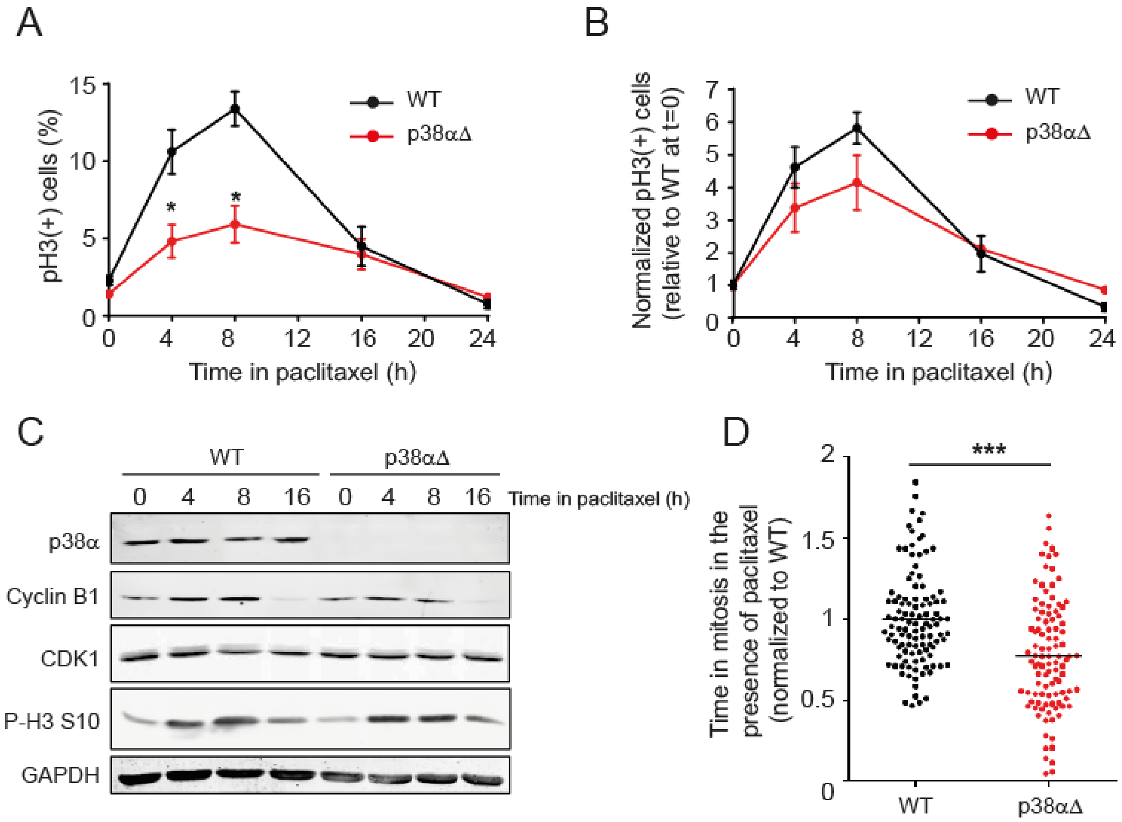

Figure 39. p38α deletion decreases mitotic arrest upon paclitaxel incubation. A) WT and p38αΔ cells were treated with 100nM paclitaxel for the indicated times and the percentage of pH3-S10(+) cells was measured by flow cytometry. Graph shows the results from three independent experiments. B) Data from A was normalized to initial pH3-S10(+) levels. C) Expression levels of the indicated proteins were analyzed after incubation in 100nM paclitaxel. Representative western blots are shown. D) H2B-GFP PyMT cancer cells were treated with 100nM paclitaxel and time-lapse was performed. Time from nuclear envelope breakdown to prometaphase exit was calculated. Graph shows the normalized results of three independent experiments.

In order to complete this analysis we made use of a known inhibitor of the SAC activity: reversine, an inhibitor of the protein kinase MPS1 whose activity is essential for the proper activation of the SAC (Winey et al., 1991, Stucke et al., 2002). The concentration range of this inhibitor in the literature was broad and it varied depending on the cell type. Therefore, we initially tested different reversine concentrations and analyzed their effects on nocodazole-treated WT cells. To determine the checkpoint activation upon nocodazole incubation, we measured the accumulation of cells in mitosis through the quantification of pH3 by FACS (Fig. 40A) and western blot (Fig. 40B). Both techniques showed that at 250nM, reversine effectively reverted nocodazole effects, indicating that MPS1 was inhibited and the checkpoint was abolished. Additionally, western blot indicated that reversine did not affect p38 MAPK phosphorylation levels, suggesting that it does not interfere with the p38α activity.

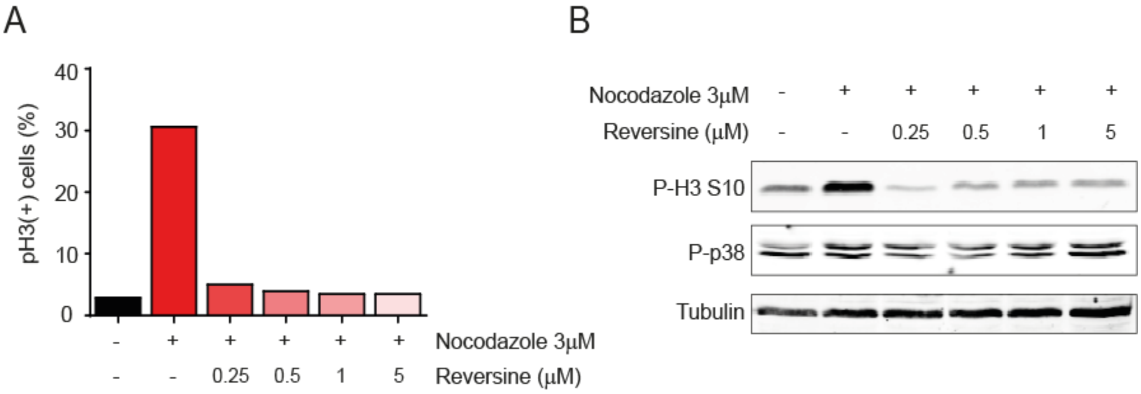

Figure 40. 250nM reversine is enough to block SAC activity in PyMT epithelial cells. Cells were incubated for 8h in 3μM nocodazole in the presence of increasing concentrations of reversine. Checkpoint activation was detected by accumulation of pH3 S10(+) cells by A) flow cytometry and B) western Blot.

Once the concentration of reversine was established, we performed time-lapse with H2B-GFP cells and observed that indeed, PyMT epithelial cells did not arrest at mitosis in the presence of reversine (Fig. 41A). Moreover, reversine did not affect mitosis entry of the cells (Fig. 41B) and did not revert the binucleation upon nocodazole incubation (Fig. 41C).

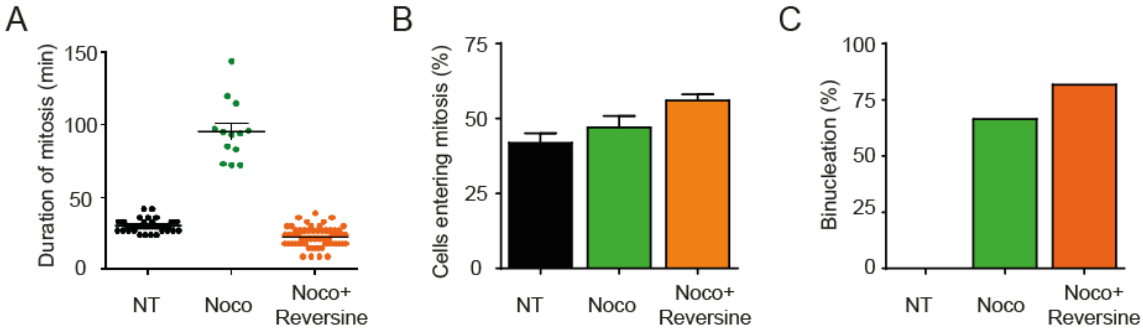

Figure 41. 250nM reversine reverts nocodazole-induced arrest. H2B-GFP PyMT epithelial cells were incubated in 3μM nocodazole in the presence or absence of 250nM reversine and time-lapse was performed. A) Duration of mitotic arrest was determined. B) The percentage of cells entering in mitosis in four frames during the whole time-lapse was calculated. C) Percentage of binucleated cells resulting from mitosis was quantified in four frames from the same experiment. Values correspond to the average binucleation percentage in each condition.

When we compared the effects of reversine and p38α downregulation, we found that reversine increased the percentage of cells showing micronuclei (Fig. 42A) and DNA bridges (Fig. 42B), indicating that abolishment of SAC could be a source of CIN in the PyMT cells. However, when we analyzed the duration of mitosis, we observed that reversine decreased normal mitosis time, while p38α deletion slightly increased it (Fig. 42C). But most strikingly, comparing the duration of normal mitoses -a parameter that we did not have into account in the first time-lapse analysis in Fig. 39D- and the duration following nocodazole-induced arrest, we observed that the decrease in mitosis arrest caused by p38α deletion was of 9% (and not 25% as calculated before), while reversine induced a 100% reversal. This 10-fold difference between the effect of p38α deletion and reversine suggested that the missegregation and CIN in p38αΔ cells were not caused by defects in SAC.

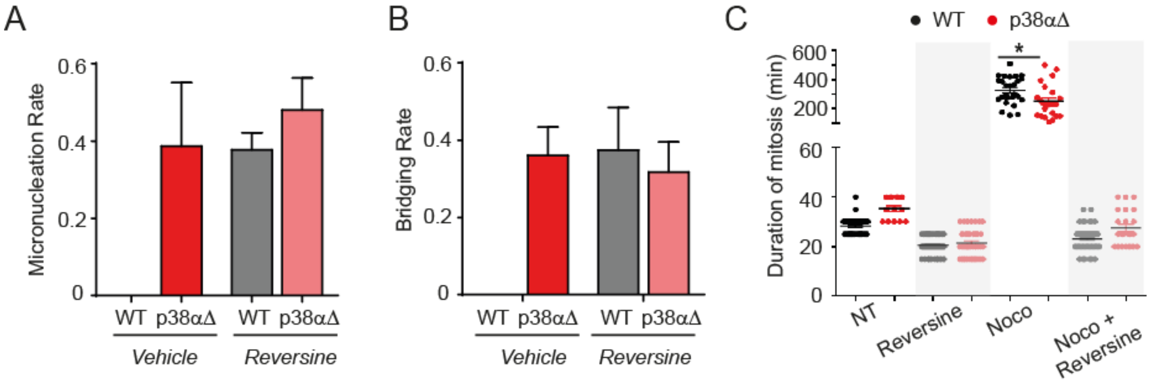

Figure 42. Reversine mimics the increase in micronucleation and DNA bridges. However, the effect of p38α deletion on SAC is not comparable to reversine. H2B-GFP PyMT derived epithelial cells were treated as indicated and time-lapse video was performed for 16h**.** A) Cells bearing micronuclei after mitosis were quantified. B) Mitoses showing DNA bridges were quantified. C) Duration of mitoses was determined. Nocodazole 3µM (Noco) was used as positive control of SAC activation.

In order to try to confirm these findings, we used monastrol, a cell-permeable small molecule inhibitor of the motor protein Eg5 that induces monoastral spindles and mitotic arrest. Unlike paclitaxel and nocodazole, monastrol causes checkpoint activation without affecting microtubule polymerization. After 16h incubation in monastrol, we observed a similar percentage of arrest escapers (mitotic cells out of the prophase block), around 20%, suggesting that both WT and p38αΔ cells were equally sensitive to the monastrol-induced spindle checkpoint. However, in p38αΔ cells most of the escaper cells showed aberrant morphologies (Fig. 43A, 43B), raising the possibility whether p38α deficient cancer cells bore previous defects which were magnified by the presence of mitotic poisons.

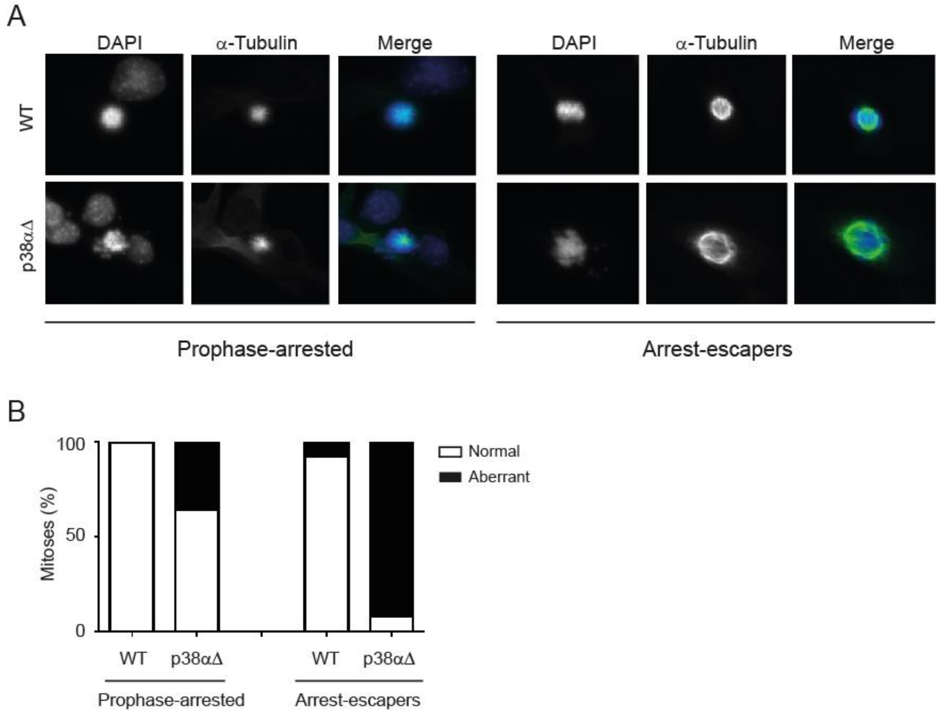
A
DAPI
α-Tubulin
Merge
DAPI
α-Tubulin
Merge
WT
p38αΔ
Prophase-arrested
Arrest-escapers
B
100
50
0
Mitoses (%)
Normal
Aberrant
WT
p38αΔ
WT
p38αΔ
Prophase-arrested
Arrest-escapers

Figure 43. p38α deleted cells arrest in mitosis upon monastrol incubation but show more aberrancies after arrest slippage. Cells were incubated for 16h in 100µM monastrol**.** A) Representative images of WT and p38αΔ cells after monastrol incubation. B) Quantification of mitotic aberrancies in arrested and escaper cells. At least 25 mitoses were analyzed in each condition.

Altogether these data suggested that the effect of p38α on the SAC was rather small and unlikely to explain the marked increase in missegregation, CIN and aneuploidy observed in p38αΔ cells.

7. p38α deletion results in elevated DNA damage and replication stress in PyMT epithelial cells

Defects in mitosis progression and regulation were not likely to be responsible for the CIN phenotype in p38αΔ cells, suggesting the existence of defects prior to mitosis. In order to support the hypothesis of a pre-mitotic origin of these defects, we stained cells with an anti-centromere antibody (ACA). Structural chromosome aberrations that arise due to pre-mitotic defects are characterized by DNA bridges and chromosome fragments without centromeres, while lagging chromosomes with centromeres often suggest mitotic dysfunctions such as merotelic kinetochore attachments (Fig. 44A) (Burrell et al., 2013). Immunofluorescence in p38αΔ cells identified DNA bridges in most of the aberrant mitoses, but only 26% of the mitoses showed lagging chromosomes stained for ACA (Fig. 44B). Therefore, although we cannot rule out some contribution of mitotic dysfunctions, our results indicated that the observed segregation errors were primarily a consequence of pre-mitotic defects.

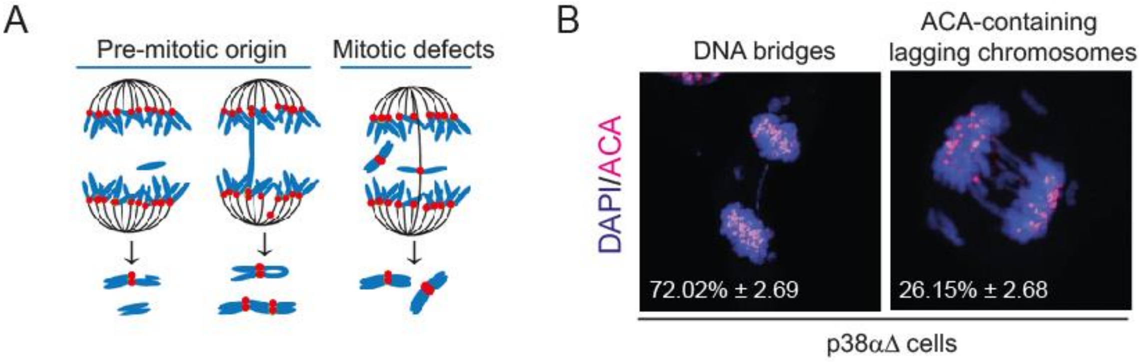

Figure 44. ACA staining in p38αΔ cells reveals pre-mitotic defects. A) Schematic illustration showing the effects of mitotic and pre-mitotic defects on chromosome segregation. Adapted from (Burrell et al., 2013). B) Representative images of p38αΔ cells in mitosis. The numbers represent the average percentage of aberrant mitoses showing DNA bridges or ACA-containing lagging chromosomes in three independent experiments. At least 20 defective mitoses were analyzed in every experiment.

Among all the undergoing events during interphase, DNA replication is the most vulnerable process, and defects in this period are known to cause genome instability. Replication stress and DNA damage have been proposed to be a major cause of CIN in tumor cells (Gorgoulis et al., 2005, Halazonetis et al., 2008, Negrini et al., 2010) leading to both numerical and structural chromosome alterations (Burrell et al., 2013). Even low levels of replication stress can hamper mitotic progression by inducing anaphase bridges or multipolar spindles, leading to aberrant chromosome segregation and aneuploidy (Wilhelm et al., 2014). Therefore, given that replication stress results in DNA damage (Lukas et al., 2011), we analyzed the levels of γH2AX, which is considered a marker of DSBs and DNA damage. We found that p38α deficient cells showed higher γH2AX staining (Fig. 45A); moreover, we observed that its localization was not restricted to the nuclei, but also appeared in DNA bridges and micronuclei (Fig. 45A), potentially reflecting DSBs resulting from chromosome segregation errors during cytokinesis (Crasta et al., 2012, Janssen et al., 2011). We also observed an increased number of 53BP1 foci, another well-characterized DSB marker (Fig. 45B). These results were complemented using neutral and alkaline COMET assays, which showed increased levels of double and single-strand breaks respectively (Fig. 45C and 45D). Altogether these results confirmed the *in vivo* data where p38α downregulated PyMT tumors showed a higher DNA damage (Fig. 16D).

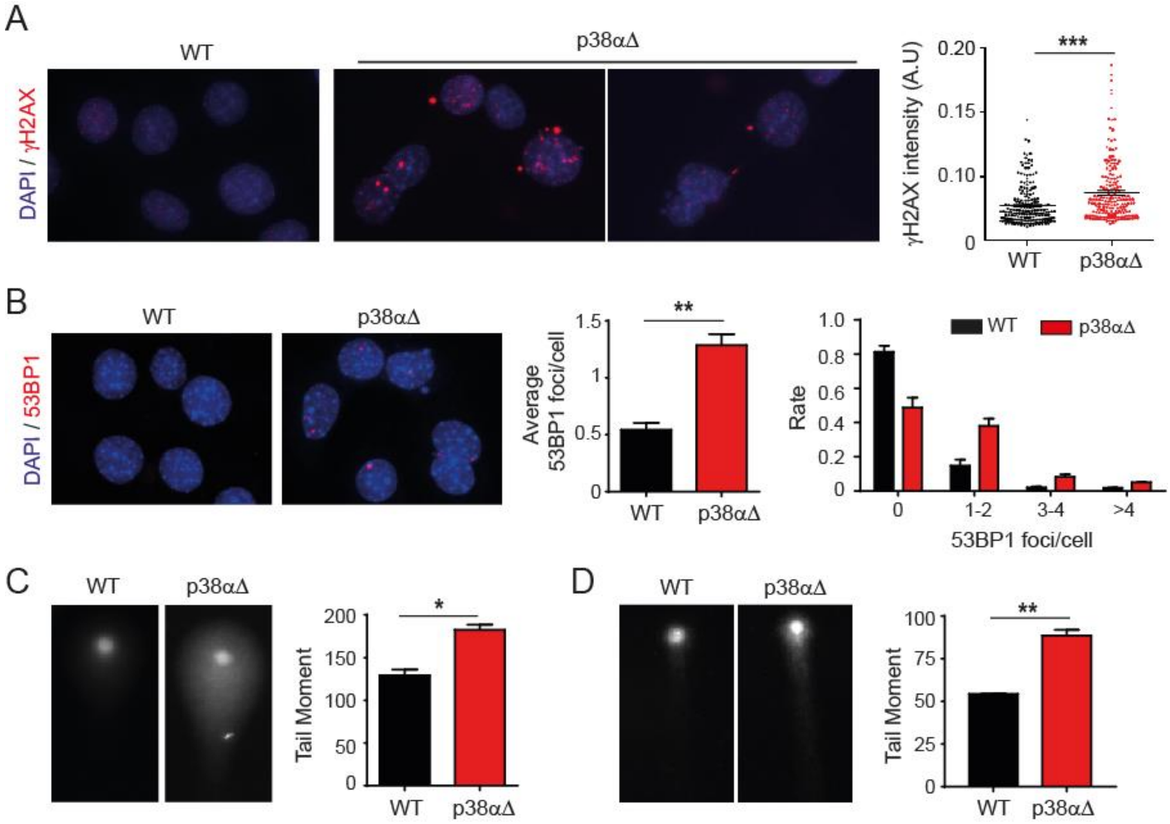

Figure 45. p38α deletion in PyMT epithelial cells results in increased DNA damage. A) Representative images of WT and p38αΔ cancer cells stained with γH2AX antibody. Nuclear γH2AX intensity was measured. Graph corresponds to one of three representative experiments. B) Representative images of WT and p38αΔ cells stained with 53BP1 antibody. Histograms show the quantification of 53BP1 foci/cell (left), and the 53BP1 foci per cell distribution of the three independent experiments (right). C) Representative images of neutral COMET assay. Graph shows quantification of the tail moment in two independent experiments. At least 50 cells per condition were analyzed in each experiment. D) Representative images of alkaline COMET assay. Graph shows quantification of the tail moment in two independent experiments. At least 50 cells per condition were analyzed in each experiment

One recognized source of endogenous DNA damage is oxidative stress, defined as an imbalance between production and elimination of ROS (Reuter et al., 2010). However, the higher level of DNA breaks found in PyMT epithelial cells following p38α deletion was not accompanied by increased ROS production (Fig. 46A) or DNA oxidation (Fig. 46B), indicating that oxidative stress was not likely responsible for the observed phenotypes.

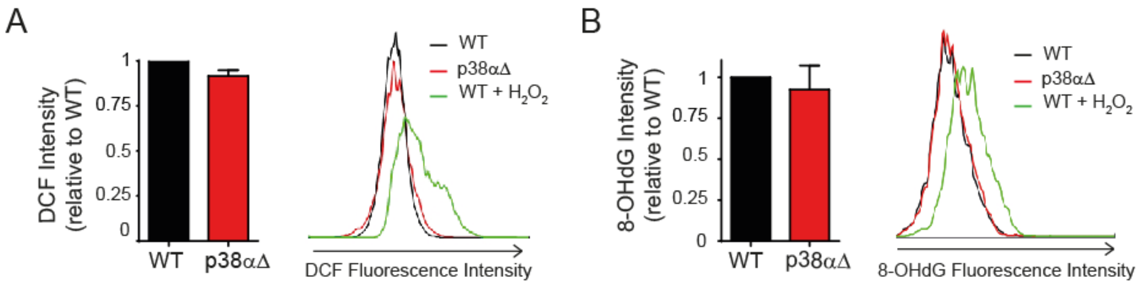

Figure 46. p38α deletion does not induce oxidative stress in PyMT cancer cells. A) ROS levels were detected using DCFDA probe. Bar graph shows the quantification of two independent experiments. B) DNA oxidation was measured by 8-oxo-guanidine antibody (8-OHdG). Bar graph shows quantification of three independent experiments. Representative DCF and 8-OHdG fluorescence intensity plots are shown including H_2O_2 treated cells as positive control.

It is well known that defects in DNA replication or DNA replication stress cause accumulation of ssDNA, SSBs or stalled replication forks, which can all promote DSBs. In turn, increased levels of DNA damage are known to impact on DNA replication and hamper its progression, both due to the generation of physical barriers for the DNA replication machinery and to activation of cell cycle checkpoints. To directly assess the effect of p38α deletion on DNA replication, we performed pulse labeling with the thymidine analogs CldU and IdU and analyzed stretched DNA fibers. We found that labeled tracks corresponding to ongoing replication forks were significantly shorter in p38αΔ cells (about 30% shorter, Fig. 47A). Shorter tracks can be interpreted as slower fork progression or as an effect of higher frequency of fork stalling. The analysis of bidirectional fibers revealed an increased rate of asymmetric forks (Fig. 47B), indicative of stalled forks. Cells usually try to respond to the replication slow-down and/or fork stalling by activating back-up origins, increasing origin density (Maya-Mendoza et al., 2009). We measured the inter-origin distance in fibers containing at least two initiation events. Although the number of these fibers analyzed was low, we could detect a decrease in the inter-origin distance (Fig. 47C), suggesting the activation of a compensatory response and activation of dormant origins, which is a common response to replication stress.

Altogether, these results indicated that p38α was required for proper fork progression and DNA replication. Therefore p38α deletion resulted, independently of ROS-induced damage and in the absence of any exogenous source of stress, in fork stalling, replication stress and DNA damage that negatively impacted the viability of the PyMT cancer cells.

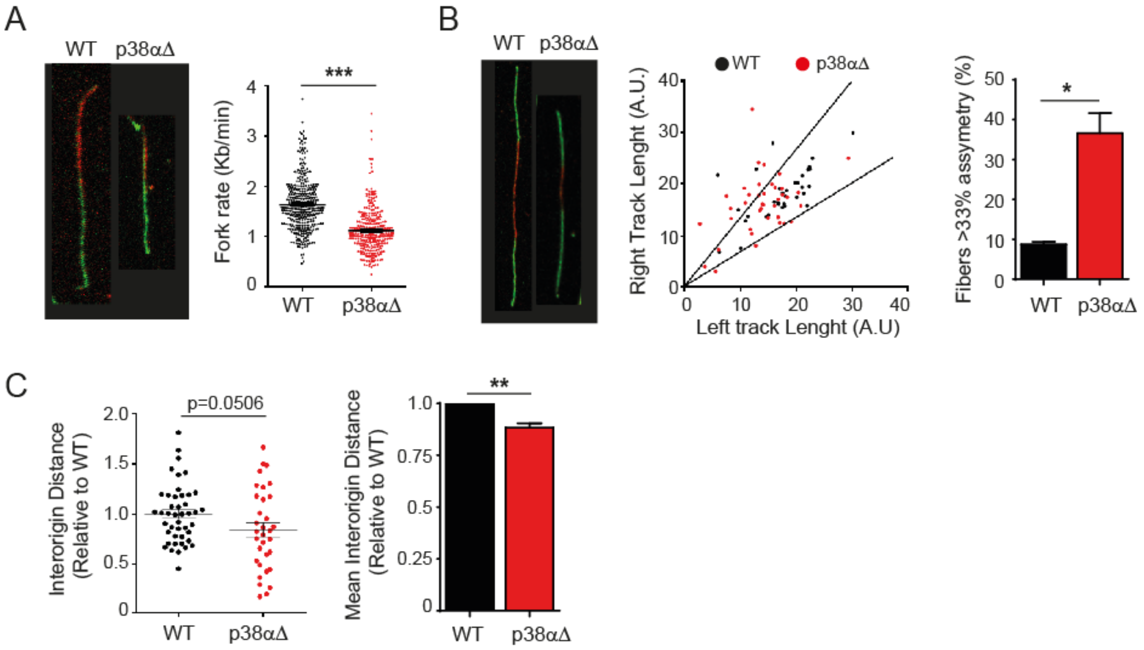

Figure 47. p38α deficient cancer cells show impaired replication fork progression. A) Representative images of DNA fibers obtained from WT and p38αΔ cells. Graph shows fork rate (Kb/min) in a representative experiment. Comparable results were obtained in three independent experiments. B) Representative images of bidirectional DNA fibers obtained from WT and p38αΔ cells. Dot plot shows the right vs left track length of every fiber in one experiment. Fibers deviating more than 33% from perfect symmetry were considered asymmetric and are located outside the black lines. Quantification of asymmetric fibers in two independent experiments is shown in the bar graph. C) Inter-origin distance was measured in multi-origin fibers. Inter-origin distances from all fibers analyzed in three independent experiments were normalized and plotted together (left panel). Bar graph (right panel) shows the mean inter-origin distance of the three independent experiments.

Next, we tried to identify the underlying mechanism leading to replication stress and DNA damage in the PyMT cancer cells following p38α deletion.

An emerging source of replication stress in cancer cells is the overexpression or activation of oncogenes such as Ras, Myc or Cyclin E, which promote origin firing, fork speed slow-down, fork stalling, and DNA damage (Zeman and Cimprich, 2014, Gaillard et al., 2015, Macheret and Halazonetis, 2015). Therefore, we studied the expression levels of these proteins in WT and p38αΔ cells, but found no increase in any of them (Fig. 48); on the contrary, we observed the downregulation of Myc in the absence of p38α. As Myc function is related to cell proliferation and survival (Soucek and Evan, 2010), this decrease in Myc protein might be explained by the lower proliferation rate of p38αΔ cells. In any case, oncogene activation did not seem to be responsible for the replication stress and CIN found in p38αΔ cells.

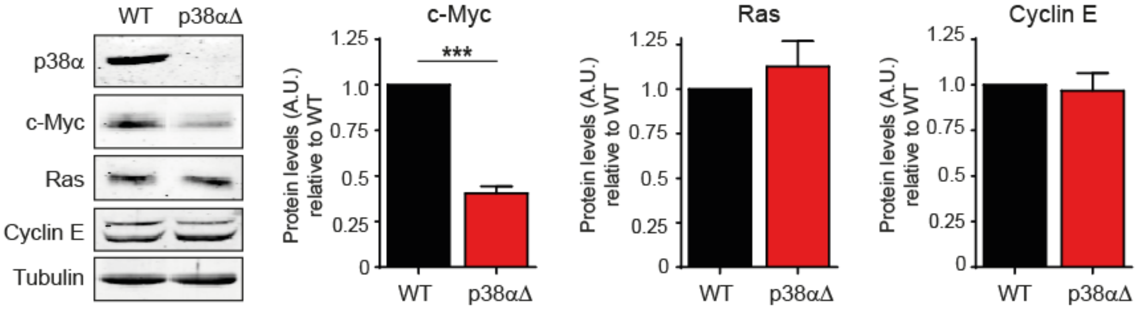

Figure 48. The key replication-inducing oncogenes are not overexpressed in p38αΔ cancer cells. The protein levels of the indicated oncogenes were analyzed by western blot in WT and p38αΔ cells. Bar graphs show the quantification in four independent samples.

Another source of replication stress relies on the de-regulation of factors involved in the initiation of replication, such as the members of the mini-chromosome maintenance complex MCMs, ORCs, CTD1 or CDC6. Recently, reduced expression of MCM proteins has been shown to induce replication stress in hematopoietic precursors (Alvarez et al., 2015, Flach et al., 2014), and increase segregation defects in several cellular models (Passerini et al., 2016, Kawabata et al., 2011). Using qRT-PCR, we found that the mRNA levels of MCM2-7, together with CDC6 and ORC1, were downregulated in p38αΔ cells compared to WT cells (Fig. 49A). Consistent with this, we observed that MCM2, 3 and 6 and, to a less extent MCM4, were downregulated at the protein level upon p38α deletion (Fig. 49B).

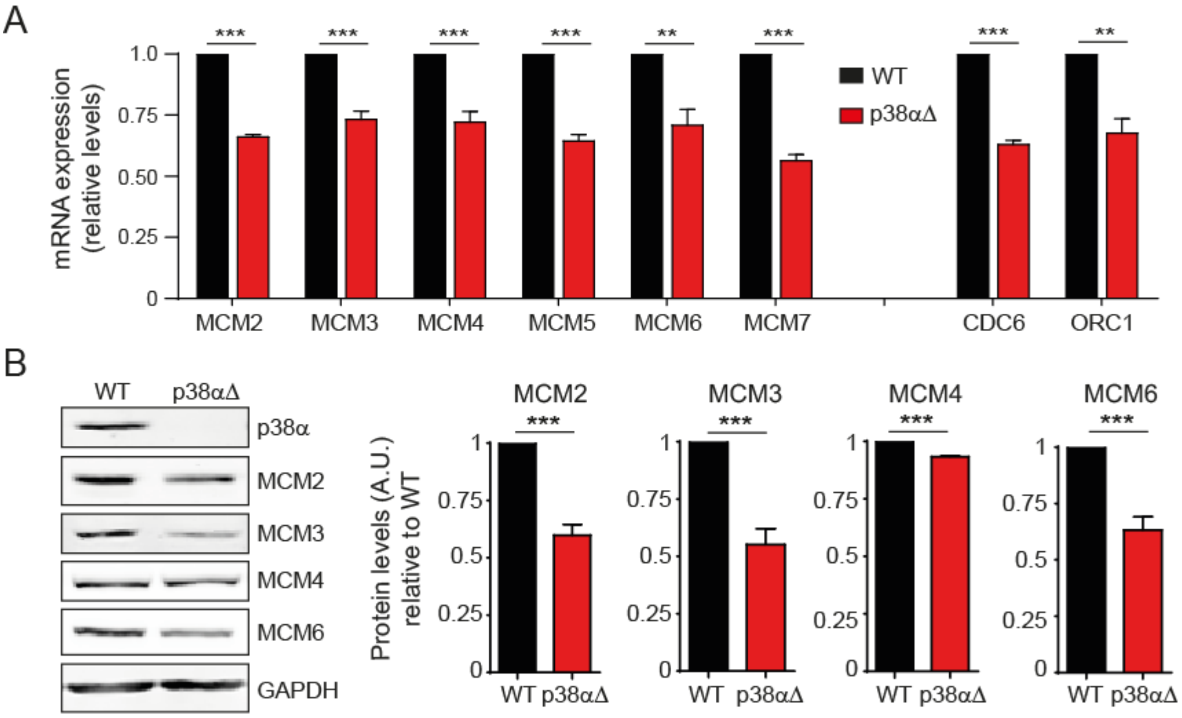

Figure 49. MCM proteins are downregulated in p38αΔ cells. A) Relative mRNA levels for the indicated MCMs, CDC6 and ORC1 genes were determined by qRT-PCR. Bar graphs show the quantification of three independent experiments. B) Total MCM2, MCM3, MCM4 and MCM6 protein levels were determined by western blot. Bar graphs show the quantification of three independent experiments.

Moreover, immunofluorescence staining of WT and p38αΔ cells with the same MCM antibodies revealed a lower nuclear expression of MCM2, 3 and 6 in p38α cells (Fig. 50A), corroborating the qRT-PCR and western blot analysis. Although MCM proteins can be localized both in the cytoplasm and the nucleus, the functional MCMs are those bound to chromatin, and more specifically, bound to replication origins. Importantly, subcellular fractionation also showed decreased MCM levels in this chromatin bound fraction in p38αΔ cells compared to WT ones (Fig. 50B).

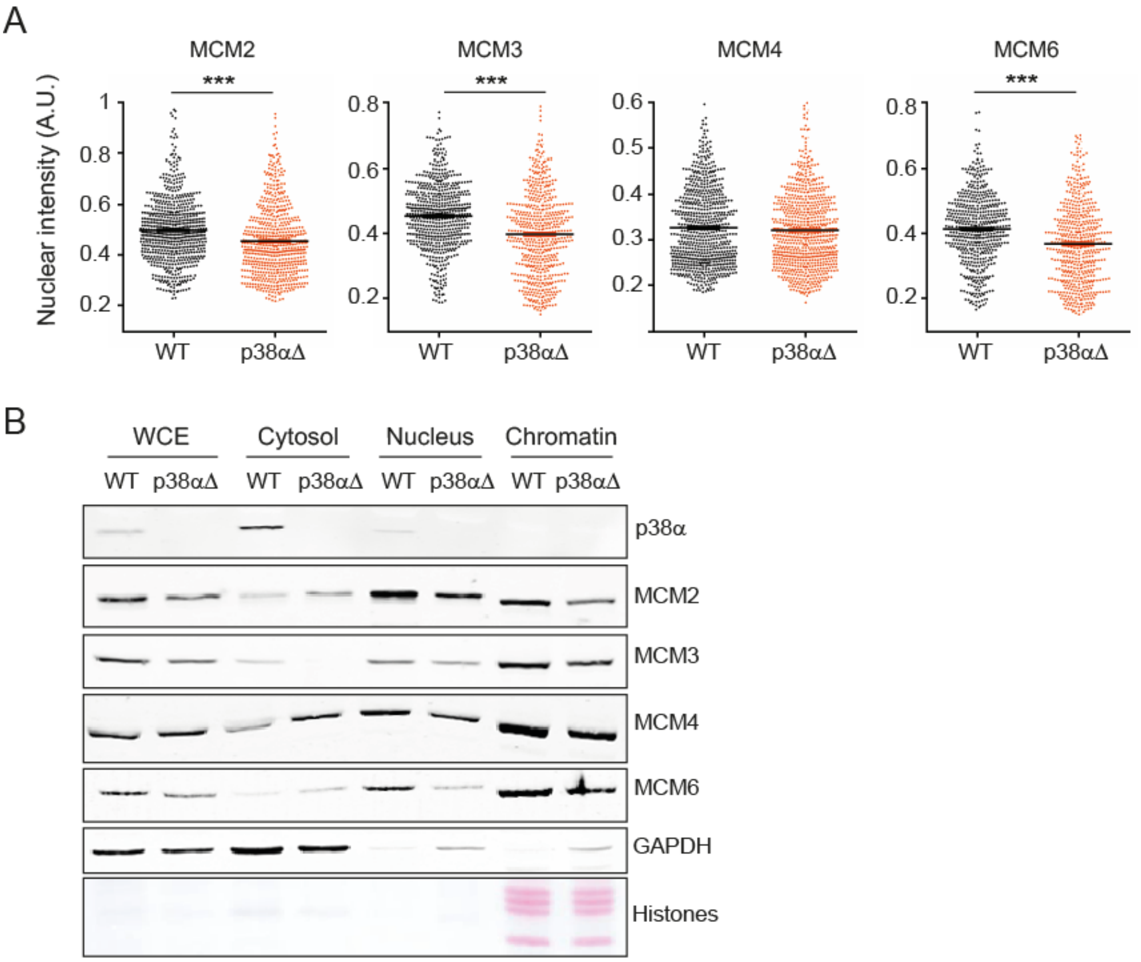

Figure 50. p38αΔ cancer cells show lower MCM levels in both the nuclear and chromatin-bound fractions A) Quantification of nuclear intensities of MCM2, MCM3, MCM4 and MCM6 were determined by immunofluorescence. Results were comparable in two independent experiments. B) MCM2, MCM3, MCM4 and MCM6 protein levels were analyzed in the different cellular compartments by subcellular fractionation and western blot. WCE, whole cell extract.

Given the global downregulation of all several MCM family members both at the mRNA and the protein level, we looked for possible common regulators. We used an online tool for searching transcription factor binding sites (MATCH) and found that all MCMs, with a higher or lower probability, could be bound by E2F family members among others. E2F is a family of transcription factors that is involved in the control of cell cycle progression, especially in the G1/S transition, and has been shown to directly and indirectly regulate MCM expression and localization (Ohtani et al., 1999, Yoshida and Inoue, 2004, Sabelli et al., 2009). We evaluated some E2F-dependent genes by qRT-PCR in WT and p38αΔ cells and observed a mild downregulation in most of them (except for cyclin A2, where a 40% reduction was detected) (Fig. 51A). However, no significant differences were found in the protein levels of E2F1 (Fig. 51B), the best characterized member of the family.

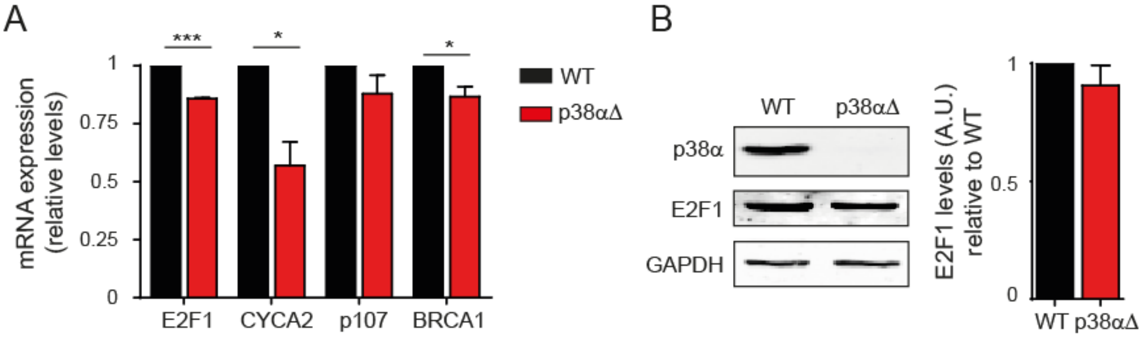

Figure 51. The E2F program does not seem to be affected after p38α deletion. A) Relative mRNA levels for the indicated E2F target genes were determined by qRT-PCR. Bar graphs show the quantification of two independent experiments. B) Total E2F1 protein levels were determined by western blot. Bar graph shows the quantification of three independent experiments.

While most of the MCMs analyzed were consistently downregulated at the mRNA and protein levels, E2F1 was barely affected at the protein level and several direct E2F targets were not strongly downregulated. Therefore, we considered unlikely that p38α could control MCM expression through the E2F program. Moreover, all these genes are related with cell proliferation programs. Hence, we hypothesized that, similarly to Myc, the downregulation of the E2F program, as well as the MCM expression, could be a consequence of a decreased DNA synthesis and slower cell proliferation and not the cause of replication stress, DNA damage and missegregation.

8. p38α deletion hampers ATR signaling and DNA repair in response to replication associated DNA damage

Next, we decided to study one of the most recognized causes of replication stress, which is the existence of unrepaired DNA lesions that represent physical obstacles to replication fork progression. For that, we investigated the status of the DNA damage response (DDR), the essential network that maintains DNA integrity by detecting DNA lesions, signaling their presence and promoting cellular responses including checkpoint activation and DNA repair (Jackson and Bartek, 2009). As a first approach, we challenged WT and p38αΔ cells with camptothecin (CPT), a topoisomerase I inhibitor that induces DNA damage specifically in S-phase. We observed that after an acute treatment with CPT, both WT and p38αΔ cells showed similar levels of γH2AX, suggesting that DNA breaks were equally sensed after p38α deletion. However, phosphorylation of two ATR substrates, RPA on serines 4, 8, and 33 and phosphorylation of Chk1 on serine 345 were reduced in p38αΔ cells (Fig. 52A), suggesting an impaired activation of the ATR kinase, a central player in the response to replication-associated DNA damage.

An essential step for fully activate ATR axis is the nucleolytic resection of DNA breaks to generate ssDNA overhangs, which are bound by RPA. We therefore quantified the number of RPA foci and noticed an increased number in the absence of p38α under basal conditions (Fig. 52B), which was consistent with the higher replication stress and increased stalled forks described above (Fig. 47A and 47B). However, in response to CPT treatment, p38αΔ cells showed reduced number of RPA foci compared to WT cells (Fig. 52B), suggesting that the DNA resection step was impaired. These results were validated by quantifying the generation of ssDNA by BrdU staining in non-denaturating conditions. Using this technique we observed that in basal conditions p38αΔ cells showed slightly more BrdU foci than WT cells, while reduced ssDNA generation was found following CPT treatment in comparison to WT cells (Fig. 52C). This confirmed the existence of replication stress in the absence of p38α and that DNA-end resection was defective following CPT incubation.

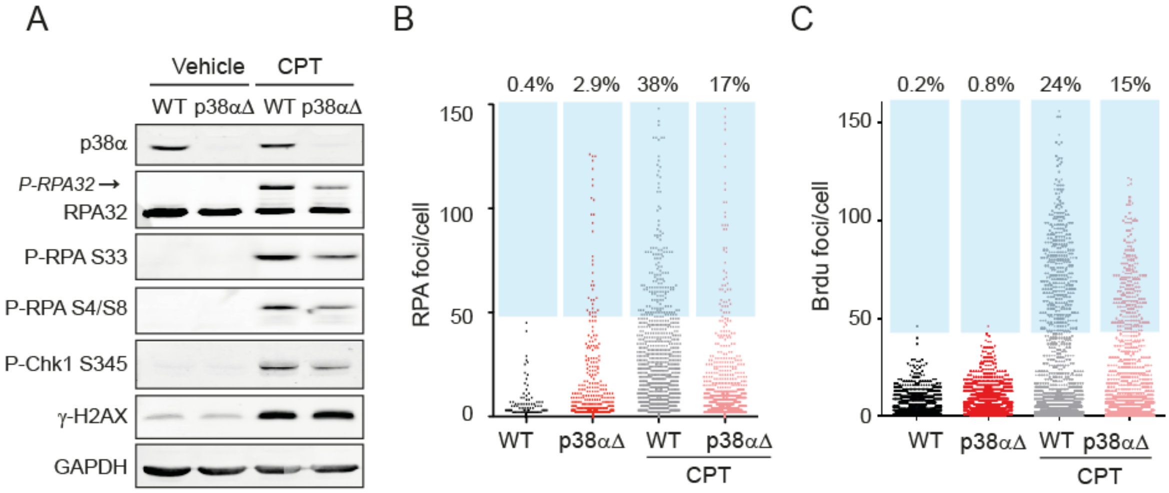

Figure 52. ATR activation and DNA-end resection after CPT incubation are impaired in the absence of p38α. A) WT and p38αΔ cells were treated or not with 1µM camptothecin (CPT) for 1h, and the phosphorylation status of RPA, Chk1 and γH2AX was analyzed by western blot. B) High-throughput microscopy quantification of RPA foci/cell in WT and p38αΔ cells treated or not with 0.1µM CPT overnight. The percentages of cells with more than 50 foci (blue boxes) are indicated. C) 10µM Brdu was incubated 48h and then cells were treated or not with 1µM CPT for 1h. BrdU was detected in non-denaturating conditions and high-throughput quantification of the BrdU foci/cell is shown. The percentages of cells with more than 40 foci (blue boxes) are indicated.

Since ssDNA generation and RPA signaling are required for homologous recombination (HR)-mediated DSB repair (Sleeth et al., 2007), we monitored RAD51 recruitment as a readout of HR efficiency. We observed fewer Rad51-containing cells in p38αΔ cells after CPT treatment (Fig. 53A), indicating reduced HR activity following DNA damage. This was further confirmed using a DR-GFP reporter to directly measure HR (Pierce et al., 1999). This reporter carries two mutant versions of GFP, none of which expresses a functional fluorescent protein *per se*. Addition of I-SceI creates a localized DSB in the first GFP copy that can be repaired using the second GFP gene, originating a wild-type glowing GFP (Fig. 53B left panel). Even if the DR-GFP integration was low, p38αΔ cells showed an approximately 50% reduction in the GFP(+) population (Fig 53B, center and right panels), indicating an impaired HR capacity in p38α deficient cells compared to WT cells.

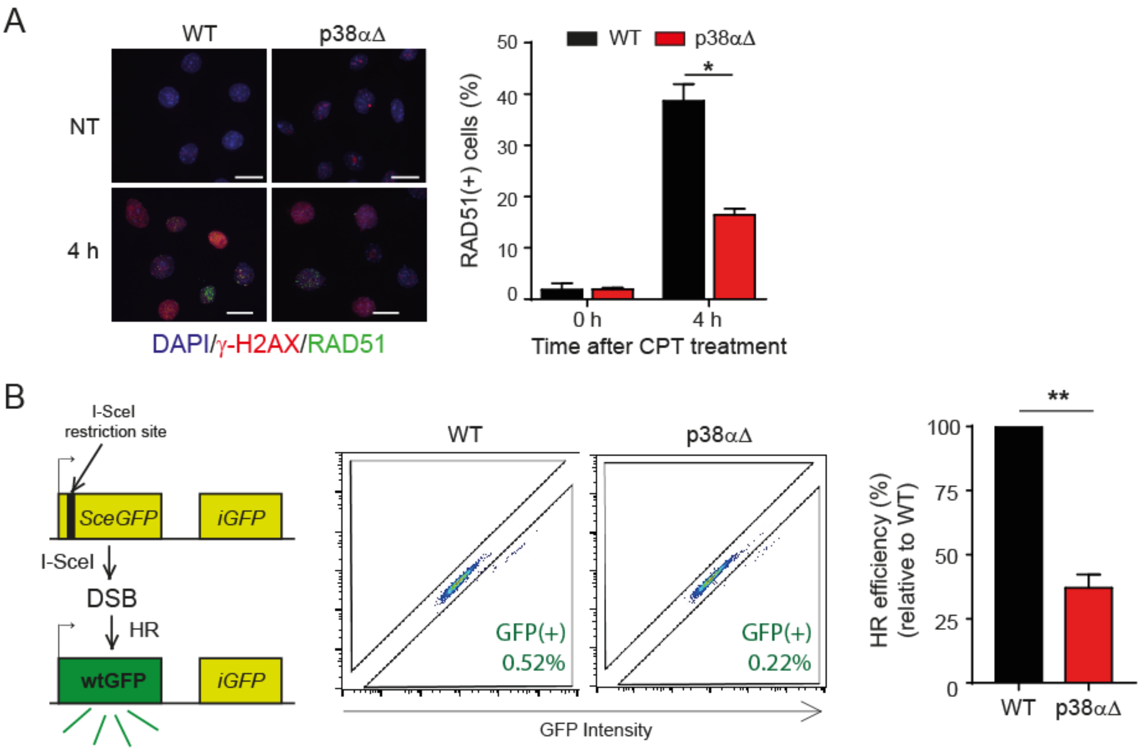

Figure 53. p38α is required for homologous recombination DNA repair in PyMT cancer cells. A) Representative images of γH2AX (red) and RAD51 (green) staining in WT and p38αΔ cancer cells treated with 1µM CPT for 1h and released for 4h. Bars=25µm. The histogram shows the quantification of two independent experiments. B) Squematic of the DR-GFP construct adapted from (Adamson et al., 2012) (Left panel). Flow cytometry plots of DR-GFP-infected WT and p38αΔ cells after I-SceI transfection (center panel). Quantification of GFP(+) cells in WT and p38αΔ cells of two independent experiments.

We repeated these experiments using ionizing radiation as source of DNA damage. γ-radiation produces several kinds of DNA lesions including damage to nucleotide bases, SSBs and DSBs and therefore different DNA repair pathways take place. Although NHEJ is considered the main repair option after ionizing radiation, HR is also involved (Mahaney et al., 2009). Accordingly, we irradiated WT and p38αΔ cells with 2.5Gy and analyzed ssDNA generation (Fig. 54A) and RAD51 recruitment (Fig. 54B). Results were comparable to those found with CPT, as p38αΔ cells showed decreased BrdU foci and reduced Rad51recruitment following radiation. These results confirmed the role of p38α as a key player in the DDR and its functions in DNA-end resection and HR independently of the DNA damage source.

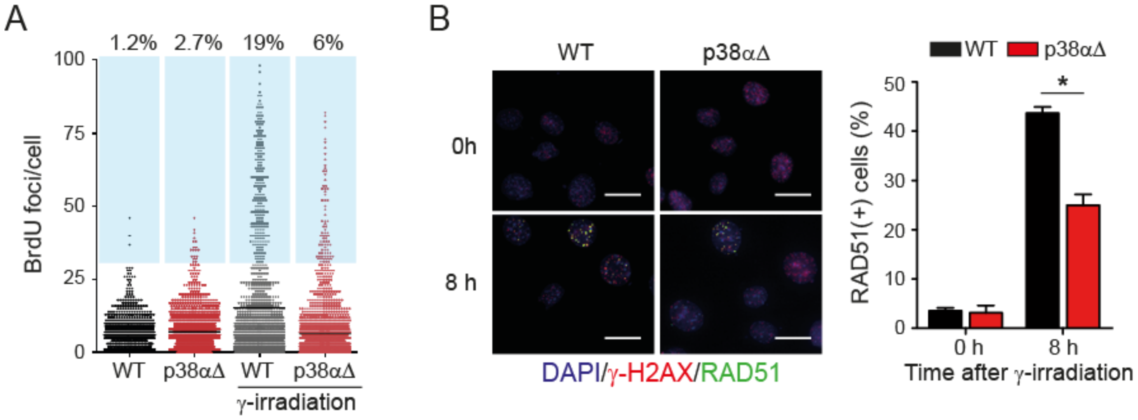

Figure 54. p38αΔ cancer cells showed reduced ssDNA generation and reduced Rad51 recruitment following ionizing radiation. A) Non-denaturating BrdU staining was used to directly detect ssDNA in WT and p38αΔ cells subjected or not to 2.5Gy radiation. Cells were harvested 2h after radiation. B) Representative images of γH2AX (red) and RAD51 (green) staining in WT and p38αΔ cancer cells irradiated with 2.5Gy released for 8h. Bars = 25µm. The histogram shows the quantification of two independent experiments.

Moreover, we performed these same assays using a p38 MAPK chemical inhibitor in order to determine if the kinase activity of p38α was required to produce all the observed phenotypes. We used PH797804, a p38 MAPK inhibitor with high affinity for the p38α isoform (Hope et al., 2009, Xing et al., 2012), currently used in clinical trials (Hope et al., 2009, Goldstein et al., 2010, MacNee et al., 2013). We observed that at the biochemical level, p38α inhibition showed an intermediate phenotype between WT and p38αΔ cells. After CPT incubation, PH797804 pretreated cells showed increased γH2AX and decreased RPA S4/S8 phosphorylation levels, comparable to those observed in p38αΔ cells. However, the effect on RPA S33 and Chk1 S345 was milder and the reduction in their phosphorylation was significantly lower than the one observed in p38α deleted cells (Fig. 55A). Meanwhile, functional assays using PH797804 offered clear results, since p38α inhibition blocked ssDNA generation (Fig. 55B) and Rad51 recruitment (Fig. 55C) to a similar extent as p38α deletion, indicating that p38α kinase activity is essential for DNA-end resection and homologous DNA repair development after DNA damage.

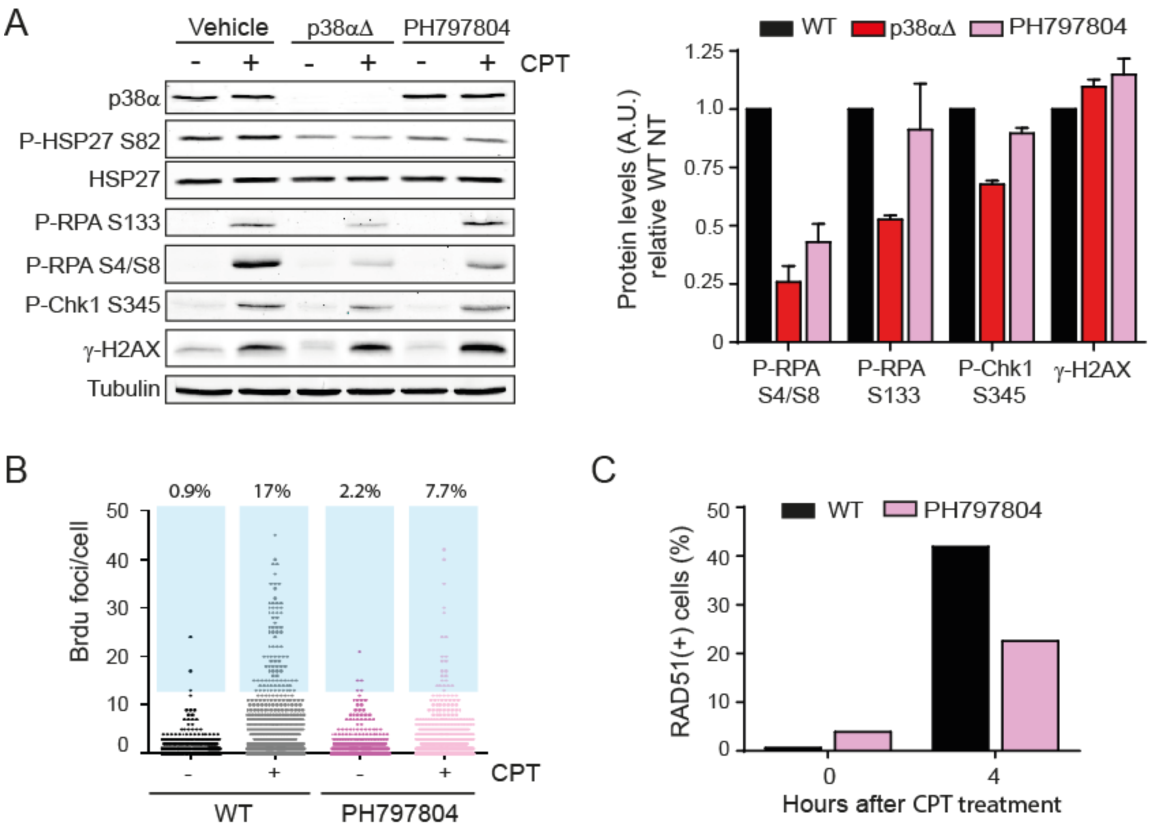

Figure 55. p38α inhibition recapitulates most of the DDR defects induced by p38α deletion in PyMT cancer cells. A) WT, p38αΔ cells and cells pretreated with 2µM PH797804 for 16h were incubated or not with 1µM CPT for 1h, and the phosphorylation status of RPA, Chk1 and H2AX was analyzed by western blot. Bar graph shows the quantification of two independent experiments. B) WT and PH797804 pretreated cells were incubated with 1µM CPT for 1h and ssDNA generation was assessed by non denaturating BrdU immunofluorescence. Percentage of cells containing more than 15 foci are indicated in the blue boxes. C) WT and PH797804 pretreated cells were incubated with 1 µM CPT for 1h and released for 4h. RAD51(+) cells were quantified by immunofluorescence.

Overall, the analysis of the DDR indicated that targeting p38α impaired ssDNA generation, RPA accumulation, ATR activation and Rad51 recruitment after DNA damage. A key factor in DNA repair pathway choice that promotes DNA-end resection in mammalian cells is CtIP, a critical regulator of the nucleolytic activity of the MRN complex (Sartori et al., 2007). CtIP contains many phosphorylation sites and twelve of them are SP/TP sites, which are potential targets for the p38α activity. Since CtIP phosphorylation has been shown to be important to control DSB resection activity (Anand et al., 2016, Huertas and Jackson, 2009, Polato et al., 2014, Makharashvili et al., 2014), we analyzed whether CtIP was a direct substrate of p38α. To test this hypothesis, recombinant CtIP was incubated *in vitro* with purified p38α and the reaction was analyzed by mass spectrometry. We found that p38α directly phosphorylated at least seven of the twelve SP/TP residues on CtIP including S276, T315, S327 and T847 (Fig. 56A, Supplementary Table 1), which have been previously involved in the regulation of CtIP activity (Cruz-Garcia et al., 2014, Huertas and Jackson, 2009, Steger et al., 2013), besides other non

SP/TP sites. We validated these results by repeating the kinase assay and performing western blot with available phospho-antibodies (Fig. 56B). We further corroborated these results by western blot using total protein lysates, which showed that the CPT-induced shift in CtIP was decreased in p38αΔ (Fig. 56C), as well as by immunofluorescence, where CPT-induced phosphorylation of CtIP on T315 was abolished in the absence of p38α (Fig. 56D).

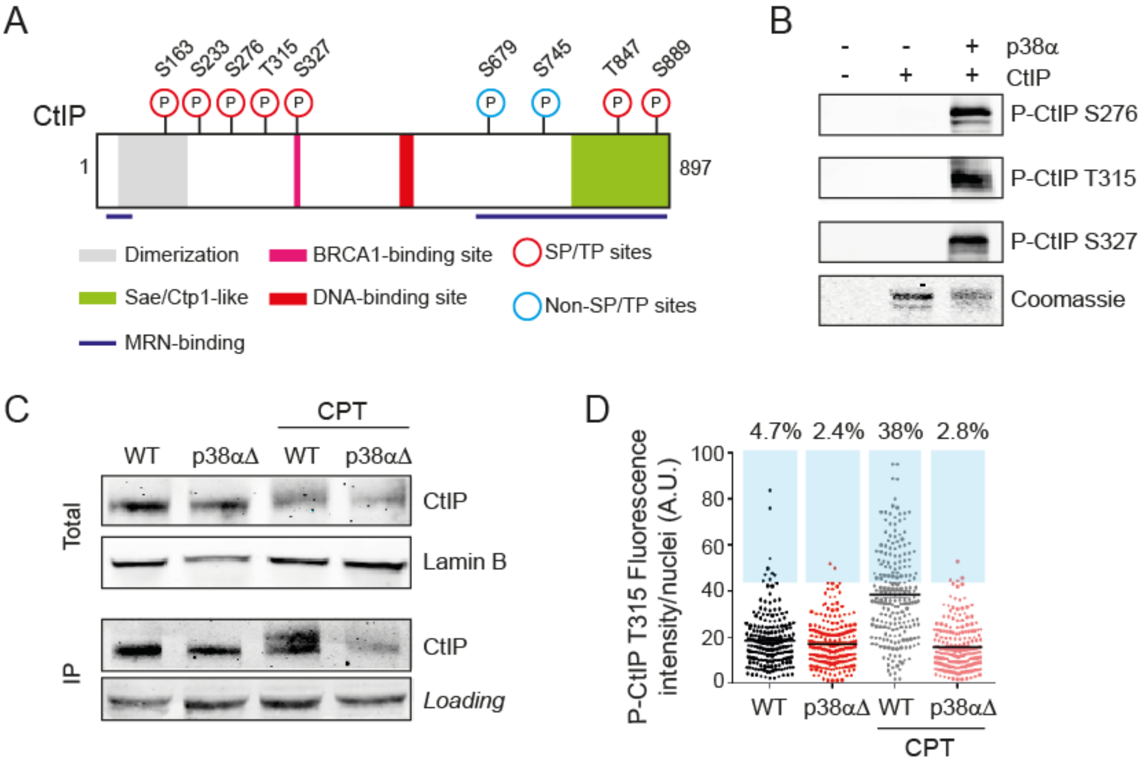

Figure 56. CtIP is directly phosphorylated by p38α *in vitro* and *in vivo*. A) Schematic indicating the CtIP sites phosphorylated by p38α *in vitro* determined by mass spectrometry analysis. B) Purified N-terminal CtIP was phosphorylated *in vitro* with p38α and then analyzed by western blot with the indicated phospho-antibodies. A representative Coomassie staining is shown. C) CtIP levels were analyzed in total lysates (up) and after CtIP immunoprecipitation (down) in WT and p38αΔ cells, incubated or not in 1µM CPT for 2h. In both cases a shift in the CtIP band corresponds to hyper-phosphorylation of the protein. D) WT and p38α-deficient cancer cells were treated with 1µM CPT for 2h, and then analyzed by immunofluorescence using the CtIP phospho-T315 antibody. The percentages of cells with an intensity value higher than 45 (blue boxes) are indicated.

Collectively, these results indicated that p38α can directly phosphorylate CtIP on sites that are required to regulate DNA-end resection, and that in the absence of p38α cells exhibited reduced ATR signaling, impaired HR, increased DNA replication stress and elevated DNA damage. These defects were compatible with un-replicated and damaged DNA entering in mitosis, giving rise to a mitotic phenotype, missegregation and CIN.

9. Inhibition of p38α potentiates the anti-tumoral effect of chromosome instability-inducing chemotherapeutic drugs

Some chemotherapeutic agents used in breast cancer therapy, such as the taxanes paclitaxel and docetaxel cause missegregation in proliferating cells and promote CIN. Our results suggested that targeting p38α could increase tumor cell sensitivity to these compounds and enhance their anti-tumoral effect. To test this hypothesis we used three chemical inhibitors of p38MAPK, PH797804, SB203580, and LY2228820. In order to address their possible cooperation with taxanes, these inhibitors were used at the lowest inhibitory dose and during a short period of time. We initially performed clonogenic assays and observed that while p38 MAPK inhibitors in these conditions had a mild effect on the viability of PyMT cancer cells, their combination with either paclitaxel or docetaxel significantly decreased colony number and size (Fig. 57A). This correlated with cell death data, as we observed barely no differences with the inhibitors alone, but their addition to taxanes significantly increased cell death in comparison with the chemotherapeutic drugs alone (Fig. 57B).

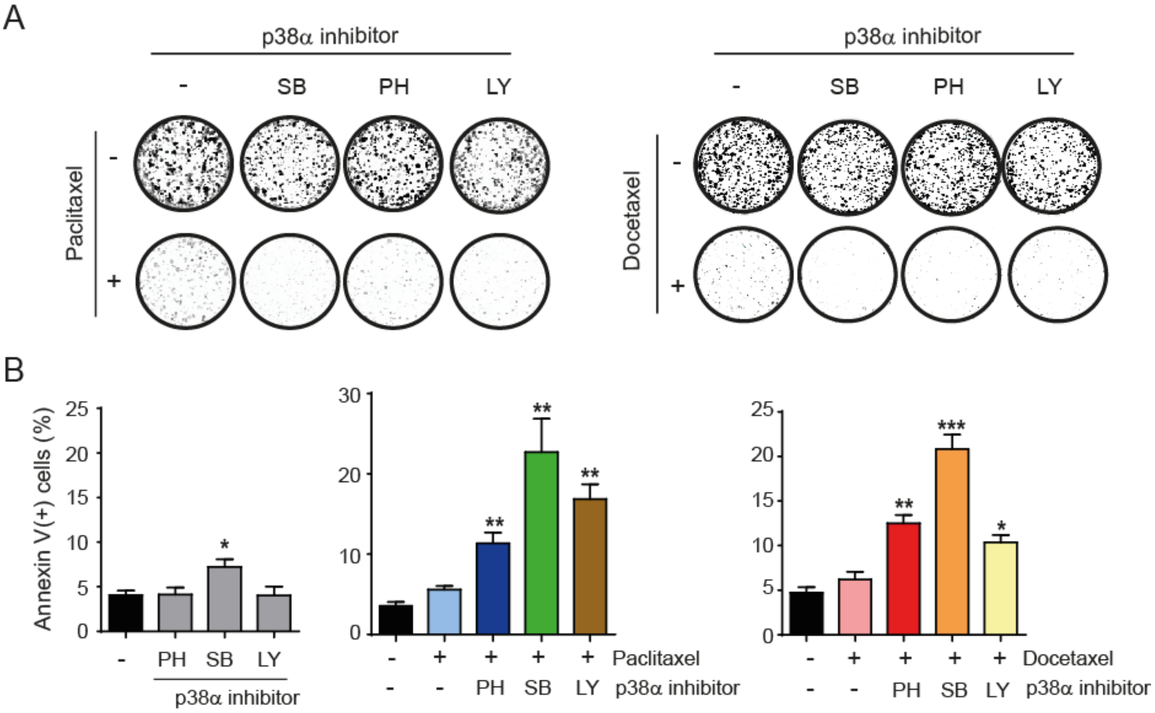

Figure 57. Targeting p38α increases sensitivity to taxanes in PyMT cancer cells. PyMT breast cancer cells were treated with 25nM paclitaxel or 5nM docetaxel and 5μM SB253080 (SB), 2μM PH797804 (PH) or 100nM LY2228820 (LY) for 48h and then subjected to the corresponding analysis. A) Survival was determined by clonogenic assay. B) Cell death was assayed by Annexin V staining. Graphs show the quantification of three independent experiments. Statistical significance was calculated between the vehicle and each of the inhibitors (left panel) and between each drug alone and the drug in combination with every p38 MAPK inhibitor (center and right panels).

We validated these results using female mice with PyMT-induced mammary tumors, which were treated with paclitaxel or docetaxel and PH797804. When administered alone, taxanes at the doses used only exerted a cytostatic effect on tumor growth. However, when combined with PH797804, we observed a substantial reduction of tumor size (Fig. 58A and 58B), which correlated with increased levels of DNA damage (Fig. 58C and 58D) and higher number of missegregation events (Fig. 58E and 58F). These results were consistent with the idea that p38α contributes to the DNA damage response and facilitates the survival of breast cancer with high levels of CIN. Moreover, they confirmed the hypothesis that targeting p38α sensitizes breast cancer cells to CIN-inducing agents such as taxanes, raising the possibility of using p38α inhibitors in the clinic.

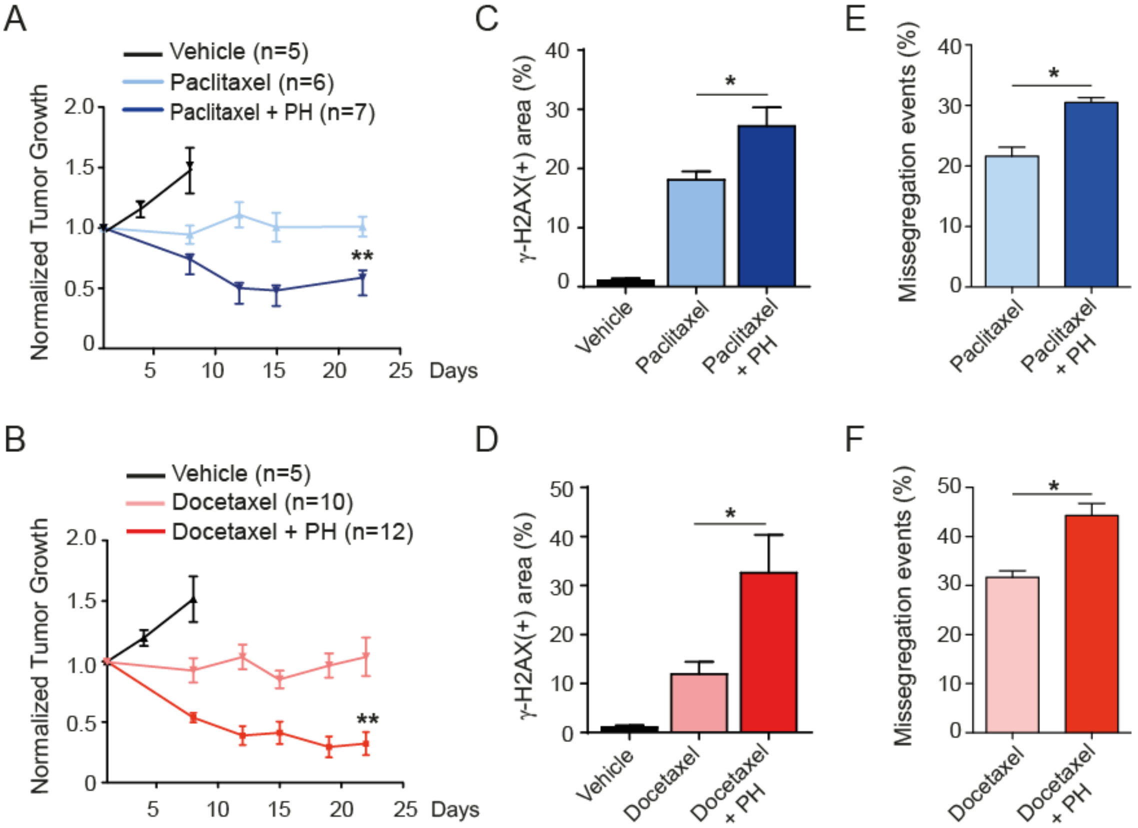

Figure 58. Targeting p38α enhances the anti-tumoral effect of taxanes in PyMT-derived tumors *in vivo*. A,B) Growth curve of PyMT-induced mammary tumors in mice treated with paclitaxel or docetaxel either alone or in combination with PH797804. The same vehicle-treated animals are represented in both graphs. Statistical analysis was performed using Student´s t-test at the endpoint of the experiment between the drugs alone or in combination with PH797804. C,D) DNA damage was measured using γH2AX staining. Graphs represent the γ-H2AX(+) area in at least 5 independent tumors, with a minimum of 15 fields quantified per tumor. E,F) Mitotic figures were analyzed at the end of the treatment using p-H3 staining. Graphs show the percentage of missegregation events in at least two independent mammary tumors, with at least 10 fields quantified per tumor.

To further support the potential clinical application of our results, we used several patient-derived xenografts (PDXs) generated from patients with triple negative or luminal tumors, which were treated with either paclitaxel or docetaxel and PH797804 as indicated in Fig. 59.

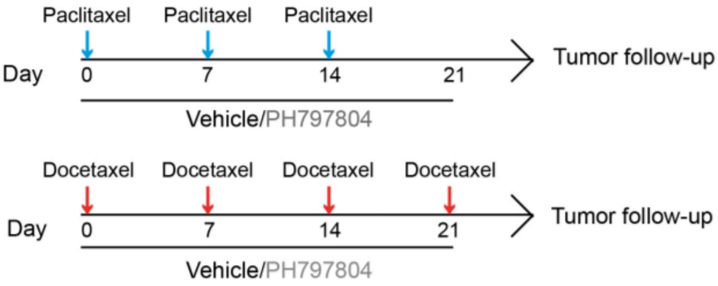
Paclitaxel
Paclitaxel
Paclitaxel
Day
0
7
14
21
Tumor follow-up
Vehicle/PH797804
Docetaxel
Docetaxel
Docetaxel
Docetaxel
Day
0
7
14
21
Tumor follow-up
Vehicle/PH797804

Figure 59. Schematic of the timeline of the combination treatments. Color arrows indicate the intraperitoneal injections of each chemotherapeutic drug. The solid line indicates the time during which mice are subjected to PH797804 treatment through oral gavage.

We found that tumor behavior was different, depending on both the drug and the PDX model, highlighting the clinical diversity of human breast cancer. However, in most cases, co-administration of PH797804 enhanced, accelerated or prolonged the anti-tumoral response observed with the taxanes alone, except for TN5 and Lum4, in which no additional benefit was observed (Fig. 60)

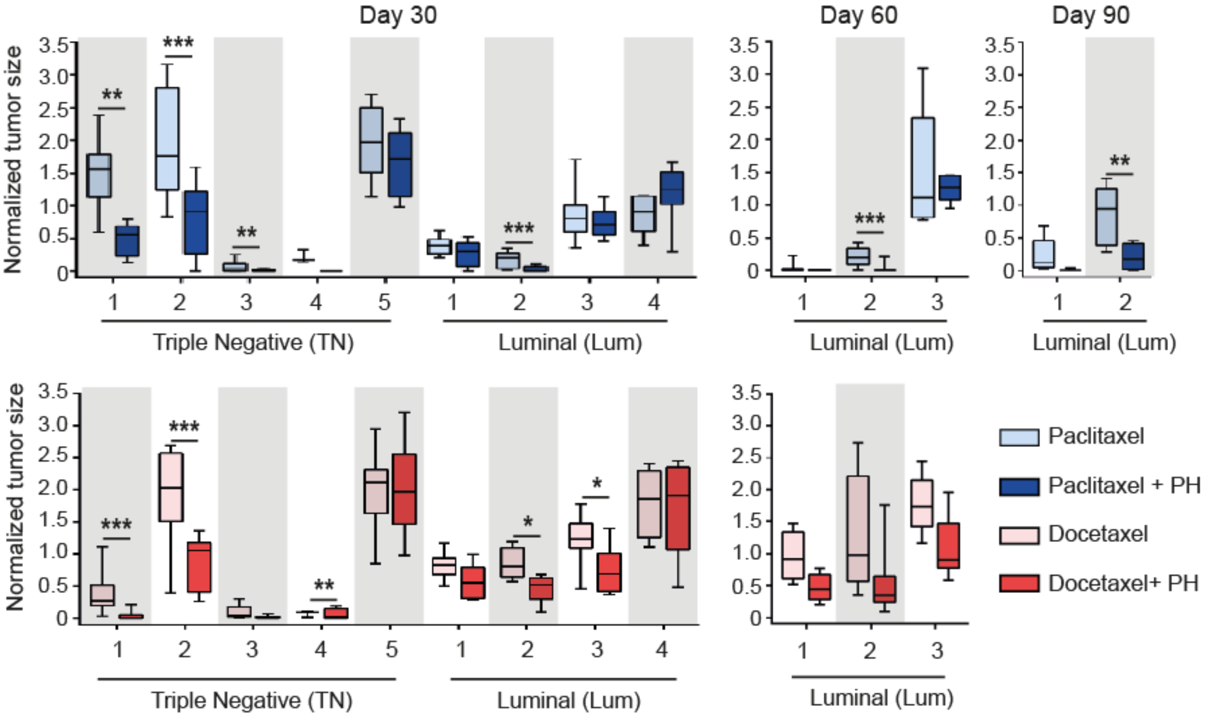

Figure 60. Response of nine PDX models to the combination of taxanes and p38α inhibition. NOD/Scid female mice implanted with human breast tumors were treated with vehicle or the indicated drugs either alone or in combination PH797804. Tumor size was followed up. Box plots show the relative tumor size compared to the initial tumor volume at the beginning of the treatment of each model at the indicated days.

We then selected four tumors that responded well to the combined treatment (TN1, TN2, Lum1 and Lum2) and the two in which the p38α inhibitor did not affect the taxane response (TN5 and Lum4), and analyzed them at an early timepoint (day 11 in case of paclitaxel and day 17 in case of docetaxel). Consistent with our previous results in the PyMT-induced mammary tumors, PDXs in which PH797804 enhanced the anti-tumoral response to taxanes showed both increased γH2AX staining (Fig. 61A) and increased percentage of missegregation events (Fig. 61B) in response to the combination therapy. Of note, this synergy was also observed in Lum1 and Lum2, which showed small differences in tumor size at this early stage, suggesting that the enhanced DNA damage and missegregation reflect an early response mechanism that translates into noticeable effects at later timepoints.

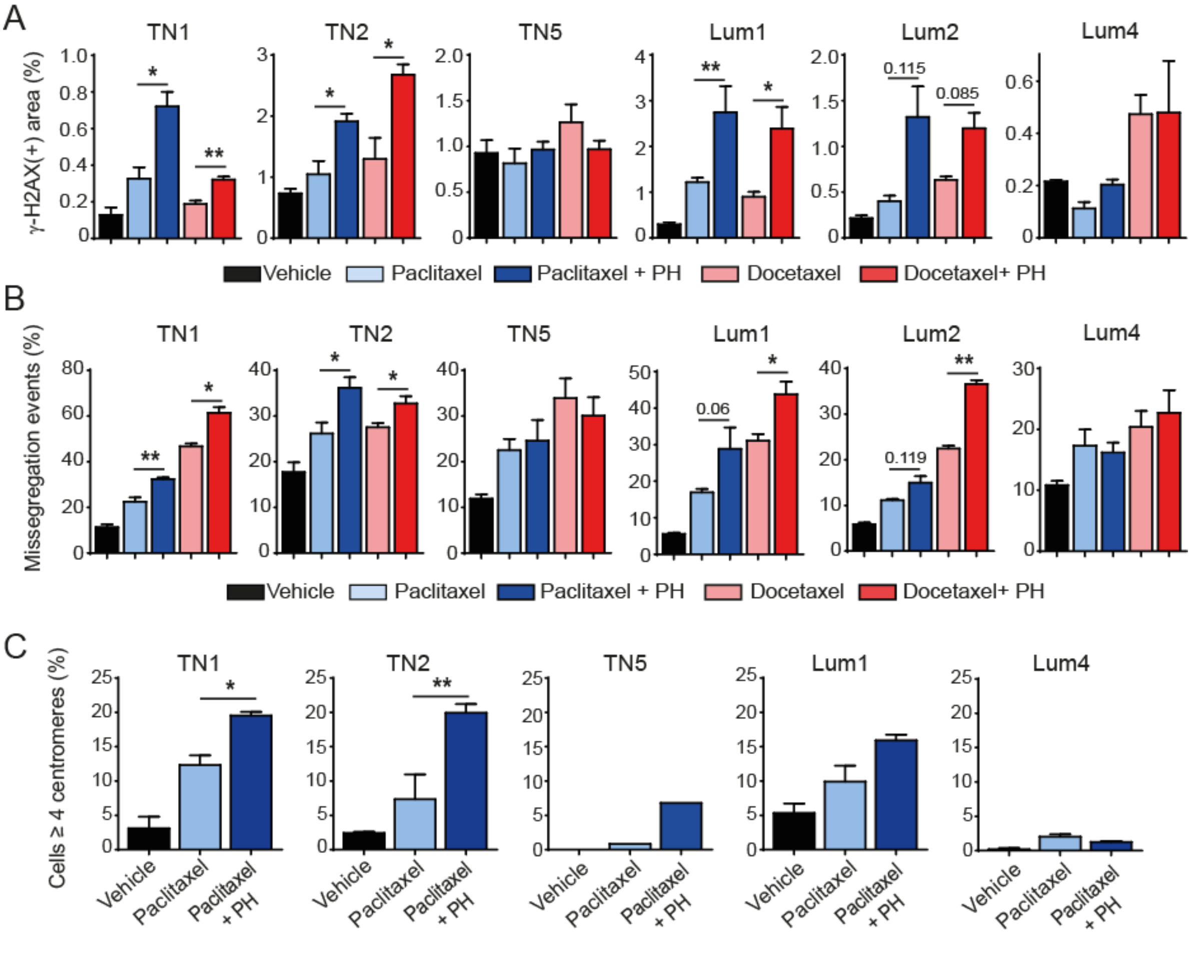

Figure 61. DNA damage, missegregation and aneuploidy are increased following the combinatory treatment in responsive PDX models. A) DNA damage was measured by γ-H2AX staining in tumor sections. γ-H2AX(+) area was determined in at least 10 fields per sample in two to six independent tumors. B) Mitotic figures were analyzed by p-H3 staining. Graphs show the percentage of missegregation events in at least 10 fields per sample in two to six independent tumors. C) Representative tumors were stained with a chromosome 17 centromeric probe, and at least 150 cells were analyzed in each group. Histograms show the percentage of cells carrying 4 or more centromeres. Two independent tumors per condition were analyzed except for model TN5, were data correspond to one representative tumor.

FISH analysis further confirmed these results, as we observed that PH797804 tended to enhance the aneuploidy induced by paclitaxel in tumors (Fig. 61C) and the PDXs where combination therapy was beneficial corresponded to those models with higher basal aneuploidy and where higher aneuploidy was reached after the treatments.

Interestingly, these results revealed a correlation between basal aneuploidy in the tumor cells and the response to taxanes (Fig. 62A) and to the combined treatment (Fig. 62B).

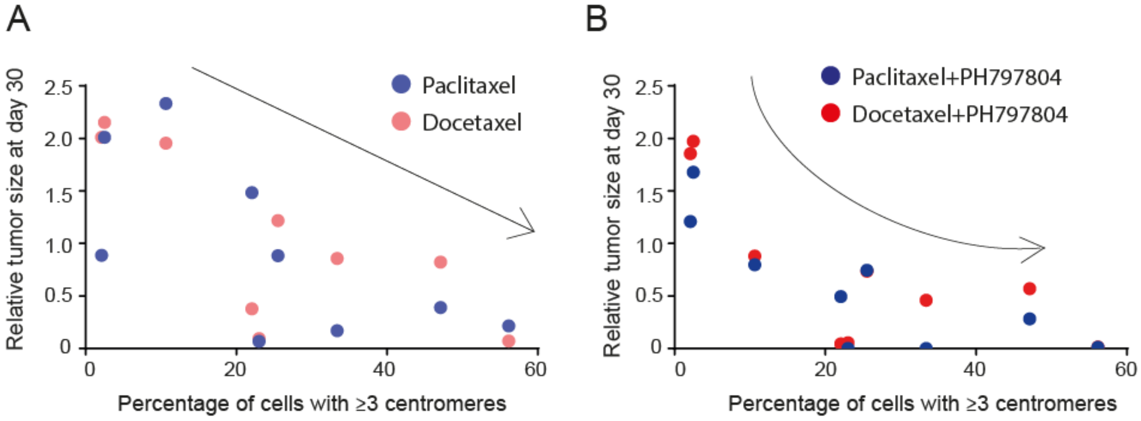

Figure 62. Correlation between aneuploidy rate and tumor size at day 30 after paclitaxel or docetaxel treatments either alone or in combination with the p38α inhibitor. A) Every dot corresponds to a single PDX model, subjected to paclitaxel (blue) or docetaxel (red) treatment. B) Every dot corresponds to a single PDX model, subjected to paclitaxel+PH797804 (blue) or docetaxel+PH797804 (red) treatment. A tendency between higher aneuploidy and smaller tumors (i.e. bigger tumor reduction) is observed. Therefore, more aneuploid tumors tend to respond better to taxanes and to the combined therapy.

Taken together, it seems that even in tumors where chemotherapy is particularly effective, interfering with p38α signaling further damages cancer cells, avoiding or delaying tumor relapse. Of note, models TN5 and Lum4, in which p38α inhibition had no evident benefit compared with the taxane treatment alone, showed no differences in DNA damage or segregation errors as well as poor aneuploidy induction in response to the combined treatment.

To try to understand why p38α inhibition did not potentiate the taxane effects in all PDX models, basal aneuploidy, DNA damage, and missegregation rates were analyzed in untreated tumors of every model. We observed that tumors with a medium to high aneuploidy level responded better to the combined taxane and p38α inhibition treatment, while tumors with more stable genomes were refractory to the combined treatment (Fig. 62A). However, we found no correlation between basal levels of DNA damage or missegregation rates and the ability of PH797804 to potentiate the taxane effects (Fig. 63B, 63C).

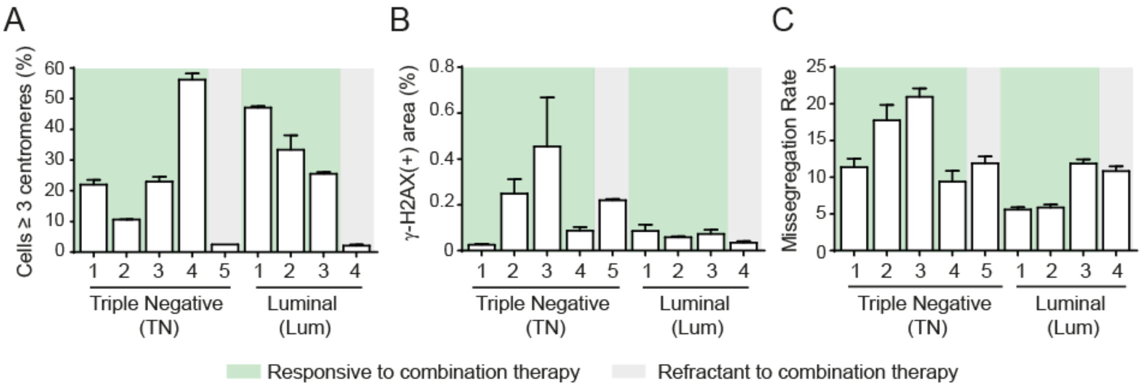

Figure 63. Analysis of basal aneuploidy, DNA damage and missegregation rate in untreated PDX models. (A - C) Aneuploidy (A) DNA damage (B) and missegregation rates (C) of the different PDXs were analyzed in untreated tumors of 150-200 mm^3. Green backgrounds indicate breast tumors where the combination therapy effectively reduced tumor size compared to taxanes alone; grey backgrounds indicate models where the combination therapy failed to significantly reduce tumor size

Altogether, our results suggest that the combination of p38α inhibition with taxane-based chemotherapy would be especially beneficial in breast tumors that have higher CIN levels.

DISCUSION

Sustained proliferation, apoptosis evasion and genomic instability are among the most prevalent hallmarks of cancer cells (Hanahan and Weinberg, 2011). A well-supported model proposes that oncogenes drive unscheduled DNA replication and induce replication stress, leading to genomic instability and cell death (Macheret and Halazonetis, 2015). This results in selective advantage for tumor cells that acquire mutations that allow them to evade apoptosis during tumor evolution, but also confers a dependency on DDR signaling that is required to prevent excessive CIN. Here we describe a novel role for p38α in maintaining genomic stability and promoting tumor cell survival by facilitating DNA replication and repair, perhaps explaining why the gene encoding p38α (MAPK14) is not frequently mutated in human tumors. According to the catalogue of somatic mutations in cancer (COSMIC), less than 0.2% of breast tumors show mutated forms of MAPK14, while almost 8% overexpress MAPK14 gene. These numbers are comparable to those found in cBioportal, where the few MAPK14 alterations found in breast cancers are mainly gene amplifications (Fig. 64), further suggesting that p38α expression is required or at least represents an advantage for cancer cells.

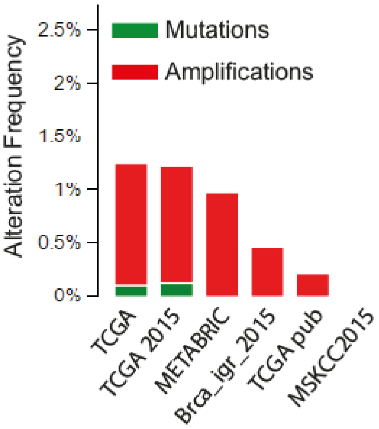

Figure 64. Genomic alterations in breast cancer collections. Graph adapted from www.cbioportal.org

1. p38α as an example of non-oncogene addiction in breast cancer cells

This idea of p38α as a "tumor-enabling" protein contradicts at first sight the classical tumor-suppressive role ascribed to p38α in the literature. p38α has been shown to impact cell proliferation by inducing apoptosis, driving differentiation, mediating senescence or regulating cell cycle checkpoints (Wagner and Nebreda, 2009). Although most of the work was initiated using *in vitro* models or cell line xenografts (Puri et al., 2000, Pruitt et al., 2002, Bulavin et al., 2002, Brancho et al., 2003), similar outcomes were found in mouse models (Ventura et al., 2007, Gupta et al., 2014). However, most of these studies analyzed the role of p38α in tumor initiation and many of them focused exclusively on Ras as the driving oncogene. More recently, several reports using established cancer cell lines and established tumors have uncovered a tumor promoter or tumor supporter role for p38α, since its targeting leads to decreased proliferation and survival in several models (Chen et al., 2009, Leelahavanichkul et al., 2014, Gupta et al., 2014, Gupta et al., 2015). Altogether, it seems that p38α is not a classical tumor suppressor such as p53, p16 or PTEN, which are commonly inactivated in human cancers (Yeang et al., 2008), but a flexible pathway which the cancer cell can benefit from. According to our work, p38α could be considered as an example of “non-oncogene addiction”, since we did not detect p38α overexpression or activation during tumor development, but it turned out to be essential for breast cancer cell homeostasis. This idea is supported by clinical data, where p38 MAPK activation has been found in high-graded breast tumors (Salh et al., 2002) and breast cancer effusions (Davidson et al., 2006), and correlated with poor prognosis (Esteva et al., 2004).

The interest of non-oncogene addiction relies on its potential application in cancer therapy. Oncogenes like Myc or Ras are not directed targetable yet and those which are, such as Her2 or BRAF, frequently lead to the appearance of resistance. On the contrary, non-oncogene addiction has been suggested as an alternative way to selectively kill cancer cells through the search of synthetically lethal interactors, or at least the induction of toxic levels of stress (Nagel et al., 2016).

In this work, we have characterized a CIN limiting role of p38α in the PyMT model. As other tumorigenesis models, PyMT is a potent oncogene driver and induces tumors that do not fully reproduce the plethora of mutations, the heterogeneity, and behavior of human tumors. However, using PDXs we showed that p38α targeting, combined with CIN-inducing drugs such as taxanes, leads to toxic levels of DNA damage, missegregation and aneuploidy, killing human cancer cells. On the one hand, this confirms the stress-buffer function of p38α and, on the other hand, validates the non-oncogene addiction of human cancer cells to p38α and the potential use of this dependency for therapy. Altogether, our results suggest that p38α inhibitors represent an unexplored treatment opportunity since p38α signaling remains functional in breast tumor cells.

Other rational combinatory strategies based on stress overload are currently being investigated to specifically target cancer cells. A promising example of a combinatorial strategy in clinical trials is the use of PARP inhibitors for treatment of HR-deficient (ex. BRCA1/2 deficient) tumors (Farmer et al., 2005, Esposito et al., 2015), or its combination with other chemotherapeutic agents (Drean et al., 2016, Oza et al., 2015) leading to synthetic lethality. More recently, ATR and Chk1 inhibitors, have been shown to increase levels of replication stress, alone or in combination with other chemotherapeutic drugs or genetic lesions (Daud et al., 2015, David et al., 2016, Dillon et al., 2017, Zhang et al., 2016). In addition, a MPS1 inhibitor that induces missegregation has been recently reported to synergize with taxanes to induce tumor regression (Janssen et al., 2009, Maia et al., 2015), further suggesting that combinatorial strategies to enhance CIN may be promising for clinical use.

2. Novel role of p38α in replication-associated DNA damage response

In this thesis we describe an essential role of p38α in the coordination of the DNA damage response and restriction of CIN, independently of its functions controlling the checkpoints and cell cycle progression.

There is good evidence implicating p38α in cell cycle regulation, either at the G2/M transition (Bulavin et al., 2001, Warmerdam et al., 2013, Cha et al., 2007, Llopis et al., 2012) or at the G1/S checkpoint in response to γ-radiation (Lafarga et al., 2009). It has also been implicated, together with p53 and p21, in the cell cycle arrest induced by centrosome disruption (Mikule et al., 2007). Moreover, the p38α pathway can contribute to the survival of cells with damaged DNA (Reinhardt et al., 2007). These are just examples of the extensive literature regarding p38α and DNA damage response regulation. Of note, most if not all of the proposed functions are related to cell cycle checkpoint activation following a plethora of stimuli; however, to our knowledge there are no studies directly linking p38α and DNA repair mechanisms.

Our results indicate that p38α directly phosphorylates CtIP, an essential factor in DSB repair pathway choice. CtIP is a large protein with many phosphorylation sites that are targets of several kinases such as CDKs, ATM, or ATR (Steger et al., 2013, Wang et al., 2013, Huertas and Jackson, 2009, Peterson et al., 2013). This might mask the role of p38α; however, we proved p38α regulation to be functionally relevant, since in its absence ATR signaling, DNA end-resection, and homologous recombination were impaired following DNA damage. All these defects are consistent with the downregulation of CtIP (Sartori et al., 2007), suggesting that p38αΔ phenotypes could be mediated by the impairment of CtIP function. Importantly, we found defects not only upon DNA damage induction, but also in basal conditions. Although the levels of RPA or Chk1 phosphorylation were barely detectable in normal proliferating cells, we found increased levels of ssDNA and RPA recruitment, as well as decreased homologous recombination efficiency upon p38α downregulation in the absence of any stimuli. This suggests that CtIP impairment not only affects the way cells respond to exogenous DNA damage, but also how cancer cells cope with their own endogenous damage, explaining why p38αΔ breast cancer cells show replication stress and higher DNA damage. Consequently, p38α-deficient cancer cells with impaired response to replication associated DNA damage and HR-mediated repair would undergo mitosis with incompletely replicated regions and damaged DNA (Lukas et al., 2011), likely accounting for the increased levels of anaphase bridges, chromosomal breaks and impaired chromosome segregation. Of note, the deletion or inhibition of MK2, a direct substrate of p38α, in U2OS cells was shown to exert a protective role in response to gemcitabine, a replication interfering agent (Kopper et al., 2013). Although the cell system and the exogenous insult were not the same, this opposite role, together with the fact that deletion of MK2 did not show any effect in the DNA fiber assay under basal conditions, suggests that the DDR phenotypes we observed are not mediated by MK2.

Moreover, we found chromosomal fusions and circular chromosomes in metaphase spreads from p38αΔ cells. These structures are thought to result from the fusion of broken chromosome arms that cannot be properly segregated and often give rise to chromosome breakage and errors in cell division. They are usually indicative of illegitimate repair by HNEJ and are found in the absence of other HR-associated factors such as Brca1 or Exo1, and reversed after downregulation of NHEJ components like 53BP1 (Eid et al., 2010, Bunting et al., 2010, Chapman et al., 2013). Although we have not directly addressed NHEJ activity, an increase in this error-prone pathway could be a compensatory response to HR repair downregulation (Ceccaldi et al., 2016, Kelley et al., 2014), and may enhance the tendency to chromosomal aberrations and missegration, cooperating in the mitotic phenotype of p38αΔ cells.

Intriguingly, p38 MAPK inhibition was shown to overcome irinotecan (a CPT derivative) resistance in some colon tumors (Paillas et al., 2011), but the underlying mechanisms remained unknown. Altogether, our results shed light on the molecular basis of this cooperation and open the window to other synergies with different DNA damaging and replication interfering drugs, especially with those inducing replication-associated DSBs. Indeed, p38 MAPK inhibition cooperates with cisplatin to cause cancer cell death in the PyMT transgenic model (Pereira et al., 2013) and has been proposed to collaborate with other chemotherapeutic agents in different cancer types (Garcia-Cano et al., 2016). Therefore, although other routes may be implicated, the p38α role in DSB repair and restricting replication stress and CIN may contribute to explain these synergies.

Our study was focused mainly on camptothecin, and validated, to a lesser extent, using γ-radiation, and the p38α role may depend on the source, intensity, and duration of the stimuli, in a similar way it does during checkpoint activation. Therefore, further analysis using a comprehensive range of damaging agents and analyzing other DNA repair pathways would be required to fully characterize the role of p38α in the DDR and predict potential synergies that could be therapeutically useful.

In addition, it would be informative to perform these experiments using both deletion and inhibition strategies. We observed that DNA-end resection and homologous recombination, measured as the generation of ssDNA and recruitment of RAD51, were downregulated in a similar way in p38α-deficient cells and p38α-inhibited cells. However, at the biochemical level we found some differences such as the phosphorylation of RPA on serine 33 or Chk1 at serine 345, which were much less affected in the case of p38α inhibition. Phosphorylation of RPA S4/S8, which was significantly downregulated both by p38α deletion and inhibition, requires CtIP

(Sartori et al., 2007). Meanwhile, CtIP depletion barely affects RPA phosphorylation on serine 33, which is mainly driven by ATR (Shiotani et al., 2013), and does not significantly impact on Chk1 phosphorylation in the early phase of CPT response, but later (Shiotani et al., 2013, Kousholt et al., 2012). Collectively, p38α deletion and inhibition coincide in the reduction of RPA S4/8 phosphorylation and decreased DNA-end resection, which are both dependent on CtIP. However, p38α absence seems to affect ATR signaling from the very beginning, impacting also on RPA S33 and Chk1 S345 phosphorylation. This would suggest that the physical presence of p38α may modulate, directly or indirectly, ATR activity, for example through ATRIP (ATR interacting protein) or TOPBP1 (an ATR activator protein).

Finally, DNA repair is closely related to DNA replication since DNA lesions are one of the most important sources of replication stress. In turn, replication defects originate SSBs that can eventually be converted into DSBs. This crosstalk suggests that p38α impairment of DNA repair would also affect DNA replication, and indeed, we found increased fork stalling and decreased inter-origin distance and replication fork rate in p38αΔ cells. Given that cancer cells are known to be genomically unstable and to be subjected to higher replication stress than normal cells (Halazonetis et al., 2008, Negrini et al., 2010), p38α targeting might be more deleterious in transformed cells than in normal cells, and would selectively or preferentially affect cancer cells. However, we have not tested this hypothesis directly.

3. p38α deletion increases chromosome instability and sensitizes breast cancer cells to CIN-inducing agents.

There is evidence implicating p38α in cell cycle arrest upon chromosome miss-segregation in a human cell line (Thompson and Compton, 2010), which connects p38 MAPK with p53 and cell cycle arrest. Additionally, p38α has been recently shown to protect epithelial cells from CIN insults such as gene dosage imbalance in *Drosophila* epithelial cells (Clemente-Ruiz et al., 2016), probably due to its relationship with JNK. Together, these reports propose different mechanisms by which p38α regulates the response to aneuploidy in different systems. In our work, however, we observed that p38α downregulation results in aneuploidy and CIN *per se*. As commented in previous sections, many roads can lead to aneuploidy and during this study some of them were evaluated.

Although we initially thought about the SAC as a main source of aneuploidy, we found no severe functional defects in this safeguard mechanism. Most of the differences that we found in terms of protein and gene expression could be explained by a decreased cell proliferation rate. Moreover, the only data pointing to SAC was the slight decrease in the duration of the mitotic arrest in response to paclitaxel. Sometimes small differences underlie marked phenotypes. However, SAC is thought to be relaxed in many cancer cells (Yamada and Gorbsky, 2006) and to be especially ameliorated in murine cells (Haller et al., 2006). Therefore, we did not consider defective SAC to be the main driver of cancer cell death in our model.

Similarly, we discarded MCM deficiency as a main cause of RS and CIN. MCM proteins can be reduced without hampering DNA replication at least in yeast, *Xenopus* and *Drosophila* (Crevel et al., 2007, Lei et al., 1996). However, MCM deficiency can cause proliferation defects, replication stress and genomic instability in several models (Flach et al., 2014, Alvarez et al., 2015, Passerini et al., 2016, Ibarra et al., 2008). Although our phenotypes were consistent with MCM downregulation, we wondered whether a 40% MCM reduction (in some, but not all of the analyzed MCMs*)* was enough to drive such effects in the absence of any exogenous stimuli. Moreover, it was unclear whether the reduction in all these proteins was a cause or a consequence of the reduced cell proliferation. Given that we were not able to answer these questions and since other replication-associated genes such as Cdc6 and ORC were also downregulated, we decided to leave aside the MCM deficiency hypothesis.

Although we cannot rule out that these or other mechanisms may cooperate in the phenotype observed in p38αΔ cancer cells, we considered CIN as the ultimate consequence of the defects in DNA repair and replication accumulated during consecutive cell cycles. Repeated cycles of defective DNA replication and segregation would lead to excessive levels of CIN, which have been reported to decrease cellular fitness in several organisms (Lynch et al., 1993, Torres et al., 2007, Torres et al., 2008) and to drive tumor regression in mouse models (Weaver et al., 2007, Silk et al., 2013). Therefore, we hypothesize that CIN overload would be the ultimate cause of cell death in p38α deficient cells.

Most of the work on CIN and its consequences in cancer have been conducted using knockouts of the SAC components, since it is a direct way to induce missegregation, DNA damage and aneuploidy. Alterations of these proteins mainly lead to increased frequency of spontaneous tumors or increased susceptibility to exogenous carcinogens (Schvartzman et al., 2010). Interestingly, some reports show that the outcome would rely on CIN levels, since low CIN would drive tumor promotion while high levels would delay tumor appearance (Silk et al., 2013). This would fit with a recent study showing that Mad2 overexpression significantly increases CIN prior to and during tumor formation and delays tumorigenesis in two breast oncogene-induced breast cancer models (Rowald et al., 2016). Of note, and similarly to what was previously commented on p38α, most, if not all of these studies focused on tumor initiation, where CIN and aneuploidy are known to produce a diversity of karyotypes that are advantageous during tumor evolution. The few studies performed on established tumors show that deletion or inhibition of SAC-related proteins results in growth inhibition (Harrington et al., 2004, Zasadil et al., 2016). Importantly, similar data have been shown using DNA damaging agents as ionizing radiation (Bakhoum et al., 2015). In this work irradiated cells show numerical and structural aberrations, and viability of the irradiated cells increased upon reduction of missegregation, again evidencing the relationship between DNA damage and missegregation and highlighting the importance of CIN in cell viability.

Collectively, it seems that the CIN role in cancer biology depends on one hand on the tumor stage, and on the other hand on the CIN rates. Accordingly, low rates of CIN would promote heterogeneity and survival while elevating these rates would impair tumor fitness and viability (Funk et al., 2016), suggesting the existence of a threshold over which cells are no longer viable. Accordingly, Kops *et al*. suggested that massive CIN would be lethal, even in aggressive cancer cells, after three divisions (Kops et al., 2004). This lapse of time is probably required to accumulate CIN and nicely fits with our results. We observed that although cell proliferation is reduced two days after p38α deletion, cell death is significantly increased later on, six days after p38α downregulation. This suggests that during this time cells undergo defective cycles of replication and segregation, accumulating DNA damage and CIN until they are not viable anymore.

Considering that excessive CIN is lethal, that the highest levels of CIN often show better outcomes (Jamal-Hanjani et al., 2015, Roylance et al., 2011, Birkbak et al., 2011) and more susceptibility to certain therapies (Zaki et al., 2014), and given that p38α restrains CIN in breast cancer cells, we hypothesized that targeting p38α would sensitize cancer cells to CIN-inducing agents and enhance cancer cell death. We validated this theory both in murine and human PDX breast cancer models, further confirming the therapeutic value of inducing high CIN in tumors.

We used taxanes as CIN-inducing agents since they were found to be effective in breast cancer twenty years ago (Bishop et al., 1997) and are still one of the preferred options for breast cancer treatment nowadays. Nevertheless, their responsiveness is calculated to be around 50% (Kellokumpu-Lehtinen et al., 2013, Perez, 1998). Perhaps, this 50% responsive-patients are those showing higher basal CIN levels and in which consequently CIN induction through chemotherapeutic drugs would exceed the “viable threshold”. This idea is supported by the fact that in our PDX models, those that better responded to the taxanes and the combination therapy were those showing higher levels of basal aneuploidy, which can be considered an indirect measure of CIN.

Since we showed that p38α is required for CIN limitation and for the viability of cells with high CIN, we believe that targeting this pathway would enhance the effect of taxanes in already responsive tumors and, in addition, open the window of responsiveness to new patients.

Although it was believed that taxane toxicity was due to cells arresting in mitosis, as it happens in cell culture, the concentrations detected in primary tumors are too low to maintain this arrest. Instead, paclitaxel induces multipolar mitoses *in vivo*, resulting in missegregation and cell death (Zasadil et al., 2014). Therefore, we hypothesize that combining taxanes with p38α targeting would impair the two most essential and delicate processes of the cell cycle, replication and segregation, giving rise to toxic levels of DNA damage, missegregation and aneuploidy, exceeding thus the "viable threshold of CIN" (Fig. 65).

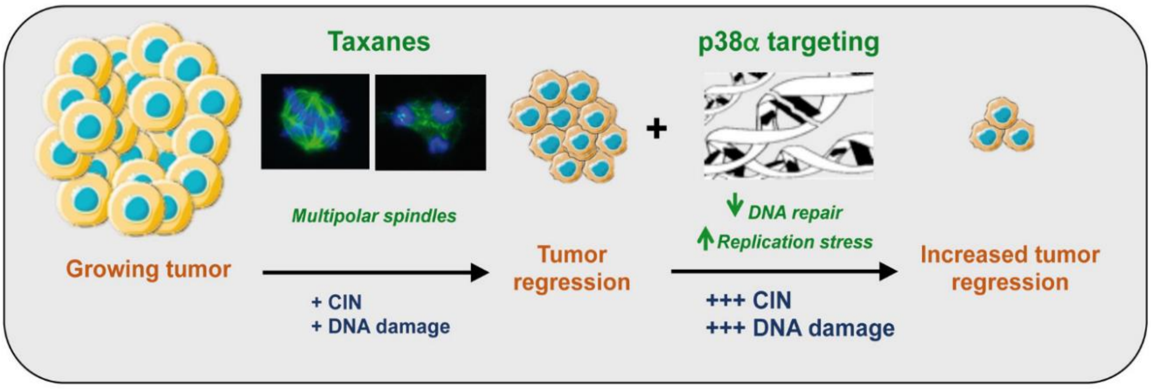

Figure 65. Proposed model for the effect of the combination of taxanes and p38α inhibition on tumor growth. Treatment with taxanes increases CIN and DNA damage levels in the cancer cells. The inhibition of p38α impairs DNA repair and increases replication stress, which potentiates the effects of taxanes leading to high levels of DNA damage, missegregation and aneuploidy that are incompatible with cancer cell viability.

Of note, this study was conducted using exclusively breast cancer models, where taxanes are normally used in therapy. However, there is no reason why the effect of p38α inhibition should be specific to taxanes and restricted to breast tumor cells. Therefore, these results may be extrapolated to other CIN-inducing drugs and to other cancer types, especially those where aneuploidy and CIN are frequently increased such as mesothelioma, small cell lung cancer, ovarian cancer or advanced colon cancer (Pikor et al., 2013, Ceccaldi et al., 2016).

4. Collateral damage of p38α targeting

Although p38α targeting could be a promising option in cancer therapy, many questions arise from this work. On the one hand CIN is a common feature of solid tumors and is suggested to be sufficient, or at least cooperate, to initiate tumorigenesis (Schvartzman et al., 2010). On the other hand, CIN promotes tumor heterogeneity and can favor tumor recurrence and therapy resistance (McGranahan et al., 2012).

We have demonstrated that p38α targeting results in tumor regression. However, we have not addressed the possible disadvantages at later stages such as higher frequency of recurrence or appearance of independent tumor foci. Studies from *Sotillo et al*. using several oncogene-induced tumorigenesis models have shown that CIN enhances tumor recurrence after oncogene withdrawal (Rowald et al., 2016, Sotillo et al., 2010), suggesting that genetic heterogeneity increases karyotype complexity and favors the generation of oncogene-independent cancer cell clones. Interestingly, a variety of chromosomal alterations and activated pathways were found in the relapsed tumors, suggesting again that CIN increases heterogeneity rather than selecting specific clones. Therefore, although excessive CIN reduces the primary tumor, it might enhance the appearance of therapy-resistant clones. In addition, given that taxanes and p38α inhibition are systemic and do not localize to the tumor site, it is possible that CIN favors the generation of side tumors in other tissues.

Moreover, p38α has diverse functions and targets in different tissues and contexts. It has been related to processes associated to metastasis such as epithelial-to-mesenchymal transition, migration and invasion, or organ colonization (del Barco et al., 2011) and its impairment enhances metastasis in some systems (Urosevic et al., 2014, Hong et al., 2015). This suggests that although p38α targeting can cooperate to achieve toxic levels of CIN and kill cancer cells in the primary tumor, it might simultaneously boost the establishment of metastatic sites.

Altogether, it is clear that we still do not understand well the function of p38α in different contexts, and further studies will be needed to analyze how targeting this pathway, along or in combination with chemotherapeutic agents, influences tumor evolution and metastasis in different cancer types, with diverse genetic alterations and distinct stromal interactions.

CONCLUSIONS

- p38α is essential for PyMT-induced mammary tumor progression *in vivo* and p38α deletion results in cancer cell death.

- Deletion of p38α in PyMT-expressing cancer cells results in replication stress, elevated DNA damage and chromosome instability.

- p38α is required for DNA-end resection, ATR activation and homologous recombination DNA repair in PyMT-expressing cancer cells.

- p38α directly phosphorylates CtIP on several sites that regulate DNA-end resection.

- Inhibition of p38α potentiates the anti-tumoral effect of chromosome instability-inducing agents such as taxanes both *ex vivo* and *in vivo*.

- Human breast tumors with high aneuploidy levels are more prone to respond to the combined treatment of taxanes and p38α inhibitors.

APPENDIX

Supplementary Table 1. Raw data for CtIP Mass spectrometry analysis containing the three analyzed replicates (R1, R2 and R3).Numbers indicate the number of peptides found with each phosphorylation or with no phosphorylation (blank). Orange background indicates the ratio of phosphorylated peptides vs. total number of peptides.

reassigned p-site	**p-site**	**CtIP_R1**	**CtIP_R2**	**CtIP_R3**
	S163		3	8
	(blank)	2	3	5
S163		0	1	1.6
	S231	1		
	S231&S233			4
	S233	9	12	11
	(blank)	35	37	31
S231		0.023	0	0.095
S233		0.250	0.324	0.484
	S276		1	1
S276			1	1
	S313		1	2
	S313-T315	1		
	S327	1	1	
	T315	5	9	7
	T323&S326-S327	1	1	3
	(blank)	2	1	2
S313		0.125	0.091	0.222
T315		2	3	1.75
	S326-S327	1	2	2
	S327	6	4	9
	S327&T333		1	2
	T333			
	(blank)	16	16	20
S326		0.045	0.095	0.065
S327		0.438	0.438	0.650
T333		0	0.045	0.065
	S347	7	7	7
	(blank)	22	32	41
S347		0.318	0.219	0.171
	S377	3	3	4
	S377-S379		4	6
	S377-S382	3	2	
	S379	6	2	
	S379-S382		1	
	S382	1		3
	T386			1
	S389	1	1	1
	(blank)	38	46	50
S377		0.133	0.184	0.189
S379		0.133	0.137	0.105
S382				
T386				
S389		0.085	0.055	0.050
	S402	1	1	1
	(blank)	6	5	5
S402		0.167	0.2	0.2
	S439	14	21	17
	(blank)	12	9	
S439		1.167	2.333	17
	S454			1
	(blank)	5	8	15
S454		0	0	0.067
	T527			1

T527				1
	S555			2
	S568			1
	(blank)	2	5	16
S555				0.118
S568				0.056
	S593		1	
	S605	1	2	2
	(blank)	16	30	29
S593		0	0.031	0
S605		0.063	0.065	0.069
	S641	1	1	1
	(blank)	18	12	4
S641		0.056	0.083	0.25
	S679		1	1
	(blank)	4	4	3
S679			0.25	0.333
	T693		1	
	(blank)	5	6	15
T693			0.167	
723	S723	4	7	7
	(blank)	64	58	50
S723		0.063	0.121	0.14
	S743			1
	S743-S745			1
	S745		1	2
	T756			1
	(blank)	1	3	11
S743				0.143
S745			0.333	0.231
T756			0	0.067
	T788-S789	2	1	
	(blank)	23	23	16
	T788			1
T788		0.087	0.043	0.063
	Y842-T847	1	3	6
	(blank)	6	9	13
Y842-T847		0.167	0.333	0.462
	S889	6	5	5
	(blank)	13	10	12
S889		0.462	0.5	0.417

REFERENCES

ADAMS, R. H., PORRAS, A., ALONSO, G., JONES, M., VINTERSTEN, K., PANELLI, S., VALLADARES, A., PEREZ, L., KLEIN, R. & NEBREDA, A. R. 2000. Essential role of p38alpha MAP kinase in placental but not embryonic cardiovascular development. *Mol Cell,* 6**,** 109-16.

ADAMSON, B., SMOGORZEWSKA, A., SIGOILLOT, F. D., KING, R. W. & ELLEDGE, S. J. 2012. A genome-wide homologous recombination screen identifies the RNA-binding protein RBMX as a component of the DNA-damage response. *Nat Cell Biol,* 14**,** 318-28.

AESOY, R., SANCHEZ, B. C., NORUM, J. H., LEWENSOHN, R., VIKTORSSON, K. & LINDERHOLM, B. 2008. An autocrine VEGF/VEGFR2 and p38 signaling loop confers resistance to 4-hydroxytamoxifen in MCF-7 breast cancer cells. *Mol Cancer Res,* 6**,** 1630-8.

ALVAREZ, S., DIAZ, M., FLACH, J., RODRIGUEZ-ACEBES, S., LOPEZ-CONTRERAS, A. J., MARTINEZ, D., CANAMERO, M., FERNANDEZ-CAPETILLO, O., ISERN, J., PASSEGUE, E. & MENDEZ, J. 2015. Replication stress caused by low MCM expression limits fetal erythropoiesis and hematopoietic stem cell functionality. *Nat Commun,* 6**,** 8548.

ALLEN, C., ASHLEY, A. K., HROMAS, R. & NICKOLOFF, J. A. 2011. More forks on the road to replication stress recovery. *J Mol Cell Biol,* 3**,** 4-12.

AMBROSINO, C., MACE, G., GALBAN, S., FRITSCH, C., VINTERSTEN, K., BLACK, E., GOROSPE, M. & NEBREDA, A. R. 2003. Negative feedback regulation of MKK6 mRNA stability by p38alpha mitogen-activated protein kinase. *Mol Cell Biol,* 23**,** 370-81.

ANAND, R., RANJHA, L., CANNAVO, E. & CEJKA, P. 2016. Phosphorylated CtIP Functions as a Co-factor of the MRE11-RAD50-NBS1 Endonuclease in DNA End Resection. *Mol Cell,* 64**,** 940-950.

ANTOON, J. W., BRATTON, M. R., GUILLOT, L. M., WADSWORTH, S., SALVO, V. A. & BUROW, M. E. 2012. Inhibition of p38-MAPK alters SRC coactivation and estrogen receptor phosphorylation. *Cancer Biol Ther,* 13**,** 1026-33.

BAKER, D. J., JEGANATHAN, K. B., CAMERON, J. D., THOMPSON, M., JUNEJA, S., KOPECKA, A., KUMAR, R., JENKINS, R. B., DE GROEN, P. C., ROCHE, P. & VAN DEURSEN, J. M. 2004. BubR1 insufficiency causes early onset of aging-associated phenotypes and infertility in mice. *Nat Genet,* 36**,** 744-9.

BAKHOUM, S. F., KABECHE, L., WOOD, M. D., LAUCIUS, C. D., QU, D., LAUGHNEY, A. M., REYNOLDS, G. E., LOUIE, R. J., PHILLIPS, J., CHAN, D. A., ZAKI, B. I., MURNANE, J. P., PETRITSCH, C. & COMPTON, D. A. 2015. Numerical chromosomal instability mediates susceptibility to radiation treatment. *Nat Commun,* 6**,** 5990.

BAKR, A., OING, C., KOCHER, S., BORGMANN, K., DORNREITER, I., PETERSEN, C., DIKOMEY, E. & MANSOUR, W. Y. 2015. Involvement of ATM in homologous recombination after end resection and RAD51 nucleofilament formation. *Nucleic Acids Res,* 43**,** 3154-66.

BARDWELL, L. & THORNER, J. 1996. A conserved motif at the amino termini of MEKs might mediate high-affinity interaction with the cognate MAPKs. *Trends Biochem Sci,* 21**,** 373-4.

BARLOW, J. H., FARYABI, R. B., CALLEN, E., WONG, N., MALHOWSKI, A., CHEN, H. T., GUTIERREZ-CRUZ, G., SUN, H. W., MCKINNON, P., WRIGHT, G., CASELLAS, R., ROBBIANI, D. F., STAUDT, L., FERNANDEZ-CAPETILLO, O. & NUSSENZWEIG, A. 2013. Identification of early replicating fragile sites that contribute to genome instability. *Cell,* 152**,** 620-32.

BEARDMORE, V. A., HINTON, H. J., EFTYCHI, C., APOSTOLAKI, M., ARMAKA, M., DARRAGH, J., MCILRATH, J., CARR, J. M., ARMIT, L. J., CLACHER, C., MALONE, L., KOLLIAS, G. & ARTHUR, J. S. 2005. Generation and characterization of p38beta (MAPK11) gene-targeted mice. *Mol Cell Biol,* 25**,** 10454-64.

BEN-LEVY, R., HOOPER, S., WILSON, R., PATERSON, H. F. & MARSHALL, C. J. 1998. Nuclear export of the stress-activated protein kinase p38 mediated by its substrate MAPKAP kinase-2. *Curr Biol,* 8**,** 1049-57.

BESTER, A. C., RONIGER, M., OREN, Y. S., IM, M. M., SARNI, D., CHAOAT, M., BENSIMON, A., ZAMIR, G., SHEWACH, D. S. & KEREM, B. 2011. Nucleotide deficiency promotes genomic instability in early stages of cancer development. *Cell,* 145**,** 435-46.

BHATT, S., XIAO, Z., MENG, Z. & KATZENELLENBOGEN, B. S. 2012. Phosphorylation by p38 mitogen-activated protein kinase promotes estrogen receptor alpha turnover and functional activity via the SCF(Skp2) proteasomal complex. *Mol Cell Biol,* 32**,** 1928-43.

BIRKBAK, N. J., EKLUND, A. C., LI, Q., MCCLELLAND, S. E., ENDESFELDER, D., TAN, P., TAN, I. B., RICHARDSON, A. L., SZALLASI, Z. & SWANTON, C. 2011. Paradoxical relationship between chromosomal instability and survival outcome in cancer. *Cancer Res,* 71**,** 3447-52.

BISHOP, J. F., DEWAR, J., TONER, G. C., TATTERSALL, M. H., OLVER, I. N., ACKLAND, S., KENNEDY, I., GOLDSTEIN, D., GURNEY, H., WALPOLE, E., LEVI, J. & STEPHENSON, J. 1997. Paclitaxel as first-line treatment for metastatic breast cancer. The Taxol Investigational Trials Group, Australia and New Zealand. *Oncology (Williston Park),* 11**,** 19-23.

BLOW, J. J., GE, X. Q. & JACKSON, D. A. 2011. How dormant origins promote complete genome replication. *Trends Biochem Sci,* 36**,** 405-14.

BOVERI, T. 1914. *Zur Frage der Entstehung maligner Tumoren*, Jena: Verlag von Gustav Fischer.

BRANCHO, D., TANAKA, N., JAESCHKE, A., VENTURA, J. J., KELKAR, N., TANAKA, Y., KYUUMA, M., TAKESHITA, T., FLAVELL, R. A. & DAVIS, R. J. 2003. Mechanism of p38 MAP kinase activation in vivo. *Genes Dev,* 17**,** 1969-78.

BROWN, A. D., SAGER, B. W., GORTHI, A., TONAPI, S. S., BROWN, E. J. & BISHOP, A. J. 2014. ATR suppresses endogenous DNA damage and allows completion of homologous recombination repair. *PLoS One,* 9**,** e91222.

BRYANT, H. E., SCHULTZ, N., THOMAS, H. D., PARKER, K. M., FLOWER, D., LOPEZ, E., KYLE, S., MEUTH, M., CURTIN, N. J. & HELLEDAY, T. 2005. Specific killing of BRCA2-deficient tumours with inhibitors of poly(ADP-ribose) polymerase. *Nature,* 434**,** 913-7.

BUISSON, R., DION-COTE, A. M., COULOMBE, Y., LAUNAY, H., CAI, H., STASIAK, A. Z., STASIAK, A., XIA, B. & MASSON, J. Y. 2010. Cooperation of breast cancer proteins PALB2 and piccolo BRCA2 in stimulating homologous recombination. *Nat Struct Mol Biol,* 17**,** 1247-54.

BULAVIN, D. V., DEMIDOV, O. N., SAITO, S., KAURANIEMI, P., PHILLIPS, C., AMUNDSON, S. A., AMBROSINO, C., SAUTER, G., NEBREDA, A. R., ANDERSON, C. W., KALLIONIEMI, A., FORNACE, A. J., JR. & APPELLA, E. 2002. Amplification of PPM1D in human tumors abrogates p53 tumor-suppressor activity. *Nat Genet,* 31**,** 210-5.

BULAVIN, D. V., HIGASHIMOTO, Y., POPOFF, I. J., GAARDE, W. A., BASRUR, V., POTAPOVA, O., APPELLA, E. & FORNACE, A. J., JR. 2001. Initiation of a G2/M checkpoint after ultraviolet radiation requires p38 kinase. *Nature,* 411**,** 102-7.

BUNTING, S. F., CALLEN, E., WONG, N., CHEN, H. T., POLATO, F., GUNN, A., BOTHMER, A., FELDHAHN, N., FERNANDEZ-CAPETILLO, O., CAO, L., XU, X., DENG, C. X., FINKEL, T., NUSSENZWEIG, M., STARK, J. M. & NUSSENZWEIG, A. 2010. 53BP1 inhibits homologous recombination in Brca1-deficient cells by blocking resection of DNA breaks. *Cell,* 141**,** 243-54.

BURRELL, R. A., MCCLELLAND, S. E., ENDESFELDER, D., GROTH, P., WELLER, M. C., SHAIKH, N., DOMINGO, E., KANU, N., DEWHURST, S. M., GRONROOS, E., CHEW, S. K., ROWAN, A. J., SCHENK, A., SHEFFER, M., HOWELL, M., KSCHISCHO, M., BEHRENS, A., HELLEDAY, T., BARTEK, J., TOMLINSON, I. P. & SWANTON, C. 2013. Replication stress links structural and numerical cancer chromosomal instability. *Nature,* 494**,** 492-6.

CAHILL, D. P., KINZLER, K. W., VOGELSTEIN, B. & LENGAUER, C. 1999. Genetic instability and darwinian selection in tumours. *Trends Cell Biol,* 9**,** M57-60.

CAHILL, D. P., LENGAUER, C., YU, J., RIGGINS, G. J., WILLSON, J. K., MARKOWITZ, S. D., KINZLER, K. W. & VOGELSTEIN, B. 1998. Mutations of mitotic checkpoint genes in human cancers. *Nature,* 392**,** 300-3.

CANNELL, I. G., KONG, Y. W., JOHNSTON, S. J., CHEN, M. L., COLLINS, H. M., DOBBYN, H. C., ELIA, A., KRESS, T. R., DICKENS, M., CLEMENS, M. J., HEERY, D. M., GAESTEL, M., EILERS, M., WILLIS, A. E. & BUSHELL, M. 2010. p38 MAPK/MK2-mediated induction of miR-34c following DNA damage prevents Myc-dependent DNA replication. *Proc Natl Acad Sci U S A,* 107**,** 5375-80.

CARGNELLO, M. & ROUX, P. P. 2011. Activation and function of the MAPKs and their substrates, the MAPK-activated protein kinases. *Microbiol Mol Biol Rev,* 75**,** 50-83.

CARTER, S. L., EKLUND, A. C., KOHANE, I. S., HARRIS, L. N. & SZALLASI, Z. 2006. A signature of chromosomal instability inferred from gene expression profiles predicts clinical outcome in multiple human cancers. *Nat Genet,* 38**,** 1043-8.

CASSIDY, J. W., CALDAS, C. & BRUNA, A. 2015. Maintaining Tumor Heterogeneity in Patient-Derived Tumor Xenografts. *Cancer Res,* 75**,** 2963-8.

CECCALDI, R., RONDINELLI, B. & D'ANDREA, A. D. 2016. Repair Pathway Choices and Consequences at the Double-Strand Break. *Trends Cell Biol,* 26**,** 52-64.

CICCIA, A. & ELLEDGE, S. J. 2010. The DNA damage response: making it safe to play with knives. *Mol Cell,* 40**,** 179-204.

CIMPRICH, K. A. & CORTEZ, D. 2008. ATR: an essential regulator of genome integrity. *Nat Rev Mol Cell Biol,* 9**,** 616-27.

CLEMENTE-RUIZ, M., MURILLO-MALDONADO, J. M., BENHRA, N., BARRIO, L., PEREZ, L., QUIROGA, G., NEBREDA, A. R. & MILAN, M. 2016. Gene Dosage Imbalance Contributes to Chromosomal Instability-Induced Tumorigenesis. *Dev Cell,* 36**,** 290-302.

COLOMER, R., LUPU, R., BACUS, S. S. & GELMANN, E. P. 1994. erbB-2 antisense oligonucleotides inhibit the proliferation of breast carcinoma cells with erbB-2 oncogene amplification. *Br J Cancer,* 70**,** 819-25.

COOK, J. G., BARDWELL, L. & THORNER, J. 1997. Inhibitory and activating functions for MAPK Kss1 in the S. cerevisiae filamentous-growth signalling pathway. *Nature,* 390**,** 85-8.

COULTHARD, L. R., WHITE, D. E., JONES, D. L., MCDERMOTT, M. F. & BURCHILL, S. A. 2009. p38(MAPK): stress responses from molecular mechanisms to therapeutics. *Trends Mol Med,* 15**,** 369-79.

COWLEY, D. O., MUSE, G. W. & VAN DYKE, T. 2005. A dominant interfering Bub1 mutant is insufficient to induce or alter thymic tumorigenesis in vivo, even in a sensitized genetic background. *Mol Cell Biol,* 25**,** 7796-802.

CRASTA, K., GANEM, N. J., DAGHER, R., LANTERMANN, A. B., IVANOVA, E. V., PAN, Y., NEZI, L., PROTOPOPOV, A., CHOWDHURY, D. & PELLMAN, D. 2012. DNA breaks and chromosome pulverization from errors in mitosis. *Nature,* 482**,** 53-8.

CREVEL, G., HASHIMOTO, R., VASS, S., SHERKOW, J., YAMAGUCHI, M., HECK, M. M. & COTTERILL, S. 2007. Differential requirements for MCM proteins in DNA replication in Drosophila S2 cells. *PLoS One,* 2**,** e833.

CRUZ-GARCIA, A., LOPEZ-SAAVEDRA, A. & HUERTAS, P. 2014. BRCA1 accelerates CtIP-mediated DNA-end resection. *Cell Rep,* 9**,** 451-9.

CUADRADO, A. & NEBREDA, A. R. 2010. Mechanisms and functions of p38 MAPK signalling. *Biochem J,* 429**,** 403-17.

CUENDA, A., COHEN, P., BUEE-SCHERRER, V. & GOEDERT, M. 1997. Activation of stress-activated protein kinase-3 (SAPK3) by cytokines and cellular stresses is mediated via SAPKK3 (MKK6); comparison of the specificities of SAPK3 and SAPK2 (RK/p38). *EMBO J,* 16**,** 295-305.

CUENDA, A. & ROUSSEAU, S. 2007. p38 MAP-kinases pathway regulation, function and role in human diseases. *Biochim Biophys Acta,* 1773**,** 1358-75.

CUEVAS, B. D., ABELL, A. N. & JOHNSON, G. L. 2007. Role of mitogen-activated protein kinase kinase kinases in signal integration. *Oncogene,* 26**,** 3159-71.

CHA, H., WANG, X., LI, H. & FORNACE, A. J., JR. 2007. A functional role for p38 MAPK in modulating mitotic transit in the absence of stress. *J Biol Chem,* 282**,** 22984-92.

CHANG, L. & KARIN, M. 2001. Mammalian MAP kinase signalling cascades. *Nature,* 410**,** 37-40.

CHAPMAN, J. R., BARRAL, P., VANNIER, J. B., BOREL, V., STEGER, M., TOMAS-LOBA, A., SARTORI, A. A., ADAMS, I. R., BATISTA, F. D. & BOULTON, S. J. 2013. RIF1 is essential for 53BP1-dependent nonhomologous end joining and suppression of DNA double-strand break resection. *Mol Cell,* 49**,** 858-71.

CHEN, L., MAYER, J. A., KRISKO, T. I., SPEERS, C. W., WANG, T., HILSENBECK, S. G. & BROWN, P. H. 2009. Inhibition of the p38 kinase suppresses the proliferation of human ER-negative breast cancer cells. *Cancer Res,* 69**,** 8853-61.

CHIBON, F., LAGARDE, P., SALAS, S., PEROT, G., BROUSTE, V., TIRODE, F., LUCCHESI, C., DE REYNIES, A., KAUFFMANN, A., BUI, B., TERRIER, P., BONVALOT, S., LE CESNE, A., VINCE-RANCHERE, D., BLAY, J. Y., COLLIN, F., GUILLOU, L., LEROUX, A., COINDRE, J. M. & AURIAS, A. 2010. Validated prediction of clinical outcome in sarcomas and multiple types of cancer on the basis of a gene expression signature related to genome complexity. *Nat Med,* 16**,** 781-7.

CHIN, L., TAM, A., POMERANTZ, J., WONG, M., HOLASH, J., BARDEESY, N., SHEN, Q., O'HAGAN, R., PANTGINIS, J., ZHOU, H., HORNER, J. W., 2ND, CORDON-CARDO, C., YANCOPOULOS, G. D. & DEPINHO, R. A. 1999. Essential role for oncogenic Ras in tumour maintenance. *Nature,* 400**,** 468-72.

CHOU, T. T., TROJANOWSKI, J. Q. & LEE, V. M. 2001. p38 mitogen-activated protein kinase-independent induction of gadd45 expression in nerve growth factor-induced apoptosis in medulloblastomas. *J Biol Chem,* 276**,** 41120-7.

DAUD, A. I., ASHWORTH, M. T., STROSBERG, J., GOLDMAN, J. W., MENDELSON, D., SPRINGETT, G., VENOOK, A. P., LOECHNER, S., ROSEN, L. S., SHANAHAN, F., PARRY, D., SHUMWAY, S., GRABOWSKY, J. A., FRESHWATER, T., SORGE, C., KANG, S. P., ISAACS, R. & MUNSTER, P. N. 2015. Phase I dose-escalation trial of checkpoint kinase 1 inhibitor MK-8776 as monotherapy and in combination with gemcitabine in patients with advanced solid tumors. *J Clin Oncol,* 33**,** 1060-6.

DAVID, L., FERNANDEZ-VIDAL, A., BERTOLI, S., GRGUREVIC, S., LEPAGE, B., DESHAIES, D., PRADE, N., CARTEL, M., LARRUE, C., SARRY, J. E., DELABESSE, E., CAZAUX, C., DIDIER, C., RECHER, C., MANENTI, S. & HOFFMANN, J. S. 2016. CHK1 as a therapeutic target to bypass chemoresistance in AML. *Sci Signal,* 9**,** ra90.

DAVIDSON, B., KONSTANTINOVSKY, S., KLEINBERG, L., NGUYEN, M. T., BASSAROVA, A., KVALHEIM, G., NESLAND, J. M. & REICH, R. 2006. The mitogen-activated protein kinases (MAPK) p38 and JNK are markers of tumor progression in breast carcinoma. *Gynecol Oncol,* 102**,** 453-61.

DEAK, M., CLIFTON, A. D., LUCOCQ, L. M. & ALESSI, D. R. 1998. Mitogen- and stress-activated protein kinase-1 (MSK1) is directly activated by MAPK and SAPK2/p38, and may mediate activation of CREB. *EMBO J,* 17**,** 4426-41.

DEL BARCO BARRANTES, I., COYA, J. M., MAINA, F., ARTHUR, J. S. & NEBREDA, A. R. 2011. Genetic analysis of specific and redundant roles for p38alpha and p38beta MAPKs during mouse development. *Proc Natl Acad Sci U S A,* 108**,** 12764-9.

DEL BARCO, D. G., MONTERO, E., CORO-ANTICH, R. M., BROWN, E., SUAREZ-ALBA, J., LOPEZ, L., SUBIROS, N. & BERLANGA, J. 2011. Coadministration of epidermal growth factor and growth hormone releasing peptide-6 improves clinical recovery in experimental autoimmune encephalitis. *Restor Neurol Neurosci,* 29**,** 243-52.

DERIJARD, B., RAINGEAUD, J., BARRETT, T., WU, I. H., HAN, J., ULEVITCH, R. J. & DAVIS, R. J. 1995. Independent human MAP-kinase signal transduction pathways defined by MEK and MKK isoforms. *Science,* 267**,** 682-5.

DEROSE, Y. S., WANG, G., LIN, Y. C., BERNARD, P. S., BUYS, S. S., EBBERT, M. T., FACTOR, R., MATSEN, C., MILASH, B. A., NELSON, E., NEUMAYER, L., RANDALL, R. L., STIJLEMAN, I. J., WELM, B. E. & WELM, A. L. 2011. Tumor grafts derived from women with breast cancer authentically reflect tumor pathology, growth, metastasis and disease outcomes. *Nat Med,* 17**,** 1514-20.

DILWORTH, S. M., BREWSTER, C. E., JONES, M. D., LANFRANCONE, L., PELICCI, G. & PELICCI, P. G. 1994. Transformation by polyoma virus middle T-antigen involves the binding and tyrosine phosphorylation of Shc. *Nature,* 367**,** 87-90.

DILLON, M. T., BARKER, H. E., PEDERSEN, M., HAFSI, H., BHIDE, S. A., NEWBOLD, K. L., NUTTING, C. M., MCLAUGHLIN, M. & HARRINGTON, K. J. 2017. Radiosensitization by the ATR Inhibitor AZD6738 through Generation of Acentric Micronuclei. *Mol Cancer Ther,* 16**,** 25-34.

DOLADO, I., SWAT, A., AJENJO, N., DE VITA, G., CUADRADO, A. & NEBREDA, A. R. 2007. p38alpha MAP kinase as a sensor of reactive oxygen species in tumorigenesis. *Cancer Cell,* 11**,** 191-205.

DREAN, A., LORD, C. J. & ASHWORTH, A. 2016. PARP inhibitor combination therapy. *Crit Rev Oncol Hematol,* 108**,** 73-85.

DUESBERG, P., RAUSCH, C., RASNICK, D. & HEHLMANN, R. 1998. Genetic instability of cancer cells is proportional to their degree of aneuploidy. *Proc Natl Acad Sci U S A,* 95**,** 13692-7.

DUESBERG, P., STINDL, R. & HEHLMANN, R. 2000. Explaining the high mutation rates of cancer cells to drug and multidrug resistance by chromosome reassortments that are catalyzed by aneuploidy. *Proc Natl Acad Sci U S A,* 97**,** 14295-300.

DYNAN, W. S. & YOO, S. 1998. Interaction of Ku protein and DNA-dependent protein kinase catalytic subunit with nucleic acids. *Nucleic Acids Res,* 26**,** 1551-9.

EID, W., STEGER, M., EL-SHEMERLY, M., FERRETTI, L. P., PENA-DIAZ, J., KONIG, C., VALTORTA, E., SARTORI, A. A. & FERRARI, S. 2010. DNA end resection by CtIP and exonuclease 1 prevents genomic instability. *EMBO Rep,* 11**,** 962-8.

ENSLEN, H., RAINGEAUD, J. & DAVIS, R. J. 1998. Selective activation of p38 mitogen-activated protein (MAP) kinase isoforms by the MAP kinase kinases MKK3 and MKK6. *J Biol Chem,* 273**,** 1741-8.

ESPOSITO, M. T., ZHAO, L., FUNG, T. K., RANE, J. K., WILSON, A., MARTIN, N., GIL, J., LEUNG, A. Y., ASHWORTH, A. & SO, C. W. 2015. Synthetic lethal targeting of oncogenic transcription factors in acute leukemia by PARP inhibitors. *Nat Med,* 21**,** 1481-90.

ESTEVA, F. J., SAHIN, A. A., SMITH, T. L., YANG, Y., PUSZTAI, L., NAHTA, R., BUCHHOLZ, T. A., BUZDAR, A. U., HORTOBAGYI, G. N. & BACUS, S. S. 2004. Prognostic significance of phosphorylated P38 mitogen-activated protein kinase and HER-2 expression in lymph node-positive breast carcinoma. *Cancer,* 100**,** 499-506.

FACHINETTI, D., BERMEJO, R., COCITO, A., MINARDI, S., KATOU, Y., KANOH, Y., SHIRAHIGE, K., AZVOLINSKY, A., ZAKIAN, V. A. & FOIANI, M. 2010. Replication termination at eukaryotic chromosomes is mediated by Top2 and occurs at genomic loci containing pausing elements. *Mol Cell,* 39**,** 595-605.

FALCK, J., COATES, J. & JACKSON, S. P. 2005. Conserved modes of recruitment of ATM, ATR and DNA-PKcs to sites of DNA damage. *Nature,* 434**,** 605-11.

FAN, L., YANG, X., DU, J., MARSHALL, M., BLANCHARD, K. & YE, X. 2005. A novel role of p38 alpha MAPK in mitotic progression independent of its kinase activity. *Cell Cycle,* 4**,** 1616-24.

FARMER, H., MCCABE, N., LORD, C. J., TUTT, A. N., JOHNSON, D. A., RICHARDSON, T. B., SANTAROSA, M., DILLON, K. J., HICKSON, I., KNIGHTS, C., MARTIN, N. M., JACKSON, S. P., SMITH, G. C. & ASHWORTH, A. 2005. Targeting the DNA repair defect in BRCA mutant cells as a therapeutic strategy. *Nature,* 434**,** 917-21.

FENECH, M., KIRSCH-VOLDERS, M., NATARAJAN, A. T., SURRALLES, J., CROTT, J. W., PARRY, J., NORPPA, H., EASTMOND, D. A., TUCKER, J. D. & THOMAS, P. 2011. Molecular mechanisms of micronucleus, nucleoplasmic bridge and nuclear bud formation in mammalian and human cells. *Mutagenesis,* 26**,** 125-32.

FERRETTI, L. P., HIMMELS, S. F., TRENNER, A., WALKER, C., VON AESCH, C., EGGENSCHWILER, A., MURINA, O., ENCHEV, R. I., PETER, M., FREIRE, R., PORRO, A. & SARTORI, A. A. 2016. Cullin3-KLHL15 ubiquitin ligase mediates CtIP protein turnover to fine-tune DNA-end resection. *Nat Commun,* 7**,** 12628.

FLACH, J., BAKKER, S. T., MOHRIN, M., CONROY, P. C., PIETRAS, E. M., REYNAUD, D., ALVAREZ, S., DIOLAITI, M. E., UGARTE, F., FORSBERG, E. C., LE BEAU, M. M., STOHR, B. A., MENDEZ, J., MORRISON, C. G. & PASSEGUE, E. 2014. Replication stress is a potent driver of functional decline in ageing haematopoietic stem cells. *Nature,* 512**,** 198-202.

FLUCK, M. M. & SCHAFFHAUSEN, B. S. 2009. Lessons in signaling and tumorigenesis from polyomavirus middle T antigen. *Microbiol Mol Biol Rev,* 73**,** 542-63, Table of Contents.

FREIJE, J. M., FRAILE, J. M. & LOPEZ-OTIN, C. 2011. Protease addiction and synthetic lethality in cancer. *Front Oncol,* 1**,** 25.

FUNK, L. C., ZASADIL, L. M. & WEAVER, B. A. 2016. Living in CIN: Mitotic Infidelity and Its Consequences for Tumor Promotion and Suppression. *Dev Cell,* 39**,** 638-652.

GAILLARD, H., GARCIA-MUSE, T. & AGUILERA, A. 2015. Replication stress and cancer. *Nat Rev Cancer,* 15**,** 276-89.

GALLUZZI, L., KEPP, O., VANDER HEIDEN, M. G. & KROEMER, G. 2013. Metabolic targets for cancer therapy. *Nat Rev Drug Discov,* 12**,** 829-46.

GARCIA-CANO, J., ROCHE, O., CIMAS, F. J., PASCUAL-SERRA, R., ORTEGA-MUELAS, M., FERNANDEZ-AROCA, D. M. & SANCHEZ-PRIETO, R. 2016. p38MAPK and Chemotherapy: We Always Need to Hear Both Sides of the Story. *Front Cell Dev Biol,* 4**,** 69.

GELOT, C., MAGDALOU, I. & LOPEZ, B. S. 2015. Replication stress in Mammalian cells and its consequences for mitosis. *Genes (Basel),* 6**,** 267-98.

GIAM, M. & RANCATI, G. 2015. Aneuploidy and chromosomal instability in cancer: a jackpot to chaos. *Cell Div,* 10**,** 3.

GISSELSSON, D., PETTERSSON, L., HOGLUND, M., HEIDENBLAD, M., GORUNOVA, L., WIEGANT, J., MERTENS, F., DAL CIN, P., MITELMAN, F. & MANDAHL, N. 2000. Chromosomal breakage-fusion-bridge events cause genetic intratumor heterogeneity. *Proc Natl Acad Sci U S A,* 97**,** 5357-62.

GODEK, K. M., VENERE, M., WU, Q., MILLS, K. D., HICKEY, W. F., RICH, J. N. & COMPTON, D. A. 2016. Chromosomal Instability Affects the Tumorigenicity of Glioblastoma Tumor-Initiating Cells. *Cancer Discov,* 6**,** 532-45.

GOLDSTEIN, D. M., KUGLSTATTER, A., LOU, Y. & SOTH, M. J. 2010. Selective p38alpha inhibitors clinically evaluated for the treatment of chronic inflammatory disorders. *J Med Chem,* 53**,** 2345-53.

GONZALEZ-LOYOLA, A., FERNANDEZ-MIRANDA, G., TRAKALA, M., PARTIDA, D., SAMEJIMA, K., OGAWA, H., CANAMERO, M., DE MARTINO, A., MARTINEZ-RAMIREZ, A., DE CARCER, G., PEREZ DE CASTRO, I., EARNSHAW, W. C. & MALUMBRES, M. 2015. Aurora B Overexpression Causes Aneuploidy and p21Cip1 Repression during Tumor Development. *Mol Cell Biol,* 35**,** 3566-78.

GORGOULIS, V. G., VASSILIOU, L. V., KARAKAIDOS, P., ZACHARATOS, P., KOTSINAS, A., LILOGLOU, T., VENERE, M., DITULLIO, R. A., JR., KASTRINAKIS, N. G., LEVY, B., KLETSAS, D., YONETA, A., HERLYN, M., KITTAS, C. & HALAZONETIS, T. D. 2005. Activation of the DNA damage checkpoint and genomic instability in human precancerous lesions. *Nature,* 434**,** 907-13.

GUPTA, J., DEL BARCO BARRANTES, I., IGEA, A., SAKELLARIOU, S., PATERAS, I. S., GORGOULIS, V. G. & NEBREDA, A. R. 2014. Dual function of p38alpha MAPK in colon cancer: suppression of colitis-associated tumor initiation but requirement for cancer cell survival. *Cancer Cell,* 25**,** 484-500.

GUPTA, J., IGEA, A., PAPAIOANNOU, M., LOPEZ-CASAS, P. P., LLONCH, E., HIDALGO, M., GORGOULIS, V. G. & NEBREDA, A. R. 2015. Pharmacological inhibition of p38 MAPK reduces tumor growth in patient-derived xenografts from colon tumors. *Oncotarget,* 6**,** 8539-51.

GUTIERREZ, M. C., DETRE, S., JOHNSTON, S., MOHSIN, S. K., SHOU, J., ALLRED, D. C., SCHIFF, R., OSBORNE, C. K. & DOWSETT, M. 2005. Molecular changes in tamoxifen-resistant breast cancer: relationship between estrogen receptor, HER-2, and p38 mitogen-activated protein kinase. *J Clin Oncol,* 23**,** 2469-76.

GUY, C. T., CARDIFF, R. D. & MULLER, W. J. 1992. Induction of mammary tumors by expression of polyomavirus middle T oncogene: a transgenic mouse model for metastatic disease. *Mol Cell Biol,* 12**,** 954-61.

HABERMANN, J. K., DOERING, J., HAUTANIEMI, S., ROBLICK, U. J., BUNDGEN, N. K., NICORICI, D., KRONENWETT, U., RATHNAGIRISWARAN, S., METTU, R. K., MA, Y., KRUGER, S., BRUCH, H. P., AUER, G., GUO, N. L. & RIED, T. 2009. The gene expression signature of genomic instability in breast cancer is an independent predictor of clinical outcome. *Int J Cancer,* 124**,** 1552-64.

HALAZONETIS, T. D., GORGOULIS, V. G. & BARTEK, J. 2008. An oncogene-induced DNA damage model for cancer development. *Science,* 319**,** 1352-5.

HALLER, K., KIBLER, K. V., KASAI, T., CHI, Y. H., PELOPONESE, J. M., YEDAVALLI, V. S. & JEANG, K. T. 2006. The N-terminus of rodent and human MAD1 confers species-specific stringency to spindle assembly checkpoint. *Oncogene,* 25**,** 2137-47.

HANAHAN, D. & WEINBERG, R. A. 2000. The hallmarks of cancer. *Cell,* 100**,** 57-70.

HANAHAN, D. & WEINBERG, R. A. 2011. Hallmarks of cancer: the next generation. *Cell,* 144**,** 646-74.

HARRINGTON, E. A., BEBBINGTON, D., MOORE, J., RASMUSSEN, R. K., AJOSE-ADEOGUN, A. O., NAKAYAMA, T., GRAHAM, J. A., DEMUR, C., HERCEND, T., DIU-HERCEND, A., SU, M., GOLEC, J. M. & MILLER, K. M. 2004. VX-680, a potent and selective small-molecule inhibitor of the Aurora kinases, suppresses tumor growth in vivo. *Nat Med,* 10**,** 262-7.

HARTLERODE, A. J., MORGAN, M. J., WU, Y., BUIS, J. & FERGUSON, D. O. 2015. Recruitment and activation of the ATM kinase in the absence of DNA-damage sensors. *Nat Struct Mol Biol,* 22**,** 736-43.

HELLEDAY, T., PETERMANN, E., LUNDIN, C., HODGSON, B. & SHARMA, R. A. 2008. DNA repair pathways as targets for cancer therapy. *Nat Rev Cancer,* 8**,** 193-204.

HOLLAND, A. J. & CLEVELAND, D. W. 2012. Losing balance: the origin and impact of aneuploidy in cancer. *EMBO Rep,* 13**,** 501-14.

HONG, B., LI, H., ZHANG, M., XU, J., LU, Y., ZHENG, Y., QIAN, J., CHANG, J. T., YANG, J. & YI, Q. 2015. p38 MAPK inhibits breast cancer metastasis through regulation of stromal expansion. *Int J Cancer,* 136**,** 34-43.

HOPE, H. R., ANDERSON, G. D., BURNETTE, B. L., COMPTON, R. P., DEVRAJ, R. V., HIRSCH, J. L., KEITH, R. H., LI, X., MBALAVIELE, G., MESSING, D. M., SAABYE, M. J., SCHINDLER, J. F., SELNESS, S. R., STILLWELL, L. I., WEBB, E. G., ZHANG, J. & MONAHAN, J. B. 2009. Anti-inflammatory properties of a novel N-phenyl pyridinone inhibitor of p38 mitogen-activated protein kinase: preclinical-to-clinical translation. *J Pharmacol Exp Ther,* 331**,** 882-95.

HOTHORN, T., BRETZ, F. & WESTFALL, P. 2008. Simultaneous inference in general parametric models. *Biom J,* 50**,** 346-63.

HUERTAS, P. 2010. DNA resection in eukaryotes: deciding how to fix the break. *Nat Struct Mol Biol,* 17**,** 11-6.

HUERTAS, P. & JACKSON, S. P. 2009. Human CtIP mediates cell cycle control of DNA end resection and double strand break repair. *J Biol Chem,* 284**,** 9558-65.

HUETTNER, C. S., ZHANG, P., VAN ETTEN, R. A. & TENEN, D. G. 2000. Reversibility of acute B-cell leukaemia induced by BCR-ABL1. *Nat Genet,* 24**,** 57-60.

IBARRA, A., SCHWOB, E. & MENDEZ, J. 2008. Excess MCM proteins protect human cells from replicative stress by licensing backup origins of replication. *Proc Natl Acad Sci U S A,* 105**,** 8956-61.

IWAIZUMI, M., SHINMURA, K., MORI, H., YAMADA, H., SUZUKI, M., KITAYAMA, Y., IGARASHI, H., NAKAMURA, T., SUZUKI, H., WATANABE, Y., HISHIDA, A., IKUMA, M. & SUGIMURA, H. 2009. Human Sgo1 downregulation leads to chromosomal instability in colorectal cancer. *Gut,* 58**,** 249-60.

JACKSON, S. P. & BARTEK, J. 2009. The DNA-damage response in human biology and disease. *Nature,* 461**,** 1071-8.

JAIN, M., ARVANITIS, C., CHU, K., DEWEY, W., LEONHARDT, E., TRINH, M., SUNDBERG, C. D., BISHOP, J. M. & FELSHER, D. W. 2002. Sustained loss of a neoplastic phenotype by brief inactivation of MYC. *Science,* 297**,** 102-4.

JAMAL-HANJANI, M., A'HERN, R., BIRKBAK, N. J., GORMAN, P., GRONROOS, E., NGANG, S., NICOLA, P., RAHMAN, L., THANOPOULOU, E., KELLY, G., ELLIS, P., BARRETT-LEE, P., JOHNSTON, S. R., BLISS, J., ROYLANCE, R. & SWANTON, C. 2015. Extreme chromosomal instability forecasts improved outcome in ER-negative breast cancer: a prospective validation cohort study from the TACT trial. *Ann Oncol,* 26**,** 1340-6.

JANSSEN, A., KOPS, G. J. & MEDEMA, R. H. 2009. Elevating the frequency of chromosome mis-segregation as a strategy to kill tumor cells. *Proc Natl Acad Sci U S A,* 106**,** 19108-13.

JANSSEN, A., VAN DER BURG, M., SZUHAI, K., KOPS, G. J. & MEDEMA, R. H. 2011. Chromosome segregation errors as a cause of DNA damage and structural chromosome aberrations. *Science,* 333**,** 1895-8.

JIANG, Y., CHEN, C., LI, Z., GUO, W., GEGNER, J. A., LIN, S. & HAN, J. 1996. Characterization of the structure and function of a new mitogen-activated protein kinase (p38beta). *J Biol Chem,* 271**,** 17920-6.

JIANG, Y., GRAM, H., ZHAO, M., NEW, L., GU, J., FENG, L., DI PADOVA, F., ULEVITCH, R. J. & HAN, J. 1997. Characterization of the structure and function of the fourth member of p38 group mitogen-activated protein kinases, p38delta. *J Biol Chem,* 272**,** 30122-8.

KASTAN, M. B. & BARTEK, J. 2004. Cell-cycle checkpoints and cancer. *Nature,* 432**,** 316-23.

KAUFMANN, W. K. & PAULES, R. S. 1996. DNA damage and cell cycle checkpoints. *FASEB J,* 10**,** 238-47.

KAWABATA, T., LUEBBEN, S. W., YAMAGUCHI, S., ILVES, I., MATISE, I., BUSKE, T., BOTCHAN, M. R. & SHIMA, N. 2011. Stalled fork rescue via dormant replication origins in unchallenged S phase promotes proper chromosome segregation and tumor suppression. *Mol Cell,* 41**,** 543-53.

KELLEY, M. R., LOGSDON, D. & FISHEL, M. L. 2014. Targeting DNA repair pathways for cancer treatment: what's new? *Future Oncol,* 10**,** 1215-37.

KELLOKUMPU-LEHTINEN, P., TUUNANEN, T., ASOLA, R., ELOMAA, L., HEIKKINEN, M., KOKKO, R., JARVENPAA, R., LEHTINEN, I., MAICHE, A., KALEVA-KEROLA, J., HUUSKO, M., MOYKKYNEN, K. & ALA-LUHTALA, T. 2013. Weekly paclitaxel--an effective treatment for advanced breast cancer. *Anticancer Res,* 33**,** 2623-7.

KIM, G. Y., MERCER, S. E., EWTON, D. Z., YAN, Z., JIN, K. & FRIEDMAN, E. 2002. The stress-activated protein kinases p38 alpha and JNK1 stabilize p21(Cip1) by phosphorylation. *J Biol Chem,* 277**,** 29792-802.

KOPPER, F., BIERWIRTH, C., SCHON, M., KUNZE, M., ELVERS, I., KRANZ, D., SAINI, P., MENON, M. B., WALTER, D., SORENSEN, C. S., GAESTEL, M., HELLEDAY, T., SCHON, M. P. & DOBBELSTEIN, M. 2013. Damage-induced DNA replication stalling relies on MAPK-activated protein kinase 2 activity. *Proc Natl Acad Sci U S A,* 110**,** 16856-61.

KOPS, G. J., FOLTZ, D. R. & CLEVELAND, D. W. 2004. Lethality to human cancer cells through massive chromosome loss by inhibition of the mitotic checkpoint. *Proc Natl Acad Sci U S A,* 101**,** 8699-704.

KOPS, G. J., WEAVER, B. A. & CLEVELAND, D. W. 2005. On the road to cancer: aneuploidy and the mitotic checkpoint. *Nat Rev Cancer,* 5**,** 773-85.

KOUNDRIOUKOFF, S., CARIGNON, S., TECHER, H., LETESSIER, A., BRISON, O. & DEBATISSE, M. 2013. Stepwise activation of the ATR signaling pathway upon increasing replication stress impacts fragile site integrity. *PLoS Genet,* 9**,** e1003643.

KOUROS-MEHR, H., BECHIS, S. K., SLORACH, E. M., LITTLEPAGE, L. E., EGEBLAD, M., EWALD, A. J., PAI, S. Y., HO, I. C. & WERB, Z. 2008. GATA-3 links tumor differentiation and dissemination in a luminal breast cancer model. *Cancer Cell,* 13**,** 141-52.

KOUSHOLT, A. N., FUGGER, K., HOFFMANN, S., LARSEN, B. D., MENZEL, T., SARTORI, A. A. & SORENSEN, C. S. 2012. CtIP-dependent DNA resection is required for DNA damage checkpoint maintenance but not initiation. *J Cell Biol,* 197**,** 869-76.

KRAJEWSKA, M., FEHRMANN, R. S., DE VRIES, E. G. & VAN VUGT, M. A. 2015. Regulators of homologous recombination repair as novel targets for cancer treatment. *Front Genet,* 6**,** 96.

KUMAR, S., BOEHM, J. & LEE, J. C. 2003. p38 MAP kinases: key signalling molecules as therapeutic targets for inflammatory diseases. *Nat Rev Drug Discov,* 2**,** 717-26.

KYRIAKIS, J. M. & AVRUCH, J. 2012. Mammalian MAPK signal transduction pathways activated by stress and inflammation: a 10-year update. *Physiol Rev,* 92**,** 689-737.

LAFARGA, V., CUADRADO, A., LOPEZ DE SILANES, I., BENGOECHEA, R., FERNANDEZ-CAPETILLO, O. & NEBREDA, A. R. 2009. p38 Mitogen-activated protein kinase- and HuR-dependent stabilization of p21(Cip1) mRNA mediates the G(1)/S checkpoint. *Mol Cell Biol,* 29**,** 4341-51.

LAFRANCHI, L., DE BOER, H. R., DE VRIES, E. G., ONG, S. E., SARTORI, A. A. & VAN VUGT, M. A. 2014. APC/C(Cdh1) controls CtIP stability during the cell cycle and in response to DNA damage. *EMBO J,* 33**,** 2860-79.

LEE, A. J., ENDESFELDER, D., ROWAN, A. J., WALTHER, A., BIRKBAK, N. J., FUTREAL, P. A., DOWNWARD, J., SZALLASI, Z., TOMLINSON, I. P., HOWELL, M., KSCHISCHO, M. & SWANTON, C. 2011a. Chromosomal instability confers intrinsic multidrug resistance. *Cancer Res,* 71**,** 1858-70.

LEE, H. & BAI, W. 2002. Regulation of estrogen receptor nuclear export by ligand-induced and p38-mediated receptor phosphorylation. *Mol Cell Biol,* 22**,** 5835-45.

LEE, J. C., LAYDON, J. T., MCDONNELL, P. C., GALLAGHER, T. F., KUMAR, S., GREEN, D., MCNULTY, D., BLUMENTHAL, M. J., HEYS, J. R., LANDVATTER, S. W. & ET AL. 1994. A protein kinase involved in the regulation of inflammatory cytokine biosynthesis. *Nature,* 372**,** 739-46.

LEE, J. H. & PAULL, T. T. 2004. Direct activation of the ATM protein kinase by the Mre11/Rad50/Nbs1 complex. *Science,* 304**,** 93-6.

LEE, K., KENNY, A. E. & RIEDER, C. L. 2010. P38 mitogen-activated protein kinase activity is required during mitosis for timely satisfaction of the mitotic checkpoint but not for the fidelity of chromosome segregation. *Mol Biol Cell,* 21**,** 2150-60.

LEE, S. H., JIA, S., ZHU, Y., UTERMARK, T., SIGNORETTI, S., LODA, M., SCHAFFHAUSEN, B. & ROBERTS, T. M. 2011b. Transgenic expression of polyomavirus middle T antigen in the mouse prostate gives rise to carcinoma. *J Virol,* 85**,** 5581-92.

LEELAHAVANICHKUL, K., AMORNPHIMOLTHAM, P., MOLINOLO, A. A., BASILE, J. R., KOONTONGKAEW, S. & GUTKIND, J. S. 2014. A role for p38 MAPK in head and neck cancer cell growth and tumor-induced angiogenesis and lymphangiogenesis. *Mol Oncol,* 8**,** 105-18.

LEI, M., KAWASAKI, Y. & TYE, B. K. 1996. Physical interactions among Mcm proteins and effects of Mcm dosage on DNA replication in Saccharomyces cerevisiae. *Mol Cell Biol,* 16**,** 5081-90.

LENGAUER, C., KINZLER, K. W. & VOGELSTEIN, B. 1997. DNA methylation and genetic instability in colorectal cancer cells. *Proc Natl Acad Sci U S A,* 94**,** 2545-50.

LIN, E. Y., JONES, J. G., LI, P., ZHU, L., WHITNEY, K. D., MULLER, W. J. & POLLARD, J. W. 2003. Progression to malignancy in the polyoma middle T oncoprotein mouse breast cancer model provides a reliable model for human diseases. *Am J Pathol,* 163**,** 2113-26.

LIU, Y., HOCK, J. M., SULLIVAN, C., FANG, G., COX, A. J., DAVIS, K. T., DAVIS, B. H. & LI, X. 2010. Activation of the p38 MAPK/Akt/ERK1/2 signal pathways is required for the protein stabilization of CDC6 and cyclin D1 in low-dose arsenite-induced cell proliferation. *J Cell Biochem,* 111**,** 1546-55.

LOPEZ-CONTRERAS, A. J. & FERNANDEZ-CAPETILLO, O. 2010. The ATR barrier to replication-born DNA damage. *DNA Repair (Amst),* 9**,** 1249-55.

LUKAS, C., SAVIC, V., BEKKER-JENSEN, S., DOIL, C., NEUMANN, B., PEDERSEN, R. S., GROFTE, M., CHAN, K. L., HICKSON, I. D., BARTEK, J. & LUKAS, J. 2011. 53BP1 nuclear bodies form around DNA lesions generated by mitotic transmission of chromosomes under replication stress. *Nat Cell Biol,* 13**,** 243-53.

LUKAS, J., LUKAS, C. & BARTEK, J. 2004. Mammalian cell cycle checkpoints: signalling pathways and their organization in space and time. *DNA Repair (Amst),* 3**,** 997-1007.

LUO, J., SOLIMINI, N. L. & ELLEDGE, S. J. 2009. Principles of cancer therapy: oncogene and non-oncogene addiction. *Cell,* 136**,** 823-37.

LYNCH, M., BURGER, R., BUTCHER, D. & GABRIEL, W. 1993. The mutational meltdown in asexual populations. *J Hered,* 84**,** 339-44.

LLOPIS, A., SALVADOR, N., ERCILLA, A., GUAITA-ESTERUELAS, S., BARRANTES IDEL, B., GUPTA, J., GAESTEL, M., DAVIS, R. J., NEBREDA, A. R. & AGELL, N. 2012. The stress-activated protein kinases p38alpha/beta and JNK1/2 cooperate with Chk1 to inhibit mitotic entry upon DNA replication arrest. *Cell Cycle,* 11**,** 3627-37.

MACNEE, W., ALLAN, R. J., JONES, I., DE SALVO, M. C. & TAN, L. F. 2013. Efficacy and safety of the oral p38 inhibitor PH-797804 in chronic obstructive pulmonary disease: a randomised clinical trial. *Thorax,* 68**,** 738-45.

MACHERET, M. & HALAZONETIS, T. D. 2015. DNA replication stress as a hallmark of cancer. *Annu Rev Pathol,* 10**,** 425-48.

MADHANI, H. D., STYLES, C. A. & FINK, G. R. 1997. MAP kinases with distinct inhibitory functions impart signaling specificity during yeast differentiation. *Cell,* 91**,** 673-84.

MAGLIONE, J. E., MOGHANAKI, D., YOUNG, L. J., MANNER, C. K., ELLIES, L. G., JOSEPH, S. O., NICHOLSON, B., CARDIFF, R. D. & MACLEOD, C. L. 2001. Transgenic Polyoma middle-T mice model premalignant mammary disease. *Cancer Res,* 61**,** 8298-305.

MAHANEY, B. L., MEEK, K. & LEES-MILLER, S. P. 2009. Repair of ionizing radiation-induced DNA double-strand breaks by non-homologous end-joining. *Biochem J,* 417**,** 639-50.

MAHTANI, K. R., BROOK, M., DEAN, J. L., SULLY, G., SAKLATVALA, J. & CLARK, A. R. 2001. Mitogen-activated protein kinase p38 controls the expression and posttranslational modification of tristetraprolin, a regulator of tumor necrosis factor alpha mRNA stability. *Mol Cell Biol,* 21**,** 6461-9.

MAIA, A. R., DE MAN, J., BOON, U., JANSSEN, A., SONG, J. Y., OMERZU, M., STERRENBURG, J. G., PRINSEN, M. B., WILLEMSEN-SEEGERS, N., DE ROOS, J. A., VAN DOORNMALEN, A. M., UITDEHAAG, J. C., KOPS, G. J., JONKERS, J., BUIJSMAN, R. C., ZAMAN, G. J. & MEDEMA, R. H. 2015. Inhibition of the spindle assembly checkpoint kinase TTK enhances the efficacy of docetaxel in a triple-negative breast cancer model. *Ann Oncol,* 26**,** 2180-92.

MAKHARASHVILI, N., TUBBS, A. T., YANG, S. H., WANG, H., BARTON, O., ZHOU, Y., DESHPANDE, R. A., LEE, J. H., LOBRICH, M., SLECKMAN, B. P., WU, X. & PAULL, T. T. 2014. Catalytic and noncatalytic roles of the CtIP endonuclease in double-strand break end resection. *Mol Cell,* 54**,** 1022-33.

MALUMBRES, M. & BARBACID, M. 2009. Cell cycle, CDKs and cancer: a changing paradigm. *Nat Rev Cancer,* 9**,** 153-66.

MALUREANU, L., JEGANATHAN, K. B., JIN, F., BAKER, D. J., VAN REE, J. H., GULLON, O., CHEN, Z., HENLEY, J. R. & VAN DEURSEN, J. M. 2010. Cdc20 hypomorphic mice fail to counteract de novo synthesis of cyclin B1 in mitosis. *J Cell Biol,* 191**,** 313-29.

MANKE, I. A., NGUYEN, A., LIM, D., STEWART, M. Q., ELIA, A. E. & YAFFE, M. B. 2005. MAPKAP kinase-2 is a cell cycle checkpoint kinase that regulates the G2/M transition and S phase progression in response to UV irradiation. *Mol Cell,* 17**,** 37-48.

MARECHAL, A. & ZOU, L. 2015. RPA-coated single-stranded DNA as a platform for post-translational modifications in the DNA damage response. *Cell Res,* 25**,** 9-23.

MARTIN, S. A., HEWISH, M., LORD, C. J. & ASHWORTH, A. 2010. Genomic instability and the selection of treatments for cancer. *J Pathol,* 220**,** 281-9.

MASSAGUE, J. 2004. G1 cell-cycle control and cancer. *Nature,* 432**,** 298-306.

MASUDA, A. & TAKAHASHI, T. 2002. Chromosome instability in human lung cancers: possible underlying mechanisms and potential consequences in the pathogenesis. *Oncogene,* 21**,** 6884-97.

MASUDA, K., SHIMA, H., WATANABE, M. & KIKUCHI, K. 2001. MKP-7, a novel mitogen-activated protein kinase phosphatase, functions as a shuttle protein. *J Biol Chem,* 276**,** 39002-11.

MATSUSAKA, T. & PINES, J. 2004. Chfr acts with the p38 stress kinases to block entry to mitosis in mammalian cells. *J Cell Biol,* 166**,** 507-16.

MAYA-MENDOZA, A., TANG, C. W., POMBO, A. & JACKSON, D. A. 2009. Mechanisms regulating S phase progression in mammalian cells. *Front Biosci (Landmark Ed),* 14**,** 4199-213.

MAZOUZI, A., VELIMEZI, G. & LOIZOU, J. I. 2014. DNA replication stress: causes, resolution and disease. *Exp Cell Res,* 329**,** 85-93.

MCGRANAHAN, N., BURRELL, R. A., ENDESFELDER, D., NOVELLI, M. R. & SWANTON, C. 2012. Cancer chromosomal instability: therapeutic and diagnostic challenges. *EMBO Rep,* 13**,** 528-38.

MIKHAILOV, A., SHINOHARA, M. & RIEDER, C. L. 2004. Topoisomerase II and histone deacetylase inhibitors delay the G2/M transition by triggering the p38 MAPK checkpoint pathway. *J Cell Biol,* 166**,** 517-26.

MIKULE, K., DELAVAL, B., KALDIS, P., JURCYZK, A., HERGERT, P. & DOXSEY, S. 2007. Loss of centrosome integrity induces p38-p53-p21-dependent G1-S arrest. *Nat Cell Biol,* 9**,** 160-70.

MOASSER, M. M. 2007. Targeting the function of the HER2 oncogene in human cancer therapeutics. *Oncogene,* 26**,** 6577-92.

MORRISON, D. K. 2012. MAP kinase pathways. *Cold Spring Harb Perspect Biol,* 4.

MUDGETT, J. S., DING, J., GUH-SIESEL, L., CHARTRAIN, N. A., YANG, L., GOPAL, S. & SHEN, M. M. 2000. Essential role for p38alpha mitogen-activated protein kinase in placental angiogenesis. *Proc Natl Acad Sci U S A,* 97**,** 10454-9.

MULLER, P. A. & VOUSDEN, K. H. 2013. p53 mutations in cancer. *Nat Cell Biol,* 15**,** 2-8.

NAGEL, R., SEMENOVA, E. A. & BERNS, A. 2016. Drugging the addict: non-oncogene addiction as a target for cancer therapy. *EMBO Rep,* 17**,** 1516-1531.

NEGRINI, S., GORGOULIS, V. G. & HALAZONETIS, T. D. 2010. Genomic instability--an evolving hallmark of cancer. *Nat Rev Mol Cell Biol,* 11**,** 220-8.

NICHOLSON, J. M. & CIMINI, D. 2013. Cancer karyotypes: survival of the fittest. *Front Oncol,* 3**,** 148.

NOWELL, P. C. 1976. The clonal evolution of tumor cell populations. *Science,* 194**,** 23-8.

OHTANI, K., IWANAGA, R., NAKAMURA, M., IKEDA, M., YABUTA, N., TSURUGA, H. & NOJIMA, H. 1999. Cell growth-regulated expression of mammalian MCM5 and MCM6 genes mediated by the transcription factor E2F. *Oncogene,* 18**,** 2299-309.

OLSON, J. M. & HALLAHAN, A. R. 2004. p38 MAP kinase: a convergence point in cancer therapy. *Trends Mol Med,* 10**,** 125-9.

OU, X. H., LI, S., XU, B. Z., WANG, Z. B., QUAN, S., LI, M., ZHANG, Q. H., OUYANG, Y. C., SCHATTEN, H., XING, F. Q. & SUN, Q. Y. 2010. p38alpha MAPK is a MTOC-associated protein regulating spindle assembly, spindle length and accurate chromosome segregation during mouse oocyte meiotic maturation. *Cell Cycle,* 9**,** 4130-43.

OWENS, D. M. & KEYSE, S. M. 2007. Differential regulation of MAP kinase signalling by dual-specificity protein phosphatases. *Oncogene,* 26**,** 3203-13.

OZA, A. M., CIBULA, D., BENZAQUEN, A. O., POOLE, C., MATHIJSSEN, R. H., SONKE, G. S., COLOMBO, N., SPACEK, J., VUYLSTEKE, P., HIRTE, H., MAHNER, S., PLANTE, M., SCHMALFELDT, B., MACKAY, H., ROWBOTTOM, J., LOWE, E. S., DOUGHERTY, B., BARRETT, J. C. & FRIEDLANDER, M. 2015. Olaparib combined with chemotherapy for recurrent platinum-sensitive ovarian cancer: a randomised phase 2 trial. *Lancet Oncol,* 16**,** 87-97.

PAILLAS, S., BOISSIERE, F., BIBEAU, F., DENOUEL, A., MOLLEVI, C., CAUSSE, A., DENIS, V., VEZZIO-VIE, N., MARZI, L., CORTIJO, C., AIT-ARSA, I., ASKARI, N., POURQUIER, P., MARTINEAU, P., DEL RIO, M. & GONGORA, C. 2011. Targeting the p38 MAPK pathway inhibits irinotecan resistance in colon adenocarcinoma. *Cancer Res,* 71**,** 1041-9.

PASSERINI, V., OZERI-GALAI, E., DE PAGTER, M. S., DONNELLY, N., SCHMALBROCK, S., KLOOSTERMAN, W. P., KEREM, B. & STORCHOVA, Z. 2016. The presence of extra chromosomes leads to genomic instability. *Nat Commun,* 7**,** 10754.

PEDRAZA-ALVA, G., KOULNIS, M., CHARLAND, C., THORNTON, T., CLEMENTS, J. L., SCHLISSEL, M. S. & RINCON, M. 2006. Activation of p38 MAP kinase by DNA double-strand breaks in V(D)J recombination induces a G2/M cell cycle checkpoint. *EMBO J,* 25**,** 763-73.

PEREIRA, L., IGEA, A., CANOVAS, B., DOLADO, I. & NEBREDA, A. R. 2013. Inhibition of p38 MAPK sensitizes tumour cells to cisplatin-induced apoptosis mediated by reactive oxygen species and JNK. *EMBO Mol Med,* 5**,** 1759-74.

PEREZ DE CASTRO, I., DE CARCER, G. & MALUMBRES, M. 2007. A census of mitotic cancer genes: new insights into tumor cell biology and cancer therapy. *Carcinogenesis,* 28**,** 899-912.

PEREZ, E. A. 1998. Paclitaxel in Breast Cancer. *Oncologist,* 3**,** 373-389.

PETERSON, S. E., LI, Y., WU-BAER, F., CHAIT, B. T., BAER, R., YAN, H., GOTTESMAN, M. E. & GAUTIER, J. 2013. Activation of DSB processing requires phosphorylation of CtIP by ATR. *Mol Cell,* 49**,** 657-67.

PIERCE, A. J., JOHNSON, R. D., THOMPSON, L. H. & JASIN, M. 1999. XRCC3 promotes homology-directed repair of DNA damage in mammalian cells. *Genes Dev,* 13**,** 2633-8.

PIKOR, L., THU, K., VUCIC, E. & LAM, W. 2013. The detection and implication of genome instability in cancer. *Cancer Metastasis Rev,* 32**,** 341-52.

PILLAIRE, M. J., SELVES, J., GORDIEN, K., GOURRAUD, P. A., GENTIL, C., DANJOUX, M., DO, C., NEGRE, V., BIETH, A., GUIMBAUD, R., TROUCHE, D., PASERO, P., MECHALI, M., HOFFMANN, J. S. & CAZAUX, C. 2010. A 'DNA replication' signature of progression and negative outcome in colorectal cancer. *Oncogene,* 29**,** 876-87.

POLATO, F., CALLEN, E., WONG, N., FARYABI, R., BUNTING, S., CHEN, H. T., KOZAK, M., KRUHLAK, M. J., RECZEK, C. R., LEE, W. H., LUDWIG, T., BAER, R., FEIGENBAUM, L., JACKSON, S. & NUSSENZWEIG, A. 2014. CtIP-mediated resection is essential for viability and can operate independently of BRCA1. *J Exp Med,* 211**,** 1027-36.

POLI, J., TSAPONINA, O., CRABBE, L., KESZTHELYI, A., PANTESCO, V., CHABES, A., LENGRONNE, A. & PASERO, P. 2012. dNTP pools determine fork progression and origin usage under replication stress. *EMBO J,* 31**,** 883-94.

POLYAK, K. 2011. Heterogeneity in breast cancer. *J Clin Invest,* 121**,** 3786-8.

PRAT, A., PINEDA, E., ADAMO, B., GALVAN, P., FERNANDEZ, A., GABA, L., DIEZ, M., VILADOT, M., ARANCE, A. & MUNOZ, M. 2015. Clinical implications of the intrinsic molecular subtypes of breast cancer. *Breast,* 24 Suppl 2**,** S26-35.

PRUITT, K., PRUITT, W. M., BILTER, G. K., WESTWICK, J. K. & DER, C. J. 2002. Raf-independent deregulation of p38 and JNK mitogen-activated protein kinases are critical for Ras transformation. *J Biol Chem,* 277**,** 31808-17.

PURI, P. L., WU, Z., ZHANG, P., WOOD, L. D., BHAKTA, K. S., HAN, J., FERAMISCO, J. R., KARIN, M. & WANG, J. Y. 2000. Induction of terminal differentiation by constitutive activation of p38 MAP kinase in human rhabdomyosarcoma cells. *Genes Dev,* 14**,** 574-84.

RAINGEAUD, J., GUPTA, S., ROGERS, J. S., DICKENS, M., HAN, J., ULEVITCH, R. J. & DAVIS, R. J. 1995. Pro-inflammatory cytokines and environmental stress cause p38 mitogen-activated protein kinase activation by dual phosphorylation on tyrosine and threonine. *J Biol Chem,* 270**,** 7420-6.

RAUCH, J., VOLINSKY, N., ROMANO, D. & KOLCH, W. 2011. The secret life of kinases: functions beyond catalysis. *Cell Commun Signal,* 9**,** 23.

REINHARDT, H. C., ASLANIAN, A. S., LEES, J. A. & YAFFE, M. B. 2007. p53-deficient cells rely on ATM- and ATR-mediated checkpoint signaling through the p38MAPK/MK2 pathway for survival after DNA damage. *Cancer Cell,* 11**,** 175-89.

REINHARDT, H. C., HASSKAMP, P., SCHMEDDING, I., MORANDELL, S., VAN VUGT, M. A., WANG, X., LINDING, R., ONG, S. E., WEAVER, D., CARR, S. A. & YAFFE, M. B. 2010. DNA damage activates a spatially distinct late cytoplasmic cell-cycle checkpoint network controlled by MK2-mediated RNA stabilization. *Mol Cell,* 40**,** 34-49.

REUTER, S., GUPTA, S. C., CHATURVEDI, M. M. & AGGARWAL, B. B. 2010. Oxidative stress, inflammation, and cancer: how are they linked? *Free Radic Biol Med,* 49**,** 1603-16.

REYNOLDS, C. H., BETTS, J. C., BLACKSTOCK, W. P., NEBREDA, A. R. & ANDERTON, B. H. 2000. Phosphorylation sites on tau identified by nanoelectrospray mass spectrometry: differences in vitro between the mitogen-activated protein kinases ERK2, c-Jun N-terminal kinase and P38, and glycogen synthase kinase-3beta. *J Neurochem,* 74**,** 1587-95.

RICKE, R. M., JEGANATHAN, K. B. & VAN DEURSEN, J. M. 2011. Bub1 overexpression induces aneuploidy and tumor formation through Aurora B kinase hyperactivation. *J Cell Biol,* 193**,** 1049-64.

ROSCHKE, A. V. & ROZENBLUM, E. 2013. Multi-layered cancer chromosomal instability phenotype. *Front Oncol,* 3**,** 302.

ROUX, P. P. & BLENIS, J. 2004. ERK and p38 MAPK-activated protein kinases: a family of protein kinases with diverse biological functions. *Microbiol Mol Biol Rev,* 68**,** 320-44.

ROWALD, K., MANTOVAN, M., PASSOS, J., BUCCITELLI, C., MARDIN, B. R., KORBEL, J. O., JECHLINGER, M. & SOTILLO, R. 2016. Negative Selection and Chromosome Instability Induced by Mad2 Overexpression Delay Breast Cancer but Facilitate Oncogene-Independent Outgrowth. *Cell Rep,* 15**,** 2679-91.

ROYLANCE, R., ENDESFELDER, D., GORMAN, P., BURRELL, R. A., SANDER, J., TOMLINSON, I., HANBY, A. M., SPEIRS, V., RICHARDSON, A. L., BIRKBAK, N. J., EKLUND, A. C., DOWNWARD, J., KSCHISCHO, M., SZALLASI, Z. & SWANTON, C. 2011. Relationship of extreme chromosomal instability with long-term survival in a retrospective analysis of primary breast cancer. *Cancer Epidemiol Biomarkers Prev,* 20**,** 2183-94.

RUDALSKA, R., DAUCH, D., LONGERICH, T., MCJUNKIN, K., WUESTEFELD, T., KANG, T. W., HOHMEYER, A., PESIC, M., LEIBOLD, J., VON THUN, A., SCHIRMACHER, P., ZUBER, J., WEISS, K. H., POWERS, S., MALEK, N. P., EILERS, M., SIPOS, B., LOWE, S. W., GEFFERS, R., LAUFER, S. & ZENDER, L. 2014. In vivo RNAi screening identifies a mechanism of sorafenib resistance in liver cancer. *Nat Med,* 20**,** 1138-46.

RUZANKINA, Y., ASARE, A. & BROWN, E. J. 2008. Replicative stress, stem cells and aging. *Mech Ageing Dev,* 129**,** 460-6.

RUZANKINA, Y., PINZON-GUZMAN, C., ASARE, A., ONG, T., PONTANO, L., COTSARELIS, G., ZEDIAK, V. P., VELEZ, M., BHANDOOLA, A. & BROWN, E. J. 2007. Deletion of the developmentally essential gene ATR in adult mice leads to age-related phenotypes and stem cell loss. *Cell Stem Cell,* 1**,** 113-26.

SABELLI, P. A., HOERSTER, G., LIZARRAGA, L. E., BROWN, S. W., GORDON-KAMM, W. J. & LARKINS, B. A. 2009. Positive regulation of minichromosome maintenance gene expression, DNA replication, and cell transformation by a plant retinoblastoma gene. *Proc Natl Acad Sci U S A,* 106**,** 4042-7.

SABIO, G., ARTHUR, J. S., KUMA, Y., PEGGIE, M., CARR, J., MURRAY-TAIT, V., CENTENO, F., GOEDERT, M., MORRICE, N. A. & CUENDA, A. 2005. p38gamma regulates the localisation of SAP97 in the cytoskeleton by modulating its interaction with GKAP. *EMBO J,* 24**,** 1134-45.

SALH, B., MAROTTA, A., WAGEY, R., SAYED, M. & PELECH, S. 2002. Dysregulation of phosphatidylinositol 3-kinase and downstream effectors in human breast cancer. *Int J Cancer,* 98**,** 148-54.

SANTAMARIA, D., VIGUERA, E., MARTINEZ-ROBLES, M. L., HYRIEN, O., HERNANDEZ, P., KRIMER, D. B. & SCHVARTZMAN, J. B. 2000. Bi-directional replication and random termination. *Nucleic Acids Res,* 28**,** 2099-107.

SARTORI, A. A., LUKAS, C., COATES, J., MISTRIK, M., FU, S., BARTEK, J., BAER, R., LUKAS, J. & JACKSON, S. P. 2007. Human CtIP promotes DNA end resection. *Nature,* 450**,** 509-14.

SAYED, M., PELECH, S., WONG, C., MAROTTA, A. & SALH, B. 2001. Protein kinase CK2 is involved in G2 arrest and apoptosis following spindle damage in epithelial cells. *Oncogene,* 20**,** 6994-7005.

SCHAEFFER, H. J. & WEBER, M. J. 1999. Mitogen-activated protein kinases: specific messages from ubiquitous messengers. *Mol Cell Biol,* 19**,** 2435-44.

SCHAFFHAUSEN, B. S. & ROBERTS, T. M. 2009. Lessons from polyoma middle T antigen on signaling and transformation: A DNA tumor virus contribution to the war on cancer. *Virology,* 384**,** 304-16.

SCHVARTZMAN, J. M., DUIJF, P. H., SOTILLO, R., COKER, C. & BENEZRA, R. 2011. Mad2 is a critical mediator of the chromosome instability observed upon Rb and p53 pathway inhibition. *Cancer Cell,* 19**,** 701-14.

SCHVARTZMAN, J. M., SOTILLO, R. & BENEZRA, R. 2010. Mitotic chromosomal instability and cancer: mouse modelling of the human disease. *Nat Rev Cancer,* 10**,** 102-15.

SETTLEMAN, J. 2012. Oncogene addiction. *Curr Biol,* 22**,** R43-4.

SHALTIEL, I. A., APRELIA, M., SAURIN, A. T., CHOWDHURY, D., KOPS, G. J., VOEST, E. E. & MEDEMA, R. H. 2014. Distinct phosphatases antagonize the p53 response in different phases of the cell cycle. *Proc Natl Acad Sci U S A,* 111**,** 7313-8.

SHELTZER, J. M., BLANK, H. M., PFAU, S. J., TANGE, Y., GEORGE, B. M., HUMPTON, T. J., BRITO, I. L., HIRAOKA, Y., NIWA, O. & AMON, A. 2011. Aneuploidy drives genomic instability in yeast. *Science,* 333**,** 1026-30.

SHELTZER, J. M., KO, J. H., REPLOGLE, J. M., HABIBE BURGOS, N. C., CHUNG, E. S., MEEHL, C. M., SAYLES, N. M., PASSERINI, V., STORCHOVA, Z. & AMON, A. 2017. Single-chromosome Gains Commonly Function as Tumor Suppressors. *Cancer Cell,* 31**,** 240-255.

SHEN, Z. 2011. Genomic instability and cancer: an introduction. *J Mol Cell Biol,* 3**,** 1-3.

SHERR, C. J. 2000. Cell cycle control and cancer. *Harvey Lect,* 96**,** 73-92.

SHEVCHENKO, A., TOMAS, H., HAVLIS, J., OLSEN, J. V. & MANN, M. 2006. In-gel digestion for mass spectrometric characterization of proteins and proteomes. *Nat Protoc,* 1**,** 2856-60.

SHILOH, Y. & ZIV, Y. 2013. The ATM protein kinase: regulating the cellular response to genotoxic stress, and more. *Nat Rev Mol Cell Biol,* 14**,** 197-210.

SHIOTANI, B., NGUYEN, H. D., HAKANSSON, P., MARECHAL, A., TSE, A., TAHARA, H. & ZOU, L. 2013. Two distinct modes of ATR activation orchestrated by Rad17 and Nbs1. *Cell Rep,* 3**,** 1651-62.

SHIOTANI, B. & ZOU, L. 2009. Single-stranded DNA orchestrates an ATM-to-ATR switch at DNA breaks. *Mol Cell,* 33**,** 547-58.

SHRIVASTAV, M., DE HARO, L. P. & NICKOLOFF, J. A. 2008. Regulation of DNA double-strand break repair pathway choice. *Cell Res,* 18**,** 134-47.

SIEGEL, R. L., MILLER, K. D. & JEMAL, A. 2016. Cancer statistics, 2016. *CA Cancer J Clin,* 66**,** 7-30.

SILK, A. D., ZASADIL, L. M., HOLLAND, A. J., VITRE, B., CLEVELAND, D. W. & WEAVER, B. A. 2013. Chromosome missegregation rate predicts whether aneuploidy will promote or suppress tumors. *Proc Natl Acad Sci U S A,* 110**,** E4134-41.

SLAMON, D. J., CLARK, G. M., WONG, S. G., LEVIN, W. J., ULLRICH, A. & MCGUIRE, W. L. 1987. Human breast cancer: correlation of relapse and survival with amplification of the HER-2/neu oncogene. *Science,* 235**,** 177-82.

SLEETH, K. M., SORENSEN, C. S., ISSAEVA, N., DZIEGIELEWSKI, J., BARTEK, J. & HELLEDAY, T. 2007. RPA mediates recombination repair during replication stress and is displaced from DNA by checkpoint signalling in human cells. *J Mol Biol,* 373**,** 38-47.

SMITS, V. A., REAPER, P. M. & JACKSON, S. P. 2006. Rapid PIKK-dependent release of Chk1 from chromatin promotes the DNA-damage checkpoint response. *Curr Biol,* 16**,** 150-9.

SOLIMINI, N. L., LUO, J. & ELLEDGE, S. J. 2007. Non-oncogene addiction and the stress phenotype of cancer cells. *Cell,* 130**,** 986-8.

SOLOMON, D. A., KIM, T., DIAZ-MARTINEZ, L. A., FAIR, J., ELKAHLOUN, A. G., HARRIS, B. T., TORETSKY, J. A., ROSENBERG, S. A., SHUKLA, N., LADANYI, M., SAMUELS, Y., JAMES, C. D., YU, H., KIM, J. S. & WALDMAN, T. 2011. Mutational inactivation of STAG2 causes aneuploidy in human cancer. *Science,* 333**,** 1039-43.

SONODA, E., HOCHEGGER, H., SABERI, A., TANIGUCHI, Y. & TAKEDA, S. 2006. Differential usage of non-homologous end-joining and homologous recombination in double strand break repair. *DNA Repair (Amst),* 5**,** 1021-9.

SORLIE, T., PEROU, C. M., TIBSHIRANI, R., AAS, T., GEISLER, S., JOHNSEN, H., HASTIE, T., EISEN, M. B., VAN DE RIJN, M., JEFFREY, S. S., THORSEN, T., QUIST, H., MATESE, J. C., BROWN, P. O., BOTSTEIN, D., LONNING, P. E. & BORRESEN-DALE, A. L. 2001. Gene expression patterns of breast carcinomas distinguish tumor subclasses with clinical implications. *Proc Natl Acad Sci U S A,* 98**,** 10869-74.

SOTILLO, R., HERNANDO, E., DIAZ-RODRIGUEZ, E., TERUYA-FELDSTEIN, J., CORDON-CARDO, C., LOWE, S. W. & BENEZRA, R. 2007. Mad2 overexpression promotes aneuploidy and tumorigenesis in mice. *Cancer Cell,* 11**,** 9-23.

SOTILLO, R., SCHVARTZMAN, J. M., SOCCI, N. D. & BENEZRA, R. 2010. Mad2-induced chromosome instability leads to lung tumour relapse after oncogene withdrawal. *Nature,* 464**,** 436-40.

SOUCEK, L. & EVAN, G. I. 2010. The ups and downs of Myc biology. *Curr Opin Genet Dev,* 20**,** 91-5.

STEGER, M., MURINA, O., HUHN, D., FERRETTI, L. P., WALSER, R., HANGGI, K., LAFRANCHI, L., NEUGEBAUER, C., PALIWAL, S., JANSCAK, P., GERRITS, B., DEL SAL, G., ZERBE, O. & SARTORI, A. A. 2013. Prolyl isomerase PIN1 regulates DNA double-strand break repair by counteracting DNA end resection. *Mol Cell,* 50**,** 333-43.

STEIN, B., BRADY, H., YANG, M. X., YOUNG, D. B. & BARBOSA, M. S. 1996. Cloning and characterization of MEK6, a novel member of the mitogen-activated protein kinase kinase cascade. *J Biol Chem,* 271**,** 11427-33.

STUCKE, V. M., SILLJE, H. H., ARNAUD, L. & NIGG, E. A. 2002. Human Mps1 kinase is required for the spindle assembly checkpoint but not for centrosome duplication. *EMBO J,* 21**,** 1723-32.

SU, W., LIU, W., SCHAFFHAUSEN, B. S. & ROBERTS, T. M. 1995. Association of Polyomavirus middle tumor antigen with phospholipase C-gamma 1. *J Biol Chem,* 270**,** 12331-4.

SULLI, G., DI MICCO, R. & D'ADDA DI FAGAGNA, F. 2012. Crosstalk between chromatin state and DNA damage response in cellular senescence and cancer. *Nat Rev Cancer,* 12**,** 709-20.

SUZUKI, M. & TAKAHASHI, T. 2013. Aberrant DNA replication in cancer. *Mutat Res,* 743-744**,** 111-7.

SWANTON, C., BURRELL, R. A. & FUTREAL, P. A. 2011. Breast cancer genome heterogeneity: a challenge to personalised medicine? *Breast Cancer Res,* 13**,** 104.

SWANTON, C., MARANI, M., PARDO, O., WARNE, P. H., KELLY, G., SAHAI, E., ELUSTONDO, F., CHANG, J., TEMPLE, J., AHMED, A. A., BRENTON, J. D., DOWNWARD, J. & NICKE, B. 2007. Regulators of mitotic arrest and ceramide metabolism are determinants of sensitivity to paclitaxel and other chemotherapeutic drugs. *Cancer Cell,* 11**,** 498-512.

SWANTON, C., NICKE, B., SCHUETT, M., EKLUND, A. C., NG, C., LI, Q., HARDCASTLE, T., LEE, A., ROY, R., EAST, P., KSCHISCHO, M., ENDESFELDER, D., WYLIE, P., KIM, S. N., CHEN, J. G., HOWELL, M., RIED, T., HABERMANN, J. K., AUER, G., BRENTON, J. D., SZALLASI, Z. & DOWNWARD, J. 2009. Chromosomal instability determines taxane response. *Proc Natl Acad Sci U S A,* 106**,** 8671-6.

TAKENAKA, K., MORIGUCHI, T. & NISHIDA, E. 1998. Activation of the protein kinase p38 in the spindle assembly checkpoint and mitotic arrest. *Science,* 280**,** 599-602.

TANG, J., QI, X., MERCOLA, D., HAN, J. & CHEN, G. 2005. Essential role of p38gamma in K-Ras transformation independent of phosphorylation. *J Biol Chem,* 280**,** 23910-7.

TANG, Y. C., WILLIAMS, B. R., SIEGEL, J. J. & AMON, A. 2011. Identification of aneuploidy-selective antiproliferation compounds. *Cell,* 144**,** 499-512.

THOMPSON, S. L. & COMPTON, D. A. 2010. Proliferation of aneuploid human cells is limited by a p53-dependent mechanism. *J Cell Biol,* 188**,** 369-81.

THORNTON, T. M., DELGADO, P., CHEN, L., SALAS, B., KREMENTSOV, D., FERNANDEZ, M., VERNIA, S., DAVIS, R. J., HEIMANN, R., TEUSCHER, C., KRANGEL, M. S., RAMIRO, A. R. & RINCON, M. 2016. Inactivation of nuclear GSK3beta by Ser(389) phosphorylation promotes lymphocyte fitness during DNA double-strand break response. *Nat Commun,* 7**,** 10553.

THORNTON, T. M. & RINCON, M. 2009. Non-classical p38 map kinase functions: cell cycle checkpoints and survival. *Int J Biol Sci,* 5**,** 44-51.

TOBIUME, K., MATSUZAWA, A., TAKAHASHI, T., NISHITOH, H., MORITA, K., TAKEDA, K., MINOWA, O., MIYAZONO, K., NODA, T. & ICHIJO, H. 2001. ASK1 is required for sustained activations of JNK/p38 MAP kinases and apoptosis. *EMBO Rep,* 2**,** 222-8.

TORRES, E. M., SOKOLSKY, T., TUCKER, C. M., CHAN, L. Y., BOSELLI, M., DUNHAM, M. J. & AMON, A. 2007. Effects of aneuploidy on cellular physiology and cell division in haploid yeast. *Science,* 317**,** 916-24.

TORRES, E. M., WILLIAMS, B. R. & AMON, A. 2008. Aneuploidy: cells losing their balance. *Genetics,* 179**,** 737-46.

TREMPOLEC, N., DAVE-COLL, N. & NEBREDA, A. R. 2013. SnapShot: p38 MAPK signaling. *Cell,* 152**,** 656-656 e1.

TSAO, J. L., TAVARE, S., SALOVAARA, R., JASS, J. R., AALTONEN, L. A. & SHIBATA, D. 1999. Colorectal adenoma and cancer divergence. Evidence of multilineage progression. *Am J Pathol,* 154**,** 1815-24.

UROSEVIC, J., GARCIA-ALBENIZ, X., PLANET, E., REAL, S., CESPEDES, M. V., GUIU, M., FERNANDEZ, E., BELLMUNT, A., GAWRZAK, S., PAVLOVIC, M., MANGUES, R., DOLADO, I., BARRIGA, F. M., NADAL, C., KEMENY, N., BATLLE, E., NEBREDA, A. R. & GOMIS, R. R. 2014. Colon cancer cells colonize the lung from established liver metastases through p38 MAPK signalling and PTHLH. *Nat Cell Biol,* 16**,** 685-94.

VAZQUEZ-NOVELLE, M. D., SANSREGRET, L., DICK, A. E., SMITH, C. A., MCAINSH, A. D., GERLICH, D. W. & PETRONCZKI, M. 2014. Cdk1 inactivation terminates mitotic checkpoint surveillance and stabilizes kinetochore attachments in anaphase. *Curr Biol,* 24**,** 638-45.

VENTURA, J. J., TENBAUM, S., PERDIGUERO, E., HUTH, M., GUERRA, C., BARBACID, M., PASPARAKIS, M. & NEBREDA, A. R. 2007. p38alpha MAP kinase is essential in lung stem and progenitor cell proliferation and differentiation. *Nat Genet,* 39**,** 750-8.

WAGNER, E. F. & NEBREDA, A. R. 2009. Signal integration by JNK and p38 MAPK pathways in cancer development. *Nat Rev Cancer,* 9**,** 537-49.

WANG, H., SHI, L. Z., WONG, C. C., HAN, X., HWANG, P. Y., TRUONG, L. N., ZHU, Q., SHAO, Z., CHEN, D. J., BERNS, M. W., YATES, J. R., 3RD, CHEN, L. & WU, X. 2013. The interaction of CtIP and Nbs1 connects CDK and ATM to regulate HR-mediated double-strand break repair. *PLoS Genet,* 9**,** e1003277.

WANG, H., WANG, H., POWELL, S. N., ILIAKIS, G. & WANG, Y. 2004. ATR affecting cell radiosensitivity is dependent on homologous recombination repair but independent of nonhomologous end joining. *Cancer Res,* 64**,** 7139-43.

WARMERDAM, D. O., BRINKMAN, E. K., MARTEIJN, J. A., MEDEMA, R. H., KANAAR, R. & SMITS, V. A. 2013. UV-induced G2 checkpoint depends on p38 MAPK and minimal activation of ATR-Chk1 pathway. *J Cell Sci,* 126**,** 1923-30.

WASKIEWICZ, A. J., FLYNN, A., PROUD, C. G. & COOPER, J. A. 1997. Mitogen-activated protein kinases activate the serine/threonine kinases Mnk1 and Mnk2. *EMBO J,* 16**,** 1909-20.

WEAVER, B. A., SILK, A. D., MONTAGNA, C., VERDIER-PINARD, P. & CLEVELAND, D. W. 2007. Aneuploidy acts both oncogenically and as a tumor suppressor. *Cancer Cell,* 11**,** 25-36.

WEINSTEIN, I. B. 2002. Cancer. Addiction to oncogenes--the Achilles heal of cancer. *Science,* 297**,** 63-4.

WELBURN, J. P., VLEUGEL, M., LIU, D., YATES, J. R., 3RD, LAMPSON, M. A., FUKAGAWA, T. & CHEESEMAN, I. M. 2010. Aurora B phosphorylates spatially distinct targets to differentially regulate the kinetochore-microtubule interface. *Mol Cell,* 38**,** 383-92.

WHITMAN, M., KAPLAN, D. R., SCHAFFHAUSEN, B., CANTLEY, L. & ROBERTS, T. M. 1985. Association of phosphatidylinositol kinase activity with polyoma middle-T competent for transformation. *Nature,* 315**,** 239-42.

WHITTLE, J. R., LEWIS, M. T., LINDEMAN, G. J. & VISVADER, J. E. 2015. Patient-derived xenograft models of breast cancer and their predictive power. *Breast Cancer Res,* 17**,** 17.

WIDMANN, C., GIBSON, S., JARPE, M. B. & JOHNSON, G. L. 1999. Mitogen-activated protein kinase: conservation of a three-kinase module from yeast to human. *Physiol Rev,* 79**,** 143-80.

WILHELM, T., MAGDALOU, I., BARASCU, A., TECHER, H., DEBATISSE, M. & LOPEZ, B. S. 2014. Spontaneous slow replication fork progression elicits mitosis alterations in homologous recombination-deficient mammalian cells. *Proc Natl Acad Sci U S A,* 111**,** 763-8.

WILLIAMS, B. R., PRABHU, V. R., HUNTER, K. E., GLAZIER, C. M., WHITTAKER, C. A., HOUSMAN, D. E. & AMON, A. 2008. Aneuploidy affects proliferation and spontaneous immortalization in mammalian cells. *Science,* 322**,** 703-9.

WINEY, M., GOETSCH, L., BAUM, P. & BYERS, B. 1991. MPS1 and MPS2: novel yeast genes defining distinct steps of spindle pole body duplication. *J Cell Biol,* 114**,** 745-54.

XING, L., DEVADAS, B., DEVRAJ, R. V., SELNESS, S. R., SHIEH, H., WALKER, J. K., MAO, M., MESSING, D., SAMAS, B., YANG, J. Z., ANDERSON, G. D., WEBB, E. G. & MONAHAN, J. B. 2012. Discovery and characterization of atropisomer PH-797804, a p38 MAP kinase inhibitor, as a clinical drug candidate. *ChemMedChem,* 7**,** 273-80.

XIU, M., KIM, J., SAMPSON, E., HUANG, C. Y., DAVIS, R. J., PAULSON, K. E. & YEE, A. S. 2003. The transcriptional repressor HBP1 is a target of the p38 mitogen-activated protein kinase pathway in cell cycle regulation. *Mol Cell Biol,* 23**,** 8890-901.

YAMADA, H. Y. & GORBSKY, G. J. 2006. Spindle checkpoint function and cellular sensitivity to antimitotic drugs. *Mol Cancer Ther,* 5**,** 2963-9.

YEANG, C. H., MCCORMICK, F. & LEVINE, A. 2008. Combinatorial patterns of somatic gene mutations in cancer. *FASEB J,* 22**,** 2605-22.

YEN, A. H. & YANG, J. L. 2010. Cdc20 proteolysis requires p38 MAPK signaling and Cdh1-independent APC/C ubiquitination during spindle assembly checkpoint activation by cadmium. *J Cell Physiol,* 223**,** 327-34.

YOSHIDA, K. & INOUE, I. 2004. Regulation of Geminin and Cdt1 expression by E2F transcription factors. *Oncogene,* 23**,** 3802-12.

YOU, Z. & BAILIS, J. M. 2010. DNA damage and decisions: CtIP coordinates DNA repair and cell cycle checkpoints. *Trends Cell Biol,* 20**,** 402-9.

YU, X. & BAER, R. 2000. Nuclear localization and cell cycle-specific expression of CtIP, a protein that associates with the BRCA1 tumor suppressor. *J Biol Chem,* 275**,** 18541-9.

ZAKI, B. I., SURIAWINATA, A. A., EASTMAN, A. R., GARNER, K. M. & BAKHOUM, S. F. 2014. Chromosomal instability portends superior response of rectal adenocarcinoma to chemoradiation therapy. *Cancer,* 120**,** 1733-42.

ZARUBIN, T. & HAN, J. 2005. Activation and signaling of the p38 MAP kinase pathway. *Cell Res,* 15**,** 11-8.

ZASADIL, L. M., ANDERSEN, K. A., YEUM, D., ROCQUE, G. B., WILKE, L. G., TEVAARWERK, A. J., RAINES, R. T., BURKARD, M. E. & WEAVER, B. A. 2014. Cytotoxicity of paclitaxel in breast cancer is due to chromosome missegregation on multipolar spindles. *Sci Transl Med,* 6**,** 229ra43.

ZASADIL, L. M., BRITIGAN, E. M., RYAN, S. D., KAUR, C., GUCKENBERGER, D. J., BEEBE, D. J., MOSER, A. R. & WEAVER, B. A. 2016. High rates of chromosome missegregation suppress tumor progression but do not inhibit tumor initiation. *Mol Biol Cell,* 27**,** 1981-9.

ZASADIL, L. M., BRITIGAN, E. M. & WEAVER, B. A. 2013. 2n or not 2n: Aneuploidy, polyploidy and chromosomal instability in primary and tumor cells. *Semin Cell Dev Biol,* 24**,** 370-9.

ZEMAN, M. K. & CIMPRICH, K. A. 2014. Causes and consequences of replication stress. *Nat Cell Biol,* 16**,** 2-9.

ZHANG, Y., LAI, J., DU, Z., GAO, J., YANG, S., GORITYALA, S., XIONG, X., DENG, O., MA, Z., YAN, C., SUSANA, G., XU, Y. & ZHANG, J. 2016. Targeting radioresistant breast cancer cells by single agent CHK1 inhibitor via enhancing replication stress. *Oncotarget,* 7**,** 34688-702.

ZOU, L. & ELLEDGE, S. J. 2003. Sensing DNA damage through ATRIP recognition of RPA-ssDNA complexes. *Science,* 300**,** 1542-8.

ACKNOWLEDGMENTS

No supondrás, ¿verdad?, que todas tus aventuras y escapadas fueron producto de la mera suerte, para tu beneficio exclusivo. Te considero una gran persona, señor Bolsón, y te aprecio mucho; pero en última instancia ¡eres sólo un simple individuo en un mundo enorme!
¡Gracias al cielo! dijo Bilbo riendo, y le pasó el pote de tabaco-

El Hobbit, J.R.R. Tolkien

Y así es, la aventura de la tesis ha llegado a su fin. Y al igual que en todo gran libro de aventuras, el final es a la par ansiado y melancólico. Ansiado ya que tras las oscuras cavernas atravesadas, las duras batallas libradas y todas las agonías sufridas, la trama se desenreda y el desenlace se desvela. Y a la vez melancólico, ya que tras tantas páginas vividas los personajes deben volar. Sin embargo, a diferencia de los libros, en la vida real los personajes no tienen por qué desaparecer y con un poco de suerte reaparecerán durante los diferentes capítulos de tu historia.

Como un gran mago dijo un día a un pequeño hobbit, "todos somos simples individuos en un mundo enorme". Nuestras alegrías y logros siempre dependen en gran parte del resto de individuos que nos rodean. Y por eso estoy orgullosa de todos aquellos individuos y personajes que me han rodeado durante esta mi aventura, a los cuales debo en gran medida haber llegado hoy hasta aquí y a los cuales quiero agradecer todo su cariño y apoyo.

En primer, último y enésimo lugar, a mi familia. A Padre, Madre y Pu. A papá, por su eterno optimismo y humor, a mamá, por su característico realismo e ironía y a Pu, mi hermana, la diva a la que siempre puedes recurrir y que tras sacarte de tus casillas será capaz de sacarte también una sonrisa. Porque sin ellos este pequeño hobbit nunca habría salido de La Comarca y porque sin ellos estaría perdida en este mundo enorme.

A Ángel, por confiar en mí para esta tarea y no dudar (espero) que completaría este viaje.
A Isabel, que con su buen humor y carácter amable amenizó el camino.
A Travis, que allanó el sendero en las tierras del DNA damage.
A todos aquellos que con sus consejos guiaron el camino y evitaron sendas oscuras.

A Ana. Ese ser que apareció en mi camino y al cual tardé en entender. Un personaje que pasó de ser circunstancial a ser parte esencial de la historia. Con ella que reí en Rivendell, batallé en Helm, ascendí la Torre oscura y espero beber y comer en la Comarca o en cualquier parte. Porque ha sido una compañera de aventuras gracias a la cual se han forjado muchas historias y con la que espero poder seguir escribiendo, ya sea una trilogía o una saga sin final cerrado.

A Nati, mi compañera de oficina, mi compañera de poyata, mi compañera de viaje y espero que compañera de muchas cosas más. A pesar de ser guiri fue ella quien me introdujo en el mundo del vermut, que tantas tardes ha servido de excusa para comentar penas y glorias. A pesar de ser deportista me enseñó muchas terrazas en las que sentarme a disfrutar de Barcelona. A pesar de ser tonta le he cogido cariño y espero que nuestros caminos se crucen a los largo de nuestras respectivas aventuras.

A las chicas del café, del vermut, de la cerveza o de lo que haga falta. Porque con gente como Eli, Sandra, Raquel, Eva…. los días son más amenos y las risas salen más fácil. Gracias por todos esos momentos memorables, momentos innombrables o momentos ridículos que han hecho de este viaje no sólo un libro de aventuras sino también un compendio humorístico.

A todos los miembros del laboratorio que están y que han estado, porque sus consejos, sus ideas, sus ocurrencias, sus conversaciones y su existencia en general han hecho de la poyata un lugar más amable.

A los colonos Carles y Marta. Porque aunque ahora se hallen en países lejanos como Bélgica o países imaginarios como Andorra, siempre nos quedarán las noches de Catán, las noches de Risk, las noches de Just Dance, las noches en las que no me pude hacer burbuja, las tardes de cine, las tardes de volley, las tardes de andar sin rumbo, la continua búsqueda de las bravas perfectas, las tardes en las que me confinasteis a sentarme en una papelera, las excursiones poco planeadas (no por la poca insistencia de Marta)… Por tantos años de increpamientos exentos de cariño y amor que espero que se repitan, ya sea en un país real o imaginario.

A las Arpías. A Ana, por su eterna sonrisa, a Pa, por su ironía y maldad, a Maca, por su imaginación y exageración, a Blanca, por su quillería y a Elma, por su perenne buen humor. Porque aunque la geografía se interponga entre nosotras, siempre habrá lugar para un buen akelarre que reconforte a las brujas.

A las de Siempre. A Laura por su tranquilidad y serenidad, a Drea, por su risa, a Caro, por su retranca y a Iara, por su amable mala baba. A esas gallegas que han hecho de la cerveza y del pulpo el mejor remedio contra la lluvia, el frío y la distancia.

A los Biolokos. Esa raza especial que conquistará la tierra media, la baja y la alta. Porque sin ellos la Biología no hubiese sido una fuente de diversión y porque sin ellos tal vez no hubiese confiado mi futuro a la Biología. Porque sin Félix el mundo no sería tan perverso, porque sin Migue no habría una constante risa de fondo y porque sin Ant el mundo sería un poco más aburrido. Gracias en especial a Ant por leer este manuscrito y criticarlo con la gran elegancia que le caracteriza y por haber hecho no sólo de esta historia, sino de cualquier historia, una historia mejor.

A Bea, una raza en extinción que me enseñó que se puede disfrutar de la ciencia y cuyos consejos y visión del mundo viajaron desde allende los mares hasta Barcelona y que llevaré allá donde vaya.

A Meri, una elfo con la que siempre puedes contar, con la que viajar, con la que reír, con la hablar y con la que disfrutar. Ya sea aquí o allá, yo sé que a Meri siempre se la podrá encontrar.

A todos aquellos que me olvido por el camino, lo cual no significa que se hayan quedado en el camino.

Y finalmente a Kiko. “Me hace feliz que estés aquí conmigo, aquí al final de todas las cosas”. “Porque aquí estamos, igual que en las grandes historias, las que realmente importan […] Ahora lo entiendo. Los protagonistas de esas historias se rendirían si quisieran pero no lo hacen. Siguen adelante.” Gracias por estar aquí, ahí y allí, y en todos lados. Por no rendirte, por evitar que me rindiese y porque espero que no nos rindamos nunca.

Aquí termina esta historia, tal como ha llegado a nosotros; y […] nada más se dice en este libro acerca de los días antiguos.

El señor de los anillos, J.R.R. Tolkien